Anti-inflammatory activity of repurposed tyrosine kinase inhibitors in macrophages

A thesis submitted for the degree of Doctor of Philosophy in Cardiovascular Science

University of Oxford

Trinity Term 2023

Laura Chaffey

St Edmund Hall

Sir William Dunn School of Pathology

Abstract

Inflammation is a driver of human disease and an unmet clinical need exists for new anti-inflammatory medicines. As a key cell type involved in pathologies of both acute and chronic inflammatory disease, macrophages are an appealing therapeutic target for novel anti-inflammatory medicines. Drug repurposing, the use of existing medicines for novel indications, is an attractive and pragmatic strategy for the discovery of novel anti-inflammatory medicines due to reduced development costs and lower toxicity-associated failure risks than *de novo* drug discovery. In this thesis I set out to identify novel drug repurposing candidates with anti-inflammatory activity in macrophages. Using inhibition of NF-κB activity as a measure of anti-inflammatory activity, I performed a drug repurposing screen of 159 FDA-approved medicines in a macrophage reporter cell-line and identified sunitinib, a multiple tyrosine kinase inhibitor currently used as a treatment for advanced kidney cancers, to be an inhibitor of NF-κB activity. Further investigation of sunitinib in bone marrow derived macrophages revealed ability to inhibit production pro-inflammatory mediator production of TNFα, IL-6, IL-1β, CCL2, and NO. *In vivo,* I show that oral sunitinib treatment prior to LPS challenge reduces TNFα production and inflammatory gene expression, inhibits NF-κB nuclear translocation and reduces organ damage in a murine model of endotoxaemia. Additionally, as NF-κB mediated inflammatory signalling plays an important role in atherosclerosis progression, effects of sunitinib treatment were investigated in a model of hypercholesterolaemia. In *Ldlr*$^{-/-}$ mice fed a high fat diet, sunitinib treatment effectively reduced TNFα production and inflammatory gene expression but did not alter atherosclerotic plaque development or stability. The findings of this thesis support drug repurposing as a strategy for investigation of novel anti-inflammatory medicines and further exploration of sunitinib in inflammatory disease models will aid in determining its feasibility as a drug repurposing candidate for inflammatory disease.

Acknowledgments

This thesis would not have been possible without the help of many people over the past 4 and a half years. Firstly, I extend my deepest gratitude to my DPhil supervisor, Professor David Greaves. It has been a privilege to work in your lab and I will be forever grateful the mentorship and guidance you have given me over the past few years. I truly couldn't have asked for a better place to have had my scientific training than the Dunn School — even when the ceilings fall down!

Secondly, I would like to thank all the staff who have been so helpful throughout my DPhil. In particular, thank you to Dr. Gillian Douglas, who dedicated so much time to helping to train me in experimental techniques over the past year.

Next, to all members of the Greaves lab present and past: Vincent, Annabell, Agata, Gareth, Conan, Ada, and Lili – thank you for all the support you have provided me, both scientifically and otherwise. You have been wonderful colleagues and created such a fun lab atmosphere in which to work. I feel exceptionally lucky to have spent my daily DPhil life with you all and hope for many more cheese and wine evenings to come!

To those I've met during my time at Oxford — to Michael, Diana, Yu, Yasemin, Faseeha and Lucy — you are all incredible and I really couldn't have gotten through the hard times without you. I am very fortunate to have made lifelong friends in you all during this DPhil.

Finally, I would not be in this position without the continuing support of my family; Jess, and my parents, Brian and Caroline, who have always supported my academic endeavours and encouraged me achieve my goals. I will be so proud to become the final Dr of the family.

Abbreviations

αSMA	Smooth muscle α actin
AKI	acute kidney injury
ALF	acute liver failure
ALI	acute lung injury
ALT	alanine aminotransferase
AP-1	activator protein 1
ARDS	acute respiratory distress syndrome
ARDS	acute respiratory distress syndrome
AST	aspartate aminotransferase
AUC	area under curve
BMDM	bone marrow derived macrophage
BSA	bovine serum albumin
BTK	Bruton's tyrosine kinase
CHF	chronic heart failure
CLP	caecal ligation and puncture
COX	cyclooxygenase
CRP	C-reactive protein
CSF-1	colony stimulating factor 1
CSF-1R	colony stimulating factor 1 receptor
CVD	cardiovascular disease
DAMP	damage-associated molecular pattern
DMARD	disease-modifying antirheumatic drug
DMEM	Dulbecco's modified eagle media
DMSO	dimethyl sulfoxide
EC	endothelial cell
EDTA	ethylenediaminetetraacetic acid
FBS	fetal bovine serum
FDA	Food and Drug Administration
FLT3	fms related receptor tyrosine kinase 3
FMO	fluorescence minus one
FSC	forward scatter
GIST	gastrointestinal stromal tumour
GR	glucocorticoid receptor
i.v	intravenous
IFNγ	interferon gamma
IKK	inhibitor of κB kinase
IL	interleukin
iNOS	inducible nitric oxide synthase
i.p	intraperitoneal
IRAK1/2	interleukin-1 receptor associated kinase 1/2
IκB	inhibitor of κB
LDH	lactate dehydrogenase
LPS	lipopolysaccharide

LVEF	left ventricular ejection fraction
MHC	major histocompatibility complex
MI	myocardial infarction
MI	myocardial infarction
MOF	multiple organ failure
MSPR	macrophage stimulating 1 receptor
MuSK	muscle specific kinase
NF-κB	nuclear receptor kappa B
NIK	NF-κB inducing kinase
NLRP3	NLR family pyrin domain containing 3
NO	nitric oxide
NSDAID	non-steroidal anti-inflammatory drug
oxLDL	oxidised low density lipoprotein
p.o	per os
P/S	penicillin plus streptomycin
PAMP	pathogen-associated molecular pattern
PBS	phosphate buffered saline
PDGFR	platelet derived growth factor receptor
PEC	peritoneal exudate cells
PFA	paraformaldehyde
PGE_2	prostoglandin E2
PRR	pattern recognition receptor
PS	phasphatidyl serine
RA	rheumatoid arthritis
RCC	renal cell carcinoma
ROS	reactive oxygen species
RTK	receptor tyrosine kinase
s.c	subcutaneous
SEAP	secreted alkaline phosphatase
SIK	salt inducible kinase
SPM	specialised pro-resolving mediator
SSC	side scatter
STEMI	ST segment elevation myocardial infarction
T2D	Type 2 Diabetes
TBS	tris-buffered saline
TDZ	thioridazine hydrochloride
TIR	Toll/interleukin-1 receptor
TKI	tyrosine kinase inhibitor
TLR	Toll like receptor
TNFα	tumour necrosis factor α
VEGFR	vascular endothelial growth factor receptor
VSMC	vascular smooth muscle cell
WBC	white blood cell
ZIP	zymosan-induced peritonitis

Contents

ABSTRACT ..... **I**

ACKNOWLEDGMENTS ..... **II**

ABBREVIATIONS ..... **III**

CONTENTS ..... **V**

LIST OF FIGURES ..... **VIII**

LIST OF TABLES ..... **IX**

CHAPTER 1: INTRODUCTION **1**

1.1 AN HISTORICAL OVERVIEW OF INFLAMMATION 1
1.2 THE ROLE OF MACROPHAGES IN INFLAMMATION 2
1.2.1 Tissue resident and monocyte-derived macrophage identities *2*
1.2.2 Monocyte recruitment and chemotaxis *4*
1.2.3 Macrophage polarisation *4*
1.2.4 Macrophage phagocytosis and efferocytosis *6*
1.2.5 Tissue repair and inflammation resolution *7*
1.3 INFLAMMATORY SIGNALLING PATHWAYS 8
1.3.1 TLR4 initiated inflammatory cascades *8*
1.3.2 NF-κB signalling in macrophages *9*
1.3.3 AP-1 signalling in macrophages *12*
1.3.4 The NLRP3 inflammasome *12*
1.4 MACROPHAGE PRO-INFLAMMATORY MEDIATORS 13
1.4.1 Tumour Necrosis Factor α *13*
1.4.2 Interleukin 6 ..... *14*
1.4.3 Interleukin 1β *15*
1.4.4 Nitric Oxide *15*
1.5 TYROSINE KINASES IN INFLAMMATORY SIGNALLING 16
1.5.1 Src family kinases *16*
1.5.2 Bruton's Tyrosine Kinase *17*
1.5.3 Colony Stimulating Factor-1 Receptor *18*
1.5.4 Tyro3, Axl, Mer (TAM) kinase family *18*
1.6 MACROPHAGE DRIVEN INFLAMMATORY DISEASES 20
1.6.1 Sepsis *20*
1.6.2 Atherosclerosis *21*
1.7 ANTI-INFLAMMATORY MEDICINES 26
1.7.1 Glucocorticoids *26*
1.7.2 NSAIDs *27*
1.7.3 DMARDs *28*
1.7.4 Limitations of current anti-inflammatory medicines *29*
1.8 ORIGINAL HYPOTHESIS AND AIMS OF THIS THESIS 30

CHAPTER 2: MATERIALS AND METHODS **31**

2.1 REAGENTS 31
2.2 ANIMAL EXPERIMENTS 31
2.2.1 Ethical statement *31*
2.2.2 Mouse strains and husbandry *32*
2.2.3 Endotoxaemia *32*
2.2.4 Hypercholesterolaemia *33*
2.3 CELL CULTURE 33
2.3.1 Murine bone marrow-derived macrophages (BMDMs) *33*
2.3.2 RAW-Blue macrophage reporter cell line *34*

2.3.3 Murine L929 fibroblast cells *34*
2.4 QUANTI-BLUE ASSAY 34
2.5 CELL VIABILITY ASSAYS 35
2.5.1 MTT viability Assay *35*
2.5.2 PrestoBlue viability assay *35*
2.5.3 Cell Titer Glo viability assay *35*
2.6 GRIESS ASSAY 35
2.7 ELISA 36
2.8 BLOOD ANALYSIS 36
2.9 FLOW CYTOMETRY EXPERIMENTS 36
2.9.1 Cell Stimulations and Sample preparation *36*
2.9.2 Aortic Digestion *37*
2.9.3 Flow cytometry staining procedure *37*
2.9.4 Flow cytometry data acquisition and analysis *39*
2.10 IMAGESTREAM ANALYSIS OF P65 NUCLEAR TRANSLOCATION 39
2.11 REAL-TIME PHAGOCYTOSIS 39
2.12 PHOSPHO-KINASE ARRAY 40
2.13 WESTERN BLOTTING 40
2.13.1 Sample preparation and protein extraction from cells *40*
2.13.2 Protein Extraction from mouse tissue *41*
2.13.3 Protein concentration quantification *41*
2.13.4 Western Blotting *41*
2.14 RT-QPCR 42
2.15 HISTOLOGY 44
2.15.1 Haematoxylin & Eosin *44*
2.15.2 En face Oil-Red-O *44*
2.15.3 Masson-Goldner's Trichrome *44*
2.15.4 Immunohistochemistry *46*
2.16 STATISTICAL ANALYSIS 46

CHAPTER 3: DRUG REPURPOSING SCREENING FOR ANTI-INFLAMMATORY ACTIVITY AND INVESTIGATION OF ANTI-INFLAMMATORY EFFECTS OF SUNITINIB *IN VITRO* 47

3.1 INTRODUCTION: 47
3.1.1 Drug Repurposing and de novo drug discovery *47*
3.1.2 Drug repurposing strategies *48*
3.2 RATIONALE AND EXPERIMENTAL AIMS OF CHAPTER 51
3.3 RESULTS: 51
3.3.1 Screen of FDA-approved medicines for NF-kB inhibition in RAW-Blue cells: *51*
3.3.2 Validation of the anti-inflammatory activity of Bosutinib and Sunitinib in cell-line macrophages *59*
3.3.3 Bosutinib and Sunitinib activity in primary macrophages *61*
3.3.4 Effect of sunitinib on macrophage polarisation *65*
3.3.5 Effect of sunitinib on macrophage phagocytosis *68*
3.3.4 Effect of sunitinib on AP-1 activity *70*
3.3.6 Effect of sunitinib on TLR4 surface expression *71*
3.3.7 Effect of sunitinib on NF-κB pathway phosphorylation *73*
3.3.8 Investigating the kinase target of sunitinib in LPS induced NF-κB activation though phosphoprotein array *75*
3.3.9 Investigating macrophage specificity of sunitinib *77*
3.4 DISCUSSION 79
3.4.1 Designing a target-based drug-repurposing screen for anti-inflammatory activity based on macrophage NF-κB inhibition *79*
3.4.2 Bosutinib identified as an inhibitor of NF-κB in macrophages *80*
3.4.3 Sunitinib identified as an inhibitor of NF-κB in macrophages *81*
3.4.4 Limitations of study *84*
3.4.5 Summary *84*

CHAPTER 4: EFFECTS OF SUNITINIB IN ACUTE INFLAMMATION *IN VIVO*..... 85

4.1 INTRODUCTION..... 85
4.1.1 Murine Models of Acute inflammation..... 85
4.1.2 Murine models of systemic inflammation and sepsis..... 85
4.1.3 Acute Lung injury in systemic inflammation..... 87
4.1.4 Liver dysfunction in systemic inflammation..... 87
4.1.5 Acute Kidney Injury in systemic inflammation..... 88
4.1.6 Animal models of inflammation in drug repurposing studies..... 88
4.2 RATIONALE AND EXPERIMENTAL AIMS OF CHAPTER..... 89
4.3 RESULTS..... 90
4.3.1 Determining an in vivo Inflammatory model in which to test sunitinib..... 90
4.3.2 Effects of sunitinib on early inflammatory responses in vivo..... 92
4.3.3 Effects of sunitinib in intermediate inflammation in vivo..... 97
4.3.4 Effects of sunitinib on advanced inflammation and organ damage..... 101
4.4 DISCUSSION..... 108
4.4.1 Characterising anti-inflammatory effects of sunitinib in vivo..... 108
4.4.2 Limitations of study..... 110
4.4.3 Summary..... 112

CHAPTER 5: EFFECTS OF SUNITINIB IN CHRONIC INFLAMMATION *IN VIVO*..... 113

5.1 INTRODUCTION:..... 113
5.1.1 Targeting inflammation in cardiovascular disease..... 113
5.1.2 Drug repurposing in atherosclerosis..... 116
5.1.3 Emerging anti-inflammatory drug repurposing candidates and molecular targets for cardiovascular disease..... 120
5.2 RATIONALE AND EXPERIMENTAL AIMS OF CHAPTER..... 122
5.3 RESULTS:..... 123
5.3.1 Safety and effect of sunitinib on the induction of hypercholesterolaemia in a $Ldlr^{-/-}$ mouse model..... 123
5.3.2 Effect of sunitinib on hypercholesterolaemia induced inflammatory mediator production..... 126
5.3.3 Effect of sunitinib on immune cell recruitment in hypercholesterolaemia..... 129
5.3.4 Effect of sunitinib on atherosclerotic plaque development..... 133
5.4 DISCUSSION..... 137
5.4.1 Sunitinib reduces inflammation but not atherosclerosis development in a model of hypercholesterolaemia..... 137
5.4.2 Potential anti-inflammatory mechanisms of sunitinib in hypercholesterolaemia..... 138
5.4.3 Targeting TNFα in chronic cardiovascular inflammation..... 139
5.4.2 Limitations of study..... 140
5.4.3 Summary..... 141

CHAPTER 6: CONCLUSIONS..... 142

6.1 SUMMARY OF KEY FINDINGS..... 142
6.2 THE FUTURE OF SUNITINIB AS A DRUG REPURPOSING CANDIDATE FOR INFLAMMATORY DISEASE..... 143

REFERENCES..... 147

APPENDICES..... 169

APPENDIX 1: AMELIA BOWMAN FHS PROJECT CYTOTOXICITY DATA..... 169
APPENDIX 2: LYNDA ZEBOUDJ ENDOTOXAEMIA DATA..... 170
APPENDIX 3: PUBLICATION CONTRIBUTIONS..... 171

List of Figures

FIGURE 1.1: BALANCING INFLAMMATION....2
FIGURE 1.2: THE NF-KB SIGNALLING CASCADE....11
FIGURE 1.3 CONTRIBUTION OF MYELOID CELLS TO ATHEROSCLEROTIC PLAQUE FORMATION....25
FIGURE 2.1: AORTIC ROOT PLAQUE ANALYSIS....45
FIGURE 3.1: RAW-BLUE SCREEN DESIGN FOR ANTI-INFLAMMATORY DRUG ACTIVITY....53
FIGURE 3.2: ANTI-INFLAMMATORY ACTIVITY OF FDA-APPROVED MEDICINES DETECTED IN A NF-KB REPORTER CELL LINE SCREEN....54
FIGURE 3.3: EFFECTS OF VORINOSTAT IN THE QUANTI-BLUE ASSAY. OPTICAL DENSITY OF RAW-BLUE SUPERNATANTS IN THE QUANTI-BLUE ASSAY....57
FIGURE 3.4: CYTOTOXICITY OF FDA-APPROVED MEDICINES IN LPS-STIMULATED RAW-BLUE CELLS....58
FIGURE 3.5: DOSE-DEPENDENT ANTI-INFLAMMATORY EFFECTS OF BOSUTINIB AND SUNITINIB IN RAW-BLUE CELLS....60
FIGURE 3.6: EFFECT OF BOSUTINIB ON PRIMARY MACROPHAGE CYTOKINE PRODUCTION....63
FIGURE 3.7: EFFECT OF SUNITINIB ON PRIMARY MACROPHAGE CYTOKINE PRODUCTION....64
FIGURE 3.8: SUNITINIB AFFECTS MACROPHAGE POLARISATION *IN VITRO*....67
FIGURE 3.9: SUNITINIB INHIBITS MACROPHAGE PHAGOCYTOSIS....69
FIGURE 3.10: ANTI-INFLAMMATORY ACTIVITY OF SUNITINIB IS NOT DUE TO INHIBITION OF AP-1....70
FIGURE 3.11: SUNITINIB DOES NOT AFFECT INTERNALISATION OF TLR4....72
FIGURE 3.12: SUNITINIB DOES NOT AFFECT CANONICAL NF-KB SIGNALLING....74
FIGURE 3.13: SUNITINIB ALTERS THE RECEPTOR TYROSINE KINASE PHOSPHORYLATION LANDSCAPE IN MACROPHAGES....76
FIGURE 3.14: SUNITINIB INHIBITS NO PRODUCTION IN FIBROBLASTS....78
FIGURE 4.1: ENDOTOXAEMIA 1 HOUR MODEL DESIGN....91
FIGURE 4.2: SUNITINIB REDUCES PLASMA TNFA IN ENDOTOXAEMIA AT 1 HOUR....92
FIGURE 4.3: SUNITINIB REDUCES INFLAMMATORY GENE EXPRESSION IN ENDOTOXAEMIA AT 1 HOUR....94
FIGURE 4.4: SUNITINIB INHIBITS NF-KB NUCLEAR TRANSLOCATION IN ENDOTOXAEMIA AT 1 HOUR....96
FIGURE 4.5: ENDOTOXAEMIA 6 HOURS MODEL DESIGN....98
FIGURE 4.6: SUNITINIB DOES NOT ATTENUATE SERUM CYTOKINE LEVELS IN ENDOTOXAEMIA AT 6 HOURS....99
FIGURE 4.7: SUNITINIB REDUCES INFLAMMATORY GENE EXPRESSION IN ENDOTOXAEMIA AT 6 HOURS....100
FIGURE 4.8: ENDOTOXAEMIA 24 HOURS MODEL DESIGN....102
FIGURE 4.9: SUNITINIB REDUCES SERUM TNFA IN ENDOTOXAEMIA AT 24 HOURS....103
FIGURE 4.10: SUNITINIB DOES NOT INHIBIT INFLAMMATORY GENE EXPRESSION IN ENDOTOXAEMIA AT 24 HOURS....104
FIGURE 4.11: SUNITINIB ATTENUATES MACROPHAGE POLARISATION *IN VIVO*....105
FIGURE 4.12: SUNITINIB REDUCES MARKERS OF ORGAN DAMAGE IN ENDOTOXAEMIA AT 24 HOURS.107
FIGURE 5.1: SUNITINIB DOES NOT AFFECT CIRCULATING LIPID LEVELS IN A MOUSE MODEL OF HYPERCHOLESTEROLAEMIA....125
FIGURE 5.2: SUNITINIB REDUCES TNFA PRODUCTION IN HYPERCHOLESTEROLAEMIC MICE....127
FIGURE 5.3: SUNITINIB REDUCES INFLAMMATORY GENE EXPRESSION IN HYPERCHOLESTEROLAEMIC MICE....128
FIGURE 5.4: SUNITINIB DOES NOT ALTER PERITONEAL IMMUNE CELL POPULATIONS IN HYPERCHOLESTEROLAEMIC MICE....130
FIGURE 5.5: SUNITINIB DOES NOT ALTER BLOOD IMMUNE CELL POPULATIONS IN HYPERCHOLESTEROLAEMIC MICE....131
FIGURE 5.6: SUNITINIB DOES NOT ALTER IMMUNE CELL COMPOSITION IN THE AORTA OF HYPERCHOLESTEROLAEMIC MICE....132
FIGURE 5.7: SUNITINIB DOES NOT AFFECT ATHEROSCLEROTIC PLAQUE BURDEN IN HYPERCHOLESTEROLAEMIC MICE....134
FIGURE 5.8: SUNITINIB DOES NOT AFFECT PLAQUE COMPOSITION IN HYPERCHOLESTEROLAEMIC MICE....136

List of Tables

TABLE 1.1: CHARACTERISTICS OF M1 AND M2 POLARISED MACROPHAGES 6
TABLE 1.2: ROLE OF CYTOKINES IN ATHEROSCLEROSIS.....23
TABLE 2.1: LIST OF ANTIBODIES USED FOR FLOW CYTOMETRY.....38
TABLE 2.2: LIST OF PRIMARY ANTIBODIES USED FOR WESTERN BLOTTING.....42
TABLE 2.3: LIST OF MOUSE PRIMERS USED 43
TABLE 3.1: COMPOUNDS CAUSING >25% INHIBITION OF NF-KB IN RAW-BLUE DRUG REPURPOSING SCREEN.....56
TABLE 3.2: IC_{50} VALUES FOR PRO-INFLAMMATORY CYTOKINE PRODUCTION IN BONE MARROW DERIVED MACROPHAGES.....62
TABLE 3.3: EXPRESSION OF NF-KB SIGNALLING COMPONENTS AND RECEPTOR TYROSINE KINASES IN DIFFERENT CELL TYPES.....78
TABLE 4.1: DRUG REPURPOSING CANDIDATES TESTED IN ANIMAL MODELS OF ACUTE INFLAMMATION.....89
TABLE 5.1: DRUG REPURPOSING CARDIOVASCULAR CLINICAL TRIALS OF ANTI-INFLAMMATORY MEDICINES.....114
TABLE 5.2: ANTI-INFLAMMATORY DRUG REPURPOSING CANDIDATES FOR USE IN CARDIOVASCULAR DISEASE.....121
TABLE 5.3: PLASMA LIPID CONCENTRATION IN $LDLR^{-/-}$ MICE FED A HIGH-FAT DIET…….....124

Chapter 1: Introduction

1.1 An historical overview of inflammation

The ability of an organism to defend itself against harmful invading pathogens as well as protect against pathological tissue damage is critical to its survival. The appearance of host immune processes equipped to confer this essential ability occurred early in the evolutionary process and can now be found throughout all domains of life to varying degrees of complexity from bacterial CRISPR/Cas 9 systems [1] to our own multicellular immune systems.

In mammals, immune processes can be broadly spilt into those of the innate immune response and of the adaptive immune response, with both arms working in tandem in a coordinated fashion to ensure maximal host protection. Adaptive immune responses are carried out largely by B and T lymphocytes and are highly specific due to amplification of clones carrying antigen-specific receptors, and can confer long-lasting immunological memory and protection against subsequent infection. Innate immune responses on the other hand are triggered more broadly by a range of stimuli and are rapidly deployed to provide front-line host defence, and offer comparatively limited immunological memory.

Inflammation is a cornerstone of the innate immune response and is characterised by the processes swelling, heat, redness, and pain, as described as early as 25 A.D by Aulus Cornelius Celsus. Since this time, key advances in understanding from John Hunter in 1794, Elie Metchnikoff in 1882 [2], and others [3] have contributed to the understanding of inflammation as a homeostatic and beneficial process; a consequence of prior insult initiated to restore normal tissue function, rather than detrimental to health in and of itself. This viewpoint holds true for inflammation that is self-resolving, however uncontrolled inflammation in instances such as sepsis, or chronic inflammation in diseases like atherosclerosis, see these once-protective processes become pathological. Therefore, a delicate balance must be struck between these two outcomes through tight regulation of inflammation initiation and resolution (Figure 1.1).

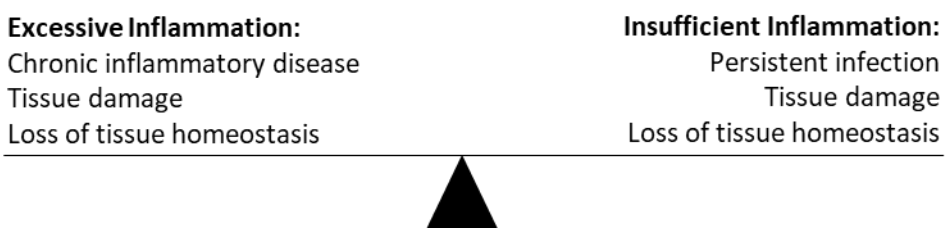


Figure 1.1: Balancing inflammation

1.2 The role of macrophages in inflammation

The significance of macrophages to host immunity was first recognised in seminal experiments in the 1880s by Elie Metchnikoff, who is widely regarded the father of innate immunity [2,4]. Metchnikoff described phagocytic cells surrounding rose thorns embedded into starfish larva and identified this as a host defence mechanism akin to an inflammatory response [2]. Macrophages are central to the process of inflammation and possess specialised properties to make them adept at protecting against infection and maintaining homeostasis. Importantly, unlike other immune cells such as effector T cells, macrophages retain a high degree of phenotypic plasticity which enables them to enact varied physiological roles. The following section will address the physiological functions and characteristics of macrophages.

1.2.1 Tissue resident and monocyte-derived macrophage identities

By definition, macrophages are found only within tissues and are not present in the blood unlike their monocyte precursors which are largely confined to the circulation [5,6]. Initially after their discovery, it was believed that all tissue resident macrophages originated from bone marrow progenitor cells and that monocytes were merely not yet differentiated macrophages [5–7]. Subsequent evidence of local tissue proliferation and the presence of mature macrophages in embryonic tissues prior to the appearance of haematopoietic stem cells has challenged these beliefs [7] and it is now widely accepted that tissue resident macrophages can arise from three distinct origins: the embryonic yolk sac, fetal liver monocytes, and bone marrow monocytes [6,7]. The balance of these populations is unique to each tissue and fluctuates over time upon tissue infection or injury, as well as with age [6,7].

Embryonically derived tissue resident macrophages are considered to play an important role in inflammation resolution and maintaining tissue homeostasis, whereas monocyte derived macrophages are key cell types in the inflammatory response and host protection [5]. These resident macrophages display a large degree of tissue heterogeneity, with expression levels of key (murine) macrophage markers like F4/80, CD68, CD11b and Dectin-1 differing between specific tissue populations including alveolar macrophages, resident peritoneal macrophages, and microglia [8]. While each tissue has its own requirements for replenishment by bone marrow monocytes, some tissue resident macrophage populations such as alveolar macrophages of the lung are almost entirely self-sustaining and are instead maintained by local proliferation [6].

Monocytes, which can also give rise to dendritic cells and osteoclasts as well as macrophages [8], contribute 4% and 10% of nucleated blood cells in mice and humans respectively [5] and are found in large numbers in marginal pools in the spleen and lungs which can be rapidly mobilised upon infection or injury [5,9]. Monocytes originate in the bone marrow from haematopoietic stem cells and depend on the growth factor macrophage colony stimulating factor 1 (CSF-1) for development and survival [5]. In the blood, monocytes are short lived with a typical half-life of 20 hours [5]. In humans, monocytes can be categorised into two main subpopulations based on their expression of the Fcγ receptor CD16, and lipopolysaccharide co-receptor CD14 [10]. The human monocytic populations $CD14^{+}CD16^{-/+}$ and $CD14^{low}CD16^{+}$ monocytes are believed to be functionally equivalent to $Ly6C^{hi}$ and $Ly6C^{low}$ populations in mice [5]. In mice, blood monocytes can be thought of as existing in differentiation states, with $Ly6C^{hi}$ cells differentiating into $Ly6C^{low}$ cells in circulation [5] that proceed to patrol the vasculature by migrating along the endothelial wall [11]. However, it is $Ly6C^{hi}$ and $CD14^{+}$ monocytes which are considered 'classical monocytes'. These monocytes are recruited to tissues upon inflammation *via* interactions with the monocyte expressed CCR2 receptor [10] where they differentiate into macrophages [5]. Emerging evidence suggests that monocytes may have a role as effector cells in their own right in processes such as angiogenesis [5].

1.2.2 Monocyte recruitment and chemotaxis

Recruitment of monocytes to inflamed tissues is essential to their function in inflammation. Monocyte recruitment during inflammation is governed by CCL2/CCR2 signalling, as is evidenced by reduced monocytes/macrophages in $CCR2^{-/-}$ mice in various inflammatory models [9]. During monocyte extravasation, CCL2 is presented by the endothelium to promote tight adhesion and extravasation *via* CCR2 induced signalling events. Once within the tissue, CCL2 gradients then induce monocyte chemotaxis, the directional movement of cells along a chemoattractant gradient, towards the site of inflammation [12].

In addition to its essential function in myeloid lineage commitment and survival, the cytokine CSF-1 can also act as a tissue chemoattractant. CSF-1 ligand binding to CSF-1R triggers morphological cell changes like membrane ruffling *via* actin skeleton reorganisation in processes involving Rac1 and Rho signalling [13].

Although to a lesser degree than monocytes, macrophages are also chemotactic cells. The processes underpinning macrophage migration are more complex and less well understood than that of monocytes, with recent evidence suggesting that they are able to display context dependent migratory behaviours, switching between ameboid and mesenchymal migration [14]. Tissue resident macrophages on the other hand can be largely immobile. For example, liver Kupfer cells and alveolar macrophages form sessile interactions with surrounding structural cells while peritoneal macrophages also display low mobility, instead patrolling their surroundings through the extension of pseudopodia [6]

1.2.3 Macrophage polarisation

As mentioned above, macrophages are highly heterogenous cells with functionally diverse roles dictated by microenvironmental cues. Macrophage polarisation refers to the functional phenotype arising from such environmental stimuli, in regards to cytokine production, surface marker expression and functional activity.

Macrophage activation, now recognised as 'classical activation', was first described by Mackaness in the 1960s upon noting macrophage-mediated resistance to bacterial infection [15,16]. This activity was later linked to Th1 T helper cell responses, although the equivalent Th2-linked macrophage function, termed 'alternative activation', initially remained elusive [15]. Another key advance was made in 1983 when Carl Nathan and colleagues identified lymphocyte-produced interferon gamma (IFNγ) as an important molecule in inducing macrophage activation and anti-microbial activity [17].

The M1/M2 macrophage polarisation framework was introduced in 2000 by Mills and colleagues. They found that macrophages in mouse strains with a Th1 or Th2 background had differing ability to respond to inflammatory stimuli lipopolysaccharide (LPS) and IFNγ, and that 'M1' macrophages made nitric oxide (NO) from arginine while 'M2' macrophages produced ornithine from arginine [15]. This was adopted by Mantovani and colleagues to describe an experimental model of macrophage polarisation in which M1 is induced by stimulation with LPS and IFNγ, and M2 is induced by IL-4 [15]. Functionally, pro-inflammatory and microbicidal M1 cells are easier to define than M2 cells, which are classically associated with an anti-parasitic role akin to Th2 responses. There has been a notable deviation from this original definition for M2 over the years, with it often being described in the literature as an 'anti-inflammatory' or 'pro-repair' phenotype [18–20]. This characterisation, more akin to that of T_{regs} than Th2 cells, is not strictly accurate, although there have been links between inflammation resolution and M2-secreted cytokines like IL-10, TGFβ [18]. Furthermore, M2 macrophages have been linked to tissue repair in certain contexts like post-myocardial infarction repair [21,22], and M2 pro-fibrotic transcriptional signatures may be favourable in instances such as atherosclerosis, where fibrosis helps to promote plaque stability [18].

It is widely agreed that the M1/M2 framework is oversimplistic and unlikely to recapitulate an *in vivo* setting where macrophages simultaneously receive multiple polarising cues and thus exist on a spectrum rather than as a dichotomy. This nomenclature is useful however to standardise research efforts, and certain cytokine secretion profiles, transcriptional regulators, and functions are associated with M1/M2 polarisation (Table 1.1). Moreover, polarisation is believed to be transient rather than terminal and is thought to merely fine-tune functions common to all macrophages such

as phagocytosis, cytokine secretion, chemotaxis and microbial killing, rather than dictate them entirely [15]. Finally, as transcriptomic and single cell techniques continue to be developed, the field's reliance on the M1/M2 classification system is diminishing and more detailed, individualised, descriptions of macrophages are evolving.

Table 1.1: Characteristics of M1 and M2 polarised macrophages [12,15,16,23,24]

	M1	**M2**
Inducing stimuli	IFNγ, LPS, viral/bacterial antigens, TLR ligands, GM-CSF	IL-4, IL-13, IL-10, glucocorticoids, CSF-1
Cytokine profile	TNFα, IL-1β, IL-6, IL-12, CCL2	TGF-β, IL-10
Markers (murine)	MHCII, Nos2	CD206, Arg1, Fizz1, CCL1, CCL17
Transcriptional regulators	NF-κB, AP-1, STAT1, IRF5	STAT6, IRF4, PPARγ
Phagocytosis	Decreased Fc-mediated and complement phagocytosis, Increased phagocytosis of bacteria	Decreased phagocytosis of bacteria with increased cytokine secretion, *Increased efferocytosis*
Nitric Oxide	Induction of iNOS leads to increase NO-mediated killing	Favours Arginase-1 mediated production of ornithine
Chemotaxis	Chemotaxis towards CCL19, CCL21, CCL24, CCL25, CXCL8, CXCL10, and XCL2, CCL7	Chemotaxis towards CCL7, CCL2, CCL5, CXCL10, CXCL12 and C1q

1.2.4 Macrophage phagocytosis and efferocytosis

Phagocytosis, defined as the uptake of particles >0.5μm in diameter within a plasma-membrane envelope [25], is the function that earned macrophages their name 'big eater' from Metchnikoff upon their initial identification [2]. The process involves ligand binding to plasma membrane receptors such as FcRs and complement receptors. This initiates cytoskeletal rearrangement, membrane invagination, and subsequent formation of a phagosome through various signalling pathways involving mediators such as Rac1. Phagosomes eventually fuse with lysosomes to form acidified phagolysosomes which begin to break down internalised cargo [25]. Although other cell types are capable of this process, macrophages, alongside neutrophils, monocytes, dendritic cells, osteoclasts, and eosinophils, have a particularly high capacity for phagocytosis and have thus been termed 'professional phagocytes' [25]. Phagocytosis is just one of many immunological processes that occur

upon detection of an invading pathogen and therefore occurs in parallel to processes such as cytokine production, and NO-mediated killing.

A specialised form of phagocytosis is the engulfment of apoptotic cells; a process termed efferocytosis. Efferocytosis involves specialised plasma membrane receptors, such as TAM family receptors, Tim3 and integrin αvβ3/5, which recognise and bind "eat me" signals on the surface of apoptotic cells including externalised phosphatidyl serine (PS) to allow engulfment. At the same time, engulfment of non-apoptotic cells is prevented though macrophage interactions with "don't eat me" molecules such as CD47 [26]. With an estimated billion cells in the human body undergoing apoptosis each day, efficient efferocytosis is essential for maintaining tissue homeostasis, and is unsurprisingly therefore highly evolutionarily conserved [27]. Notably, the engulfment of apoptotic debris has been shown to result in the production of anti-inflammatory mediators such as IL-10, TGF-β and PGE_2 [28–30] and is regarded to actively promote inflammation resolution *in vivo*. Interestingly, there are considerable metabolic consequences to apoptotic cell ingestion and the mechanism which allow macrophages to cope with internalised apoptotic cell-derived cargo is a topic of ongoing interest [31–33].

1.2.5 Tissue repair and inflammation resolution

Inflammation resolution, the return to tissue homeostasis after an inflammatory response, is an essential yet somewhat enigmatic step of the inflammatory cascade. The question of whether resolution of inflammation is an active process requiring signalling arising from events such as neutrophil apoptosis, efferocytosis, and production of pro-repair mediators [9], or a passive process — simply the dying down of pro-inflammatory signalling that allows for these processes to occur — remains poorly understood and the underlying mechanisms continue to prove controversial [34].

A number of pro-resolution pathways and signalling events have been described. Firstly, the removal of the inciting inflammatory stimulus such as bacterial or viral infection is essential for resolution, and when this is defective the result is chronic or hyperinflammation [35]. The next requirement is cessation of proinflammatory signalling, achieved via regulatory negative feedback loops in cytokine production, and catabolism of mediators such as prostaglandins and chemokines[35]. As discussed

above, efferocytosis is an important event in inflammation resolution, particularly efferocytosis of apoptotic neutrophils that have been recruited to the site of inflammation [35,36].

Much of the research into inflammation resolution has focused on specialised pro-resolving mediators (SPMs) spearheaded by the work of Charles Serhan and colleagues [37,38]. SPMs are a subset of omega-3 derived lipids that have been shown reduce inflammation *via* enhancement of resolution pathways through binding specific immune-cell expressed receptors. SPMs include Lipoxins A_4 and B_4, Resolvins E1, D1 and D2, and Protectin D1, and all are reported to inhibit granulocyte trafficking, dampen pro-inflammatory signalling, promote efferocytosis and induce pro-repair macrophage polarisation [35,38]. There is widespread interest in understanding these processes and therapeutically exploiting them in instances of hyperinflammation and chronic inflammatory disease.

1.3 Inflammatory signalling pathways

1.3.1 TLR4 initiated inflammatory cascades

Inflammation is initiated when pattern recognition receptors (PRRs) on innate immune cells are bound and activated by pathogen- or damage-associated molecular patterns (PAMPs or DAMPs, respectively). Unlike the B cell and T cell receptors of the adaptive immune system, PRRs are germline encoded and expressed by multiple different immune and non-immune cell types. The most intensively studied class of PRR is the family of Toll like receptors (TLR). These receptors, first described in *Drosophila* in 1985 [39] include TLR4, the receptor responsible for sensing Gram negative bacteria derived lipopolysaccharide (LPS), also known as endotoxin [40,41]. Since its discovery, TLR4 activation and downstream signalling pathways have been extensively studied and the LPS/TLR4/NF-κB signalling axis is regularly used as a paradigm for inflammatory signalling.

TLR4 is a transmembrane protein consisting of a leucine-rich repeat extracellular domain and cytoplasmic Toll/Interleukin-1 receptor (TIR) domain, which shares homology with the IL-1 receptor [42]. TLR4 alone is unable to directly bind LPS and instead relies upon interactions with adaptor proteins. Extracellular LPS micelles are readily bound by serum LPS binding protein, which in turn enables binding to myeloid CD14. CD14 aids TLR4 receptor internalisation and chaperones LPS

monomers to MD-2, an adaptor protein that complexes with TLR4. Two LPS-bound LPS/MD-2/TLR4 complexes then dimerise to form an active signalling unit[42,43].

Once activated, the TIR domain of TLR4 can be bound by TIR domain containing adaptor proteins TIRAP and TRIF, and subsequent signalling is dependent on which of these adaptor proteins is recruited. In the plasma membrane, MyD88 is recruited *via* TIRAP and recruits the serine-threonine kinase interleukin-1 receptor associated kinase 1/2 (IRAK1/2) to form the 'myddosome'[40,43,44]. From here, the E3 ubiquitin ligase TRAF6 is recruited followed by the serine/threonine kinase TAK1. Instead of MyD88, endosomal TLR4 binds to the adaptor proteins TRAM/TRIF, then RIP1 and TRAF6 before converging with the MyD88-dependent pathway with the activation of TAK1 [43]. TAK1 phosphorylates inhibitor of κB kinase β (IKKβ) at key serine residues, allowing serine phosphorylation of inhibitor of κB (IκB). IκB phosphorylation triggers its ubiquitination and subsequent degradation [45]. This action disinhibits NF-kB dimers, normally held in the cytoplasm by inhibitory IκB complexes, allowing nuclear translocation and DNA binding to occur [40]. The above signalling cascade is known as the 'canonical NF-κB pathway' (Figure 1.2).

1.3.2 NF-κB signalling in macrophages

NF-κB (Nuclear Factor κ light chain enhancer of activated B cells) was first described in 1986 [46] and has since been recognised as the central mediator of inflammatory signalling in macrophages. This transcription factor is responsible for the transcription of its many gene targets *via* binding of κB enhancer elements in response to environmental stimuli such as infection, stress and damage. The NF-κB family consists of five subunits: p65 (RelA), RelB, c-Rel, p50 (NF-κB1), and p52 (NF-κB2), which dimerise to form NF-κB complexs [47,48]. The most common dimer combination is the P65/p50 heterodimer, and exact configuration is postulated to be cell-type and environment dependent [49]. In the absence of stimuli, NF-κB is sequestered in the cytoplasm by IκB family proteins and is released only upon IκB degradation induced by signalling cascades that are initiated downstream of external stimuli sensing receptors [45]. Gene targets of NF-κB include cytokines, chemokines, antimicrobial peptides, interferon stimulated genes and amass to thousands of genes [47,49]. A vast array of different input signalling pathways lead to NF-κB activation from TLR signalling, interleukin receptor

signalling, viral-sensing STING signalling, NOD-like receptors, and signalling through B and T cell receptors. Evidence suggests that NF-κB DNA-binding and transcriptional patterns are stimulus-specific [49].

As well as the canonical signalling pathway described above in the context of TLR4 signalling, NF-κB can be activated by the non-canonical/alternative signalling pathway (Figure 1.2). Canonical signalling is triggered by a broad range of stimuli, whereas non-canonical signalling is more selectively activated by ligands including a subset of the TNF receptor superfamily and CSF-1 signalling through CSF1R [50]. In this pathway activation of NF-κB-inducing kinase (NIK) phosphorylates and activates IKKα thereby causing phosphorylation, ubiquitination, and proteasomal processing of p100 NF-κB subunits to generate mature p52 [51]. Non-canonical NF-κB signalling is slower than canonical signalling and believed to serve an auxiliary function of sorts, with a particular role in regulation of adaptive immune responses and lymphoid organ development[49,51].

In macrophages, NF-κB signalling is associated with M1 polarised cells, and production of pro-inflammatory cytokines like TNFα, IL-1β, IL-6 that are synonymous with the M1 phenotype are under the direct transcriptional control of NF-κB [47]. Although p50/p65 is the predominant NF-κB dimer in most cell types, c-REL-containing dimers are of increased importance in macrophages and are required for IL-12 p40 production [52] and discrimination between high- and low-level LPS exposure [53]. Loss of both p50 and c-Rel in mice leads to impaired innate immune response in a model of sepsis, with defective phagocytosis, bacterial killing and AMP production [54]. However, evidence suggests that c-Rel plays different roles in tissue resident *versus* monocyte derived macrophages [55].

Furthermore, NF-κB signalling dynamics are believed to differ in macrophages *versus* non-haematopoietic cells. In non-haematopoietic cell types, signalling is characterised by oscillations of NF-κB nuclear occupancy, governed by negative feedback mechanisms such as the NF-κB mediated transcription of *IκBα* [56]. In macrophages however, target gene transcription is believed to be achieved *via* sustained NF-κB nuclear occupancy in a stimulus dose-dependent manner partially attributed to positive feedback loops whereby NF-κB proteins p65 and c-Rel induce their own transcription [49].

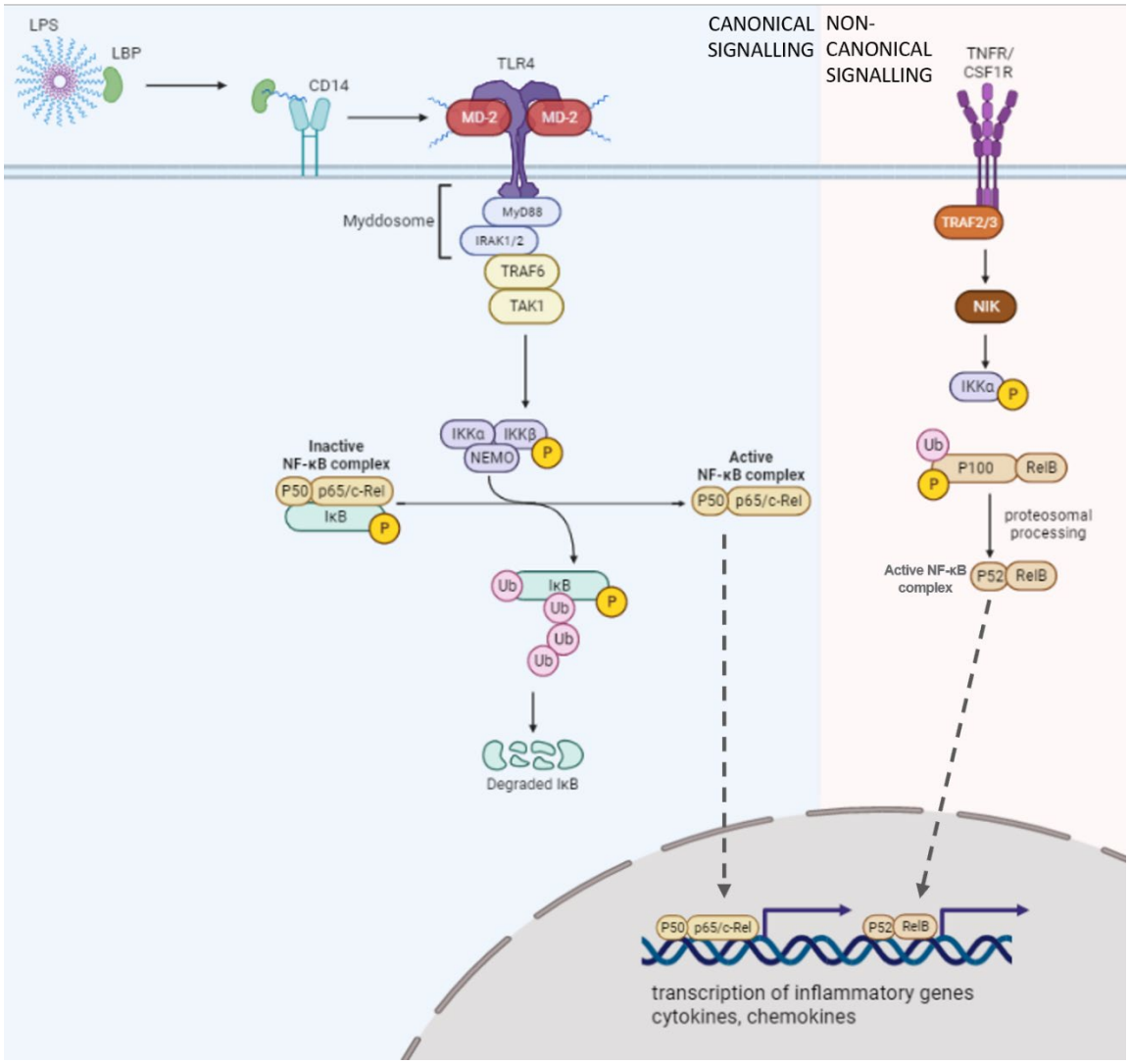


Figure 1.2: The TLR4-NF-κB signalling cascade. Pattern recognition receptors on immune cells become activated upon detecting and binding pathogen- or damage- associated molecular patterns. This interaction triggers intracellular signalling cascades that activate the canonical and non-canonical NF-κB pathways in a stimulus-dependent manner. Both canonical and non-canonical NF-κB signalling result in nuclear translocation and DNA binding of NF-κB dimers to induce transcription of immune genes such as cytokines (TNFα, IL-1β, IL-6), chemokines and their receptors (CCL2, CCL5, CCR5), adhesion molecules (ICAM-1) and pro-inflammatory mediators (iNOS).

1.3.3 AP-1 signalling in macrophages

TLR4 signalling also activates MAPK pathways *via* MyD88 [43]. Activation of the serine/threonine MAPKs ERK, p38 and JNK results in activation of the Activator Protein 1 (AP-1) transcription factor. AP-1 exists predominantly as a heterodimer of c-Jun and c-Fos subunits and controls the transcription of inflammatory genes including cytokines such as TNFα [57]. AP-1 signalling often occurs in tandem with NF-κB signalling, and the two factors share common upstream activating stimuli like inflammatory cytokines and TLR ligands. Although their activating mechanisms are distinct, the NF-κB and AP-1 pathways act cooperatively and involve crosstalk between upstream components [57]. Furthermore, AP-1 and NF-κB mediated responses are found to be enhanced when both factors are present [57], suggesting integration of the two pathways and possible mutual regulation.

1.3.4 The NLRP3 inflammasome

Closely connected to NF-κB signalling is inflammasome activation. The inflammasome is a group of multimeric protease complexes which act together as a molecular machine to ultimately result in production of the proinflammatory cytokines IL-1β and IL-18, and inflammatory cell death *via* gasdermin D-mediated pyroptosis [58,59]. Inflammasome signalling is initiated upon activation of a sensor PRR, for example NLR family pyrin domain containing 3 (NLRP3), which oligomerises and recruits the adaptor protein ASC. In the case of NLRP3 the serine/threonine kinase NEK7 is also necessary for this assembly[58]. Caspase-1 is then recruited by ASC and cleaves pro-IL-1β and pro-IL-18 to their mature forms. Gasdermin D is also cleaved by caspase-1, enabling it to insert itself into the plasma membrane and oligomerise to form a pore thereby causing cell death by pyroptosis [58].

In order for inflammasome signalling to occur, two events are required. The first is inflammasome priming 'signal 1' induced by NF-κB signalling downstream of PRR activation. NF-κB is a transcriptional regulator of *nlrp3* and *il1b* and so these genes are transcribed and translated to high levels upon NF-κB signalling [58,59]. Although all components are expressed following signal 1, inflammasome assembly and activation occurs only in the presence of a 'signal 2'. This is the signal

responsible for inflammasome sensor activation and is diverse in its nature. For example, NLRP3 has been shown to be activated by ATP, heme, pathogenic RNA, and bacterial components, but as this group is chemically dissimilar and none of these signals have been shown to directly interact with NLRP3, it has been proposed that they induce a common downstream cellular signal such as ionic flux, mitochondrial dysfunction, or lysosomal damage [58].

LPS has been shown to activate the inflammasome independently of TLR4 signalling *via* the non-canonical inflammasome pathway. This is activated though binding of LPS to caspases (4/5 in humans and 11 in mice) and induction of pyroptosis. Caspase activation also drives NLRP3 inflammasome assembly and IL-1β production [58].

1.4 Macrophage pro-inflammatory mediators

1.4.1 Tumour Necrosis Factor α

Tumour necrosis factor α (TNFα) is a cytokine that was first discovered in 1975 as a host-derived factor found in the sera of endotoxin stimulated mice, that is capable of inducing necrosis of tumour cells [60]. TNFα is primarily produced by monocytes/macrophages, however other cells such as Th1 cells, mast cells, natural killer cells, neutrophils, osteoclasts, fibroblasts are also capable of secreting TNFα at lower levels [61].

TNFα is encoded by the TNFA gene in humans and shares a locus with major histocompatibility complex (MHC) II genes [62]. The TNFA promoter contains consensus binding sites for several transcription factors, including NF-κB, allowing transcription upon a range of stimuli and cell type specific transcriptional control. TNFα is produced as a 26 kDa transmembrane protein (mTNF-α), the extracellular domain of which can be cleaved by TNFα cleaving enzyme (TACE, ADAM17) to form 17 kDa soluble TNFα (sTNFα) [63]. mTNFα and sTNFα exist in their biologically active form as homotrimers that are recognised by their cognate receptors TNFR1 and TNFR2. TNFR1, which is largely activated by sTNFα, is constitutively expressed in the majority of cell types whereas TNFR2, which has greater affinity for mTNFα, is expressed primarily by immune cells (as well as endothelial cells and cardiomyocytes [62]) in response to pro-inflammatory mediators [62,63]. Signalling through both

TNFR1 and TNFR2 can result in NF-κB and MAPK signalling pathway activation; TNFR1 through interactions with RIPK1, TRADD, and TRAF2/5 adaptor proteins, and TNFR2 through recruitment of TRAF2, TRAF1 [64]. Only TNFR1 signalling however can trigger cell death due to its death domain allowing interactions with apoptotic pathway components that also contain death domains. [63]. Functionally, TNFR1 signalling is associated with induction of inflammatory and cell death pathways, whereas TNFR2 signalling is associated with homeostatic functions such as tissue regeneration, cell proliferation and survival [64].

Produced at in large quantities immediately following inflammatory insult, the early response cytokine TNFα is a potent regulator of macrophage biology and is considered a 'master regulator' of pro-inflammatory cytokine production as well as lipid mediator signal transduction e.g. prostaglandins [65].

1.4.2 Interleukin 6

Interleukin 6 (IL-6) is a highly glycosylated protein of around 26 kDa produced by many different cell types including macrophages, DCs, T cells, B cells and endothelial cells [66]. Signalling of IL-6 is initiated upon its binding to two transmembrane proteins mIL-6Rα and gp130, which are expressed by a variety of immune cell types as well as hepatocytes [67]. This mechanism is described as classic IL-6 signalling however mIL-6Rα can be cleaved to form a soluble receptor (sIL-6Rα) which is also capable of binding IL-6, complexing with gp130, and inducing IL-6 signalling pathways [68]. This mechanism, termed trans-signalling, allows IL-6 to act on a broad range of cell types including those which do not typically express mIL-6Rα [67,68]. Intracellular pathways activated by IL-6 include JAK/STAT signalling, MAPK/AP-1, and NF-κB , which induce diverse and cell type dependent biological functions [69]. In hepatocytes, IL-6 promotes production of acute-phase proteins such as C-reactive protein (CRP), serum amyloid A, and fibrinogen [69]. In T cells, IL-6 signalling promotes Th17 differentiation through STAT3 activation and inhibits T_{reg} differentiation [68]. Trans-signalling of IL-6 in endothelial cells induces upregulation of adhesion molecules ICAM-1 and VCAM-1 thereby promoting leukocyte transmigration [70,71].

IL-6 also has anti-inflammatory properties that are not fully understood. In a mouse model of endotoxaemia, administration of LPS to IL6$^{-/-}$ mice results in significantly increased TNFα and IL-1β production than that in mice with IL-6 [72]. Additionally, Mauer *et al.* showed that loss of IL-6 signalling through myeloid specific IL-6Rα ablation resulted in increased metabolic dysfunction in an obese mouse model and that IL-6 signalling primes adipose tissue macrophages to an anti-inflammatory, insulin-sensitivity protective M2 phenotype though an IL-4 dependent mechanism [73].

1.4.3 Interleukin 1β

IL-1α/IL-1β are IL-1 family cytokines that signal through a common receptor, IL-1R and therefore exert the same biological functions [74]. However, these two cytokines are differentiated by the fact that they are produced by distinct cell types, with myeloid cells primarily producing IL-1β [75]. Production of biologically active mature IL-1β requires inflammasome activation and caspase-1 mediated cleavage [58]. Two forms of IL-1R exist, functional IL-1R and IL-R2, which is not capable of inducing downstream signalling and acts as a decoy receptor. Different cell types express different ratios of these two receptors, with immune cell types like neutrophils expressing relatively high levels of IL-1R2 and therefore requiring high levels of IL-1 for activation [74]. IL-1R1 signalling induces intracellular signalling pathways such as p38, MAPK, and NF-κB to promote transcription of pro-inflammatory genes [75]. Additionally, IL-1β signalling can promote Th1 and Th17 differentiation and B cell proliferation [74].

1.4.4 Nitric Oxide

Nitric oxide (NO) is a soluble gas mediator produced by the enzyme inducible NO synthase (iNOS) in macrophages upon inflammatory signalling. NO also has important homeostatic roles in neurons and in endothelial cells where it is produced at low levels by constitutively expressed neuronal- amd endothelial- NO synthase respectively (nNOS/eNOS) and mediates essential functions such as vascular tone [76]. Additionally, NO has several pro-inflammatory functions including causing cytotoxicity to pathogens [77], suppression of lymphocyte apoptosis [76,78], and regulating macrophage metabolism [76]. Macrophage production of NO is associated with M1 polarised macrophages, whereas M2 macrophages preferentially metabolise arginine to ornithine [79].

1.5 Tyrosine kinases in inflammatory signalling

The phosphorylation and dephosphorylation of proteins is central to almost all cellular signalling cascades and is one of the most common post-translational modifications. Kinases are responsible for phosphorylation, the addition of a phosphate group (PO_4) to polar R group of an amino acid typically on serine, threonine, or tyrosine residues. Protein phosphorylation can have diverse and context-specific implications such as protein activation, deactivation or degradation. In the inflammatory signalling pathways described above, a particularly important role is played by serine/threonine kinases; IRAK, TAK1, IKKα/β in NF-κB signalling, MAPKs in AP-1 signalling, and NEK7 in NLRP3 inflammasome signalling. However, tyrosine kinases also make a significant contribution to inflammatory signalling and, importantly, can be pharmacologically targeted with the use of tyrosine kinase inhibitors (TKIs). The following section will discuss key tyrosine kinases involved in inflammatory pathways.

1.5.1 Src family kinases

The Src kinases are a family of nine structurally similar non-receptor tyrosine kinases: SRC, LCK, LYN, BLK, HCK, FYN, FGR, YES, and YRK. Src kinases are implicated in many signalling pathways including cellular proliferation, survival, migration and angiogenesis which drive oncogenesis [80]. This, coupled with the fact that Src is frequently overexpressed in human malignancies, has made it a popular therapeutic target in cancer, with tyrosine kinase inhibitors (TKIs) such as dasatinib, saracatinib, and bosutinib being developed against Src [80]. Src kinases are also involved in many immune signalling pathways, with different family members having cell-specific expression and function; Lck is involved in TCR signalling in T lymphocytes, Blk and Lyn are involved in B lymphocyte function [80], and in neutrophils Src has been shown to mediate migration towards the chemoattractant fMLP [81]

In macrophages, Src family kinases have been reported to play a role in signalling downstream of TLRs. Both TLR3 which senses dsRNA, and TLR9 which senses non-methylated CpG are phosphorylated by Src [44,82]. Downstream of TLR2 signalling, Src has been shown to activate NF-κB *via* platelet derived growth factor receptor (PDGFR) signalling [83], and in synovial fibroblasts it

induces IL-6 production *via* NF-κB activation [84]. Furthermore, Src has been shown to interact with TLR4 *via* CD14 [44]. Phosphorylation of TLR4 itself has been shown to be essential for downstream signalling through experiments using phospho-null TLR4 mutants. However, the kinase responsible for TLR4 phosphorylation remains unclear [44]. Src as well as other myeloid-expressed Src family members Lyn, Hck and Fgr are induced downstream of LPS stimulation [85,86]. Triple *Lyn*$^{-/-}$*Hck*$^{-/-}$*Fgr*$^{-/-}$ knockout mice however, have no defects in their response to LPS indicating that these genes are dispensable for LPS signalling [85]. Pharmacological inhibition of Src on the other hand has been shown to supress NF-κB activation [87], reduce TNFα and NO production [86] and reduce phagocytosis [88] in macrophages *in vitro* in response to LPS stimulation.

1.5.2 Bruton's Tyrosine Kinase

Bruton's Tyrosine Kinase (BTK) has been well documented for it's critical role in B cell development and survival through BCR and subsequent NF-κB signalling [89]. BTK has a fairly restricted expression pattern and is highly expressed only in B cells and myeloid cells [90]. In myeloid cells, BTK has been shown to interact with TLRs and their adaptor molecules including MyD88, promoting induction of NF-κB and inflammatory gene transcription [91]. Loss of function mutations in the *Btk* gene cause the immunodeficiency x-linked agammaglobulinaemia (XLA), and patients with this condition display dysregulated TLR signalling [91]. Due to its importance in B cell survival and critical role in driving B cell malignancies, BTK inhibitors such as ibrutinib, acalabrutinib and others have been developed to specifically target BTK. Use BTK inhibitors in inflammatory models have shown anti-inflammatory benefits. For instance, previous work in the Greaves lab has shown that inhibition of BTK reduces neutrophil and monocyte recruitment and cytokine production in a model of zymosan-induced peritonitis (ZIP), and attributed this effect to inhibition of NF-κB [92]. Similarly, loss of BTK has been shown to have role in macrophage and neutrophil phagocytosis [91,93]. Additionally, BTK directly interacts with NLRP3 and ASC and is required for IL-1β release from murine macrophages [94,95], and BTK inhibitor treatment shows benefit in models of ischemic stroke [94], sepsis induced cardiac failure [96], and obesity [97] due to inflammasome targeting.

1.5.3 Colony Stimulating Factor-1 Receptor

CSF-1 (also known as M-CSF) is an essential regulator of macrophage development and homeostasis. The key role that this growth factor plays in myeloid development can be demonstrated by the fact that purified CSF-1 is sufficient to promote macrophage differentiation from bone marrow progenitors *in vitro* [10]. The receptor for CSF-1, which is shared with IL-34, is the Type III Receptor Tyrosine Kinase (RTK) family member CSF-1R (also known as CD115 and c-fms). CSF-1 binding triggers CSF-1R dimerization and phosphorylation and induces diverse intracellular pathways. For macrophage survival and proliferation the PI3K and Akt signalling pathways are important [10], whereas induction of the myeloid transcription factor PU.1 is important in macrophage differentiation [13]. CSF-1 also acts as chemoattractant and induces macrophage chemotaxis through CSF-1R and activation of Rho and Rac pathways, thereby promoting cell migration through actin polymerisation [13].

In terms of mediating macrophage effector functions, a clear role for CSF-1R signalling is not well defined. Microarray data suggests that CSF-1R signalling promotes an M2-like phenotype away from antigen presentation towards an immunosuppressive role [10]. Additionally, CSF-1 is thought to promote macrophage phagocytosis, extracellular proteolysis and tissue repair [10]. Irvine *et al.,* reported that application of a CSF-1R targeted TKI reduces pro-inflammatory cytokine production in LPS stimulated murine bone marrow derived macrophages (BMDMs) [98], suggesting a more typical M1-like role for CSF-1R signalling. Interestingly, in humans but not in mice, continuous CSF-1 exposure is pro-atherogenic [10], with CSF-1 being found in human atherosclerotic lesions and CSF-1 differentiated macrophages having increased LDL uptake, promoting foam cell phenotype [99].

1.5.4 Tyro3, Axl, Mer (TAM) kinase family

TAM is a family of receptor tyrosine kinases consisting of the members Tyro3, Axl, and Mer, with Mer being the family member predominantly expressed by macrophages [100]. An immune role for TAM family kinases was discovered when Mer^{KD} mice with inactive Mer kinase were found to display hypersensitivity to LPS due to immune hyperactivation and enhanced pro-inflammatory mediator production due to excessive NF-κB activation [101]. Subsequently triple TAM knockout mice

were found to have hyper lymphoproliferation and autoimmunity due to impaired clearance by TAM-expressing macrophages and DCs during lymphopoiesis [102]. The key role of TAMs is to mediate efferocytosis though the recognition of phosphatidyl serine (PS), a phospholipid normally found only on the inner leaflet of cell membranes that becomes exposed due to loss of membrane asymmetry during apoptosis [26]. PS can be recognised by TAM receptor bridging molecule ligands Gas6 and Protein S, and activation of TAM receptors through these ligands induces phagocyte-apoptotic cell tethering to allow subsequent phagocytosis.

A key feature of efferocytosis is that it is innately anti-inflammatory, as it induces pro-resolution pathway signalling and promotion of tissue homeostasis [36]. TAM receptors themselves are immunomodulatory and act to limit the magnitude of an inflammatory response. For instance, TAM expression is induced by TLR signalling and TAM signalling upon Gas6 stimulation inhibits NF-κB activity in a negative feedback mechanism [100]. Similarly, protein S is upregulated by macrophages in the resolution phase in a ZIP model, and loss of Protein S/TAM signalling increases production of TNFα, CCL3, IL-6 and reduces pro-resolution IL-10 production and efferocytosis [103]. Although macrophages express both Mer and Axl (little is known about Tyro3 function), distinct roles have been proposed for the two receptors. Whereas Mer is induced by anti-inflammatory stimuli such as dexamethasone in BMDMs, Axl expression is inhibited [104]. Axl is instead upregulated by inflammatory stimuli like LPS, Poly(I:C), and IFNα [104,105] suggesting that Axl and Mer are responsible for apoptotic cell clearance in inflammatory and homeostatic environments respectively [104].

In the context of cardiovascular disease, loss of MerTK signalling through receptor cleavage or mutation promotes plaque necrosis *via* impaired efferocytosis in atherosclerotic lesions [106,107] whereas Axl signalling in cardiac macrophages promotes IL-1β secretion and impairs cardiac function post myocardial infarction [108], presenting a possible therapeutic target.

1.6 Macrophage driven inflammatory diseases

1.6.1 Sepsis

Sepsis continues to be a major global health burden with an estimated 31.5 million cases and 5.3 million deaths annually [109,110]. Sepsis is defined as a life-threatening condition of organ dysfunction caused by dysregulated host immune responses to infection [109], and symptoms of severe sepsis include hypotension and hypoperfusion resulting in organ dysfunction and acute respiratory distress syndrome (ARDS). Septic shock is a severe form of sepsis associated with increased risk of mortality due to underlying circulatory, cellular and metabolic dysfunction [109]. The term septicaaemia has previously been used to describe sepsis, but is now generally considered outdated as presence of infection in the blood is not necessarily detected in sepsis patients [109].

The excessive host response in sepsis is primarily mediated by activation of the innate immune system upon simultaneous recognition of both PAMPs and DAMPs [109]. Activation of pathways such as TLR signalling, MAPKs, JAK/STAT signalling, NF-κB, and interferon regulatory factors in macrophages leads to high levels of cytokine production and 'cytokine storm' initiation [109]. Cytokines, primarily produced by macrophages, are key orchestrators of innate immune responses in sepsis with TNFα and IL-1β being the major drivers of pathology [110]. Other important cytokines in sepsis include pro-inflammatory IL-8, IL-12, IFNγ, IL-6 which has dual pro- and anti-inflammatory properties, and the anti-inflammatory cytokine IL-10 [110].

Complement activation is also central to the pathogenesis of sepsis. Rapid production of complement peptides such as C5a and C3a upon PAMP/DAMP recognition triggers monocyte and neutrophil chemotaxis, production of reactive oxygen species (ROS) and granular enzyme release in neutrophils, and cytokine production in macrophages [110]. These processes contribute to immune response amplification, cause tissue damage and help to sustain a hyper-coagulative state seen in sepsis [109].

Somewhat paradoxically, sepsis is also associated with immunosuppression at both early and late stages of disease. In early disease, attenuation of the adaptive immune response is seen in sepsis in

the form of lymphopenia with increased T and B cell apoptosis[109]. Additionally, innate responses are also impaired due to immature neutrophil phenotype, loss of monocyte inflammatory cytokine production, increased circulating myeloid derived suppressor cell (MDSC) populations, and M2-skewed macrophage polarisation [109]. These processes occur simultaneously with pro-inflammatory pathways and therefore this complex pathology has made targeting sepsis with anti-inflammatory drugs, such as TNFα or IL-1β inhibiting therapies, particularly challenging and of limited success [109,110].

1.6.2 Atherosclerosis

Atherosclerosis is a pathology of medium and large vessel walls that underpins cardiovascular disease such as chronic heart failure (CHF) and myocardial infarction (MI), which collectively remain the leading cause of death worldwide. A link between inflammation and atherosclerosis has been long recognised, with increased incidence of CVD in patients with inflammatory conditions such as rheumatoid arthritis [111]. More solid evidence was gathered in the 1990s when a correlation between high C-reactive protein (CRP) levels and cardiovascular disease (CVD) was identified, and HLA was identified in human plaques [112,113]. Today, substantial experimental evidence suggests that inflammation is a driver of atherogenesis [59,114–118].

Monocytes and macrophages are central to the pathogenic process of atherosclerosis from early plaques to advanced lesions[118]. Early atherosclerotic lesions are formed upon CCR2/CCR5/CX3CR1 dependent recruitment of classical $Ly6c^{hi}$ (murine) or $CD14^{hi}CD16+$ (human) monocytes to activated endothelium characterised by overexpression of adhesion molecules such as VCAM-1 and ICAM-1 that occurs in hypercholesterolaemia [5,119]. Recruited monocytes transmigrate through the endothelium to the intima where they differentiate into macrophages that can locally proliferate to accelerate plaque growth. In early lesions, plaque macrophages are generally derived from recruited monocytes, whereas in more advanced plaques local proliferation of lesional macrophages becomes the predominant source of macrophage replenishment [115]. Other immune cells including B cells, T cells (mostly Th1 subtype), neutrophils, NK cells and mast cells are also present within atherosclerotic lesion and have been shown to also contribute to atherogenesis [114]. Single cell

techniques have revealed plaque macrophages to be phenotypically diverse [115], however M1-like plaque macrophages with NF-κB driven production of pro-inflammatory cytokines such as IL-1β, TNFα, as well as expression of matrix metalloproteases are predominant in unstable lesions[114,120] (Table 1.2). These M1-like macrophages also produce chemokines and promote activation of the endothelium to perpetuate blood monocyte plaque recruitment [119], and crosstalk with vascular smooth muscle cells to maintain a pro-inflammatory environment [120]. IL-6 production is also associated with M1 macrophages. Interestingly however studies of IL-6 signalling in atherosclerosis development have yielded conflicting results [121–123]. On the other hand, M2-like plaque macrophages that produce IL-10 and TGFβ and carry out functions such as efferocytosis and collagen deposition are associated with increased plaque stability and plaque regression [114,120,124] (Table 1.2)

Accumulation of lipid-laden foam cells is a hallmark of atherosclerotic lesions and are formed upon sustained oxidised low density lipoprotein (oxLDL) uptake by intimal macrophages over time *via* scavenger receptors such as CD36 [120]. Foam cells, which can alternatively be of vascular smooth muscle cell origin [120], have pro-atherogenic properties such as release of matrix metalloproteases which can degrade the plaque fibrous cap and promote plaque instability [124].

A feature of advanced, rupture prone-plaques is the presence of a necrotic core — a region of dead foam cells within the centre of the atherosclerotic plaque [26] (Figure 1.3). Necrotic core formation is due in part to defective efferocytosis by plaque phagocytes, resulting in reduced apoptotic cell clearance and secondary necrosis [26,125]. The mechanisms by which efferocytosis becomes ineffective in atherosclerosis are not clear, however, it is hypothesised to be the result of reduced apoptotic cell recognition or clearance ability by phagocytes, rather than overwhelming rates of apoptosis [26]. Studies by Tabas and colleagues have revealed that Mer tyrosine kinase of the TAM family of phagocytic receptors may play a role in atherogenesis as atheroprone *Apoe*$^{-/-}$ mice with kinase-null Mer exhibit increased plaque necrosis and reduced efferocytosis, despite no difference in plaque area [107]. Another proposed mechanism of impaired efferocytosis in atherosclerosis is by upregulation of CD47 in atherosclerosis [126]. In healthy state, CD47 is rapidly downregulated during apoptosis to abolish the balance of "don't eat me" with "eat me" signals to allow recognition by efferocytes. In

atherosclerosis however, this expression reduction is inhibited *via* NF-κB dependent TNFα signalling, thereby inhibiting apoptotic cell recognition [26,126].

Table 1.2: Role of cytokines in atherosclerosis. Table adapted from Fatkhullina *et al.,* 2016 [127]

Cytokine	Source	Role in atherosclerosis
TNFα	M1 macrophages	Pro-atherogenic
	Th1 cells	Induces upregulation of adhesion molecules ICAM-1, VCAM-1 [128]
		Promotes monocyte plaque recruitment through induction of CCL2 [128]
		Promotes monocyte activation and scavenger receptor upregulation [129]
IFNγ	Th1 cells	Pro-atherogenic
	$CD8^+$ T cells	Induces upregulation of macrophage scavenger receptor SR-A to promote oxLDL uptake [130]
IL-6	M1 macrophages	Dual pro- and anti-atherogenic properties [121–123]
	Endothelial cells	
IL-12	Macrophages	Pro-atherogenic [131]
	Dendritic cells	
IL-1β	M1 macrophages	Pro-atherogenic
		Regulates endothelial cell activation [132]
IL-10	T_{reg} cells	Anti-atherogenic
	M2 macrophages	Supresses Th1 and macrophage activation [133,134]
TGFβ	Epithelial cells	Anti-atherogenic
	Endothelial cells	Promotes T_{reg} differentiation
	M2 macrophages	Promotes fibrosis and plaque stability [135,136]

Another feature of advanced atherosclerotic lesions is a fibrous cap made up of collagenous extracellular matrix that overlies the plaque. Upon thinning of this cap, breaches can be formed which expose blood to thrombogenic material within the plaque. This can cause acute occlusive thrombosis and tissue infarction [114].

Experimental evidence suggests that NF-κB signalling contributes to atherogenesis, both in macrophages and in other cell types. For example, phosphorylated NF-κB has been reported in human atherosclerotic plaques [137], and is induced in C57Bl/6 mice fed an atherogenic diet [138]. Similarly, patients with familial hypercholesterolaemia (caused by genetic mutations in LDLR or other genes) have increased NF-κB activation in circulating monocytes [139]. In early atherosclerotic lesions, NF-κB promotes monocyte plaque recruitment by regulating transcription of CCL2, ICAM-1, VCAM-1[140–142] , and upregulates enzymes involved in LDL oxidation [143]. In advanced lesions, NF-κB drives the inflammatory phenotype of lesional macophages.

In addition to the inflammatory processes discussed above, an intrinsic aspect of atherogenesis is dysregulated lipid processing leading to hyperlipidaaemia and hypercholesterolaemia. Apolipoprotein B-containing lipoproteins, such as low density lipoprotein (LDL) enter the subendothelial space of vulnerable vessel walls such as areas with low shear stress due to haemodynamic forces (e.g. vessel branchpoints)[115]. Here, lipoproteins can undergo modifications such as oxidisation (oxLDL) or acetylation (acLDL) and are recognised by innate immune cells such as macrophages through scavenger receptors (e.g. CD36) and TLRs (e.g. oxLDL and TLR4) thereby driving the inflammatory response [116,118].

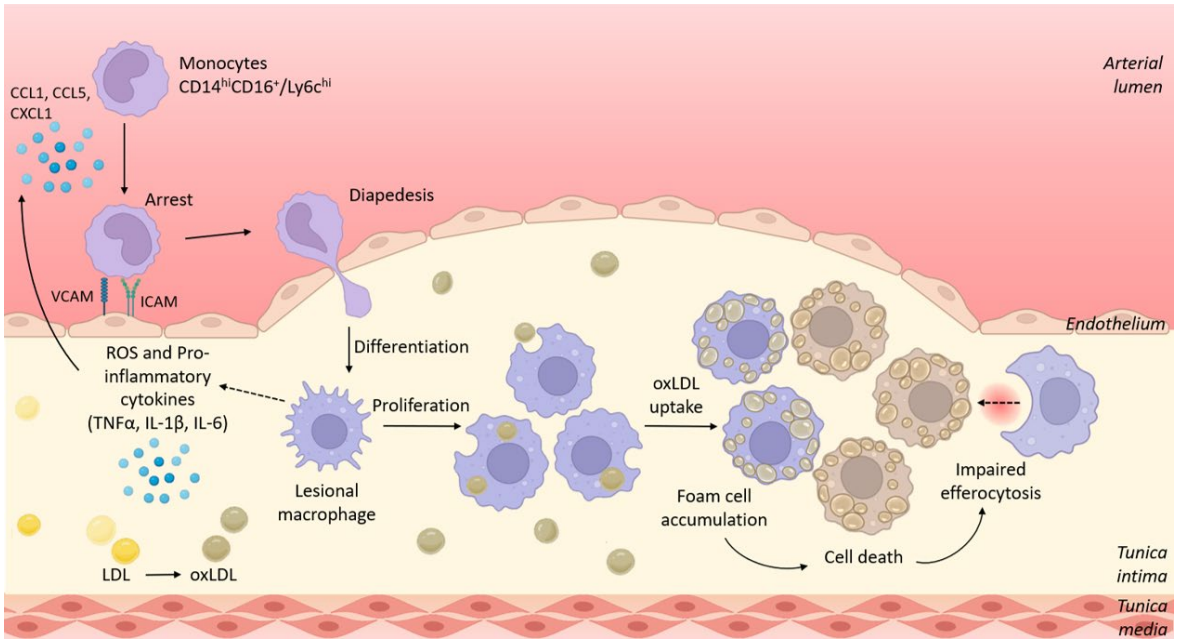


Figure 1.3 Contribution of myeloid cells to atherosclerotic plaque formation. Monocytes are recruited to atherosclerotic lesions and adhere to activated endothelium expressing adhesion molecules ICAM-1 and VCAM-1. Within the tunica intima, plaque macrophages are characterised by production of inflammatory cytokines and ROS. Endocytosis of oxLDL by lesional macrophages results in lipid-laden foam cell formation. Continued proliferation and apoptosis of foam cells coupled with impaired clearance by efferocytosis leads to necrotic core formation and plaque growth. Figure adapted from Chaffey, Roberti and Greaves, 2022 [144]

1.7 Anti-inflammatory medicines

1.7.1 Glucocorticoids

Glucocorticoids such as cortisone and hydrocortisone are cholesterol derived endogenous steroid hormones that are synthesised mainly in the cortex of the adrenal glands. Glucocorticoid release into the bloodstream is regulated by the hypothalamic-pituitary-adrenal (HPA) axis in a circadian manner and is increased in response to physiological stress [145]. The biological effects of glucocorticoids are initiated upon binding to the glucocorticoid receptor (GR). GR is a nuclear receptor transcription factor that is ubiquitously expressed in many cell types and induces transcription of GR response genes through promoter binding. Despite expression in almost all cell types, outcomes of GR signalling are context dependent and cell-type specific due to plasticity in expression of regulating proteins, differing GR isoforms, and post translational modifications [145,146]. For example, GR signalling induces apoptosis in developing thymocytes, whereas its signalling in macrophages promotes anti-inflammatory signalling and M2 polarisation [146]. In inflammation biology, genes known to be inhibited by GR include TNFα, IL-6, IL-4, GM-CSF, CCL1, CCL5 [147].

GR and NF-κB signalling can be considered to generally have mutually antagonistic effects in inflammation and there is a considerable deal of cross-talk between the two pathways. For instance, GR increases binding affinity of NF-κB to IκB [148], and is able to interact with NF-κB subunits p65 and p50 to preclude nuclear translocation, thereby inhibiting NF-κB activation [149,150]. At the transcriptional level, the GR and NF-κB display transrepression, the repression of inflammatory NF-κB gene targets by GR, and transactivation , activation of NF-κB inhibiting genes by GR.

The therapeutic potential of glucocorticoids was first recognised in a seminal study by Hench *et al.* in 1949 when it was reported that a hormone isolated from adrenal cortex extracts, later to be known as cortisol, had potent anti-inflammatory effects in rheumatoid arthritis patients [151]. Today, several synthetic glucocorticoids are routinely used in medicine due to their immunosuppressive and anti-inflammatory effects in diseases such as rheumatoid arthritis, lupus erythematosus, inflammatory bowel disease and asthma [147]. Common synthetic glucocorticoid drugs including dexamethasone,

prednisone, and methylprednisolone share chemical similarity, all modelled on the structure of the cortisone backbone [147].

Despite being widely prescribed, glucocorticoids cause frequent adverse effects such as fluid retention, weight gain, infection, and hyperglycaaemia, and long term use can lead to osteoporosis, insulin resistance, hypertension [147]. These adverse effects are partially due to the pleiotropic nature of GR signalling. Additionally, some patients do not respond to glucocorticoid therapy, either due to genetic mutations in GR signalling relevant genes, or due to downregulation of GR induced by chronic glucocorticoid therapy [145]. Therefore, dosing and prescribing of glucocorticoids requires careful regulation.

1.7.2 NSAIDs

Non-steroidal anti-inflammatory drugs (NSAIDs) are a class of commonly used drugs that target the arachidonic acid pathway [152]. Although effective in a broad range of pharmacological settings, NSAIDs are typically used for their anti-inflammatory activity. The biological target of NSAIDs is cyclooxygenases (COX), the enzymes that catalyse the synthesis of prostaglandins, prostacyclins and thromboxanes (collectively referred to as prostanoids) from arachidonic acid [153].

Two isoforms of COX exist and largely carry out different biological roles, although some functional overlap is being uncovered [154]. COX-1 is constitutively expressed throughout the body and has homeostatic and tissue-specific roles such as platelet aggregation, kidney function, and haematopoiesis. COX-2 is induced in response to inflammatory stimuli, for example by NF-κB activity, hormone signalling, and growth factors, and has important roles in pain, nociception and fever. In macrophages, inflammatory signalling triggers COX-2 mediated synthesis of prostaglandin E2 (PGE_2) which in turn induces production of IL-6 [155]. PGE_2 has various pro-inflammatory roles beyond macrophages, including promoting arterial dilation and microvascular permeability and pain sensation in peripheral sensory neurons [154].

Through suppression of prostanoid synthesis, NSAIDs are effective anti-inflammatory drugs and are widely used to inhibit inflammation and associated pain. NSAIDs as a class of drug contains several

members, including aspirin and ibuprofen. Specific NSAIDs such as celecoxib have been developed to selectively inhibit COX-2 over COX-1, thereby supressing inflammatory effects of COX-2 but allowing continued homeostatic functions of COX-1 [152].

In addition to its contribution to pro-inflammatory processes, immunomodulatory and anti-inflammatory roles for COX-2 activity and specifically for PGE_2 have more recently been recognised. PGE_2 has been found to inhibit T cell proliferation, and mice lacking both COX-1 and COX-2 display exaggerated inflammatory responses in the lung [35]. Additionally, PGE_2 signalling through EP2/4 receptors has been found to inhibit production of TNFα and IL-6 in LPS challenged mice [156] and to polarise macrophages towards an M2 phenotype [157]. This demonstrates a more complex profile for prostanoid signalling than previously appreciated and therefore broad inhibition *via* COX inhibitors may not be desirable in all contexts. Furthermore, serious adverse effects such as gastrointestinal injury are associated with NSAID use, largely due to inhibition of COX-1 function in maintaining gastric mucosal protection [152], making their use in inflammatory bowel disease particularly challenging .

1.7.3 DMARDs

Disease-modifying antirheumatic drug (DMARD) describes a chemically diverse class of drugs used for the treatment of rheumatoid arthritis, psoriatic arthritis and ankylosing spondylitis, as well as other inflammation-driven conditions. Conventional DMARDs including methotrexate, hydroxychloroquine and sulfasalazine typically have varied mechanisms of action that cause broad spectrum immunomodulation and immunosuppression. Biologic DMARDs on the other hand are targeted antibody therapeutics that act on specific molecular targets such as cytokines or cell-specific antigens. Examples include adalimumab, infliximab and etanercept (anti-TNFα), tocilizumab (anti-IL-6), and rituximab (anti-CD20 B cell targeted)[158].

Similar adverse effect profiles are associated with conventional DMARDs and include gastrointestinal injury, hepatotoxicity, and increased risk of infection. Additionally, specific effects are associated with specific DMARDs, such as methotrexate and folic acid deficiency [158]. Due to their more targeted mechanism of action, biologic DMARDs are associated with fewer side effects,

although risk of infection is still a serious concern and some patients fail to respond to treatment. Another major limitation of biologic DMARDs is their high cost, particularly for the treatment of chronic inflammatory conditions [159]. The use of DMARDs to treat inflammation in cardiovascular disease is discussed in greater detail in the introduction to Chapter 5.

1.7.4 Limitations of current anti-inflammatory medicines

The drugs described above have been used as effective anti-inflammatory agents in many inflammatory conditions and have been widely prescribed for decades despite the aforementioned drawbacks associated with each. Since the introduction of these drugs however, little progress has been made towards successfully developing novel anti-inflammatory drugs, despite extensive research efforts.

Promising pre-clinical studies have investigated novel drugs target such as chemokines, JAK/STAT signalling, cannabinoid signalling and TRPV1/2 ion channels, with some of these progressing to clinical studies [159]. Similarly, drug repurposing strategies have yielded success in pre-clinical and clinical studies, and these are discussed in greater detail in Chapter 3.

One explanation for the lack of success in anti-inflammatory drug development is a large translational gap between pre-clinical animal models and humans. This was demonstrated in a 2013 systematic review comparing genomic signatures of inflammatory responses in patient cohorts and animal models of acute inflammation. The authors found that while there was high correlation between gene expression responses in human burn and trauma patients, these responses correlated poorly with corresponding mouse models [160].

Overall, one of the most significant challenges with targeting inflammation in human disease is the fact that the very same mechanisms that are pathogenic in the context of inflammatory disease play a vital role in host protection from infection and initiation of tissue repair. Hence a delicate balance must be struck between these two extremes (Figure 1.1). This should be considered in the development of novel anti-inflammatory medicines and increasingly the research focus has shifted to pro-resolution or pro-tissue repair strategies such as SPMs [38].

1.8 Original hypothesis and aims of this thesis

Inflammation is a driver of acute and chronic human diseases such as sepsis and chronic cardiovascular disease. Macrophages play a key role in pathological and homeostatic inflammatory processes though the production of inflammatory mediators. In addition, macrophages display a high degree of phenotypic plasticity, with different polarisation phenotypes being associated with inflammatory processes such as bacterial killing, or tissue repair processes. This versatility makes macrophages an attractive cell target in inflammatory disease.

NF-κB is the master regulator of pro-inflammatory programming in macrophages and its activation induces transcription of cytokines, chemokines, adhesion molecules. NF-κB dysregulation is observed in many inflammatory pathologies such as atherosclerosis and contributes to disease progression. NF-κB is therefore a logical molecular target for novel anti-inflammatory medicines.

Drug repurposing is a pragmatic approach to drug discovery has been used previously to identify novel activity of existing drugs. The original hypothesis of this thesis is that there are existing medicines with NF-κB inhibiting activity that is yet to be uncovered, and that any such medicines would be potential drug repurposing candidates for inflammatory disease.

Building on this hypothesis, the aims of this thesis are:

1) Screen existing medicines for novel NF-κB inhibitory activity in macrophages to identify potential drug repurposing candidates, and characterise these the anti-inflammatory effects of these drugs *in vitro*
2) Explore anti-inflammatory activity of drug repurposing candidates in acute inflammation *in vivo*
3) Investigate effects of drug repurposing candidates in a mouse model of chronic cardiovascular inflammation *in vivo*
4) Determine the feasibility of repurposing existing drugs as anti-inflammatory medicines

Chapter 2: Materials and Methods

2.1 Reagents

All reagents were purchased from Merck unless otherwise stated. TOCRIScreen library of 159 FDA-approved medicines, Sunitinib malate, and Bosutinib were all purchased from Tocris. IKK-16 and T-5224 were purchased from Selleckchem. Dulbecco's Modified Eagle Media (DMEM), RPMI 1640, penicillin plus streptomycin (P/S) and ACK lysis buffer were purchased from Gibco. Fluorophore-conjugated antibodies for flow cytometry and unconjugated CD16/32 antibody were bought from BioLegend. p65-PE and all western blot antibodies were purchased from Cell Signalling Technologies. UltraComp eBeads™ and pHrodo-red labelled *E. coli* bioparticles were bought from InVitrogen. RAW-Blue™ cells, Quanti-Blue™ solution and Zeocin™ were purchased from InvivoGen. LPS used *in vitro* was from *E.coli* serotype O111:B4. LPS used *in vivo* was from *E.coli* serotype O127:B8. Cell Titer Glo and Griess assay kits were purchased from Promega. ELISA DuoSet kits were purchased from R&D Systems. Western blotting subcellular fractionation kit, Pierce BCA assay kit, NuPage gels, and nitrocellulose/PVDF membranes were purchased from ThermoFisher Scientific.

2.2 Animal experiments

2.2.1 Ethical statement

All animal experiments were conducted in accordance to the Animal Scientific Procedures Act 1986, with procedures reviewed by the Sir William Dunn School of Pathology ethical review body (AWERB) and conducted under project license P144E44F2 at the University of Oxford. I hold a personal licence (PIL) I73241866 and have been authorised to perform Schedule 1 procedures. All animal experiments were designed and performed in adherence with the guidelines from the National Centre for the Replacement Refinement & Reduction of Animal Research (NC3Rs). Group sizes were chosen by performing power calculations with previous data from the Greaves lab (Endotoxaemia experiments) or pilot data ($Ldlr^{-/-}$ high fat diet) to achieve 80% power.

2.2.2 Mouse strains and husbandry

C57Bl/6 mice were bred locally (to harvest bone marrow for experiments in Chapter 3) in the Pathology Support Building at the University of Oxford, or bought from Charles River (endotoxaemia experiments in Chapter 4). The *Ldlr*$^{-/-}$ mouse colony was maintained by breeding homozygous males and females in the Pathology Support Building at the University of Oxford. Animals were housed in individually ventilated cages (between 2 and 10 mice per cage) in specific pathogen free conditions. All animals were provided with standard chow and water *ad libitum* and, maintained on a 12 h light: 12 h dark cycle at controlled temperature (20–22°C) and humidity.

2.2.3 Endotoxaemia

Endotoxaemia experiments were performed in batches of 8-10 mice at a time, with at least two batches per experimental time point. 8-10 week old male C57Bl/6 mice (n=98) were assigned into groups to receive either vehicle (5%DMSO, 30% PEG300, 65% dH_2O), sunitinib (30mg kg^{-1}), or IKK-16 (10mg kg^{-1}). Mice were weighed prior to dosing and group assignment, with individual mice being assigned to groups so as to minimise differences between groups. The appropriate substance (vehicle, 30mg kg^{-1} sunitinib, or 10mg kg^{-1} IKK-16) was administered in a body-weight adjusted volume from a 100X stock solution (i.e. 250µL for a 25g mouse) by oral gavage at T= -24 and T= -4 hours. At T=0, mice were intraperitoneally injected with LPS (10mg kg^{-1}) or sterile Phosphate Buffered Saline (PBS). For each experimental timepoint, vials of LPS were pooled prior to use to minimise experimental batch-batch variation. Mice were sacrificed at T=1, 6 or 24 hours and tissues were harvested for collection. Peritoneal exudate cells (PECs) were harvested by injecting 7mL ice cold PBS containing 5mM ethylenediaminetetraacetic acid (EDTA) into the peritoneal cavity. Cells were dissociated from tissues by rubbing a needle across the surface of the peritoneum and fluid was then retrieved and placed onto ice. Blood was harvested from the inferior vena cava and divided into anticoagulant tubes containing EDTA powder (Teklab) for flow cytometry, and collection tubes containing clot activating gel (Sarstedtstr) for processing serum. Mice were then perfused with 12mL ice cold PBS through the left ventricle. Liver was harvested by collecting half of the same lobe from each mouse and snap freezing for western blot and mRNA analysis by storing on dry ice before long

term storage at -80°C. Small sections of lung, liver and kidney were placed into PBS containing 4% paraformaldehyde (PFA) for histology.

2.2.4 Hypercholesterolaemia

Hypercholesterolaemia experiments were performed in three experimental cohorts of 6-12 mice at a time. Male *Ldlr*$^{-/-}$ mice aged between 7 and 9 weeks were fed a Paigen diet containing 15% Cocoa butter, 1.25% cholesterol (cat E15106-3470; Ssniff) with *ad lib* access to the diet. After 4 weeks mice were assigned into treatment groups and dosed daily with either vehicle (5% DMSO, 30% PEG300, 65% dH_2O) or sunitinib (30mg kg^{-1}) five days per week (5 days on, 2 days off) by oral gavage for a further 4 weeks (Model design is illustrated in Figure 5.1). At sacrifice, PECs, blood, liver, and tissues for histology including hearts were collected as described in 2.2.3. Plasma was harvested into anticoagulant tubes containing EDTA powder (Teklab). Aortas were harvested by microdissection, cleaned of perivascular adipose tissue and placed into RPMI 1640 + 5% FBS (for flow cytometry) or PBS with 4% PFA (*en face* preparation).

2.3 Cell culture

2.3.1 Murine bone marrow-derived macrophages (BMDMs)

BMDM culture was performed following standard Greaves lab procedure [161,162]. Bone marrow was obtained from tibae and femurs of 8-12 week old C57Bl/6 mice by flushing bones with PBS using a 26G needle. Whole bone marrow isolates were cultured for 6 days in DMEM, 10% Fetal Bovine Serum (FBS), 10% L929 fibroblast-conditioned media as a source of M-CSF [163], 1% Penicillin/Streptomycin (P/S) in non-tissue culture treated 9cm petri dishes and incubated at 37°C, 5% CO_2. On day 5 3mL media was replaced with 5mL fresh media. On day 6, cells were detached from dishes using a cell scraper, counted, and plated for experiments in DMEM containing 2% FBS in either 96 well plates at a density of 100,000 cells per well, or in 6 well plates at 1 million cells per well. Cells were allowed to settle overnight before experiments were performed on day 7.

2.3.2 RAW-Blue macrophage reporter cell line

The commercially available NF-kB/AP-1 reporter RAW-Blue™ cell line was used for compound screening. RAW-Blue cells are derived from the murine macrophage cell line RAW-264.7 and contain a secreted alkaline phosphatase (SEAP) reporter construct that is expressed upon binding of NF-kB and AP-1 to promoter consensus sequences. Cells were cultured in T175 culture dishes in DMEM supplemented with 10% FBS, 1% P/S and incubated at 37°C, 5% CO_2. RAW-Blue cell clones were selected through additional supplementation with 200µg/ml Zeocin™ for 5 days and grown to 80% confluency. For experiments, cells were rinsed with PBS, detached by aspiration, centrifuged and resuspended at desired concentrations. To reduce variability in the initial screen performed in section 3.3.1, cells were grown up in culture dishes at the same passage number and then frozen at -80°C in FBS 10% dimethyl sulfoxide (DMSO) and defrosted 24 hours prior to experimentation. For all other experiments, only cells at 5 passages or below were used. For LPS stimulations, cells were seeded in 96 well plates at 100,000 cells per well. Cells were treated with the indicated drug concentration in technical quadruplicates for 1 hour and then LPS (100ng/mL) or PBS (for non-stimulated control) was added to each well for a further 6 hours.

2.3.3 Murine L929 fibroblast cells

L929 cells were cultured in DMEM containing 10% FBS 1% P/S in tissue culture flasks until 80% confluency was reached. Cells were detached using Trypsin (Life Technologies) and plated for experiments DMEM containing 2% FBS. For experiments, cells were seeded in 96 well plates at 100,000 cells per well. Cells were treated with the indicated drug concentration in technical quadruplicates for 1 hour and then LPS (100ng/mL) or PBS (for non-stimulated control) was added to each well for a further 6 hours.

2.4 Quanti-Blue Assay

NF-κB/AP-1 activity-induced SEAP production results in colour change from pink to blue in the Quanti-Blue assay. Following cell stimulations, RAW-Blue cells were centrifuged (300g, 2 minutes) and supernatant was collected. 180µL Quanti-Blue solution was added to 20µL supernatant and

incubated for 2 hours at 37°C. Optical density was measured at 620nm using a PHERAstar microplate reader (BMG Labtech).

2.5 Cell Viability Assays

2.5.1 MTT viability Assay

Following cell stimulations, RAW-Blue cells were centrifuged (300g, 2 minutes) and supernatant was collected. Cells in remaining 100µL media were incubated with MTT reagent for 1 hour at 37°C. Yellow tetrazolium salt MTT is reduced to purple formazan crystals by metabolically active viable cells. Optical density was measured at 570nm using a PHERAstar microplate reader (BMG Labtech).

2.5.2 PrestoBlue viability assay

Presto Blue assays were performed by Amelia Bowman under my supervision. Following cell stimulations, supernatant was collected from BMDMs. PrestoBlue reagent containing blue resazurin was added to cells (1:10) and incubated at 37°C for 20 minutes. Viable cells reduce blue resazurin to red resorufin which was detected by reading absorbance at 570nm using a PHERAstar plate reader (BMG Labtech). Data were normalised to average vehicle + LPS signal.

2.5.3 Cell Titer Glo viability assay

Following cell stimulations, supernatant was collected from RAW-Blue cells, BMDMs or L929 cells. Cells in remaining 100µL media were incubated with cell titer glo reagent (1:1) for 1 hour at 37°C. CTG Reagent causes cell lysis and ATP release proportional to amount of viable cells. ATP catalyses a luciferase reaction and resulting luminescence was measured using a PHERAstar microplate reader (BMG Labtech). Data were normalised to average vehicle + LPS signal.

2.6 Griess Assay

Following cell stimulations, supernatant was collected from BMDMs or L929 cells then incubated with Sulfanilamide solution for 5 minutes at room temperature, protected from light. N-1-napthylethylenediamine dihydrochloride solution was added and incubated for an additional 5 minutes. Absorbance was read at 520nm using a PHERAstar microplate reader (BMG Labtech). Nitrite standards were prepared on each plate and used to create a standard curve. Standard curve

calculation and extrapolation was performed in GraphPad Prism. Results which fell below the lower limit of detection were recorded as 0.

2.7 ELISA

Following cell stimulations, supernatant was collected from RAW-Blue cells and BMDMs and stored at -80°C until use. Serum collected from mice was stored at -80°C until use. ELISAs for TNFα, IL-6, CCL2, IL-β, IL-10 and TGFβ were performed using DuoSet ELISA kits (R&D systems) according to the manufacturer's protocol. Samples were thawed and diluted as appropriate in PBS 1% Bovine Serum Albumin (BSA); 1:10 for RAW-Blue cells, 1:50 for BMDMs, 1:2 for 1 hour endotoxaemia mouse serum samples; 1:6 for 6 hours and 24 hours endotoxaemia serum samples. HFD-fed *Ldlr*$^{-/-}$ mouse serum samples were used undiluted. Absorbance was measured using a PHERAstar microplate reader (BMG Labtech) at 450nm (signal) and 570nm (background). Protein standards were prepared on each plate and used to create a standard curve. Standard curve calculation and extrapolation was performed in GraphPad Prism. Results which fell below the lower limit of detection were recorded as 0.

2.8 Blood analysis

Murine serum and plasma were isolated from whole blood by centrifuging collection tubes at 10000g, 5 minutes. Both were then collected and stored at -80°C. Analysis of serum damage markers and plasma lipid analytes was performed externally (Mary Lyon Centre, MRC Harwell, Oxfordshire) measured using an AU680 analyser.

2.9 Flow cytometry experiments

2.9.1 Cell Stimulations and Sample preparation

For macrophage polarisation experiments, BMDMs (n=5 mice) were plated in 6 well plates at 2 million cells/well in 2mL DMEM and polarised to M1 or M2 by stimulating with IFNγ (20ng/mL) + LPS (100ng/mL), or IL-4 (20ng/mL) respectively for 16 hours. M0 cells were left untreated. To study TLR4 internalisation, BMDMs were plated in 6 well plates at 2 million cells/well in 2mL DMEM then stimulated with LPS (100ng/mL) for up to 60 minutes.

For flow cytometry of *ex vivo* samples, 1mL of PECs was pelleted and resuspended in flow cytometry buffer. 50µL blood was mixed with Ammonium–chloride–potassium (ACK) lysis buffer (1:10, 10 minutes) to remove erythrocytes. Cells were pelleted and resuspended in flow cytometry buffer. Aortas were enzymatically digested as described in section 2.9.2 and were resuspended in flow cytometry buffer.

2.9.2 Aortic Digestion

Tissues were prepared using the protocol reported by Park *et al.* [164]. Following microdissection, whole aortas were placed in RPMI-1640 Medium with 5% FBS. Tissues were cut into small ~2mm pieces and digested in the enzyme cocktail (450 U/ml collagenase I, 125 U/ml collagenase XI 60 U/ml hyaluronidase and 60 U/ml DNase I) for 50 minutes in a 37 °C shaker. Cells were retrieved by passing tissue pieces through a 70 µm cell strainer. Entire samples were processed for flow cytometry staining.

2.9.3 Flow cytometry staining procedure

Following cell stimulations, reactions were terminated by placing on ice. Samples in 5mL flow cytometry tubes were washed with flow cytometry buffer (PBS with 2mM EDTA, 1% BSA), then anti-CD16/32 (1:50; 10µg/mL) was added to block non-specific antibody binding *via* FCγRII/FCγRIII, and incubated 15 minutes on ice. Cells were incubated with fluorophore-conjugated antibodies (all 1:40; 0.5µg/mL) (Antibodies used are listed in Table 2.1) for 30 minutes on ice and protected from light then washed X3 in flow cytometry buffer. Unstained, single stained and fluorescence-minus-one (FMO) samples were created by pooling together multiple biological samples and preparing as described above. Due to limited sample, beads (UltraComp^{TM}, InVitrogen) were used instead of cells for staining controls for *Ldlr*$^{-/-}$ aortas. All samples were resuspended in 200µL flow cytometry buffer for data acquisition.

Target	Fluorophore	Clone	Experiment
CD11b	Brilliant Violet 421	M1/70	Endotoxaemia PECs *Ldlr*$^{-/-}$ PECs *Ldlr*$^{-/-}$ blood *Ldlr*$^{-/-}$ aorta
CD11c	Brilliant Violet 650	N418	*Ldlr*$^{-/-}$ blood
CD64	APC	X54-5/7.1	*Ldlr*$^{-/-}$ aorta
CD45	APC/Cyanine7	30-F11	*Ldlr*$^{-/-}$ aorta
B220	APC	RA3-6B2	*Ldlr*$^{-/-}$ PECs
CD115	PE/Cyanine7	AFS98	*Ldlr*$^{-/-}$ PECs *Ldlr*$^{-/-}$ blood *Ldlr*$^{-/-}$ aorta
Siglec-F	APC	S17007L	*Ldlr*$^{-/-}$ blood
Ly-6C	PE	HK1	*Ldlr*$^{-/-}$ blood
Ly-6C	PerCP/Cyanine5.5	HK1.4	*Ldlr*$^{-/-}$ aorta
Ly-6G	Brilliant Violet 510	1A8	*Ldlr*$^{-/-}$ blood *Ldlr*$^{-/-}$ aorta
F4/80	APC	BM8	ImageStream, TLR4 internalisation Endotoxaemia PECs
F4/80	FITC[i]	BM8	*Ldlr*$^{-/-}$ aorta
F4/80	APC/Cyanine7	BM8	BMDM polarisation *Ldlr*$^{-/-}$ PECs
MHCII	PE	M5/114.15.2	BMDM polarisation Endotoxaemia PECs *Ldlr*$^{-/-}$ PECs *Ldlr*$^{-/-}$ aorta
MHCII	FITC[i]	M5/114.15.2	*Ldlr*$^{-/-}$ blood
CD206	BV605	C068C2	*Ldlr*$^{-/-}$ PECs *Ldlr*$^{-/-}$ aorta
CD206	APC	C068C2	BMDM polarisation
CD206	FITC[i]	C068C2	Endotoxaemia PECs
p65	PE	DA1E	ImageStream
TLR4	PE	SA15-21	TLR4 internalisation

Table 2.1: List of antibodies used for flow cytometry

[i] FITC was avoided for *in vitro* due to sunitinib fluorescence, however unstained controls showed that sunitinib fluorescence was not detectable in *ex vivo* samples, so FITC channel was used when unavoidable

2.9.4 Flow cytometry data acquisition and analysis

Data acquisition was performed on either a BD Fortessa X-20 flow cytometer (BD Biosciences) or CytoFLEX LX flow cytometer (Beckman Coulter). The same cytometer was used for all replicates or batches for a complete experiment. Compensation was performed for all experiments except TLR4 internalisation, which did not require compensation as fluorophores used were sufficiently non-overlapping . Samples were gated as described in figure legends. FMO cell samples were used to gate: Ly6C, Ly6G, CD115, MHCII, and CD11c in *Ldlr*$^{-/-}$ blood samples; MHCII and CD206 in *Ldlr*$^{-/-}$ PECs; and MHCII and CD206 in polarised BMDM samples. Data analysis was performed using FlowJo (v10.8.1) according to the gating strategies shown in figure legends.

2.10 ImageStream analysis of p65 nuclear translocation

PECs were isolated as described in section 2.2.3. PECs (1mL) were pelleted and resuspended in flow cytometry buffer. FCγRII/III binding was blocked by incubation with anti-CD16/32 (1:50; 10µg/mL) in flow cytometry buffer for 10 minutes on ice. Cells were surface stained with anti-F4/80-APC for 30 minutes on ice, washed X3 with flow cytometry buffer, and fixed for 15 minutes in PBS with 4% PFA. For intracellular staining, samples were permeabilized in flow cytometry buffer + 0.1% Triton X-100 for 15 minutes then stained with anti-p65-PE (1:100; 200µg/mL) for 1 hour at room temperature. Immediately prior to acquisition, nuclei were labelled using DAPI (1µg/mL). Data were acquired using an Amnis ImageStream MKII imaging flow cytometer (Amnis Corporation) F4/80+ single cells were gated by plotting FSC vs SSC, then FSC vs F4/80. A minimum of 8000 F4/80+ events were counted and imaged at 60X magnification. Data were analysed using IDEAS software (v.6.2; Amnis Corporation). NF-kB nuclear translocation in F4/80+ cells was assessed using the built-in nuclear translocation analysis wizard, which assigns a similarity score according to overlap of DAPI and p65 staining signal.

2.11 Real-time phagocytosis

BMDMs (n=5) were seeded in 96 well plates (100,000 cells per well) and treated with sunitinib (1 - 3µM), cytochalasin D (1µM) or DMSO vehicle. After 1 hour, pHrodo-red labelled heat-killed E. coli bioparticles (Invitrogen) (5µg) were added to cells. The pH-dependent dye pHrodo is non-fluorescent

at neutral pH and becomes fluorescent in the acidic environment of the phagolysosome following phagocytosis. Plates were centrifuged (300g, 5 minutes) to settle bioparticles onto the cells then placed into the IncuCyte ZOOM live cell imaging system (Sartorius) and incubated at 37°C, 5% CO_2 for 24 hours. Phase and fluorescent images were taken every 15 minutes for 24 hours at 10X magnification, 4 images per well. Data analysis was performed using IncuCyte analysis software (Sartorius). Red fluorescence (phagosome area) was measured per image and averaged for each well.

2.12 Phospho-Kinase Array

Phospho-kinase array was performed using the Mouse Phospho-RTK Proteome Profiler Array kit (R&D Systems). BMDMs (n=5) plated in 6 well plates (1 million cells per well) were treated with sunitinib (3μM) or DMSO vehicle for 1 hour then cells were stimulated with LPS (100ng/mL) for 10 minutes. Cells were washed in PBS then lysed in Lysis Buffer 17 (R&D Systems). To obtain a sufficient quantity of protein, lysed samples from n=5 BMDMs were pooled together to create one sunitinib and one vehicle sample. Protein concentration was calculated using BCA assay as described in 2.13.3 480μg protein was used for each array and array kit steps were performed as per the manufacturer's protocol (R&D systems). Chemiluminescent signal was detected using an Amersham Imager 600 (GE Healthcare). Signal quantification was performed using ImageJ (v1.54) by measuring signal pixel intensity averaged across kinase duplicates and normalised to local background signal.

2.13 Western Blotting

2.13.1 Sample preparation and protein extraction from cells

BMDMs (n=5) in 6 well plates (1 million cells per well) were treated with sunitinib (3μM), IKK-16 (1μM) or DMSO vehicle for 1 hour then stimulated with LPS (100ng/mL) for 0, 5 or 15 minutes. Following stimulation, cells were placed on ice to terminate signalling and washed with ice-cold PBS. Cells were lysed in lysis buffer containing 1X RIPA buffer, 1X cOmplete protease inhibitor, phosphatase inhibitor cocktails II and III (1:100 each) and phenylmethylsulfonyl fluoride protease inhibitor (200nM). Samples were then stored at -80°C until use.

2.13.2 Protein Extraction from mouse tissue

Cytosolic and nuclear protein was collected using the subcellular protein fractionation kit for tissues (ThermoFisher Scientific) according to manufacturer's protocol. Frozen mouse liver (~50mg cut into 2mm pieces) was homogenised in lysis cytosolic extraction buffer (ThermoFisher) in tubes containing 1mm glass beads for 20 seconds in a FastPrep-24 tissue homogeniser (MP Biomedicals). Samples were next passed through a 250µM cell strainer and centrifuged (500g, 5 minutes) to collect the cytoplasmic fraction. Nuclear fractions were collected using nuclear extraction buffer (Thermofisher scientific) as per manufacturer's instructions.

2.13.3 Protein concentration quantification

Lysed protein samples were centrifuged at 10,000g for 20 minutes at 4°C. Protein concentration was calculated using the Pierce BCA protein assay kit (ThermoFisher Scientific). Absorbance at 562nm was measured using a PHERAstar (BMG Labtech) and BSA standards within each assay plate were used to generate a standard curve (GraphPad Prism v9) from which sample protein concentrations were interpolated.

2.13.4 Western Blotting

Protein samples (6ug nuclear, 20ug cytosolic liver; 10µg BMDM lysate) were incubated with 4X NuPAGE LDS sample buffer (Invtirogen), 10X NuPAGE reducing agent (Invitrogen) at 70°C for 10 minutes to denature proteins. Proteins were separated by electrophoresis using NuPAGE 10% Bis-Tris gels (Invitrogen) at 200V, 30-40 minutes. Proteins were then transferred to NuPAGE nitrocellulose or PVDF membranes (Invitrogen) at 15V, 1 hour. Membranes were blocked in tris-buffered saline (TBS) with 5% BSA for 1 hour at room temperature then incubated with primary antibodies in TBS + Tween-20 (TBS-T) with 5% BSA overnight at 4°C (See Table 2.2 for list of western blotting primary antibodies). Histone H3 and GAPDH were used as loading controls for nuclear and cytosolic samples, respectively. The following day, membranes were incubated with fluorophore-conjugated secondary antibodies DyLight 800 Goat anti-rabbit IgG (1:5000) or Alexa Fluor 680 Goat anti-mouse IgG (1:5000) (Invitrogen) for 30 minutes at room temperature in TBS-T with 5% skimmed milk powder. Membranes were imaged using an Odyssey SA Imgager (LI-COR

Biosciences) and analysed using Image Studio Lite software (v5.2.5; LI-COR Biosciences). Where required, membranes were stripped using stripping buffer, 15 minutes at room temperature (ThermoFisher Scientific), then the blotting process was repeated from the blocking step.

Table 2.2: List of primary Antibodies used for western blotting

Target	Species	clone	Cat	dilution
p65	Rabbit	D14E12	8242	1 in 1000
p-p65 (Ser536)	Rabbit	93H1	3033	1 in 1000
IkBa	Rabbit	44D4	4812	1 in 1000
p-IkBa (Ser32/36)	Mouse	5A5	9246	1 in 1000
IKKalpha/beta	Rabbit	D30C6	8943	1 in 1000
pIKKalpha/beta`(S176/180)	Rabbit		2694	1 in 1000
Src	Mouse	L4A1	2110	1 in 1000
p-Src (Ser17)	Rabbit	D7F20	12432	1 in 1000
p38	Rabbit	D13E1	8690	1 in 1000
p-p38 (Thr180/Tyr182)	Mouse	28B10	9216	1 in 1000
GAPDHkj	Rabbit	D16H11	5174	1 in 1000
Histone H3	Rabbit	D1H2	4499	1 in 3000

2.14 RT-qPCR

Frozen liver tissue (~50mg cut into 2mm pieces) was homogenised by mechanical disruption using a FastPrep tissue homogeniser (MP Biomedicals) in tubes with glass beads in TRIzol reagent (Invitrogen). Total RNA was then extracted using the Direct-zol RNA miniprep kit (Zymo Research) according to the manufacturer's protocol. Isolated RNA yields were measured using a NanoDrop 1000 spectrophotometer (NanoDrop). cDNA was synthesised from 1000ng RNA using the QuantiTect Reverse Transcription kit (Qiagen). Quantitative PCR was carried out using a StepOnePlus™ thermal cycler (Applied Biosystems) with SYBR green reagents (Life Technologies).

Primers were purchased from Qiagen (*tnfα, il-6, ccl2, il-1b, il-12b, cxcl1, nos2, ccl5, 18s)* and Eurofins (*icam-1, il-10)* (See Table 2.3 for primer sequences/ID). Relative expression was calculated using the ΔΔCT method [165] with *18s* used as the housekeeping gene.

Table 2.3: List of mouse primers used

Gene	Supplier	ID/Sequence
18s	Qiagen	QT02448075
tnf	Qiagen	QT00104006
il-6	Qiagen	QT00098875
ccl2	Qiagen	QT00167832
il-1b	Qiagen	QT01048355
1l-12b	Qiagen	QT00153643
cxcl1	Qiagen	QT00115647
nos2	Qiagen	QT01547980
ccl5	Qiagen	QT01747165
icam1	Eurofins	Fw: 5'-TAC CCT CAG CCA CTT CCT-3' Rv: 5'-GTT CAC AGT CTT GCT CCA TC-3'
il-10	Eurofins	Fw: 5'-CAT ACT GCT AAC CGA CTC CT-3' Rv: 5'-CTG GGG CAT CAC TTC TAC-3'
vcam1	Eurofins	Fw: 5'-ATA GGC AAA CGG TAA AGA GG -3' Rv: 5'-CAA TGA AGA AAC AGG TCC C-3'

2.15 Histology

2.15.1 Haematoxylin & Eosin

Tissues were fixed in PBS containing 4% PFA for 24 hours and then dehydrated in 70% ethanol before embedding into paraffin blocks. 5µM sections were cut using a microtome (Leica RM2255) and mounted onto glass slides. Sections were deparaffinised using Histoclear II, and rehydrated through a series of graded ethanol solutions (100%, 90%, 70%), methanol, and finally ddH_2O. Sections were stained in Haematoxylin solution for 5 minutes, washed with tap water and 95% ethanol. Samples were then counterstained with Eosin solution for 45 seconds, and finally passed back through alcohol (95%, 100%), Histoclear II and mounted using DPX mountant and cover slip. Sections were imaged at 10X and 20X magnification using an EVOS M7000 microscope (ThermoFisher Scientific).

2.15.2 *En face* Oil-Red-O

Aortas cleaned of perivascular fat were fixed in 4% PFA for 24 hours and then stored in PBS at 4°C until use. Aortas were washed in absolute propylene glycol for 5 minutes then incubated with pre-made Oil-Red-O solution for 60 minutes. The stain was differentiated using 3X washes of 85% propylene glycol, then 2X ddH_2O. Samples were placed back into 4% PFA, then opened longitudinally and pinned onto pinning beds using 0.1mm diameter minutien pins (InterFocus). Images were taken using a microscope-attached AxioCam Erc5s (Zeiss). Image analysis was performed in ImageJ (v.1.54). Plaque area was measured by manually drawing around total area of aortic arch and areas of Oil-Red-O stained plaque and calculating the relative plaque area per sample.

2.15.3 Masson-Goldner's Trichrome

Quantification of atherosclerotic plaque size was performed based on the protocol described in Douglas *et al.* [166] with guidance from Dr Gillian Douglas. 5µM aortic root sections were obtained, deparaffinised, and rehydrated as described above in 2.15.1. Sections were stained according to the manufacturer's protocol. In detail, samples were stained with Weigert's iron Haematoxylin for 5 minutes and washed with tap water. Samples were then stained with trichrome reagents Azophloxine,

Tungstophosphoric acid orange G, and light green SF and washed with acetic acid 1% between solutions. Samples were dehydrated using an ascending ethanol series (70%, 96%, 100%), clarified with Histoclear II and mounted using DPX mountant and cover slip. Sections were imaged at 4X magnification using an EVOS M7000 microscope (ThermoFisher Scientific).

Image analysis was performed by Liliana Som who was blinded to the samples' identity. At least 3 sections at 60nm intervals were analysed per sample, with the first section being defined as the first section where 3 aortic valves are visible. Plaque area was measured by manually drawing around cellular areas of plaque attached to the inner vessel wall and calculated as a percentage of total vessel area. Necrotic core was determined using a colour threshold to select acellular regions within areas defined as plaque and calculated as a percentage of total vessel area. Image analysis was performed using QuPath software (v0.4.1). An example of aortic root plaque analysis is shown in Figure 2.1a.

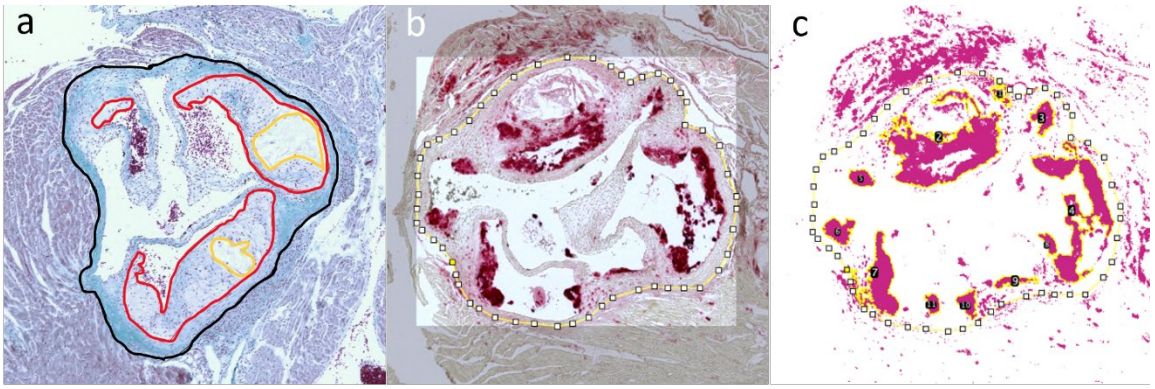


Figure 2.1: Aortic root plaque analysis. (a) Representative image of Masson-Goldner's trichrome stained aortic root section showing definition of total vessel area (black line), plaque area (red line), and necrotic core (yellow line). **(b-c)** Immunohistochemistry samples showing Galectin 3 staining. Only staining within the vessel wall was analysed **(b)** and a saturation threshold was applied to determine stained area **(c)**

2.15.4 Immunohistochemistry

5μM aortic root sections were obtained, deparaffinised, and rehydrated as described above in 2.15.1. Samples were blocked with DAKO serum free protein block (DAKO) for 1 hour, then incubated with primary antibody for 2 hours (goat anti-mouse IgG, goat polyclonal anti-mouse Galectin 3 (Gal3), or alkaline phosphatase conjugated mouse monoclonal α-smooth muscle actin (αSMA) clone 1A4, all 1:100 in PBS) then washed 3X in PBS. For Gal3 staining, samples were then incubated with biotinylated rabbit anti-goat secondary antibody (1:200 in PBS)(Vector labs) for 1 hour, washed 3X in PBS, incubated with ABC-AP (Vector labs) for 30 minutes, and washed again 3X in PBS. Gal3 and αSMA samples were washed in Tris-HCL 100mM pH 8.2 then incubated with Vector Red Alkaline Phosphatase substrate until colour was developed. Samples were washed in Tris-HCL, ddH_2O and dehydrated and clarified as described in 2.15.2. Samples were mounted using Neo-mount and cover slip. For Gal3 staining, slides containing three tissue sections were stained; one primary only IgG isotype control, one secondary only control, and one section stained with both primary and secondary antibodies. Samples were imaged using an Evos M7000 at 4X magnification.

Image analysis was performed by Liliana Som using ImageJ (v.1.54). First, a selection was made around the vessel area. Inside this region of interest a threshold (Huang) was created and 'analyse particles' was utilised to measure areas of staining above the threshold. An example of Galectin 3 image analysis is shown in Figure 2.1b-c.

2.16 Statistical Analysis

Statistical analyses were performed using GraphPad Prism (v.9) software. Tests for outliers were performed using the ROUT method and outliers were excluded where appropriate. Datasets were tested for normality using the Shapiro-Wilk test, then parametric or non-parametric tests were performed as appropriate for normally distributed data, differences between group means were assessed by one-way ANOVA with Tukey's post-hoc test for multiple comparisons when more than two groups were present, or student's T-test was used for data with only two groups. For non-normally distributed data, Mann Whitney test was used. For all analyses, $p<0.05$ was considered statistically significant. Data shown are mean ± S.E.M unless otherwise stated.

Chapter 3: Drug repurposing screening for anti-inflammatory activity and investigation of anti-inflammatory effects of sunitinib *in vitro*

3.1 Introduction:

3.1.1 Drug Repurposing and *de novo* drug discovery

The repurposing of existing medicines for novel indications is a concept that has been around since the very idea of using medicines to treat disease. Throughout history, treatments found to be effective for one particular ailment have been applied in other contexts either due to shared symptoms across diseases or as a result of serendipitous clinical observations. A prominent example of this is aspirin, which has been used for centuries in the form of Willow bark to treat a range of inflammatory conditions from back pain to fever to headaches [167]. Since 1897, aspirin has been used in its purified form of acetylsalicylic acid for many of these same conditions, and in 1971 Vane and colleagues delineated the molecular mechanism for this activity through inhibition of cyclooxygenases (COX1/2) and prostaglandin production [167,168]. Alongside its anti-inflammatory effects, additional anti-thrombotic activity attributed to aspirin has seen it become one of the most widely used drugs for prevention of cardiovascular disease today [167].

Nowadays, drug repurposing has several advantages over '*de novo*' strategies in which drugs are developed 'of new'. Foremost is the cost benefit to repurposing an existing medicine. The average cost of bringing a new drug to market has been estimated at US$2-3bn, whereas repurposing an existing drug for a novel indication typically costs just a fraction of that at an average of US$300m [169]. Moreover, a large number of prospective medicines fail at early stage safety and efficacy testing hurdles meaning that overall approval are estimated as low as between 10-20% of all Phase I investigated drugs [170–173] . Drug repurposing aims to address this issue by using drugs that are known to be safe and effective in humans for new medical indications, thereby allowing early development stages to be bypassed. This streamlined development pipeline also means that while *de novo* drugs typically require 10-15 years before market approval, drug repurposing can be achieved in an average of 6.5 years [169], allowing medicines to be provided for unmet clinical needs much quicker than *de*

novo development can offer. This strategy was employed during the COVID-19 pandemic in drug repurposing trials such as RECOVERY where the efficacy of dexamethasone in patients with severe SARS-Cov2 related inflammation was discovered [174]. Overall, drug repurposing presents a low-risk, low-cost, pragmatic option for drug development. Together, these economic incentives have led to increased interest in drug repurposing projects in recent years.

3.1.2 Drug repurposing strategies

Serendipitous discoveries

Historically, approaches to drug repurposing have largely relied on serendipity and clinical observations in patients taking the drug for its original indication. A famous example of this is sildenafil. Originally developed by Pfizer for the treatment of angina, sildenafil is a phosphodiesterase 5 inhibitor that induces vasodilation in patient coronary arteries to reduce blood pressure [175]. Early on during clinical trials erectogenic effects of the drug were reported which were later determined to also be achieved through a PDE5 dependent mechanism [175,176]. Sildenafil has gone on to be marketed for erectile disfunction under the brand name Viagra, generating peak annual sales of over $2bn USD [176]. Since then, sildenafil and other PDE5 inhibitors have been researched for their activity in cancers including brain, breast, colon, lung and prostate cancer [175] suggesting potential for repurposing once again.

Often, the new indication of a repurposed drug will be similar to that of the original and thus somewhat predictable. This trend is exemplified well by previously used examples of Aspirin and its use in various inflammatory disease, and Sildenafil with its common mechanism of action across different conditions. However, occasionally drugs are discovered to have unpredictable properties vastly different from those known previously. An example of such serendipitous drug repurposing is Thalidomide. Thalidomide was first developed in 1954 and was widely used in the late 1950s as a sedative to relieve symptoms of morning sickness during pregnancy. By 1961 thalidomide was withdrawn from the market due to its teratogenic effects which caused severe developmental abnormalities in children born to mothers taking the drug during pregnancy [177]. At the same time it was noticed that thalidomide resulted in clinical improvement in patients with leprosy who were

taking thalidomide for its sedative properties [178]. Today, thalidomide remains a standard treatment for Leprosy and is effective in up to 90% patients [177,179], with its anti-inflammatory effects attributed to its ability to supress TNFα production. More recently, structurally similar compounds with increased potency have been derived from thalidomide for use in leprosy and other inflammatory conditions [179]. Using repurposed drugs in this way, as lead compounds for the development of novel compounds, is becoming increasingly popular as drug screening methods are identifying more and more repurposing candidates and offers the opportunity to limit adverse drug effects that are associated with older drugs such as thalidomide.

Serendipitous discoveries such as these however are rare and so more reliable screening based strategies have taken over as the more common approach to drug repurposing.

Experimental Screening Strategies

Experimental drug repurposing screens are typically medium to high throughput screens that take place in cell-free, cell-based, or whole organism systems. These studies can be broadly categorised into phenotypic or target-based studies [180], with both having been utilised in studies for new anti-inflammatory drugs. Target-based approaches rely on prior mechanistic knowledge on the target pathway or disease, whereas phenotypic screens aim to detect a biological effect at the cellular or organismal level without any mechanistic knowledge required.

Zebrafish have been used as a model organism in phenotypic screens for repurposing candidates. In their 2015 study, Rihel *et al.* [181], took advantage of the lack of blood brain barrier in early zebrafish embryos to screen medicines for behavioural changes by adding them into the water of developing embryos. Using this system, the authors were able to classify drugs by the behavioural signature they induced. Anti-inflammatory medicines such as glucocorticoids and non-steroidal anti-inflammatory drugs (NSAIDs) were found to induce specific sleep/wake patterns which clustered with that of other anti-inflammatory drugs. Intriguingly, this behavioural assay identifies drugs without anti-inflammatory activity yet reported [181]. Further investigation of other medicines could reveal previously unknown anti-inflammatory activity. Elsewhere, zebrafish have been used to screen approved drugs for their ability to inhibit neutrophil migration *in vivo* in aim of uncovering novel

anti-inflammatory drug activity [182]. Such approaches allow interrogation of complex biological processes like inflammation, that are challenging to re-capitulate in an *in vitro* system.

Target based approaches aim to identify drugs that interfere with a specified cellular pathway or molecular interaction, often based on prior knowledge of shared pathways across different disease contexts or similarity in drug structures. For example, tyrosine kinase inhibitors (TKIs) are commonly used against cancer due to the key role of kinases such as KIT, Ret, and Src in cancer pathogenesis [183]. However, these and related kinases also play an important role in inflammatory processes such as cytokine signalling where they possess potential to act as druggable points of convergence for multiple cytokine signalling pathways [184]. In one drug repurposing study, the TKI dasatinib was investigated for its activity in a model of rheumatoid arthritis (RA) due to its target profile similarity to other TKIs imatinib and nilotinib, which were found to be active animal models of RA previously. Dasatanib was found to inhibit production of IL-1β, TNFα and IL-6 and disease progression in a mouse model of collagen induced arthritis [185].

Computational screening strategies

In silico screens are increasingly being performed alongside or prior to experimental drug repurposing investigations due to their huge testing capacity and low requirement for reagents and resources. A typical drug repurposing virtual screen may aim to identify compounds with a similar structure or target profile to a reference drug known to be active in the desired context, or may use molecular docking techniques to find novel drug interactions for a protein of interest. As a consequence of this rapidly expanding field, a wealth of resources, databases, and artificial intelligence approaches have been developed to aid computational drug repurposing studies [180].

In the field of inflammatory disease, this strategy has been used by Baig *et al.* to identify novel inhibitors of IKKβ [186]. The study involved using an inhibitor bound crystal structure of IKKβ as a docking surface to predict inhibition ability of compounds from an FDA-approved drug library. Thioridazine hydrochloride (TDZ), an antipsychotic dopamine-2 receptor inhibitor was predicted to be a strong affinity inhibitor of IKKβ, which was subsequently confirmed in a mouse model of sepsis [186].

3.2 Rationale and experimental aims of chapter

There is an ongoing need for new generation anti-inflammatory drugs that have high target specificity and minimal off target effects compared to traditionally used anti-inflammatory medicines. This goal is hampered by high failure rates in the *de novo* drug discovery pipeline and so drug repurposing offers a pragmatic solution to this challenge. As NF-kB governs inflammatory programming in macrophages and its signalling can become dysregulated in inflammatory disease, an experimental target-based screen of approved medicines for NF-κB activity could uncover novel anti-inflammatory properties of existing medicines for repurposing in inflammatory disease. Macrophages are an ideal target cell for such novel anti-inflammatory medicines due to their key role in both acute and chronic inflammation and their phenotypic plasticity which can be exploited therapeutically.

Therefore the experimental aims of this chapter were:

1) Screen current clinically used medicines for anti-inflammatory activity in a macrophage cell-based phenotypic screen of NF-kB activity
2) Characterise anti-inflammatory drug activity in primary murine macrophages by measuring pro-inflammatory mediator production and cell polarisation
3) Determine mechanism of action of anti-inflammatory drug candidates through interrogation of the NF-kB pathway

3.3 Results:

3.3.1 Screen of FDA-approved medicines for NF-kB inhibition in RAW-Blue cells:

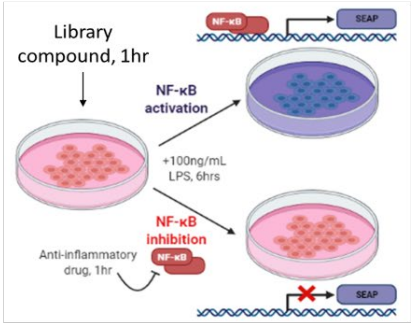
We utilised the RAW-Blue cell-line for drug-repurposing screening. RAW-Blue is a commercially available reporter cell line derived from RAW264.7 murine macrophage cells. These reporter cells contain consensus binding sequences for the inflammatory transcription factors NF-kB and AP-1 within the promotor region of the reporter gene, secreted alkaline phosphatase (SEAP) (Figure 3.1a). Consequently, NF-kB and AP-1 activity can be inferred through measurement of SEAP in the supernatant of RAW-Blue cells (Figure 3.1b). I therefore chose this system to screen existing

medicines for anti-inflammatory activity, using inhibition of NF-kB activation as the primary readout. I opted to use lipopolysaccharide (LPS) as the immune stimulus in the screen as well as for the majority of experiments throughout this chapter as LPS is a widely used, well characterised and potent inducer of NF-kB activity. The concentration 100ng/mL and stimulation duration of 6 hours were chosen based on previous experiments performed with RAW-Blue cells in the Greaves lab [92].

The chosen compound library for screening was the TocriScreen library of 159 FDA-approved medicines. Several specifically curated drug libraries exist for drug repurposing projects, however this particular library was chosen for its broad range of drug classes from various medical fields and for its practicable size for a manual experimental screening approach such as the one taken here. Compounds were screened at 1, 3 and 10μM concentrations in order to detect dose-dependent effects and screening was performed using technical quadruplicate wells (Figure 3.1b). First, RAW-blue cells seeded in 96-well plates were treated with anonymised drugs from the compound library dissolved in dimethyl sulfoxide (DMSO). In-plate controls included were a 0.1% DMSO vehicle control and the glucocorticoid dexamethasone (Dex; 1μM). Following a 1 hour incubation with the drugs, cells were stimulated with LPS (100ng/mL), or PBS for the 0.1% DMSO vehicle non-stimulated (vehicle NS) control. Cells were then incubated for 8 hours to allow NF-kB signalling and accumulation of reporter SEAP in cell supernatant. Supernatant was taken and incubated for a further 2 hours with Quanti-Blue solution for quantification of supernatant SEAP. Optical density readouts were then normalised to the average vehicle LPS signal within the same plate, and results across 23 independent plates were un-anonymised and pooled into one heat map (Figure 3.2).

Results show that the used concentration of LPS reliably induced NF-kB activation and little variation was seen within technical replicates. Variation in optical density between plates was accounted for by normalising data to vehicle LPS treated wells for each plate, and this was validated by consistently obtaining similar values for vehicle NS and Dex control groups, with averages of 0.203 and 0.590 of vehicle LPS signal respectively, and standard deviations of 0.043 and 0.068 and 0.075 for Vehicle NS, vehicle LPS and Dex controls across the entire screen.

a



Supernatant for Quanti-Blue assay
→ read absorbance at 620nm

Cells for MTT assay
→ read absorbance at 570nm

b

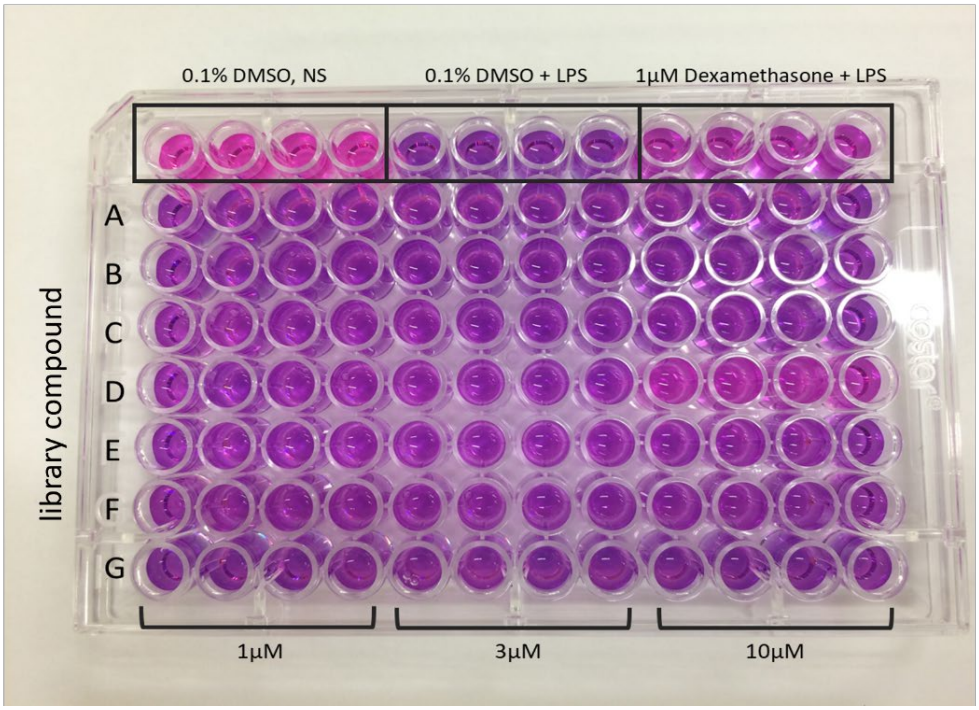


Figure 3.1: RAW-Blue Screen design for anti-inflammatory drug activity. (a) screen design illustrating assay principle. RAW-blue cells containing the reporter gene secreted embryonic alkaline phosphatase (SEAP) under the control of NF-κB and AP-1 transcription factors. Cells were first pre-treated for 1 hour with compounds from the TocriScreen library of 159 FDA-approved medicines. LPS (100ng/mL) was then added for to induce NF-κB activation and SEAP production. Cell supernatant was mixed with Quanti-Blue solution and optical density was read at 620nm in order to quantify SEAP concentration. MTT reagent was added to cells and optical density was read at 570nm to measure cell viability. **(b)** representative primary data from Quanti-Blue assay in initial drug repurposing screen. Assay was performed with four technical replicates all in 0.1% DMSO. Seven compounds were analysed per plate. Dexamethasone (1μM) was used as a positive control. NS= non-stimulated.

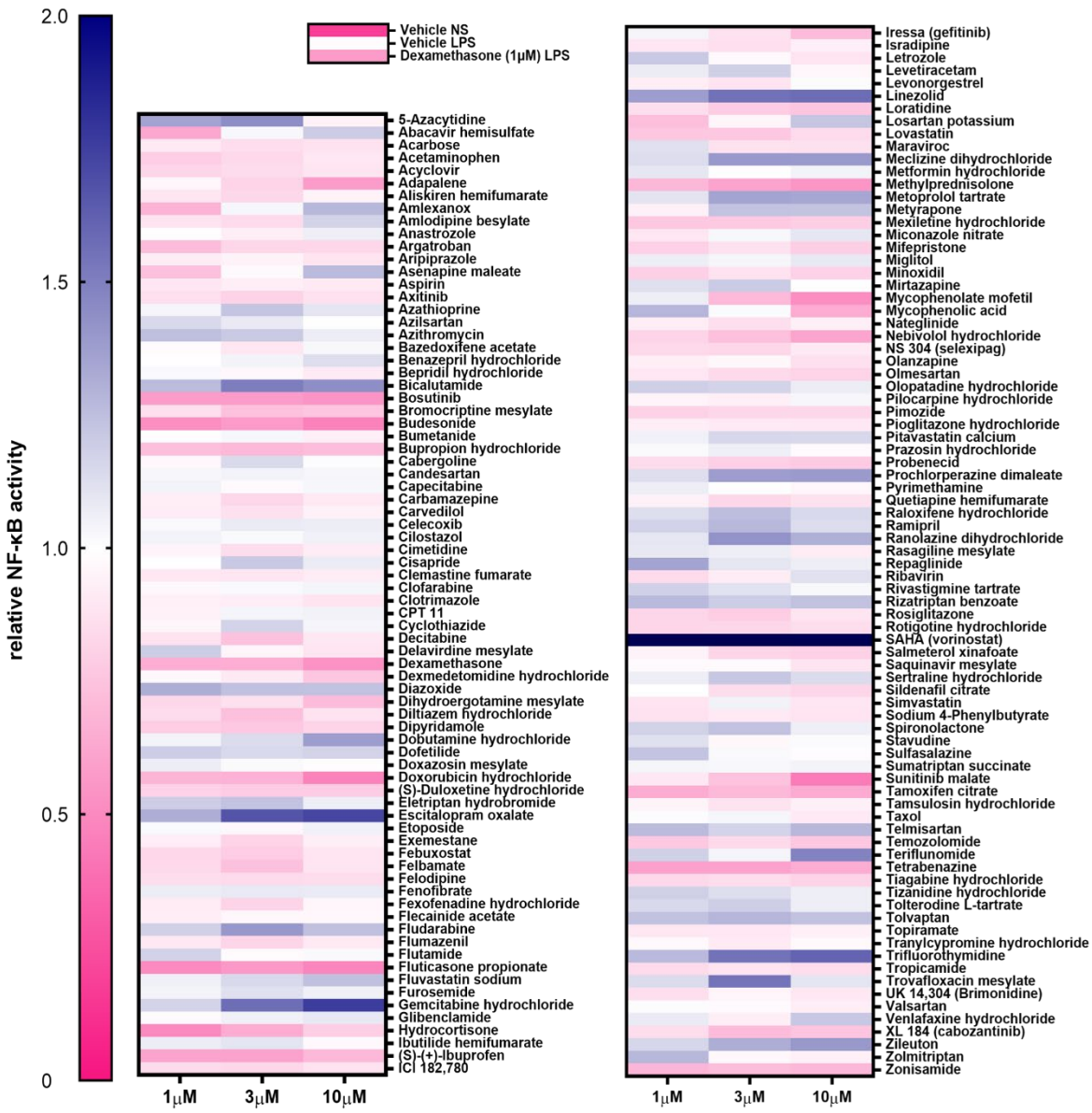


Figure 3.2: Anti-inflammatory activity of FDA-approved medicines detected in a NF-KB reporter cell line screen. RAW-blue cells (n=1) were pre-treated with the indicated compound at 1, 3, or 10μM in 0.1% DMSO for 1 hour prior to stimulation with LPS (6 hours, 100ng/mL). NF-kB activity was assessed from supernatant in the Quanti-Blue colorimetric assay and is plotted as a mean of technical quadruplicates, relative to vehicle LPS treated cells mean.

To define screening 'hits' I set an efficacy threshold at ≥25% reduction in relative NF-kB activity at any of the three tested concentrations. These criteria revealed 19 active compounds in the current screen (Table 3.1), which performed in both a dose-dependent and dose-independent manner. As predicted due to their well-known NF-kB inhibitory activity [187,188], among these compounds were several glucocorticoid receptor agonists; methylprednisolone, fluticasone propionate, budesonide, hydrocortisone and dexamethasone, with the latter also used independently as a positive control. Additionally, anti-inflammatory drugs including COX1/2 inhibitor Ibuprofen, and retinoic acid receptor agonist adapalene were identified as hits for NF-kB inhibition in the screen. As these results offered limited novelty these compounds were not investigated further. Interestingly, we noted that a significant number of compounds identified in the screen were tyrosine kinase inhibitors (TKIs). The list included TKIs with a range of molecular kinase targets, such as; the multi-target TKI sunitinib, BCR-ABL inhibitor bosutinib, EGFR inhibitor gefitinib, and VEGFR inhibitor cabozantinib.

Another notable finding from the screen was that the histone de-acetylase (HDAC) inhibitor and T-cell lymphoma medicine vorinostat caused a 2.07 fold *increase* in SEAP production compared to vehicle, the largest effect size of the screen. Given that HDACs are believed to have anti-inflammatory activity and that vorinostat has previously been shown to inhibit inflammatory processes in LPS-stimulated macrophages [189], I hypothesised that one explanation for this could be that vorinostat itself interferes with the Quanti-Blue colorimetric assay, which relies on the enzymatic activity of SEAP against substrate in the Quanti-Blue solution. To test this, the Quanti-Blue assay was repeated with supernatant from vehicle NS and vehicle LPS cells which had 10μM vorinostat added immediately prior to incubation with Quanti-Blue solution, without exposure to cells or ability to influence SEAP production. This experiment revealed no difference in optical density and therefore SEAP activity upon the addition of vorinostat (Figure 3.3), indicating that the drug itself is not interfering with the assay. The activity of vorinostat metabolites however is not ruled out by this experiment.

Table 3.1: Compounds causing >25% inhibition of NF-κB in RAW-Blue drug repurposing screen

Name	Biological target	Indicated Use	NF-kB activity at 10uM (relative to vehicle LPS)	anti-inflammatory activity reported	NF-κB inhibition reported	Effect in macrophages
Mycophenolic acid **Mycophenolate mofetil**	Inosine monophosphatase dehydrogenase	immunosupressant, organ transplant rejection prevention	0.646 0.520	yes [190]	yes [191]	treatment reduces expression of inflammatory cytokines in murine macrophage cell line [192]
Iressa (gefitinib)	EGFR	breast/lung cancer	0.714	no	no	reported reduced M2 markers upon gefitinib treatment in RAW cells/BMDMs[193]
Doxorubicin hydrochloride	DNA topoisomerase II	breast/bladder cancer, leukaaemias	0.471	no	no	pro-inflammatory, induces upregulation of TLR4 [194]
Adapalene	RARβ/RARγ	topical acne treatment	0.576	yes [195]	no	retinoids decrease inflammatory cytokine production in cell lines [196]
Nebivolol hydrochloride	β1-adrenoceptor	hypertension	0.615	yes [197]	yes [198]	
Sunitinib malate	Type III RTK family	renal cell carcinoma	0.441	yes [199]	yes [200]	may promote M2 phenotype in TAMs [201]
Tamoxifen citrate	Estrogen receptor	breast cancer	0.639	no	no	antiatherogenic: reduces CD36 exp, reduces FABP4 exp [202]
Tetrabenazine	vesicular monoamine (dopamine, noradrenaline, serotonin) transporters	hyperkinetic movement disorders	0.647	yes [203]	no	
Ibuprofen	Cyclooxygenase	Anti-inflammatory	0.698	yes [204]	yes [205]	modulates phenotype of primary lung macrophages [206]
Zonisamide	Voltage-sensitive Na+ and Ca2+ channels (T-type)	epilepsy, Parkinson's disease	0.696	yes [207]	no	
Bupropion hydrochloride	dopamine/ noradrenalin transporters	antidepressant	0.721	no	no	
Methylprednisolone	Glucocorticoid receptor	Anti-inflammatory	0.550	yes [208]	yes [208]	inhibit inflammatory signalling
Fluticasone propionate			0.483	yes [209]	yes [210]	

Dexamethasone			0.536	yes [211]	yes [211]	through NF-kB pathway [188]
Budesonide			0.464	yes [212]	yes [213]	
Hydrocortisone			0.795	yes [214]	yes [214]	
Bosutinib	Src-Abl	chronic myleloid leukaaemia	0.546	yes [215]	no	promotes anti-inflamm phenotype through SIK inhibition [216]
XL-184 (cabozantinib)	Type III RTK family; selective for VEGFR2	thyroid cancer, renal cell carcinoma	0.753	yes [217]	yes[217]	

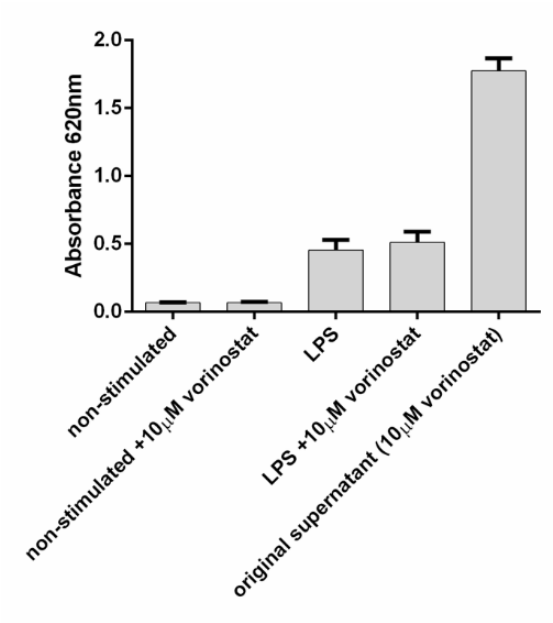


Figure 3.3: Effects of Vorinostat in the Quanti-Blue assay. Optical density of RAW-Blue supernatants (n=3 technical triplicates) in the Quanti-Blue assay. Supernatants from vehicle non-stimulated and vehicle LPS cells in the original screen were measured with and without vorinostat (10μM) added directly just prior to analysis. Supernatant from RAW-Blue cells treated with Vorinostat (10μM) then stimulated for 6 hours with LPS (100ng/mL) in the original screen.

Among hit compounds were those suspected to have been falsely identified due to cytotoxicity preventing SEAP production, such as by the chemotherapeutic agent doxorubicin hydrochloride (Table 2). To combat this issue, a counter screen for cytotoxicity using the MTT cytotoxicity assay was built into the original screen design, however poor MTT reagent solubility and high replicate variation caused the resulting data to have poor reliability (Figure 3.4). A secondary screen was therefore performed by Amelia Bowman as part of an undergraduate dissertation project under my supervision[ii]. Taking together the results of the secondary cytotoxicity screen along with existing literature, two compounds were taken forward for further investigation on the basis of their potency, limited cytotoxicity, and relative novelty: sunitinib and bosutinib.

[ii] Unpublished data by A. Bowman. See Appendix 1

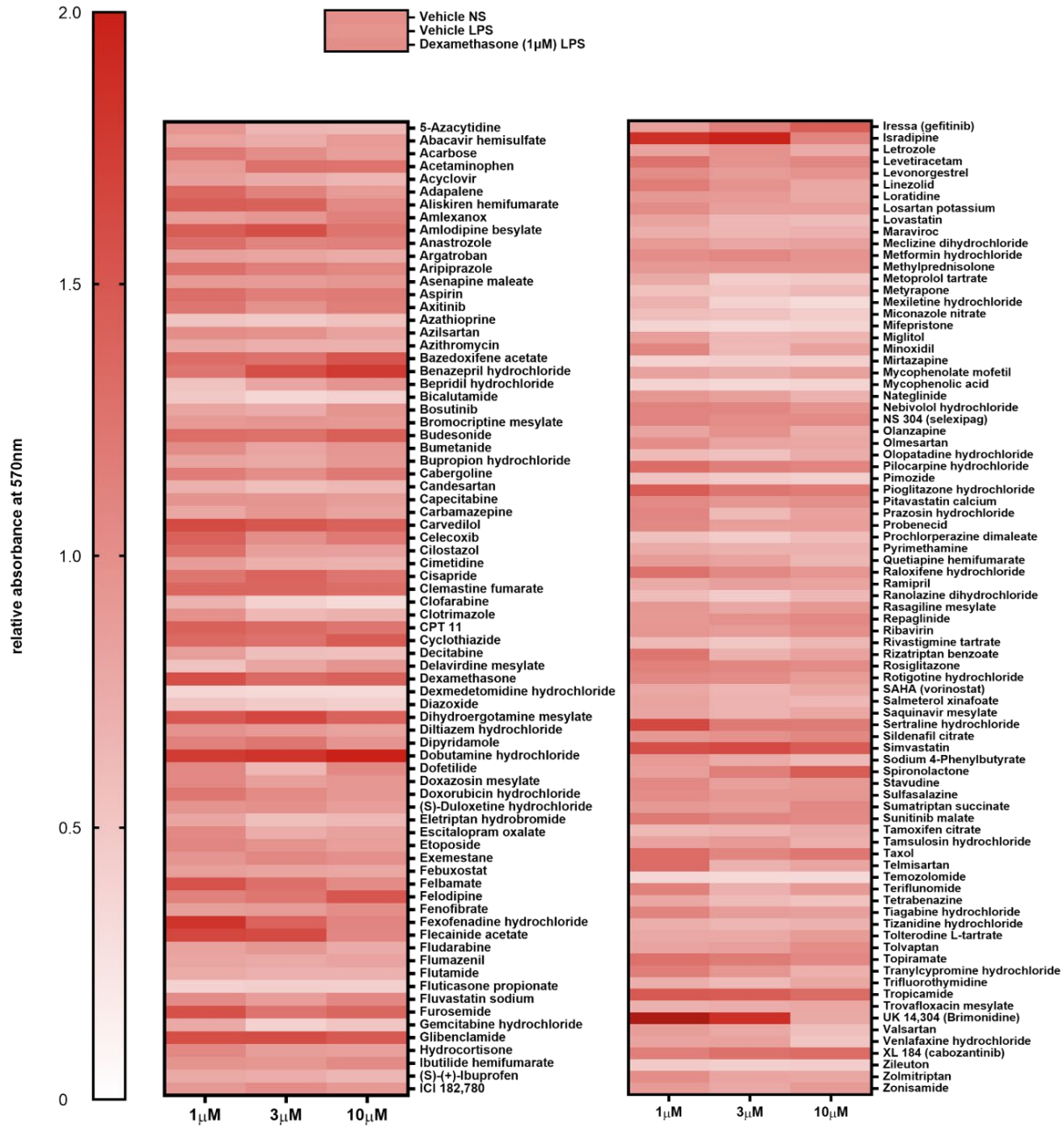


Figure 3.4: Cytotoxicity of FDA-approved medicines in LPS-stimulated RAW-Blue cells. RAW-Blue cells were treated with the indicated compound at 1, 3, or 10μM in 0.1% DMSO for 1 hour prior to stimulation with LPS (6 hours, 100ng/mL). Cell cytotoxicity was measured and is plotted as the mean of technical quadruplicates relative to vehicle LPS treated mean.

3.3.2 Validation of the anti-inflammatory activity of Bosutinib and Sunitinib in cell-line macrophages

To validate the activity of sunitinib and bosutinib in the RAW-Blue cell line, a wider range of drug concentrations was investigated. On the basis of a concentration dependent pattern being observed for both drugs in the original screen at 1,3 and 10μM, an 8-point 3-fold dilution series was chosen ranging from 31.25μM to 0.0014μM. Using the same RAW-Blue stimulation protocol as in the original screen, concentration response curves were generated for SEAP activity in both Bosutinib and Sunitinib treated cells (n=4 independent experiments performed in triplicate, Figure 3.5a-b). From this, I was able to calculate IC_{50} values for both drugs in this assay at 3.03μM for bosutinib and 1.26μM for sunitinib. Using the same samples, I assessed cell viability using the cell titre glo assay, which is dependent on ATP production. I found that both drugs only caused significant cell death at the highest concentration tested, 31.25μM ($p<0.001$, one-way ANOVA), well above active concentrations (Figure 3.5c-d). To assess whether SEAP production was an accurate measure of NF-κB production TNFα production was also tested in the same samples by ELISA. IC_{50} values for TNFα production largely mirrored that of NF-kB inhibition, and were calculated at 1.27μM for bosutinib, and 0.69μM for Sunitinib (Figure 3.5e-f).

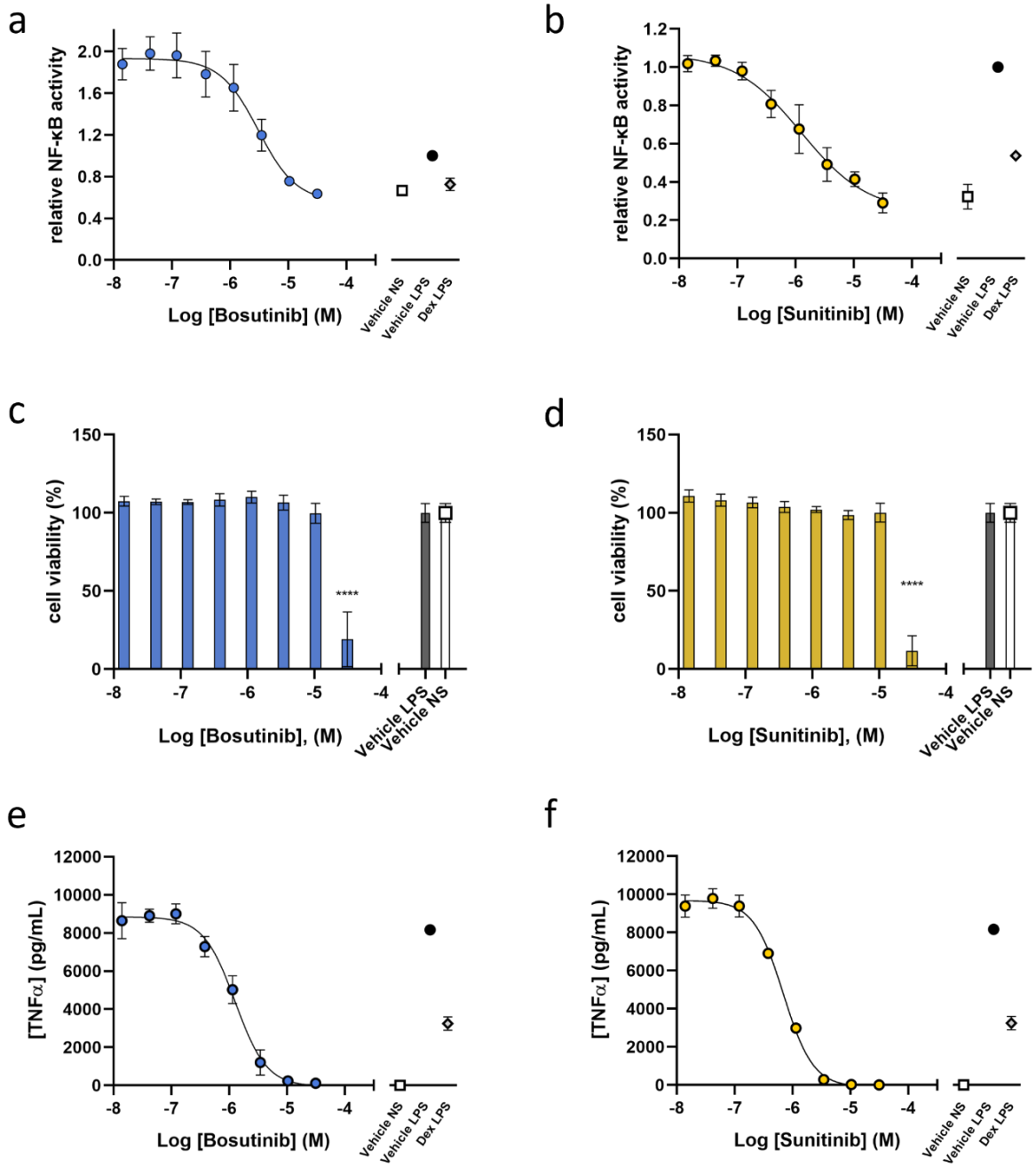


Figure 3.5: Dose-dependent anti-inflammatory effects of bosutinib and sunitinib in RAW-Blue cells. RAW-Blue cells (n=4) were treated with a concentration range of either bosutinib **(a,c,e)** or sunitinib **(b,d,f)** for 1 hour prior to stimulation with LPS (6 hours, 100ng/mL). NF-kB activity **(a-b)** and cell cytotoxicity **(c-d)** relative to vehicle LPS were measured via QuantiBlue assay and MTT assay respectively. Supernatant TNFα concentration was measured by ELISA **(e-f)**. NS=non stimulated, Dex= Dexamethasone, 1µM. All data are shown as means ± SEM. ****p>0.0001 vs vehicle LPS treated cells . Statistical significance determined by one-way ANOVA followed by Tukey's post-hoc test.

3.3.3 Bosutinib and Sunitinib activity in primary macrophages

Having shown anti-inflammatory and NF-kB inhibitory activity of both bosutinib and sunitinib in a macrophage cell-line, I next investigated whether the same activity was seen in primary macrophages in experiments conducted with Amelia Bowman. To do this, I analysed pro-inflammatory mediator production in LPS-stimulated murine bone marrow derived macrophages (BMDMs) treated with a concentration range of either bosutinib or sunitinib. Doing this, I was able to generate concentration response curves for the cytokines TNFα, IL-6, and IL-1β, neutrophil recruitment chemokine CCL2, and pro-inflammatory reactive oxygen mediator nitric oxide (NO) (Figure 3.6-7). As before, controls included were vehicle NS, in which little to no cytokine production was observed, vehicle LPS, which showed robust induction of cytokine production, and Dexamethasone (1μM) LPS, which consistently showed >50% reduction of the vehicle LPS signal. To analyse NO production, BMDMs were stimulated with LPS for 20 hours rather than 8 hours, as used for other cytokines in order to allow NO to accumulate to detectable levels in the supernatant. No additional cytotoxicity testing was performed at this timepoint, but it was noted that all sunitinib-treated cells except the 31.25μM condition appeared to show viable morphology when examined under the microscope. A selective iNOS inhibitor, 1400W dihydrochloride (100μM), was also included as a control and showed almost complete inhibition of NO production (Figure 3.7e). IC_{50} values for all tested pro-inflammatory mediators listed in Table 3.2.

Sunitinib was a potent suppressor of cytokine production, with consistent IC_{50} values around 1μM (Figure 3.7; Table 3.2). Bosutinib on the other hand did not show such a consistent pattern of inhibition, with only TNFα and CCL2 displaying dose dependent inhibition (Figure 3.6a,d). Despite bosutinib's ability to dose-dependently inhibit NF-kB, it was unable to supress IL-6 and IL-1β production with drug treated cells and caused up to 7 fold higher production than vehicle LPS stimulated cells (Figure 3.6b-c). Cell viability was also tested in these cells using the PrestoBlue assay. This revealed significant cytotoxicity with sunitinib only at 31.25μM and none with Bosutinib (Figure 3.6e, Figure 3.7f). Considering the higher potency and more consistent anti-inflammatory

profile seen with sunitinib versus bosutinib, I chose to focus the remainder of this project studying sunitinib.

Table 3.2: IC_{50} values for pro-inflammatory cytokine production in Bone Marrow Derived Macrophages. N/A indicates lack of dose dependent inhibition. (n=5-7)

	bosutinib	***sunitinib***
TNFα	*1.238μM*	*0.968μM*
IL-6	*N/A*	*1.028μM*
IL-1β	*N/A*	*1.736μM*
CCL2	*1.434μM*	*0.318μM*
NO	*untested*	*0.593μM*

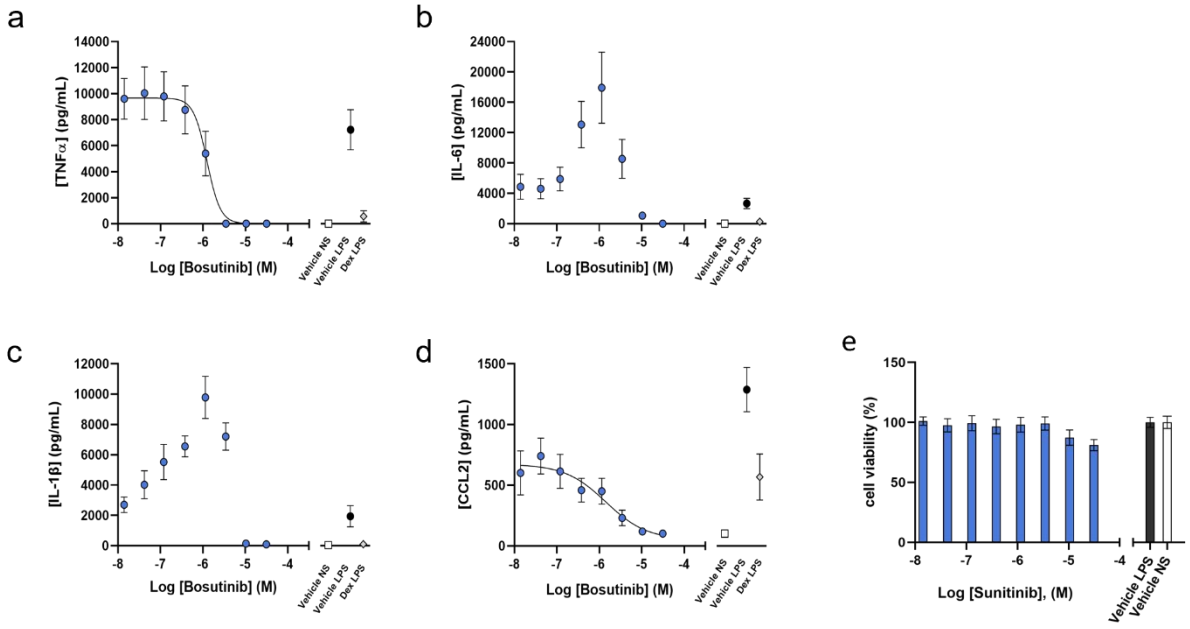


Figure 3.6: Effect of bosutinib on primary macrophage cytokine production. Bone marrow derived macrophages (n=5) were treated with a concentration range of bosutinib prior to stimulation with LPS (100ng/mL, 8 hours) and supernatant cytokine levels were measured **(a-d).** To measure IL-1β, ATP (100μM) was added after 7 hours LPS incubation **(d).** Cell viability was measured using PrestoBlue assay **(e).** NS=non stimulated, Dex= Dexamethasone, 1μM. All data are shown as means ± SEM.

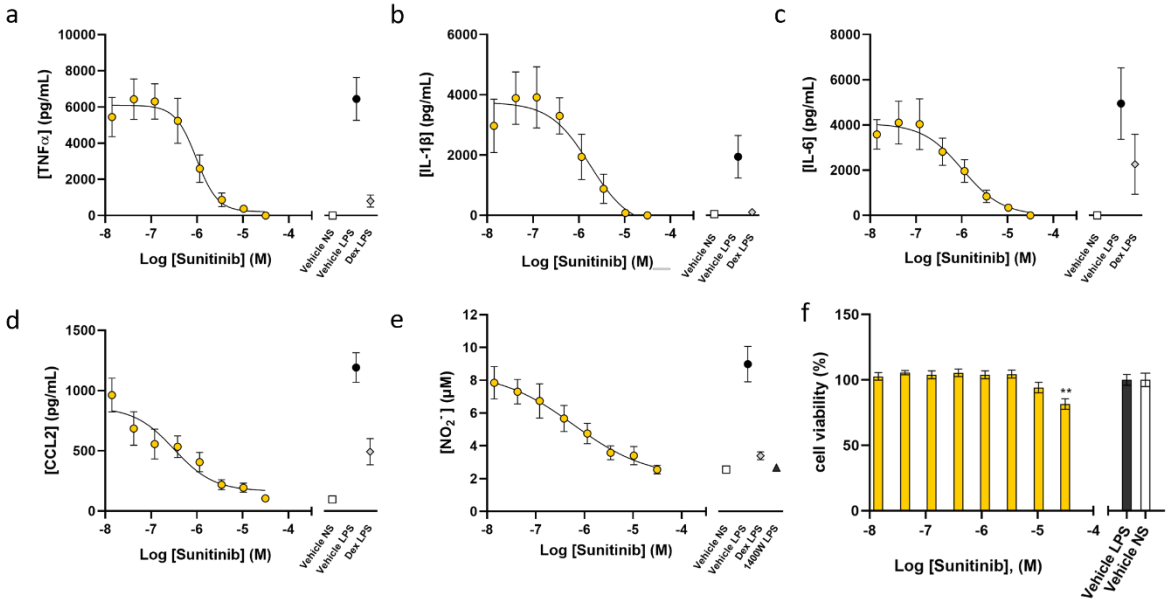


Figure 3.7: Effect of sunitinib on primary macrophage cytokine production. BMDMs (n=5-7) were treated with a concentration range of sunitinib prior to stimulation with LPS (100ng/mL). Supernatant cytokine levels were measured after 8 hours **(a-d)**.To measure IL-1β, ATP (100μM) was added after 7 hours LPS incubation **(d)**. Nitrite concentration was measured after 20 hours LPS stimulation by Griess assay **(e)**. Cell viability after 8 hours LPS stimulation was measured using PrestoBlue assay **(e)**. NS=non stimulated, Dex= Dexamethasone, 1μM. All data are shown as means ± SEM. **p<0.01 vs vehicle LPS treated cells. Statistical significance measured by One-Way ANOVA followed by Tukey's post-hoc test.

3.3.4 Effect of sunitinib on macrophage polarisation

The production of pro-inflammatory mediators *via* NF-kB signalling is largely attributed to macrophages of a M1-like state. Anti-inflammatory drugs have been previously shown to inhibit M1-associated signalling pathways and downregulate expression of M1 markers as well as actively promote M2 macrophage polarisation with increased expression of M2-associated markers [218]. Previous work in the Greaves lab has shown that the Bruton's tyrosine kinase (BTK) inhibitor ibrutinib not only inhibits NF-kB signalling, but skews macrophages towards an M2 phenotype with increased macrophage CD206 surface expression and metabolic reprogramming [162,219].

Here, I tested the effect of Sunitinib on macrophage polarisation in BMDMs. For further experiments requiring a single concentration of sunitinib, 3μM was chosen as previous results show that this is sufficient for reducing NF-kB signalling without causing cytotoxicity. Unpolarised (M0) BMDMs were first pre-treated with sunitinib or DMSO vehicle for one hour before polarisation to either M1 (LPS 100ng/mL, IFNγ 20ng/mL) or M2 (IL-4 20ng/mL) macrophages for 16 hours. Unpolarised M0 cells were also included as a control. Following polarisation, cell surface expression of M1/M2 markers were assessed by flow cytometry. An important consideration for this experiment and for all readouts involving fluorescence is the strong fluorescence of sunitinib itself. As sunitinib has a peak emission wavelength of 540nm [220], fluorophores in the green and ultraviolet range of the fluorescence spectra were avoided.

The gating strategy for analysis of macrophage polarisation is shown in Figure 3.8a. Briefly, cells were gated by size on forward scatter (FSC) *versus* side scatter (SSC) plots. Single cells were then identified using double exclusion by FSC height *versus* area and height *versus* width plots. F4/80hi cells were gated and subsequently used to gate $F4/80^{hi}MHCII^{+}$ M1 cells and $F4/80^{hi}CD206^{+}$ M2 cells (Figure 3.8a). Analysis of BMDM surface marker expression reveals similarly high expression of the resident macrophage marker F4/80 across all treatment conditions and polarisation states (Figure 3.8b). M1 polarisation was successfully induced, with 35-50% of F4/80+ vehicle treated M1-polarised cells expressing the M1 marker MHCII, and little expression seen in M0 and M2 groups. This number was significantly increased to 58% when cells were pre-treated with sunitinib ($p<0.05$,

Figure 3.8c). Conversely, M2-polarised cells showed reduced MHCII expression with sunitinib treatment ($p<0.001$). To assess M2 polarisation, CD206 expression was interrogated. As expected, M2 polarised cells showed the highest expression of CD206 (Figure 3.8d), although expression was lower in sunitinib-treated compared to vehicle-treated cells ($p<0.01$). The same pattern was seen in M1-polarised cells, with sunitinib treated cells having a modest but significant reduction in CD206 expression ($p<0.05$).

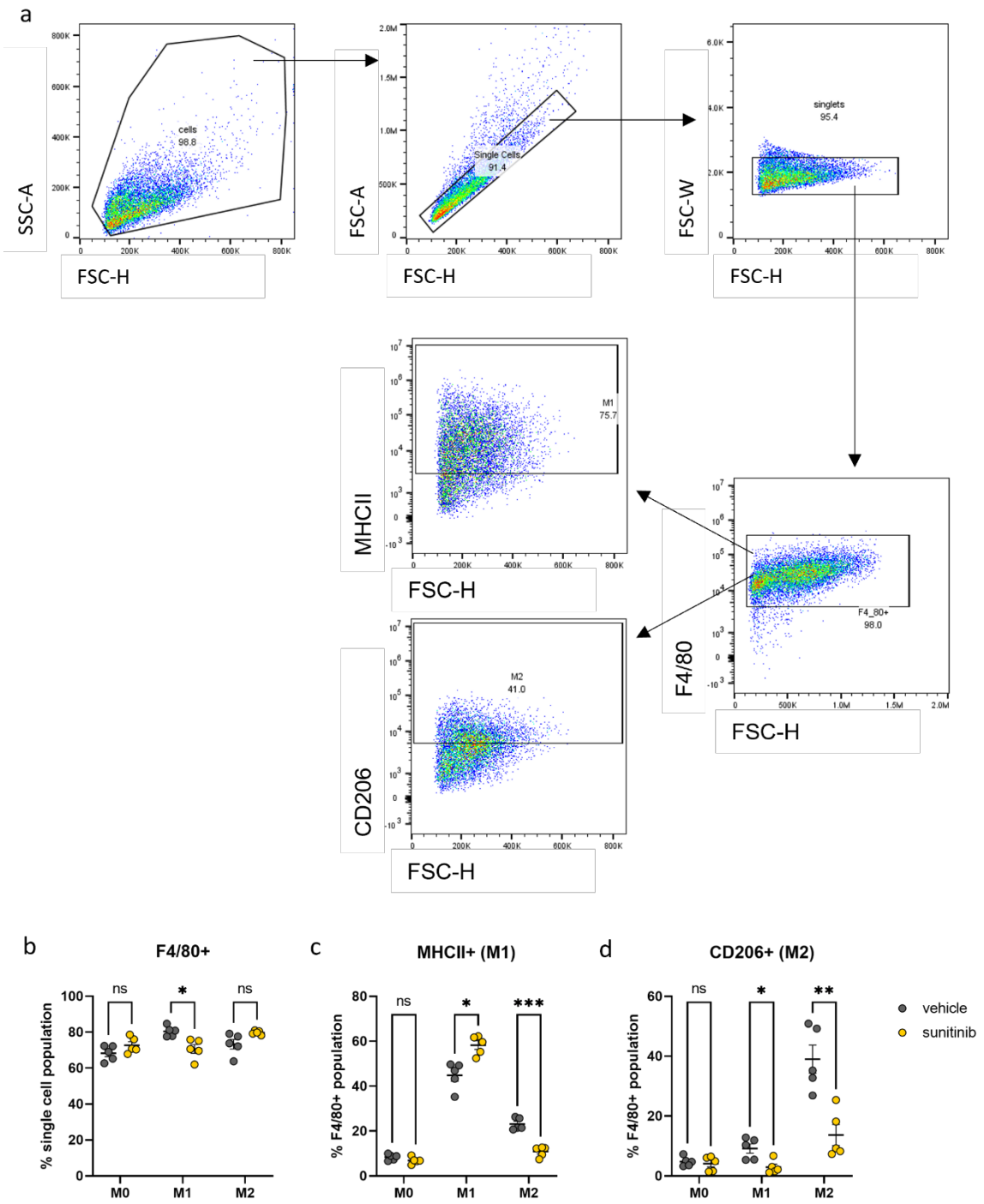


Figure 3.8: Sunitinib affects macrophage polarisation *in vitro*. Bone marrow derived macrophages (n=5) were pre-treated with sunitinib (3μM) or DMSO vehicle for 1 hour prior to polarisation to M1, M2, or control (M0) and cell surface marker expression was assessed by flow cytometry. Gating strategy for analysis **(a)**. Expression of F4/80 **(b)**, MHCII **(c)**, and CD206 **(d)**. Data shown are biological replicates ± SEM. *p<0.05, **p<0.01, ***p<0.0001. Statistical significance determined by one-way ANOVA followed by Tukey's post-hoc test.

3.3.5 Effect of sunitinib on macrophage phagocytosis

To assess whether sunitinib has an effect on macrophage effector function, I examined its activity in a macrophage phagocytosis assay. In the assay, fragments of dead *E coli* labelled with a pH-dependent fluorescent dye (pHrodo-*E. coli* bioparticles) were added to plated BMDMs and imaged every 15 minutes over a 24 hour period to assess phagocytosis. Non-phagocytosed pHrodo-*E. coli* bioparticles are non-fluorescent, but upon phagocytosis and acidification of the phagolysosome, the pHrodo signal becomes activated therefore fluorescence, read as phagosome area, can be used to calculate rate of phagocytosis (Figure 3.9a). Area under the curve (AUC) can for these analyses can be calculated to directly compare conditions (Figure 3.9b). A cells-only well lacking bioparticles was used as a control, and revealed no background fluorescence. Sunitinib exhibited a dose-dependent effect on phagocytosis, with cells treated at 1μM and at 3μM both showing significant phagocytosis inhibition ($p<0.0001$; Figure 3.9b). Cytochalasin D, an inhibitor of actin cytoskeleton polymerisation was used as a phagocytosis-inhibiting control, and showed significantly less phagocytosis than vehicle only control ($p<0.0001$; Figure 3.9b), and inhibition to a similar degree as 1μM sunitinib.

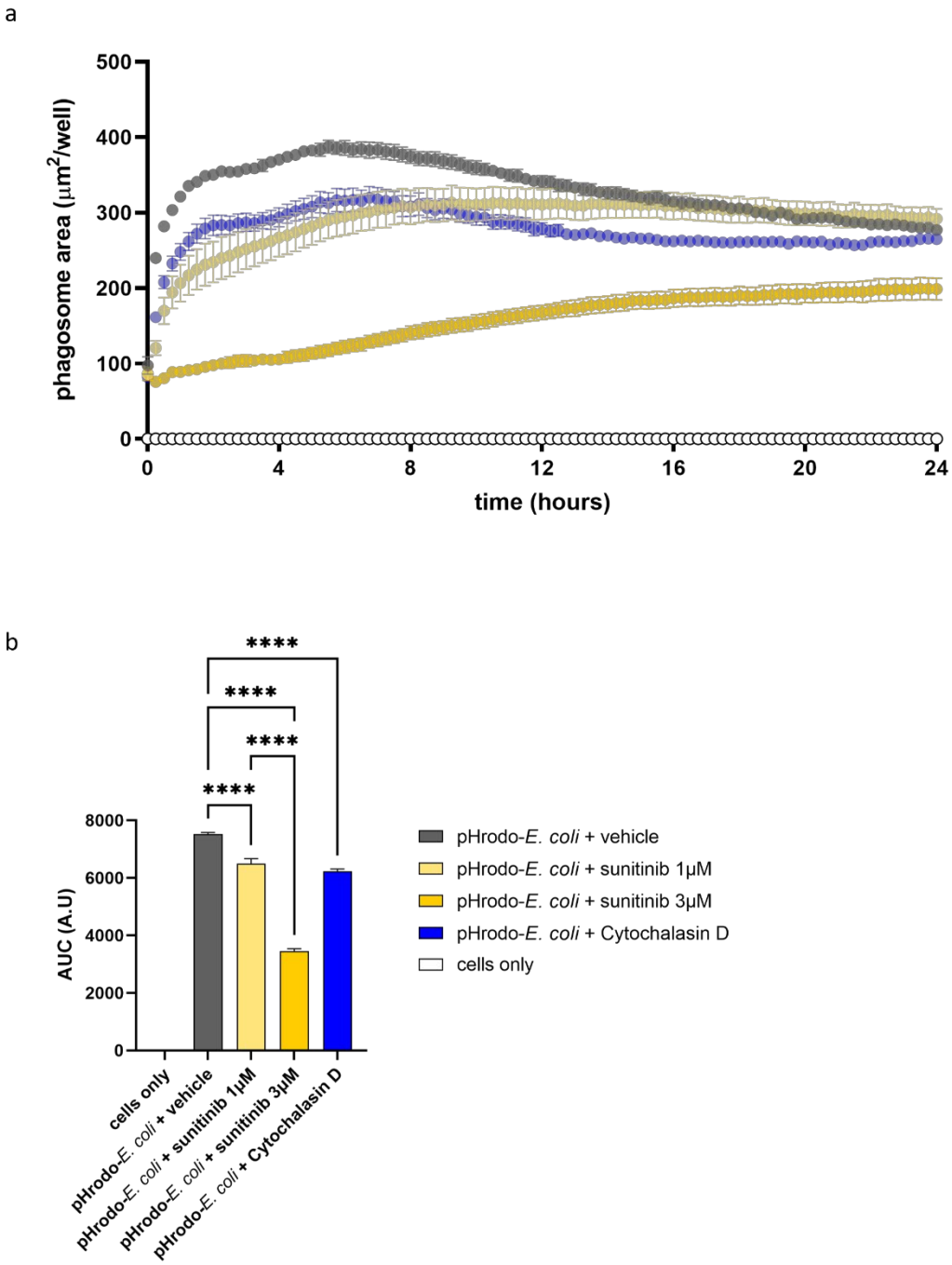


Figure 3.9: Sunitinib inhibits macrophage phagocytosis. Bone marrow derived macrophages (n=5) were pre-treated with sunitinib (1 or 3μM), cytochalasin D (1μM) or vehicle for 1 hour prior to addition of pHrodo-red labelled *E.coli* bioparticles (5μg). Uptake of bioparticles was measured by fluorescence imaging over 24 hours **(a)** and area under the curve (AUC) was calculated for the average of each condition **(b)**. ****p<0.0001. Statistical significance determined by one-way ANOVA followed by Tukey's post-hoc test.

3.3.4 Effect of sunitinib on AP-1 activity

Next, I wanted to investigate the molecular mechanism by which sunitinib attenuates macrophage NF-kB signalling. Thus far, the anti-inflammatory effects of sunitinib have been attributed to its NF-κB inhibitory activity, based on its activity in the RAW-Blue NF-κB reporter cell line. However, RAW-Blue cells also report on AP-1 activity, and as AP-1 signalling is also stimulated by LPS in the assays used here, AP-1 could be responsible for the anti-inflammatory activity of sunitinib.

To test this hypothesis, the sunitinib concentration response experiments in Figure 3.5a were repeated with and without the addition of the AP-1 chemical inhibitor T-5224 (10μM). AP-1 inhibition reduced overall response to LPS, however sunitinib treatment still caused a concentration-dependent decrease in signal (Figure 3.10). IC_{50} values were calculated at 1.34μM and 1.05μM with and without AP-1 inhibition, respectively. This result indicates sunitinib activity in RAW-Blue cells is largely not due to AP-1 inhibition and is therefore primarily caused by inhibition of NF-κB.

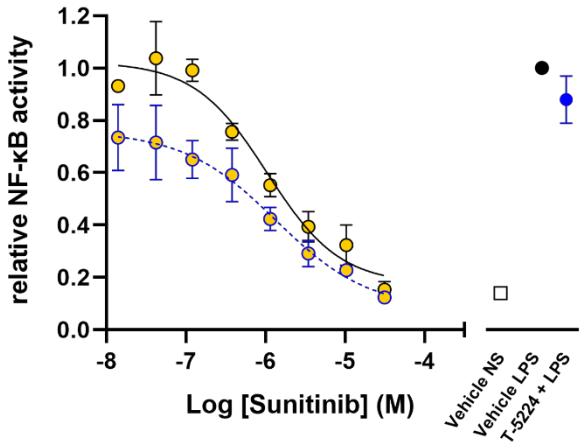


Figure 3.10: Anti-inflammatory activity of sunitinib is not due to inhibition of AP-1. RAW-Blue cells (n=3) were treated with a concentration range of sunitinib for 1 hour prior with (dotted blue line) or without (solid black line) AP-1 inhibitor T-5224 (10 μM) prior to stimulation with LPS (6 hours, 100ng/mL). NF-κB activity was measured by QuantiBlue assay. Data are shown relative to vehicle LPS without T-5224.

3.3.6 Effect of sunitinib on TLR4 surface expression

A possible explanation for the reduced response to LPS seen with sunitinib is that sunitinib inhibits signalling at TLR4, either by preventing LPS-receptor binding, or by perturbing subsequent signal transduction and receptor internalisation, particularly through the TRIF-dependent pathway that is initiated by endosomal TLR4 signalling. To interrogate this mechanism, cell surface expression of TLR4 following stimulation with LPS was assessed by flow cytometry in order to measure receptor internalisation that occurs upon ligand-receptor binding as reported previously by Richard *et al* [221]. In this assay BMDMs were pre-treated with 3μM sunitinib or DMSO vehicle for 1 hour prior to stimulation with LPS for 0, 10, 30 or 60 minutes. Signalling was arrested by placing cells on ice, and samples were harvested and stained with fluorophore-conjugated antibodies. The flow cytometry gating strategy is shown in Figure 3.11a. Single cells were isolated based on FSC and SSC profiles, and F4/80 expression was used as an additional quality control gate for macrophages. Notably, fewer cells were collected from 60 minute samples, possibly due to cell fragmentation and loss during the straining procedure. Geometric mean fluorescence intensity (gMFI) was used to assess TLR4 expression. As expected, TLR4 expression was found to gradually decline over an hour of LPS stimulation, with a significant loss after 30 minutes in both vehicle and sunitinib groups ($p<0.05$, Figure 3.11b). At 60 minutes this difference was only significant in sunitinib treated cells, likely due to higher variance in the vehicle group ($p<0.05$; Figure 3.11b). Overall, no difference was observed between vehicle and sunitinib treated cells (Figure 3.11b-c), demonstrating that sunitinib does not inhibit LPS-induced NF-kB activation in BMDMs by inhibiting TLR4 internalisation.

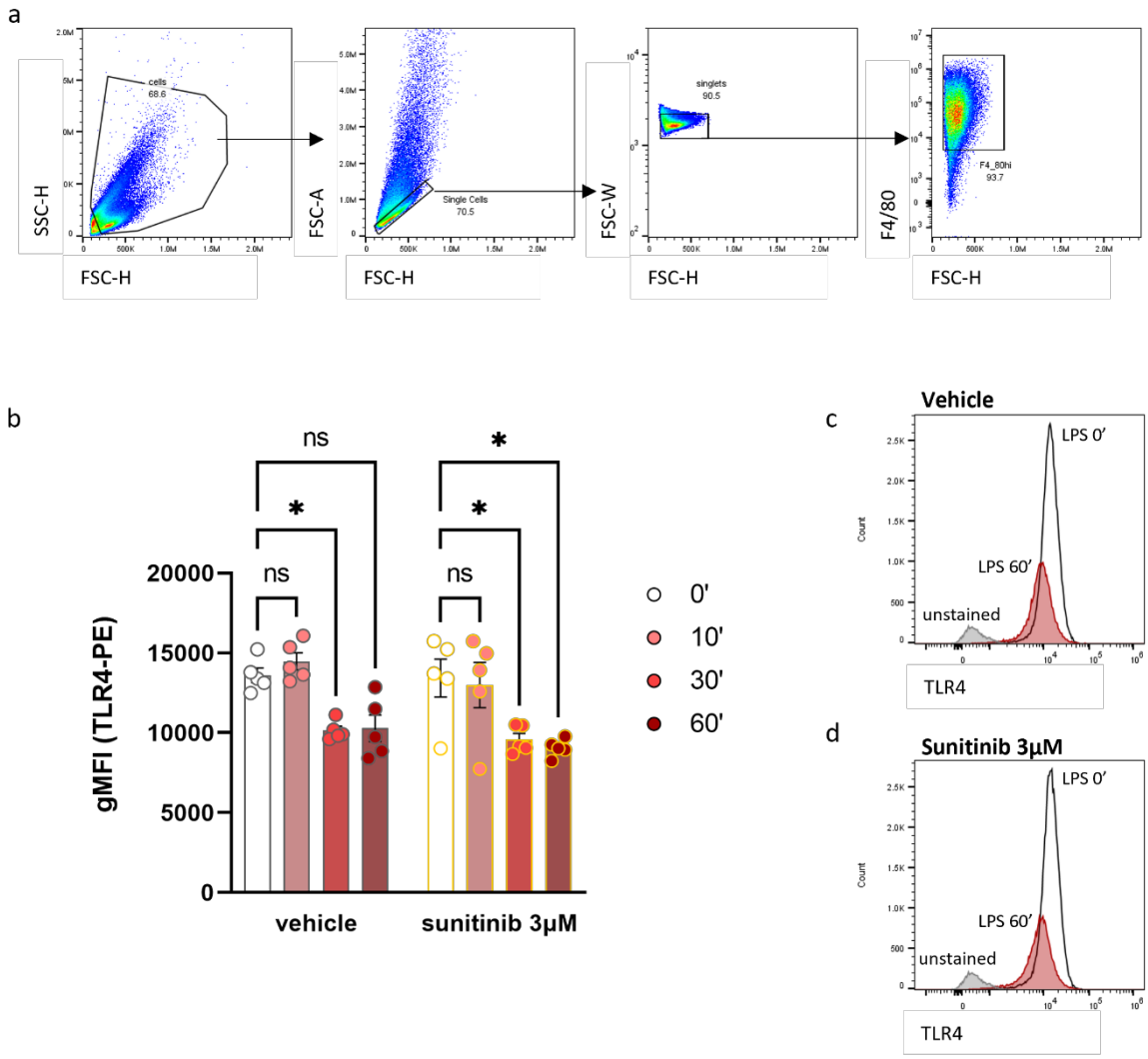


Figure 3.11: Sunitinib does not affect internalisation of TLR4. Bone marrow derived macrophages (n=5) were pre-treated with sunitinib (3µM) or DMSO vehicle for 1 hour prior to stimulation with LPS (100ng/mL) and cell surface TLR4 expression was assessed by flow cytometry at the indicated timepoints. Flow cytometry gating strategy **(a)**. Geometric MFI (gMFI) of TLR4 **(b)** and representative histograms **(c)**. Data shown are biological replicates ± SEM. *p<0.05. Statistical significance measured by 2-way ANOVA followed by Sidak's post-hoc test.

3.3.7 Effect of sunitinib on NF-κB pathway phosphorylation

So far, I have deduced that sunitinib causes inhibition of NF-κB activity at a point downstream of TLR4 signalling and so I next sought to examine upstream signalling components in the NF-κB pathway that might be inhibited by sunitinib treatment. Using BMDMs stimulated with LPS over a timecourse of 15 minutes, phosphorylation of canonical NF-κB signalling pathway components IKKα/β, IκBα, and p65 were examined by western blotting (Figure 3.12a). IKKα/β kinase activity is activated upon phosphorylation at key serine residues (Ser 176/180 of IKKα and Ser177/181 of IKKβ), and activated IKKα/β subsequently phosphorylates IκBα at Ser32/Ser36, triggering its ubiquitination and degradation [222]. The NF-κB subunit p65 is itself phosphorylated by IKKα/β at Ser536, resulting in transactivation [48]. Here, it was found that levels of phosphorylated p-p65 (Ser536) modestly increased after 15 minutes of LPS stimulation, relative to total p65 protein expression in vehicle treated cells (Figure 3.12b), although this increase was not statistically significant. In sunitinib treated cells, this increase was abolished but in cells treated with the selective IKKα/β inhibitor IKK-16, an increase in phosphorylation was still observed over time. IκBα protein expression was detected in BMDMs but signal for p- IκBα was too low to be detected. As proteasomal degradation is a direct consequence of IκBα phosphorylation, levels of total protein were quantified relative to the GAPDH loading control but this remained consistent over the 15 minute LPS stimulation (Figure 3.12). One consistent observation made was the relatively high level of p-p65 present in unstimulated cells, possibly due to background NF-κB signalling as a result of culturing technique or cell harvesting technique.

As a tyrosine kinase involved in TLR4/NF-κB signalling, phosphorylation of Src was also interrogated in LPS-stimulated BMDMs (Figure 3.12d-e). In absence of LPS, Src phosphorylation is significantly lower in sunitinib treated cells than in BMDMs treated with vehicle ($P<0.05$) or IKK-16 ($p<0.01$) (Figure 3.12e). Upon addition of LPS, the only significant difference observed is between sunitinib and IKK-16 treated cells at 15 minutes ($p<0.05$; Figure 3.12e). These data suggest that sunitinib may have a role in inhibiting Src phosphorylation in inflammatory signalling, yet as

these effects are modest, Src is unlikely to be solely responsible for sunitinib anti-inflammatory activity.

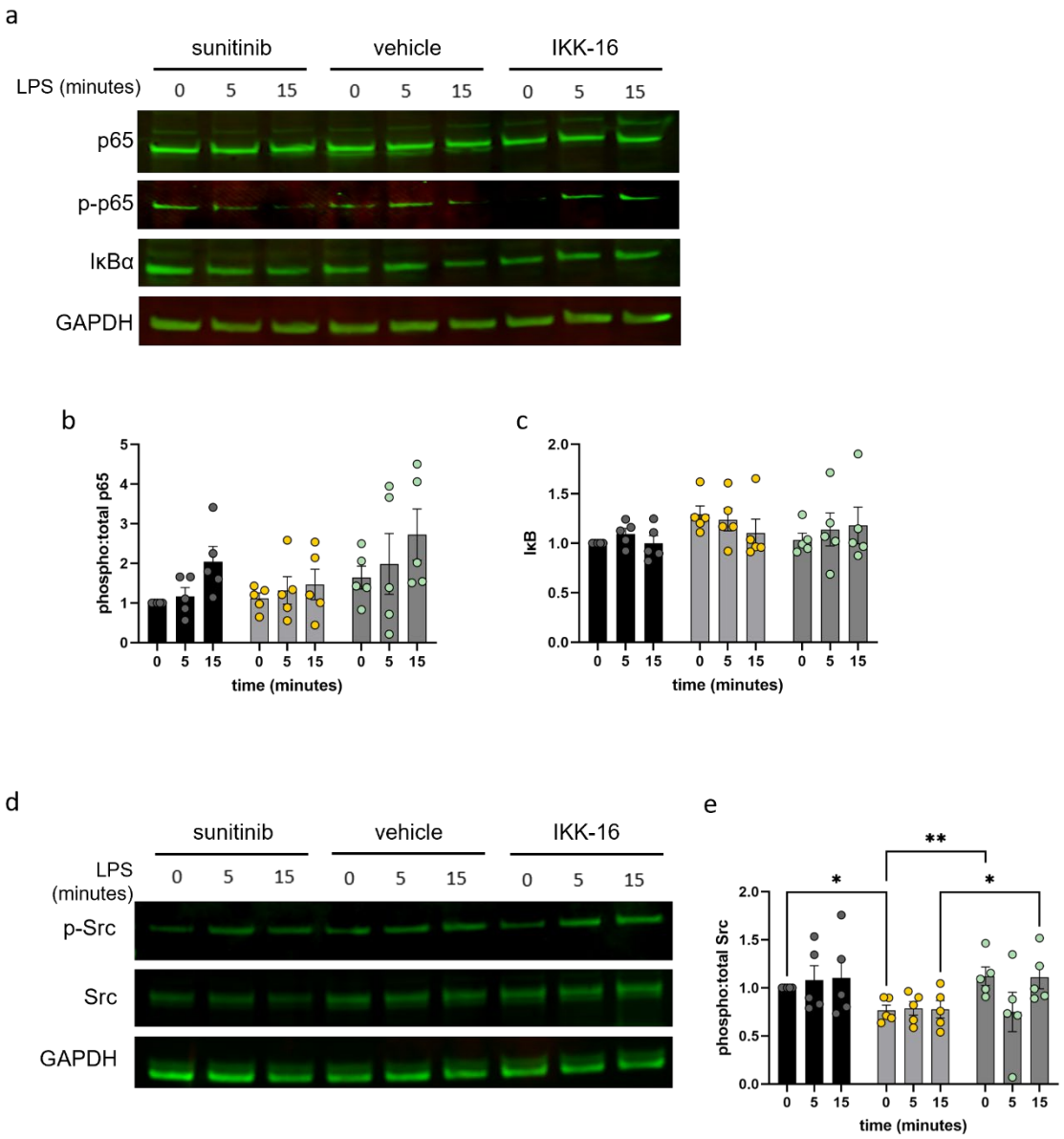


Figure 3.12: Sunitinib does not affect canonical NF-κB signalling. (a) Representative western blots for total and phosphorylated p65, and total IκB and **(d)** total and phosphorylated Src in BMDMs pre-treated with either vehicle (grey symbols), sunitinib (3μM; yellow symbols), or IKK-16 (1μM; green symbols) and stimulated with LPS for the indicated time. GAPDH was used as the loading control. Quantification of **(b)** phospho:total p65, **(c)** total IκB , and **(e)** phospho:total Src relative to unstimulated vehicle for each replicate.*p<0.05, **p<0.01. Only significant pairwise comparisons are shown. Statistical significance measured by 2-way ANOVA followed by Sidak's post-hoc test. Data are plotted as means of biological replicates (n=5) ± SEM.

3.3.8 Investigating the kinase target of sunitinib in LPS induced NF-κB activation though phosphoprotein array

Having ruled out TLR4, as the key molecular target through which sunitinib exerts its anti-inflammatory effects, I sought to further explore other potential kinase targets. Sunitinib is widely described as a multi-target kinase inhibitor, however it has particularly high affinity for type III Receptor Tyrosine Kinases (RTKs), including PDGFR, VEGFR and CSF1R. To test whether any of these targets are important in the LPS induced inflammatory response in macrophages, a protein phospho-array of RTKs was performed on BMDMs following 1 hour of LPS stimulation. This experiment reveals widespread expression and phosphorylation of RTKs in LPS-stimulated BMDMs (Figure 3.13a). The vehicle blot contained a substantial degree of noise which made analysis challenging (Figure 3.13a). Nevertheless, data were quantified and expression was compared between vehicle and sunitinib treated samples (Figure 3.13b).

Unexpectedly, the greatest signal came from phospho-muscle specific kinase (MuSK) (Figure 3.13a), an RTK important in the development and maintenance of the neuromuscular junction [223]. High expression of this receptor has not been reported in macrophages and no literature has yet linked MuSK activity to LPS-induced inflammatory signalling pathways. It is therefore possible that this result is caused by non-specific antibody binding. Similarly, tropomyosin receptor kinase C TrkC (also known as neurotrophic receptor tyrosine kinase type 3) is thought to have a neuronal restricted expression pattern [90] and is therefore also an unlikely candidate to be important in macrophage inflammatory signalling. Conversely, receptors known to be highly expressed on macrophages such as colony stimulating factor 1 receptor (CSF-1R) [13], Mer [100] and insulin-like growth factor 1 receptor [224] were not detected at high levels in the array, although it is possible that they were not phosphorylated in response to LPS stimulation.

Other kinases that showed a strong signal in the array included members of the epidermal growth factor receptor family EGFR and ErbB2, platelet derived growth factor receptor alpha (PDGFRa), fms related receptor tyrosine kinase 3 (FLT3), and Axl. Of detectable phospho-kinases, epidermal

growth factor (EGFR), PDGFRa and vascular endothelial growth factor receptor 1 (VEGFR1) were reduced in sunitinib cells versus vehicle cells (Figure 3.13b).

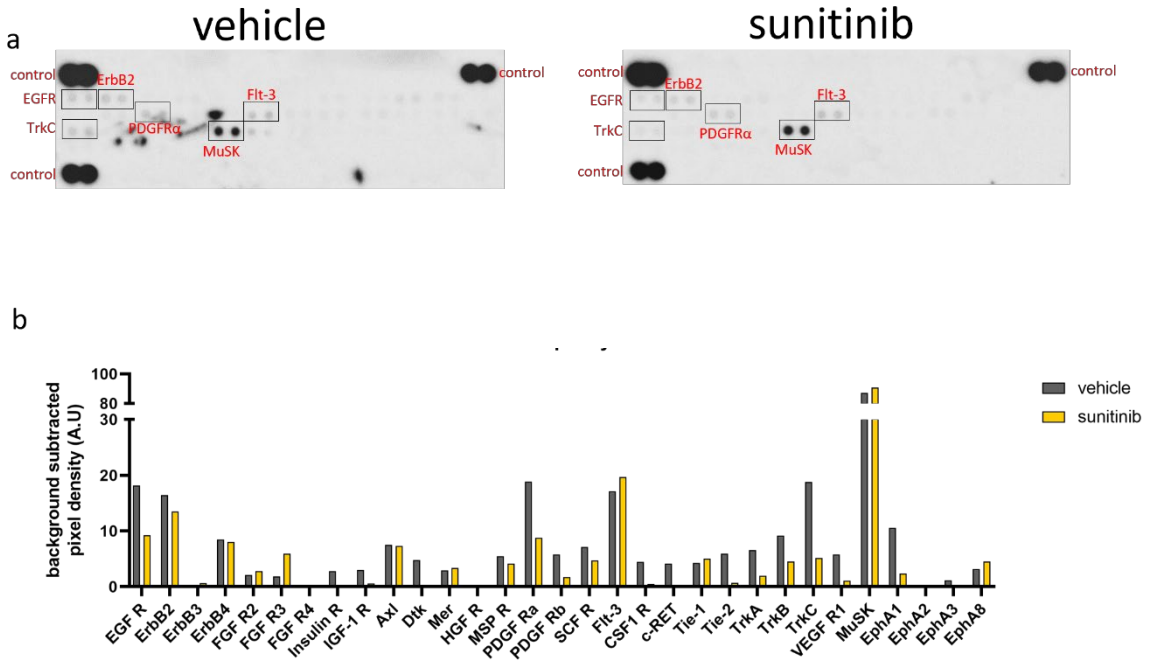


Figure 3.13: Sunitinib alters the receptor tyrosine kinase phosphorylation landscape in macrophages. Phospho-kinase array for receptor tyrosine kinases in bone marrow derived macrophages (n=3, pooled) treated with either DMSO vehicle (left) or sunitinib (3μM) (right) for 1 hour prior to stimulation with LPS for 10 minutes **(a)**. Signal quantification is shown in **b**.

3.3.9 Investigating macrophage specificity of sunitinib

Despite not being able to delineate the exact mechanism of sunitinib mediated NF-κB inhibition, an important question to address is whether this activity is specific to, or selective for, macrophages, or whether sunitinib inhibits NF-κB across cell types. While almost all cells express NF-κB and upstream signalling components, for the sake of using the same LPS stimulus I wanted perform experiments using a cell line which also expresses TLR4. While TLR4 expression is mostly restricted to innate immune cells, other cell types including endothelial cells and fibroblasts are known to also express TLR4 [90]. The mouse derived fibroblast cell line L929 has been reported to express TLR4 [225] and respond to LPS stimulation by producing NO. As with BMDMs in Figure 3.7, cultured L929s were pre-treated with a concentration range of sunitinib for 1 hour before stimulation. LPS alone was found to induce little NO production so LPS (100ng/mL) and IFNγ (20ng/mL) were used in combination for 24 hours. NO production was strongly induced under these conditions and was dose-dependently inhibited by sunitinib (IC_{50}=4.856μM) (Figure 3.14a). Dexamethasone (1μM) and IKK-16 (1μM) were once again used as positive controls and inhibited NO production by 98% and 64% respectively. Cell viability in L929s with sunitinib was comparable to that of BMDMs up to 10μM, but was dramatically compromised at 31.25μM ($p<0.0001$, Figure 3.14b). These results indicate that the anti-inflammatory activity of sunitinib is not specific to macrophages, ruling out the sole molecular target as a macrophage-specific kinase such as CSF1R (Table 3.3). A direct comparison of potency in BMDMs *versus* L929s is challenging given the different stimuli used. It is however tempting to speculate that with an IC_{50} of 4.856μM in L929s and 0.593μM in BMDMs, that BMDMs are more sensitive to sunitinib mediated anti-inflammatory activity.

Table 3.3: Expression of NF-κB signalling components and Receptor Tyrosine Kinases in different cell types

	BMDMs	*L929 fibroblasts*
TLR4	✓	✓
IKKα/β	✓	✓
IκBα	✓	✓
NF-κB	✓	✓
CSF-1R	✓	*x*
VEGFR	✓ *(VEGFR2)*	✓ *(VEGFR1)*
EGFR	✓	✓
PDGFRs	✓	✓
Src	✓	✓

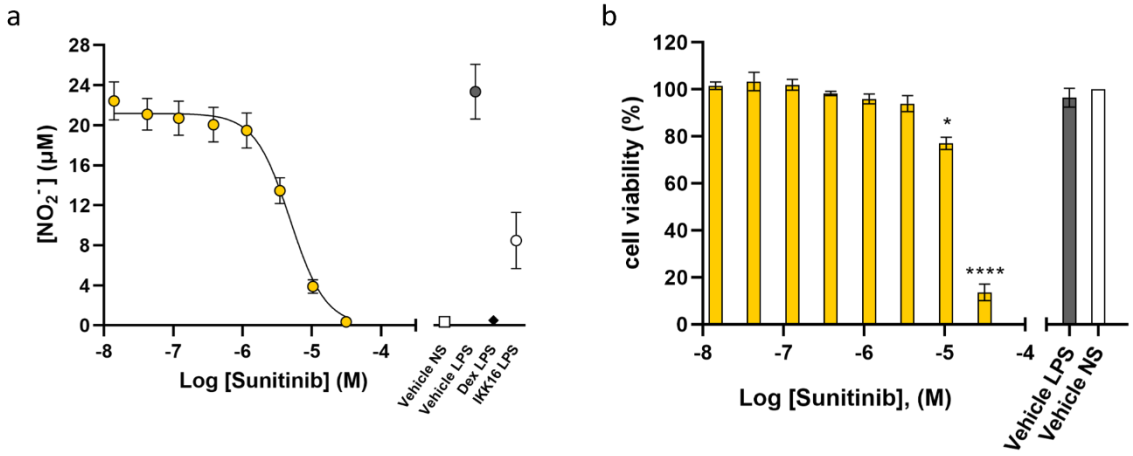


Figure 3.14: Sunitinib inhibits NO production in fibroblasts. L929 fibroblasts were treated with a concentration range of sunitinib for 1 hour prior to stimulation with LPS (100ng/mL) and IFNγ (20ng/mL) for 24 hours. Supernatant NO concentration was measured **(a)**, and cell viability was assessed **(b)**. Dexamethasone (1μM) and IKK-16 (1μM) were used as positive controls. Data are expressed as means ± SEM. *p<0.05, ****p<0.0001 vs vehicle LPS treated cells. Statistical significance determined by one-way ANOVA followed by Tukey's post-hoc test.

3.4 Discussion

In this chapter I sought to perform a drug-repurposing screen of existing medicines for novel anti-inflammatory activity. From this screen the TKIs bosutinib and sunitinib were identified as potent inhibitors of NF-κB activity in a macrophage NF-κB reporter cell line, and subsequent experiments revealed that this remained true in primary murine macrophages. Finally, I aimed to determine the molecular mechanism through with sunitinib inhibits NF-κB, however this remains elusive.

3.4.1 Designing a target-based drug-repurposing screen for anti-inflammatory activity based on macrophage NF-κB inhibition

Drug repurposing screening projects increasingly use sophisticated computational approaches to screen thousands of compounds in high-throughput studies. Here, an experimental approach was taken to perform a medium-throughput screen of a library of 159 FDA-approved medicines for anti-inflammatory activity in macrophages (Figure 3.1-2).

NF-κB is a central mediator of inflammatory signalling in macrophages with characterised upstream signalling pathways and its dysregulation has been implicated in both chronic and acute inflammatory diseases such as rheumatoid arthritis, atherosclerosis, and sepsis [47,180,226]. Curiously, despite extensive research efforts, most specific NF-κB inhibitors have failed to progress through clinical trials due to lack of efficacy [47,227,228]. This, coupled with the fact that NF-κB pathway is renowned for its many context-dependent effects from survival, to proliferation, to inflammatory signalling, which would all be affected by pathway inhibition, mean that it could be argued that NF-κB is not an ideal target for investigating anti-inflammatory medicines. Nevertheless, NF-κB was chosen for the current screen as its importance to the inflammatory response in macrophages is undeniable. Additionally, as a hugely intricate signalling pathway with many upstream components feeding into it, there is a high chance that the screen will generate a positive hit from one of these components being inhibited.

Another important decision was the choice of inflammatory stimulus to be used in the screen. Physiologically relevant stimuli such as oxLDL, a driver of atherosclerosis [117,229], or recombinant

TNFα which is present at high concentrations in the milieu in most inflammatory diseases [229,230], may be advantageous in uncovering compounds applicable to chronic inflammatory disease. Similarly, PAMPs such as LPS, ssRNA or viral particles can be triggers of acute inflammation upon infection. For this project, LPS was chosen due to its reliability at inducing inflammatory signalling and cytokine production. LPS is also inexpensive and widely used, with well-known upstream signalling pathways [44,47].

This screen successfully identified 19 active compounds to cause over 25% signal inhibition (Table 3.1). The presence of known immunomodulators such as adapalene, ibuprofen and several glucocorticoid receptor agonists supports the validity of the screen. There were however surprising compounds that were not picked up in the screen. Namely, statins have been previously reported to inhibit NF-κB in myeloid cells [231] however here, the statins Lovastatin and Simvastatin were not found to meet the signal reduction threshold. Moreover, sulfasalazine, a DMARD used in the treatment of RA is believed to act through the NF-κB pathway [232] yet here it was not found to affect NF-κB activity.

One of the key findings from the screen was the number of TKIs that were identified as to be active. Phosphorylation is key to NK-κB signalling, but primarily hinges on Serine/Threonine kinases for IKK/IκB/NF-κB phosphorylation. Tyrosine kinase activity is important in the NF-κB pathway upstream of this. In TLR4 signalling, phosphorylation of TLR4 tyrosine residues is thought to be required for signalling, with phosphorylation-null mutants failing to activate NF-κB and MAPK [233]. The kinase responsible for this is not fully known, but TLR4 has been shown to interact with Src, BTK, Lyn and Syk [44], and it has been proposed that EGFR is also involved in TLR4 activation [44]. Furthermore, Src [87,234,235] and BTK [162,236] have been implicated in NF-κB signalling independently from TLR4. Most TKIs, including those screened here, are used for cancer therapy, so their use as anti-inflammatory agents is largely unexplored outside of a tumour context.

3.4.2 Bosutinib identified as an inhibitor of NF-κB in macrophages

Bosutinib was first approved in 2013 for the treatment of chronic myeloid leukaaemia [237]. It was developed as an inhibitor of the BCR-ABL fusion-protein found in Philadelphia Chromosome

positive patients as a result of oncogenic translocation of the *ABL1* and *BCR* genes[237]. Bosutinib is also an inhibitor of Src [237], and BTK [238] but is not known to inhibit growth factor RTKs such as PDGFR, IGFR1 or EGFR[237]. Previous literature has implicated bosutinib in inflammatory signalling pathways. Bosutinib has been reported to reduce production of TNFα, IL-6 and IL-12 in LPS stimulated BMDMs and induce IL-10 production as a result of its inhibition of salt inducible kinase (SIK) family proteins [239]. Building from this, Ma *et al.* reported that intranasal bosutinib reduced TNFα release and inhibits NF-κB nuclear in a mouse model of intracerebral haemorrhage, and also linked this activity to SIK2 inhibition [216]. Here, it was found that bosutinib inhibited NF-κB in RAW-Blue cell line macrophages (Figure 3.5) and inhibited TNFα production in BMDMs as well as CCL2, but its effect on other cytokines was not linear (Figure 3.6).

3.4.3 Sunitinib identified as an inhibitor of NF-κB in macrophages

Sunitinib malate, originally marketed by Pfizer as SUTENT, has been routinely used since its approval in 2006 for the treatment of advanced renal cell carcinoma (RCC), advanced pancreatic neuroendocrine tumours, and as a second-line treatment for gastrointestinal stromal tumour (GIST). Sunitinib malate is a broad-spectrum kinase inhibitor known to target type III RTKs including PDGFRα and PDGFRβ, VEGFR, FLT3 and CSF-1R among others[240]. Of these, CSF-1R is of particular interest in the context of inflammation due to the critical role of CSF-1 signalling in myeloid lineage commitment during haematopoiesis [241].

Previous literature had linked anti-inflammatory activity to sunitinib both in cancer patients, where there is evidence that sunitinib reduces tumour myeloid derived suppressor cell [242–244] and Treg populations [244,245], as well as *in vitro* studies in which sunitinib's ability to attenuate cytokine production has been noted. In particular, sunitinib has been shown to reduce cytokine production of TNFα and IL-6 in RAW-264 macrophages, mouse bone marrow derived dendritic cells and human peripheral blood mononuclear cells upon TLR7 signalling [199] and in human monocyte derived M1 macrophages, sunitinib has been reported to induce IL-10 production [201]. The present study added to this knowledge by reporting that sunitinib dose dependently reduces production of cytokines

TNFα, IL-6, CCL2, IL-1β and NO in murine macrophages (Figure 3.7) and skews macrophage polarisation towards an M1 phenotype (Figure 3.8).

In animal models of disease, sunitinib, in combination with the TKI erlotinib, has been found to reduce infectivity and IL-18 cytokine levels in a model of dengue infection [246] and reduces endotoxaemia associated cytokine storm [199]. There are conflicting reports on sunitinib's ability to modulate immune cell recruitment. In patients, sunitinib's tumour growth inhibiting ability has been partially attributed to increased CD11b+ cell recruitment to tumours [247]. In animal models however, sunitinib has been reported to inhibit macrophage recruitment in a model of corneal injury, possibly via VEGFR inhibition [248] and in a different murine model of peritonitis it was found that sunitinib does not affect leukocyte recruitment [247].

Here, we report that sunitinib is a potent inhibitor of NF-κB activity in macrophages, with an IC_{50} of 1.26μM in the RAW-Blue reporter cell line (Figure 3.5). Previous literature has alluded to effects of sunitinib on the NF-κB pathway. In neurons, sunitinib induces pro-inflammatory signalling of NF-κB, COX2, and iNOS [249] whereas in dendritic cells, sunitinib has no effect on NF-kB signalling in response to LPS *in vitro* [245]. Additionally, sunitinib has previously been identified in a screen for NF-κB inhibitors using the ME180 human cervical cancer cell line [200]. These findings suggest that sunitinib's inhibition of NF-κB may therefore be cell specific, although in this chapter I found that both macrophages and L929 fibroblasts respond to treatment in a dose dependent manner, with perhaps some differences in potency (Figure 3.14). Nevertheless, I report here effects of sunitinib on macrophage polarisation (Figure 3.8) and effector functions such as cytokine production (Figure 3.7) and phagocytosis (Figure 3.9)

It is likely that differences in sunitinib mediated NF-κB activity are the result of the cell type specific kinase expression profiles. Although attempts were made here to delineate the key kinase target responsible for sunitinib mediated NF-κB inhibition (Figures 3.11-13), I was not able to successfully determine where in the signalling pathway sunitinib acts however AP-1 and TLR4 were ruled out as key targets (Figure 3.9-10). As the IKK/IκB/p65 phosphorylation cascade relies primarily on serine/threonine and not tyrosine residue phosphorylation, I speculate that these proteins are not

being directly inhibited by sunitinib. Indeed, the screen in which sunitinib was previously identified as an inhibitor of NF-κB found that sunitinib did not affect IκB phosphorylation in a reporter cell line assay although its mechanism of action was not further explored [200].

Ultimately, as sunitinib is by nature a multi-tyrosine kinase inhibitor [240] it is unlikely that one key target is responsible for all its observed anti-inflammatory effects. A more plausible explanation is that partial inhibition of multiple pathways that feed into NF-κB activation are targeted by sunitinib. Nevertheless, prime candidates for this activity are the primary targets of sunitinib; RTKs including MSPR, PDGFR, VEGFR, CSF1R, Kit and Flt3. Although previous reports have linked sunitinib anti-inflammatory signalling to VEGFR and PDGFR pathways [199,248], it is not obvious how signalling by these receptors would be directly implicated in the LPS/TLR4/NF-κB pathway unless *via* an autologous feedback mechanism, whereby macrophage stimulation induces ligand production and a positive feedback loop.

An interesting mechanism proposed by Glenn and van der Geer [250] involves proteolytic cleavage of CSF1R induced by TLR signalling ultimately promoting macrophage activation. In this case, a feedback mechanism initiated upon inhibition of CSF1R with sunitinib would lead to overall reduced macrophage activation and cytokine production. Moreover, CSF-1/CSF1R signalling has been shown to induce activation of the non-canonical NF-κB pathway and M2 macrophage polarisation [10]. It would be interesting to repeat experiments in this chapter in CSF1R deficient cells or in the presence of a blocking antibody to further interrogate a CSFF1R dependent mechanism.

It has also been reported that another RTK, EGFR, is phosphorylated and activated in RAW264.7 macrophages upon LPS stimulation inducing upregulation of TLR4, and this can be blocked with EGFR inhibitor Erlotinib [251]. Indeed, phosphor-EGFR was identified in the phosphor-kinase array presented in this chapter and was reduced with sunitinib (Figure 3.13). Although it has been reported that sunitinib does not inhibit EGFRs in a kinase activity assay [240], this type of RTK-TLR4 crosstalk could be responsible for results seen in this chapter. Here, surface TLR4 was measured upon LPS stimulation and although expression was not found to increase over the 1 hour time period studied

(Figure 3.8), increased surface TLR4 expression with longer LPS stimulations cannot be ruled out and could be a mechanism through which sunitinib acts.

3.4.4 Limitations of study

A major limitation of the current study is that all experiments have been performed in a murine system and therefore the effects of sunitinib on human cells are unknown. Although species differences are inevitable, one benefit of drug-repurposing studies is that the drug is known to have activity at human isoforms of target proteins. However, as the target of sunitinib in regards to NF-κB inhibition is unknown and therefore possibly different in mice and humans, it will be important to repeat the experiments in this chapter using human monocyte derived macrophages to determine whether anti-inflammatory activity is seen in a human system.

Another limitation is the reliance on LPS signalling as a paradigm for inflammatory responses. As discussed already in this chapter, there are several advantages to using LPS to interrogate macrophage mediated inflammatory responses, hence its use throughout this chapter. However, distinct signalling pathways are induced by different inflammatory stimuli and so the action of sunitinib in non-LPS induced inflammation remains unknown.

Another key limitation of this study was that only 159 medicines were tested, leaving many more — potentially more potent — repurposing candidates unexplored. Having shown here the reliability and efficacy of the repurposing screen design used here, future studies could expand this framework to include other medicines. In particular, a screen of all clinically used TKIs should be prioritised given the class effects of TKIs seen here in the present screen.

3.4.5 Summary

In this chapter I have found that the tyrosine kinase inhibitors Bosutinib and Sunitinib are potent inhibitors of NF-κB activity in macrophages *in vitro*. While Bosutinib has only partial cytokine suppressive activity, sunitinib broadly inhibits production of pro-inflammatory cytokines. The mechanism by which sunitinib exerts these effects remains unclear, but is not likely achieved through direct inhibition of TLR4.

Chapter 4: Effects of sunitinib in acute inflammation *in vivo*

4.1 Introduction

4.1.1 Murine Models of Acute inflammation

Animal models have been indispensable in the study of inflammation biology and pre-clinical investigation of anti-inflammatory drugs. Mouse models are the most common, with availability of genetic knockouts and ease of handling contributing to their popularity. Murine models can be used to study local inflammatory responses for example in peritonitis [9] or disease models like gouty arthritis [252], or to assess systemic inflammation such as that associated with sepsis [253].

Peritonitis models are regularly used to study local inflammation with readouts including leukocyte trafficking and recruitment [254]. Of such models, Zymosan Induced peritonitis (ZIP) is the best characterised and serves as a relatively simple-to-perform model of self-resolving acute inflammation [254]. Zymosan is a yeast cell wall extract from *Saccharomyces cerevisiae* that is recognised *via* TLR2 and Dectin-1 receptors [9]. The kinetics of this model have been well studied, with F4/80+^{hi} macrophages initially leaving the peritoneum for local lymph nodes [9]. Peak neutrophil recruitment is observed at around 4 hours after initial insult, followed by infiltration of Ly6C^{hi} monocytes at 16-24 hours [9]. Inflammatory cytokine production of TNFα, CCL2, IL-6 can also be measured in the peritoneal lavage fluid in this model [254].

4.1.2 Murine models of systemic inflammation and sepsis

Murine models of sepsis and septic shock can be useful tools for studying the biological processes involved in acute systemic inflammation. However, despite this use as a research tool, the translatability of findings from murine sepsis models to human disease has been scrutinised [253,255], owing to the fact that drugs found to be promising in pre-clinical animal studies have gone on to fail in sepsis patients [253,255,256].

The perhaps most commonly used sepsis-like model is endotoxaemia, where isolated LPS is injected, usually intraperitoneally, into mice. The consequences include high levels of cytokine production, hypotension and hypothermia, although host responses are closely linked to LPS dose used. Low

LPS doses for example (<1mg kg^{-1}) can be used to study immune tolerance or priming processes [257,258] whereas higher doses (>10mg kg^{-1}) cause systemic inflammatory responses and are typically lethal [253]. Notably, production of cytokines such as TNFα, IL-6 and CCL2 is found to peak more rapidly and at higher concentrations than in other models, but levels also decline at a faster rate [253]. A major limitation of this model and important distinction from human sepsis is that there is no source of ongoing stimulation as there are no living, dividing bacteria present. For this reason, endotoxaemia cannot be considered a true model of sepsis, and is perhaps more accurately described as a PAMP-initiated model of systemic acute inflammation, that can nevertheless be useful in studying the biological processes involved in sepsis and systemic inflammation.

A slightly improved model is the bacterial injection sepsis model. Here, live bacteria of a particular species such as *Escherichia coli, Staphylococcus aureus,* or *Pseudomonas aeruginosa* are injected intraperitoneally or intravenously resulting in increased systemic cytokine production comparable to endotoxaemia models [253]. Although the option of including Gram positive or Gram negative bacteria adds some power to this model over endotoxaemia, there are several drawbacks. Firstly, large bolus doses are often required due to the inability of most bacterial strains to replicate *in vivo,* which does not well mimic the continual bacterial stream seen in human sepsis [253]. Secondly, antibiotic administration and fluid resuscitation are often required to avoid haemodynamic collapse and survival long enough to observe organ damage end points [253].

The considered gold standard murine sepsis model is caecal ligation and puncture (CLP) [253,259]. CLP is a surgical procedure that occurs under anaesthesia and involves needle puncture of the caecum, allowing caecal bacteria to leak into the peritoneal cavity thereby causing polymicrobial peritonitis, bacteraemia, multi-organ failure and ultimately death [259]. CLP is considered to be the most physiologically relevant of the sepsis models due to shared symptoms with human disease such as polymicrobial insult, hyper- then hypo-haemodynamic transition, and bacteraemia, the presence of bacteria in the bloodstream [253]. Like bacterial injection models, CLP relies on fluid resuscitation and antibiotics, although the timing of administration and choice of antibiotics can vary. As well as this, another source of inter-lab variability in this model can arise from differences in surgical techniques,

such as size and number of needle punctures and placement of caecal ligature, making this model difficult to standardise [253]. The greatest challenges with this model are the technical difficulties of performing surgery as well as severity-limiting animal welfare constraints, both of which limit the widespread adoption of this specialised procedure.

An elegant model which overcomes some of these technical limitations is the caecal slurry model. This model involves isolating the caecal contents from donor mice and purifying the contents to a bacterial suspension that can be quantified, standardised, and batch stored [253]. This polymicrobial suspension is then re-injected intraperitoneally into test mice to cause polymicrobial infection and inflammation much like bacterial injection models, only with the advantage of having a true polymicrobial insult.

4.1.3 Acute Lung injury in systemic inflammation

Acute Lung Injury (ALI) and related acute respiratory distress syndrome (ARDS) are clinical conditions characterised by alveolar injury, hypoxaemia, and pulmonary oedema [260]. This damage can be the direct result of inflammatory mediators produced in sepsis [109,261] and therefore murine models of ALI are typically analogous to models of sepsis. Several stimuli are used to induce ALI in mouse models, including intraperitoneal or intravenous injection of LPS or inhalation of live bacteria as well as techniques such as mechanical ventilation, saline lavage and pulmonary ischaemia-reperfusion injury [260]. In addition to pro-inflammatory mediator production, histological features of ALI can be assessed including diffuse alveolar damage with thickening of alveolar septa, diffuse alveolar haemorrhage and immune cell infiltration [262]. Alveolar barrier injury is mediated by pro-inflammatory cytokines such as TNFα and IL-1β, neutrophil extracellular trap formation, and endothelial barrier dysfunction [261].

4.1.4 Liver dysfunction in systemic inflammation

Liver injury and dysfunction commonly occurs as part of multiple organ failure (MOF) in sepsis, although acute liver failure (ALF) is relatively rare and seen only in <2% patients [109]. Sepsis-associated liver dysfunction involves high levels of pro-inflammatory cytokine production by liver

resident Kupfer cells, and liver damage caused by hepatocyte necrosis due to poor perfusion [109,261]. A defining feature of sepsis-associated liver damage in human disease in animal models is elevated serum levels of liver enzymes including aspartate aminotransferase (AST) and alanine aminotransferase (ALT) [261,263].

4.1.5 Acute Kidney Injury in systemic inflammation

Similarly to ALI and liver failure, acute kidney injury (AKI) can occur as part of MOF in sepsis [264]. AKI results in electrolyte and acid-base dysregulation, disruption of extracellular volume and accumulation of nitrogenous waste products [265]. Various animal models of AKI have been developed, with surgical animal models inducing renal ischaemia reperfusion injury and CLP, and non-surgical AKI models including techniques such as LPS injection and bacterial injection. Physiological markers of AKI are elevated creatinine and blood urea nitrogen [264], and histological features include immune cell infiltration, vascular endothelial injury, glomerulonephritis, and acute tubular necrosis caused by renal hypoperfusion [266].

4.1.6 Animal models of inflammation in drug repurposing studies

The animal models discussed above, as well as others, have been used to test drug repurposing candidates in inflammation *in vivo* (table 4.1). In particular, endotoxaemia models have been the go-to model for many of drug repurposing studies, likely due to the simplicity of the model itself and ability to measure a wide range of inflammatory readouts. In many cases insights from animal models have helped lead to new insights into drug mechanism.

Table 4.1: Drug repurposing candidates tested in animal models of acute inflammation

Drug	Biological target	Original indication	Murine model of inflammation used	Key findings	Reference
Momelotinib	JAK/JAK2	Myelofibrosis	Endotoxaemia and *E. coli* induced sepsis	Improved survival, decreased cytokine production of TNFα, IL-6 decreased markers of organ damage Inhibits NF-κB signalling *via* TBK-1 inhibition	[267]
Thioridazine	Dopaminergic D1/D2 receptors	Schizophrenia	Endotoxaemia	Improves survival Decreases lung damage Inhibits NF-κB signalling *via* inhibition of IKKβ	[186]
Sorafenib	RTKs (VEGFR, PDGFR, c-Kit)	Renal cell carcinoma	Endotoxaemia	Reduced cytokine production, and improved lung histology	[268]
Ibrutinib **Acalabrutinib**	BTK	Chronic myeloid leukaemia	CLP	Reduced cytokine and chemokine production Reduced NF-κB and inflammasome signalling Improved cardiac function	[96]
Escitalopram	Serotonin transporter	Antidepressant	Intratracheal LPS-induced acute lung injury	Reduces immune infiltration and injury to lung tissue *via* SIK2 inhibition	[269]
Bosutinib	BCR-ABL	Chronic myeloid leukaemia	Intracerebral haemorrhage	Reduces TNFα and NF-κB translocation *via* inhibition of SIK2	[216]

4.2 Rationale and experimental aims of chapter

In the previous chapter, I report that the multi-tyrosine inhibitor sunitinib has anti-inflammatory activity in primary and cell-line macrophages *in vitro*. Here, I hypothesise that sunitinib will have a similar anti-inflammatory effect *in vivo* due to its anti- NF-κB activity.

Therefore, the specific aims of this chapter are to:

1) Explore activity of sunitinib in a mouse model of acute inflammation
2) Determine whether anti-inflammatory activity is linked to NF-κB inhibition *in vivo*

4.3 Results

4.3.1 Determining an *in vivo* Inflammatory model in which to test sunitinib

In the previous chapter, I characterised the *in vitro* anti-inflammatory activity of sunitinib. In order to determine *in vivo* efficacy, the first task was to select an appropriate inflammatory murine model. It was decided to initially test sunitinib in a short term model of acute inflammation to ensure that an efficacious dose could be selected. As the mechanism was suspected to involve NF-κB signalling, it was important to select an inflammatory model that is NF-κB driven in which activity of NF-κB effectors can be measured. Technical limitations and model severity constraints were also considered. Therefore, I decided that endotoxaemia would be an appropriate model given its ability to produce high levels of NF-κB induced cytokines, its relative ease to perform, and for continuity with TLR4- driven *in vitro* experiments using LPS. Endotoxaemia is a highly dynamic model, with quick onset and rapid amplification of inflammation and with various inflammatory mediators showing different kinetic profiles. Consequently, endotoxaemia models of different durations allow for different inflammatory effectors to be assessed. Previous work from the Greaves lab in experiments performed by Dr Lynda Zeboudj showed that peak production of early response cytokine TNFα is observed at 1 hour following intraperitoneal (i.p) injection of 10mg kg^{-1} LPS in male C57Bl/6 mice, and that levels rapidly decline after this (see Appendix 2). I therefore decided to initially test the effects of sunitinib in a 1 hour model of endotoxaemia induced by 10mg kg^{-1} LPS i.p in male C57Bl/6 mice using TNFα production as the primary readout.

Next, the dose and treatment schedule of sunitinib were considered. As a clinically-approved drug, pharmacokinetic and pharmacodynamic data for sunitinib exist already in the literature. Welti *et al.* (2014) published data showing plasma concentration of sunitinib over 18 hours in Balb/c mice given a 30 mg kg^{-1} oral bolus. The authors reported that sunitinib plasma concentration steadily increases for the first 6 hours, peaking at just over 1μM, then declining slowly to ~0.5μM at 12 hours and remaining detectable above 10nM at 18 hours [270]. From these data, I concluded that 30mg kg^{-1} would be a suitable dose to achieve plasma levels comparable to concentrations found to be efficacious *in vitro* and would not cause significant toxicity. I decided that due to the short experimental timeframe

and scale of inflammatory insult, administration of a sunitinib pre-loading dose prior to LPS challenge would be appropriate. Based on data published by Jun *et al.* using a similar endotoxaemia model to study drug activity [271], it was decided that pre-loading with an oral dose at 24 hours, and a second dose at 4 hours prior to injection would be beneficial to maximise target inhibition.

A positive control to determine that NF-κB inhibition does reduce inflammation in this model was added to the study by including a group receiving the specific IKK inhibitor IKK-16, which was also used as a control for *in vitro* experiments in chapter 3. IKK-16 has previously been found to inhibit NF-κB and TNFα production in endotoxaemia models when used at 30mg kg^{-1} orally or 1mg kg^{-1} intravenously [272,273]. For this study, a 10mg kg^{-1} oral dose was chosen and administered following the same dosing timeline as sunitinib.

Finally, in adherence with the 3Rs research guidance as the safety and tolerance of sunitinib in mice is well documented, it was decided that a sunitinib PBS group was unnecessary in this study. The final study design is shown in Figure 4.1a.

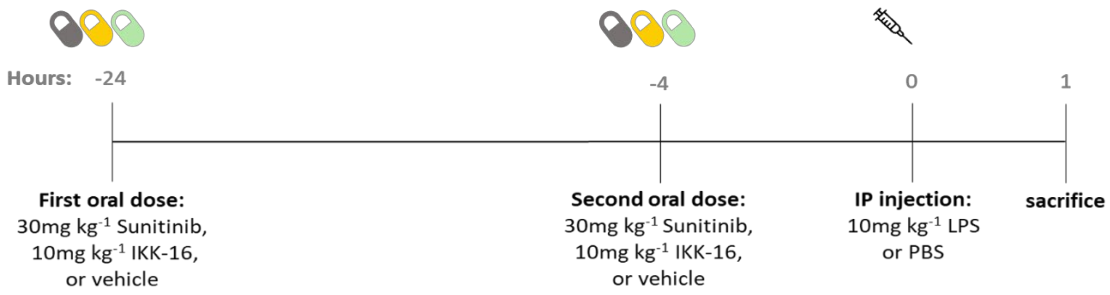


Figure 4.1: Endotoxaemia 1 hour model design. Experimental timeline. Mice were randomly assigned into groups to receive an oral dose of sunitinib (30mg kg^{-1}), IKK-16 (10mg kg^{-1}) or vehicle 24 hours before IP injection, and were given the same dose again 4 hours prior to injection. At time 0, mice were IP injected with LPS (10mg kg^{-1}) or PBS and then sacrificed after 1 hour (n=10-11 per group).

4.3.2 Effects of sunitinib on early inflammatory responses *in vivo*

Overall, 10-14 mice were used per group, based on power calculations performed using previous data from the lab [iii]. Multiple experimental batches of 8-10 mice were pooled together for analysis. Experiments followed a block design, where at least one mouse was added to each control group for every experimental batch.

The primary readout from this 1 hour endotoxaemia model is serum TNFα level as measured by ELISA. Here, I found that mice that received PBS i.p had barely detectable baseline serum concentrations of TNFα and IL-6, and CCL2 at around 60pg/mL. However, production of all three cytokines was substantially induced in LPS challenged groups, although variation between individual animals was notably high (Figure 4.2). In the sunitinib treated group, TNFα concentration was reduced by 51% compared with vehicle ($p<0.05$; Figure 4.2a), whereas IL-6 and CCL2 levels were not significantly altered. Unexpectedly, IKK-16 did not have a significant effect on TNFα or IL-6 production and caused a statistically significant increase in CCL2 ($p<0.001$; Figure 4.2c).

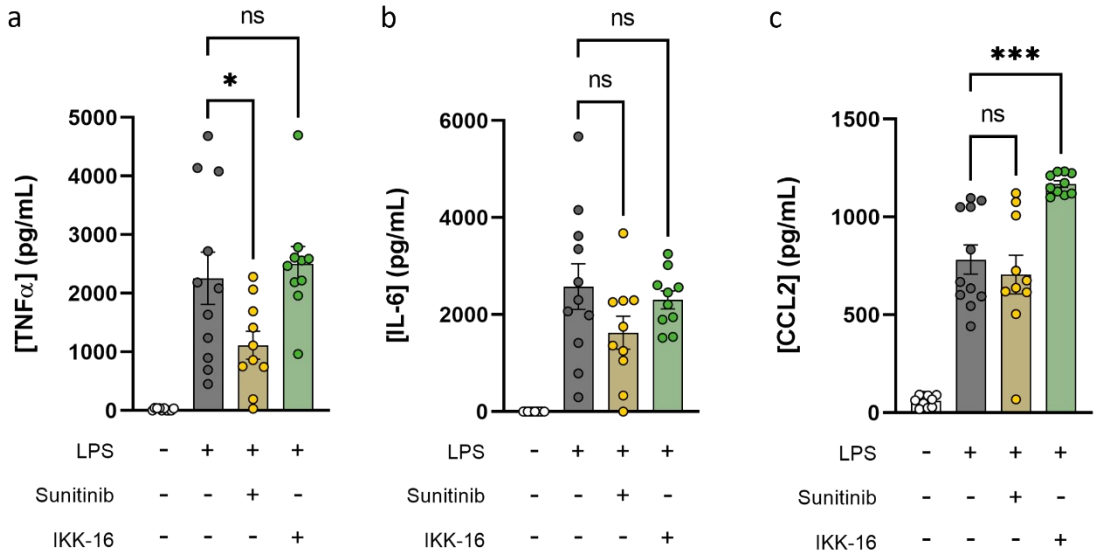


Figure 4.2: Sunitinib reduces plasma TNFα in endotoxaemia at 1 hour. Serum cytokine levels for TNFα **(a)**, IL-6 **(b)**, and CCL2 **(c)** in endotoxaemia mice were measured by ELISA. Data points represent individual animals (n=10-12). Error bars show S.E.M. *p<0.05, ***p<0.001. Statistical significance determined by one-way ANOVA followed by Tukey's post-hoc test.

[iii] Unpublished data by L. Zeboudj. See Appendix 2.

Due to a short experimental timeframe, only early response cytokines can be measured from serum samples in this model. To get a more comprehensive view of the global inflammatory environment in this model and to infer potential subsequent protein production, transcription of inflammatory genes and NF-κB targets was measured in the liver (Figure 4.3). Genes investigated included: cytokines *tnf, il1b, il6, il12* which mediate pro-inflammatory signalling, the enzyme responsible for macrophage NO production, *Nos2* (iNOS), chemokines *ccl5, ccl2, cxcl1* responsible for continued monocyte and neutrophil recruitment, and adhesion molecule *icam1,* which plays a key role in immune cell recruitment, platelet adhesion, and the coagulation cascade. Liver was chosen for sampling due to its significant macrophage populations of both tissue resident Kupfer cells and recruited monocyte derived macrophages. As with analysis of serum cytokines, I found a global upregulation of inflammatory genes in LPS treated groups compared to the vehicle PBS control group. Consistent with a reduction in serum protein concentration, sunitinib was found to significantly reduce *tnf* mRNA expression ($p<0.01$; Figure 4.3). Furthermore, sunitinib was also found to inhibit *il1b* mRNA expression ($p<0.05$; Figure 4.3), which notably cannot be assessed at the protein level due to absence of inflammasome signal 2 in this model. Taking cytokine and gene expression data together, these results indicate anti-inflammatory activity of sunitinib *in vivo* at 1 hour post LPS challenge.

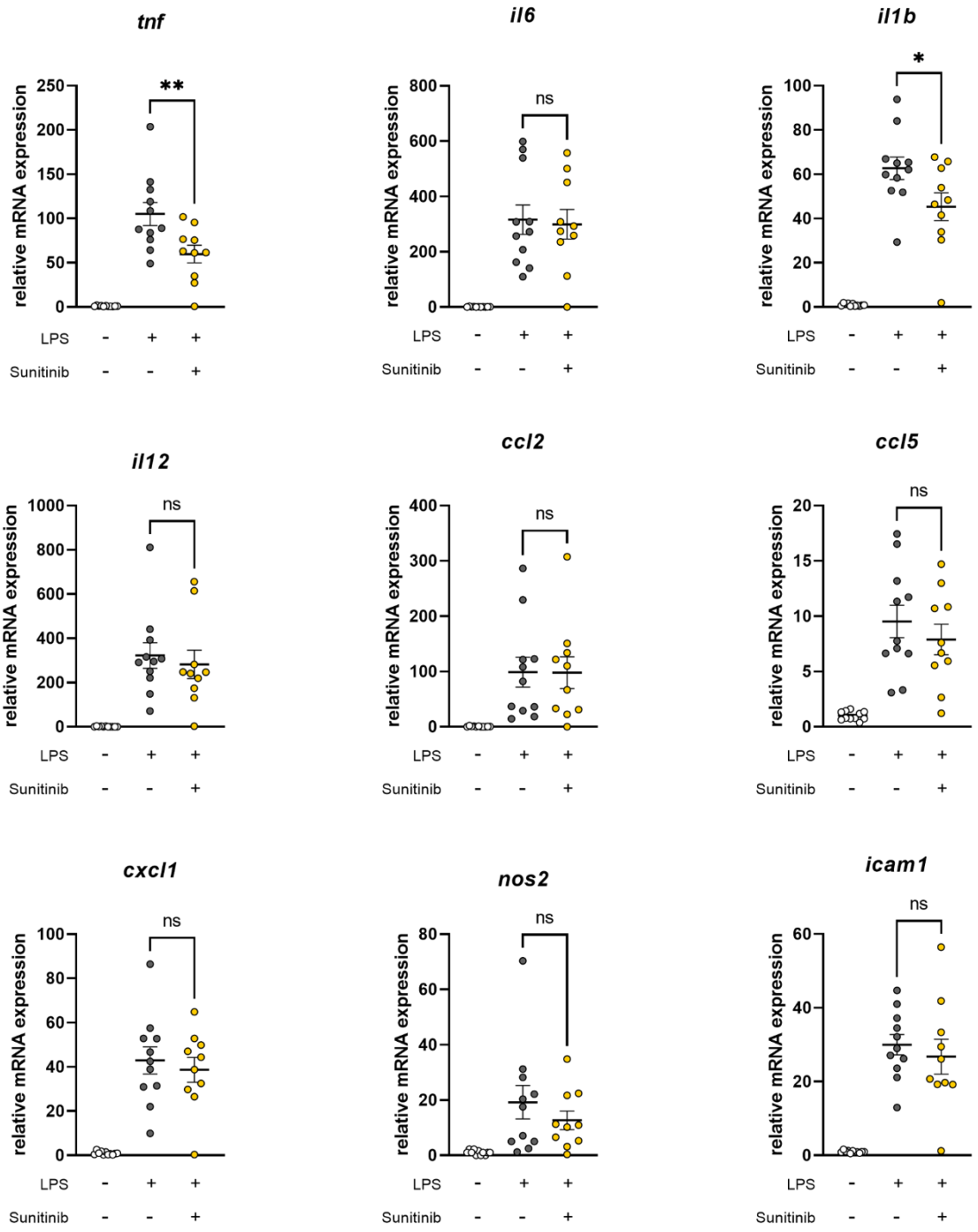


Figure 4.3: Sunitinib reduces inflammatory gene expression in endotoxaemia at 1 hour. mRNA expression of inflammatory genes in livers from endotoxaemia mice measured by RT-qPCR. Data are normalised to average vehicle + PBS group. Data points represent individual animals (n=10-12). Error bars show S.E.M. *p<0.05, **p<0.01. Statistical significance determined by one-way ANOVA followed by Tukey's post-hoc test.

Having identified *in vivo* anti-inflammatory effects of sunitinib in this model, I next sought to determine whether this was being achieved *via* NF-κB inhibition as *in vitro* data suggest. To do this, I initially attempted to assess NF-κB activity by p65 nuclear translocation by imaging flow cytometry using an ImageStream analyser (Figure 4.4). F4/80 was used as a marker to identify macrophages from the peritoneal exudate (Figure 4.4a) and a built-in ImageStream analysis algorithm was used to quantify signal similarity between p65-PE and DAPI, with high degree of similarity indicating translocation (Figure 4.4b). This method did allow for detection of translocation upon LPS stimulation, with significant increase in cells with translocated p65 in LPS treated groups versus PBS only ($p<0.01$; Figure 4.4c) and did not detect any difference between vehicle and sunitinib treated mice. However, variation within groups was unacceptably high, and results were highly dependent on the experimental batch in which the analysis was performed (Figure 4.4c). Moreover, the built in co-localisation analysis algorithm was regarded to be inaccurate, with poor distinction between nuclear and cytosolic p65 in many cases.

Due to these limitations, I decided to additionally assess *in vivo* NF-κB activation by western blot for p65 subcellular localisation in the remaining mice (n=5-6). Using liver samples isolated into cytosolic and nuclear subcellular fractions (Figure 4.4c), relative nuclear:cytosolic p65 was measured. As expected, PBS animals had low nuclear p65 protein expression compared to LPS mice. Here, sunitinib was found to significantly inhibit nuclear translocation of p65 ($p<0.05$; Figure 4.4d). This suggests that the anti-inflammatory activity of sunitinib seen in this inflammatory model is, at least in part, due to *in vivo* inhibition of NF-κB transcriptional activity.

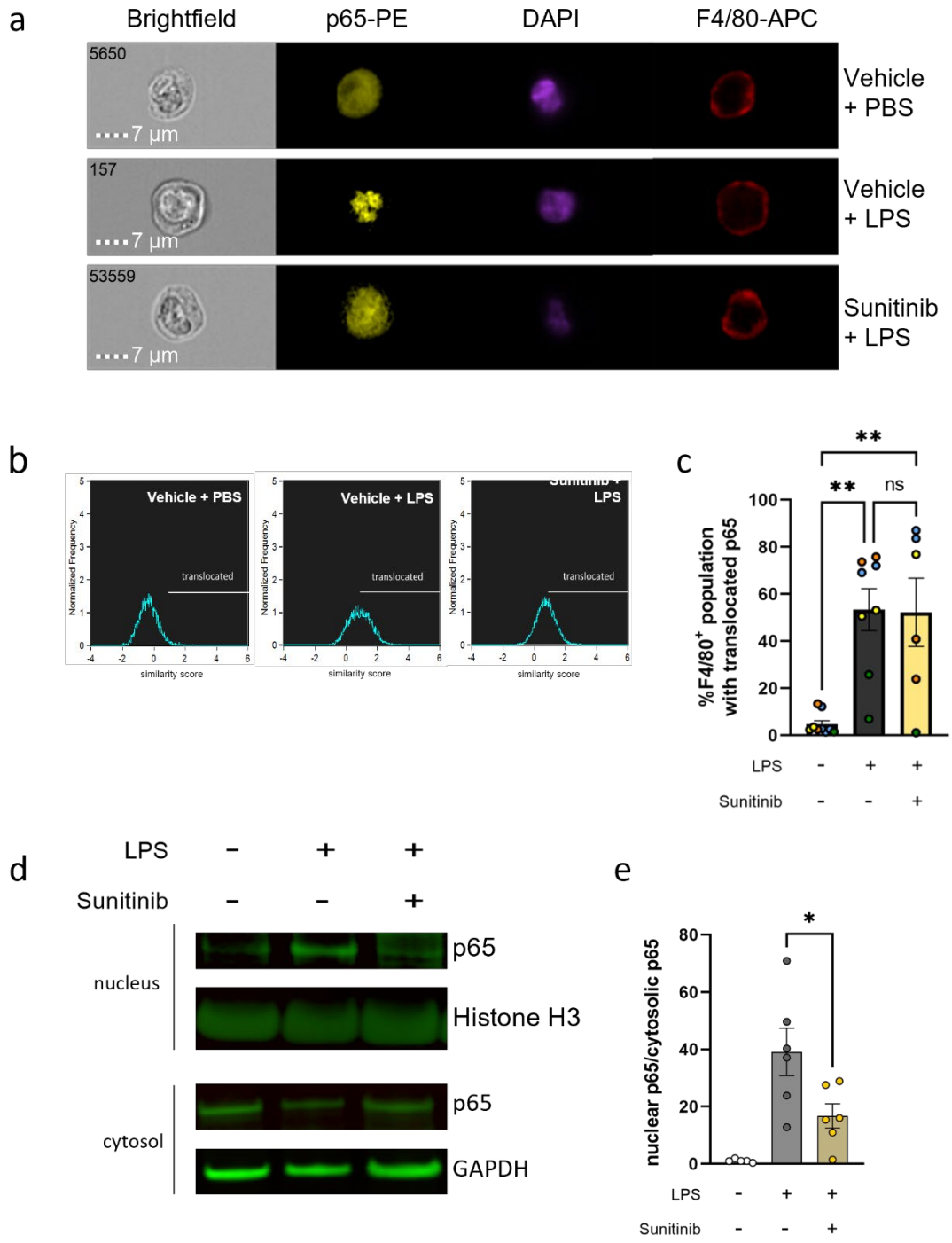


Figure 4.4: Sunitinib inhibits NF-κB nuclear translocation in endotoxaemia at 1 hour. (a) representative images of peritoneal exudate cells stained with DAPI, and p65-PE and F4/80-APC antibodies then analysed using ImageStream. **(b)** Representative histograms showing similarity of PE-65 and DAPI signals with gate added to indicate translocation. **(c)** Quantification of cells within translocated p65. Data points represent individual animals and those of the same colour show samples analysed on the same day. **(d-e)** Representative western blot **(d)** and quantification **(e)** showing nuclear and cytosolic p65 in livers of 1 hour endotoxaemia mice. Histone H3 and GAPDH were used as loading controls for nuclear and cytoplasmic samples respectively. Data points represent individual animals (n=10-12). Error bars indicate S.E.M. *p<0.05, **p<0.01. Statistical significance determined by one-way ANOVA followed by Tukey's post-hoc test.

4.3.3 Effects of sunitinib in intermediate inflammation *in vivo*

Although the 1 hour endotoxaemia model was able to confirm anti-inflammatory effects of sunitinib *in vivo*, the short term nature of this model limits the inflammatory readouts that can be obtained. Therefore, I decided to extend the LPS challenge model to 6 hours, keeping all other parameters the same as previously (Figure 4.5a). PBS and IKK-16 groups were not included in this experiment. At this timepoint, mice showed behavioural changes such as reduced feeding and water intake. Loss of body weight was observed as a consequence of this, with increased health deterioration suggesting increased severity of inflammation. Body weight immediately prior to LPS injection and again immediately prior to sacrifice was recorded in the second of two experimental batches and found to decrease in all animals receiving LPS, with no significant difference between sunitinib and vehicle treated mice (Figure 4.5b-c).

Assessing serum cytokines in the 6 hour model, TNFα remained elevated but was lower than levels seen in the 1 hour model. In contrast to the 1 hour timepoint, TNFα production was not significantly affected by sunitinib at 6 hours (Figure 4.6a). CCL2, IL-6, and the pro-resolution cytokine IL-10 were all detected at high levels at this timepoint, although none were attenuated by sunitinib (Figure 4.6b-d).

Analysis of mRNA expression in the liver was also performed in this 6 hour model, and previously obtained vehicle + PBS samples from the 1 hour experiment were used as a baseline control. Compared to 1 hour endotoxaemia, *tnf, il6*, and *il1b* expression was lower at 6 hours, although expression remained elevated in LPS-challenged mice versus PBS only controls. Expression of *ccl2, ccl5, cxcl1* and *nos2* were all higher at the 6 hour timepoint than at 1 hour. Sunitinib treatment significantly inhibited expression of five of the inflammatory genes tested at 6 hours: *tnf, il1b, ccl2, ccl5,* and *nos2* ($p<0.05$-0.001; Figure 4.7).

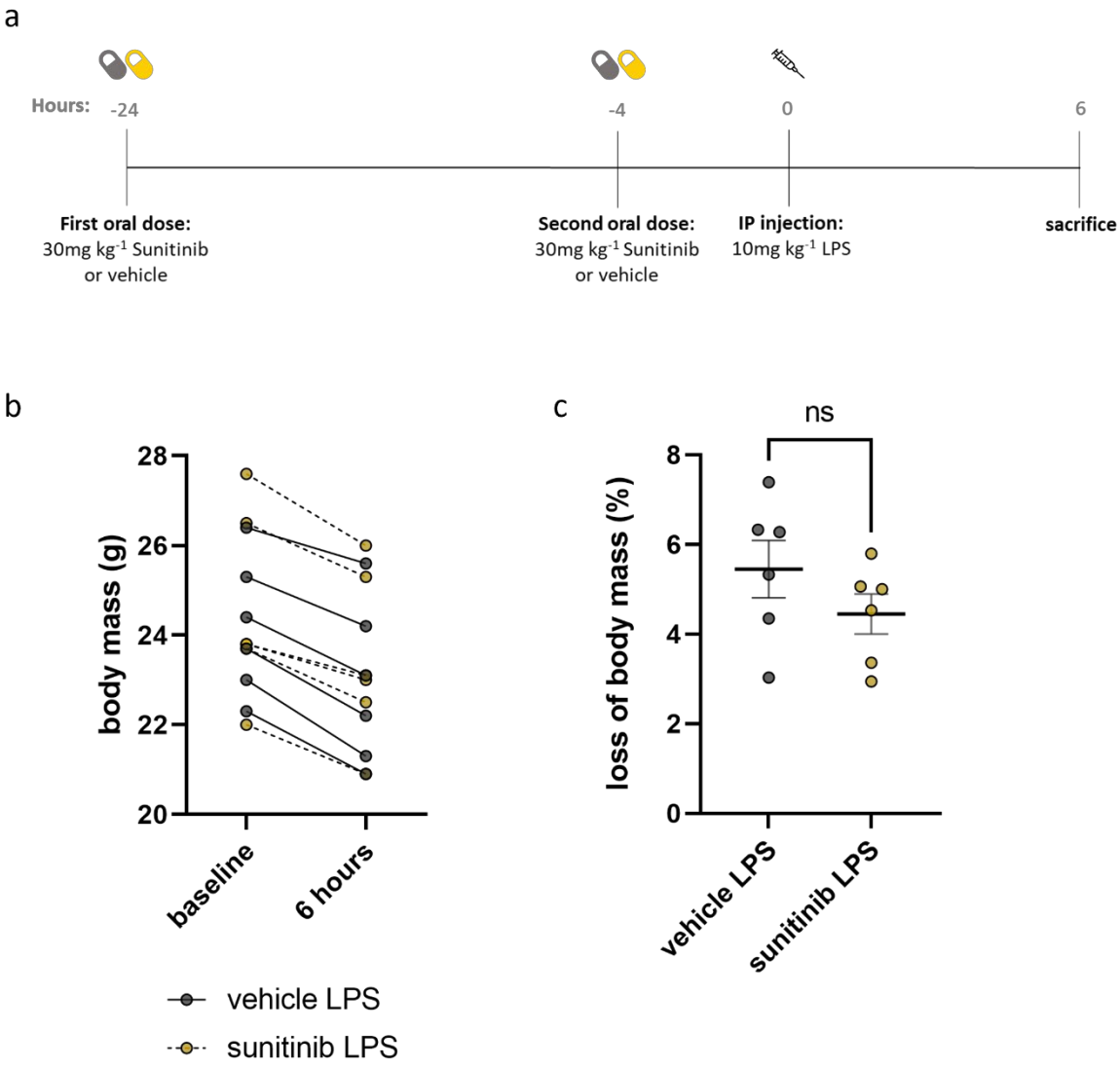


Figure 4.5: Endotoxaemia 6 hours model design. (a) Experimental timeline. Mice were randomly assigned into groups to receive an oral dose of sunitinib (30mg kg^{-1}) or vehicle 24 hours before IP injection, and were given the same dose again 4 hours prior to injection. At time 0, mice were IP injected with LPS (10mg kg^{-1}) and then sacrificed after 6 hours. **(b)** body mass at baseline and at sacrifice and **(c)** percentage loss of body mass over duration of experiment. Data points represent individual animals (n=6 per group). Error bars show S.E.M. All non-significant. Statistical significance determined by Mann-Whitney test.

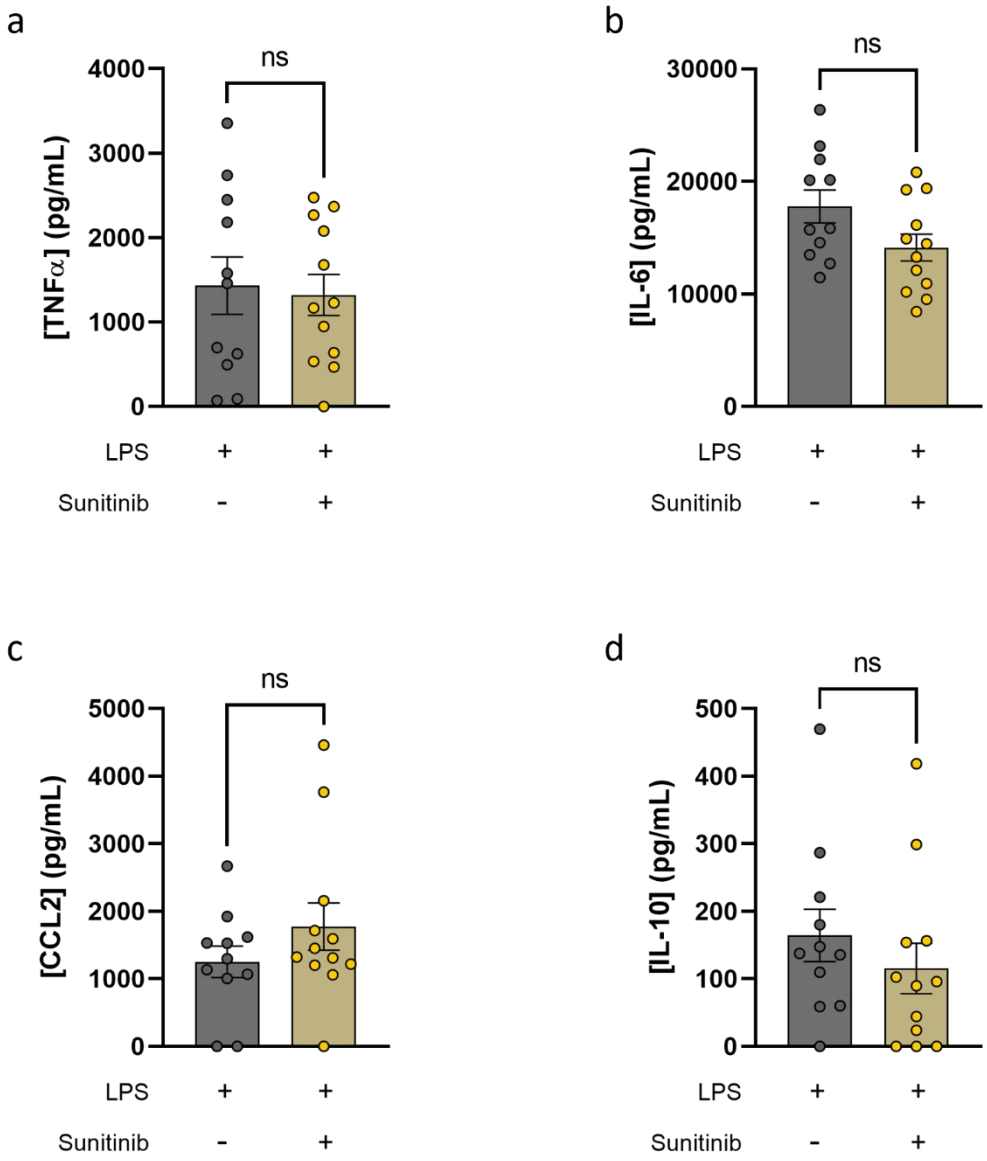


Figure 4.6: Sunitinib does not attenuate serum cytokine levels in endotoxaemia at 6 hours. Serum cytokine levels for TNFα **(a)**, IL-6 **(b)**, CCL2 **(c)** and IL-10 **(d)** in endotoxaemia mice were measured by ELISA. Data points represent individual animals (n=11-12). Error bars show S.E.M. All non-significant. Statistical significance determined by T-test.

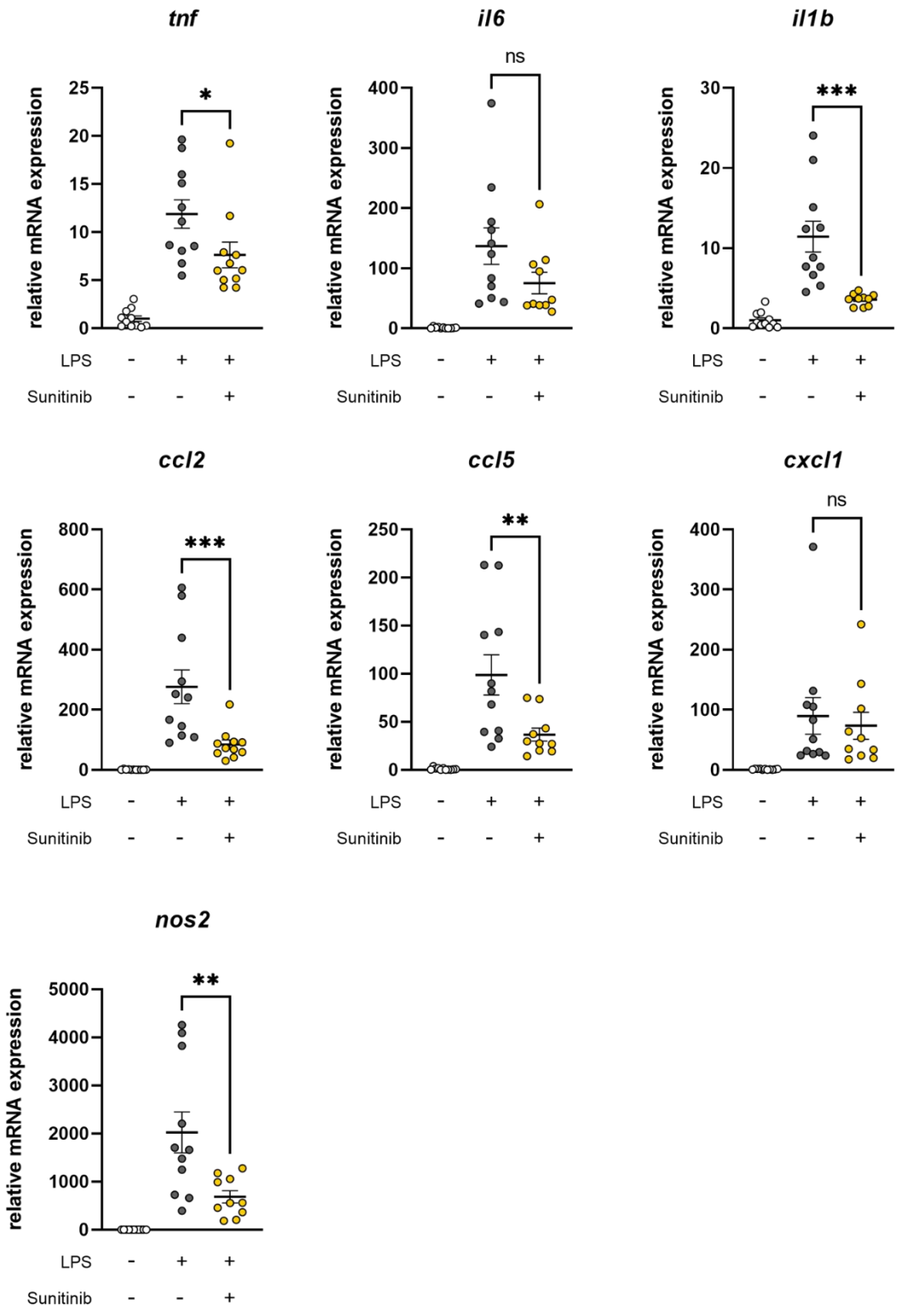


Figure 4.7: Sunitinib reduces inflammatory gene expression in endotoxaemia at 6 hours. mRNA expression of inflammatory genes in livers from endotoxaemia mice measured by RT-qPCR. Data are normalised to average vehicle + PBS 1 hour group. Data points represent individual animals (n=11-12). Error bars show S.E.M. *p<0.05, **p<0.01. Statistical significance determined by one-way ANOVA followed by Tukey's post-hoc test.

4.3.4 Effects of sunitinib on advanced inflammation and organ damage

Systemic inflammation leads to organ damage in both human disease and experimental animal models. Next, I wanted to determine whether attenuation of early inflammatory responses, identified in 4.3.2 and 4.3.3, would be protective against organ damage in advanced inflammation. This was investigated by extending the endotoxaemia model to 24 hours, keeping other parameters the same (Figure 4.8a). As weight loss was a significant welfare concern in this model, body weight was monitored throughout the experiment at the indicated times. No significant differences in raw body weight were seen between vehicle and sunitinib groups at any timepoint tested (Figure 4.8b). However, when normalised to the baseline weight for each animal, sunitinib-treated mice lost significantly more of their body weight compared to vehicle-treated mice at later timepoints. Body weight losses were 8.9% and 11.4% for vehicle- and sunitinib- treated mice respectively at 21 hours, and 10.2% and 12.9% at 24 hours (Figure 4.8c; $p<0.05$).

Inflammatory cytokine levels were drastically reduced at 24 hours compared to 1 or 6 hours timepoints and CCL2 and IL-10 were not detectable by ELISA. However, sunitinib treated mice did have significantly lower serum TNFα than vehicle treated mice ($p<0.05$; Figure 4.9a) while IL-6 levels did not differ between the two groups. At the mRNA level, inflammatory gene expression at 24 hours was not significantly higher than vehicle PBS mice for *tnf, il10, nos2, icam1,* or *ccl2.* Genes that were still upregulated at 24 hours included *il1b, il6,ccl5* and *cxcl1,* although none of these analytes were significantly affected by sunitinib treatment (Figure 4.10). Together, this suggests that inflammatory signalling becomes exhausted in late stage endotoxaemia.

Next, I sought to assess whether sunitinib altered macrophage polarisation within the peritoneum at 24 hours in this endotoxaemia model. Peritoneal exudate cells were isolated and analysed by flow cytometry using the gating strategy shown in Figure 4.11a. Using counting beads to accurately compare samples, the total number of cells in the peritoneal exudate was found to not be statistically different between vehicle and sunitinib treated mice (Figure 4.11b), suggesting immune cell recruitment is not altered by sunitinib. Similarly, proportion of F4/80+ cells remained unchanged between groups, suggesting similar sized populations of macrophages (Figure 4.11c). Sunitinib did

however significantly reduce proportion of both F4/80+MHCII+ M1 and F4/80+CD206+ M2 macrophages ($p<0.05$; Figure 4.11d-e).

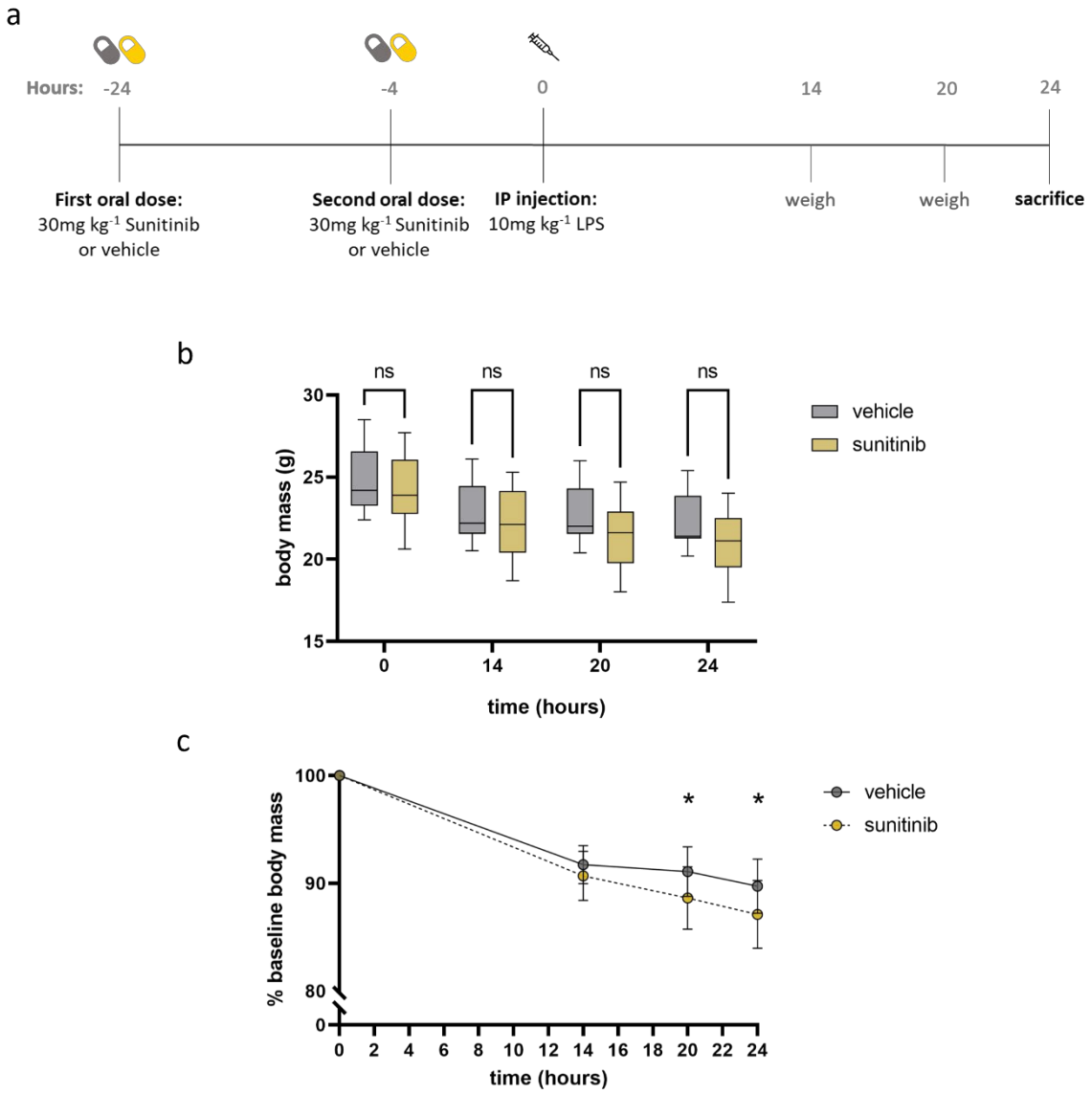


Figure 4.8: Endotoxaemia 24 hours model design. (a) Experimental timeline. Mice were randomly assigned into groups to receive an oral dose of sunitinib (30mg kg^{-1}) or vehicle 24 hours before IP injection, and were given the same dose again 4 hours prior to injection. At time 0, mice were IP injected with LPS (10mg kg^{-1}) and then sacrificed after 24 hours. **(b)** body mass at indicated time points **(c)** percentage loss of body mass over duration of experiment. *$p<0.05$. Statistical significance determined by two-way ANOVA followed by Sidak's post-hoc test. Data shown are means of biological replicates (n=13) ± S.E.M.

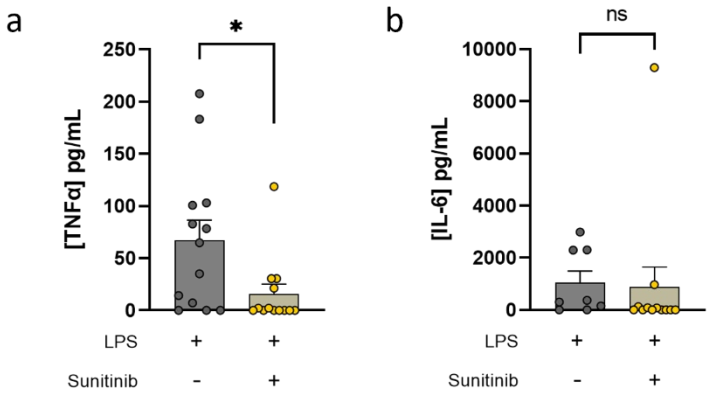


Figure 4.9: Sunitinib reduces serum TNFα in endotoxaemia at 24 hours. Serum cytokine levels for TNFα **(a)** and IL-6 **(b)** in endotoxaemia mice were measured by ELISA. Data points represent individual animals (n=13). Error bars show S.E.M. All non-significant. Statistical significance determined by T-test.

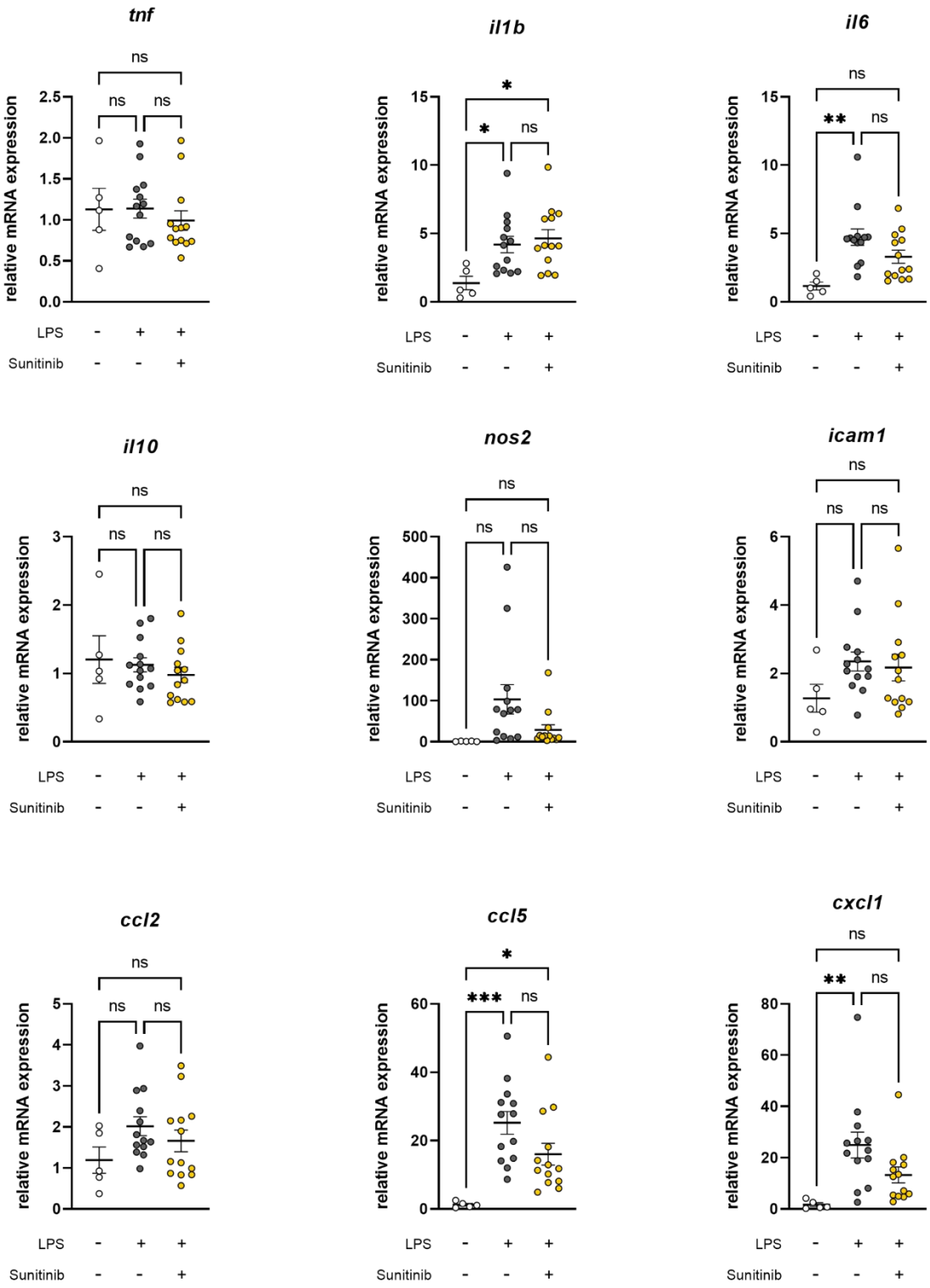


Figure 4.10: Sunitinib does not inhibit inflammatory gene expression in endotoxaemia at 24 hours. mRNA expression of inflammatory genes in livers from endotoxaemia mice measured by RT-qPCR. Data are normalised to average vehicle + PBS 1 hour group. Data points represent individual animals (n=13). Error bars show S.E.M. *p<0.05, **p<0.01, ***p<0.001. Statistical significance determined by one-way ANOVA followed by Tukey's post-hoc test.

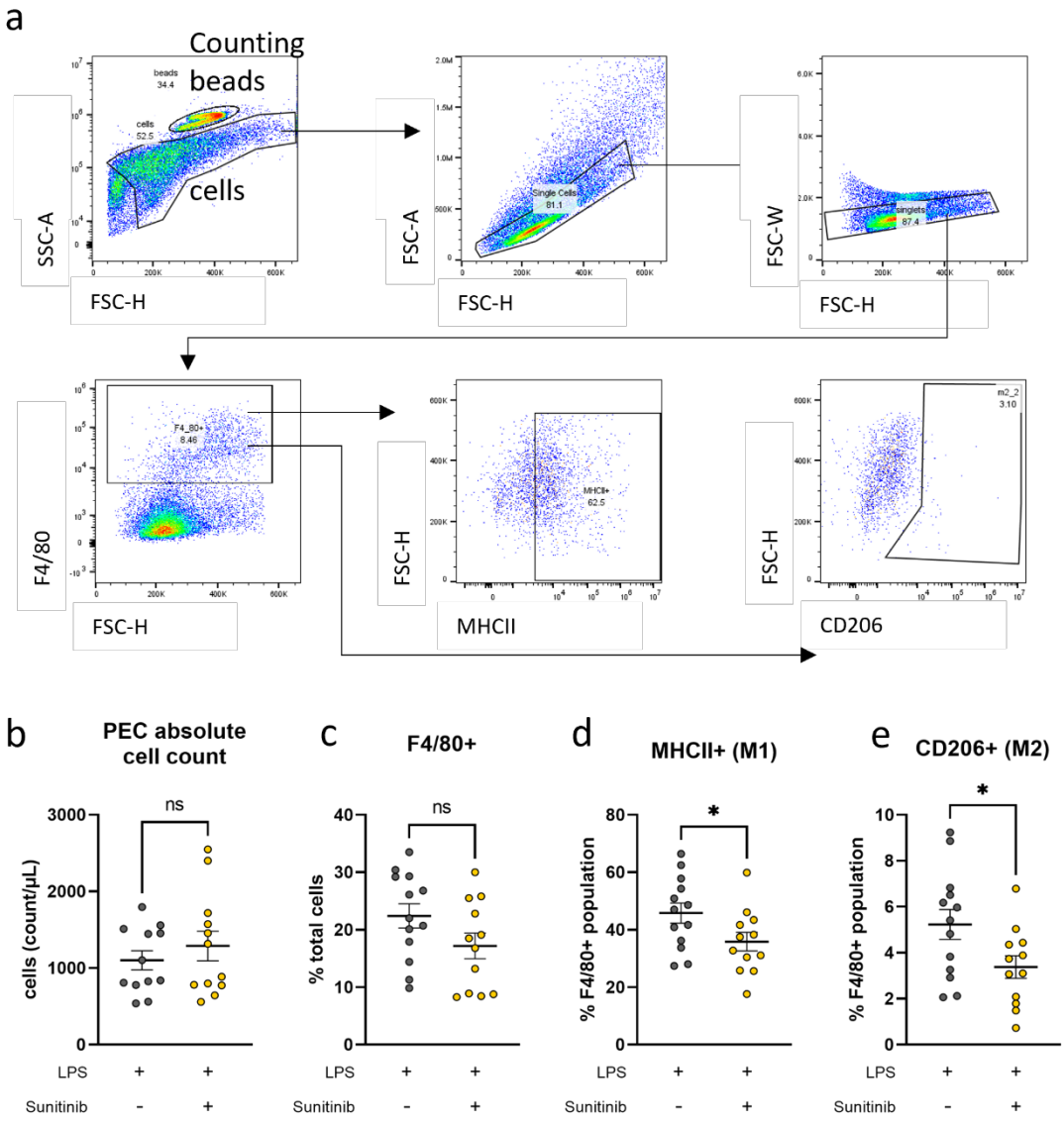


Figure 4.11: Sunitinib attenuates macrophage polarisation *in vivo*. (a) flow cytometry gating strategy for characterisation of peritoneal exudate cells in 24 hour endotoxaemia mice. **(b)** Counting beads were used to quantify total cellular infiltrate. F4/80 was used to identify macrophages **(c)**, and MHCII and CD206 were used to identify M1 and M2 macrophages respectively Data points represent individual animals (n=13). Error bars show S.E.M. *p<0.05. Statistical significance determined by T-test.

Pronounced inflammation can lead to organ damage and multi organ failure due to circulatory dysfunction, hypoxia, and cytokine-mediated cellular damage [253,261]. In this 24 hour model, I wanted to determine whether attenuation of early inflammatory responses by sunitinib is protective against organ damage in late stage inflammation. To assess liver damage, serum levels of liver enzymes alanine aminotransferase (ALT) and aspartate aminotransferase (AST) were measured. Sunitinib caused a striking reduction in both ALT ($p<0.05$; Figure 4.12a) and AST ($p<0.001$; Figure 4.12b). Kidney dysfunction was assessed by measuring serum creatinine and urea, both of which were significantly reduced by sunitinib ($p<0.001$ and $p<0.0001$; Figure 4.12c-d). Similarly, lactate dehydrogenase (LDH) was measured as a marker of cell-death and was also significantly reduced in sunitinib treated mice ($p<0.01$; Figure 4.12e). Despite these pronounced effects, analysis of haematoxylin and eosin stained kidney and liver sections reveals little difference between the groups and histological features of inflammation such as necrosis and immune cell infiltration are difficult to distinguish in these samples (Figure 4.12f,g,i,j). Lung tissue however shows marked inflammation, with thickening of the alveolar septa that appears reduced in sunitinib treated mice (Figure 4.12h,k). Overall, these quantitative and qualitative results indicate that sunitinib treatment has a protective role against organ damage in systemic inflammation.

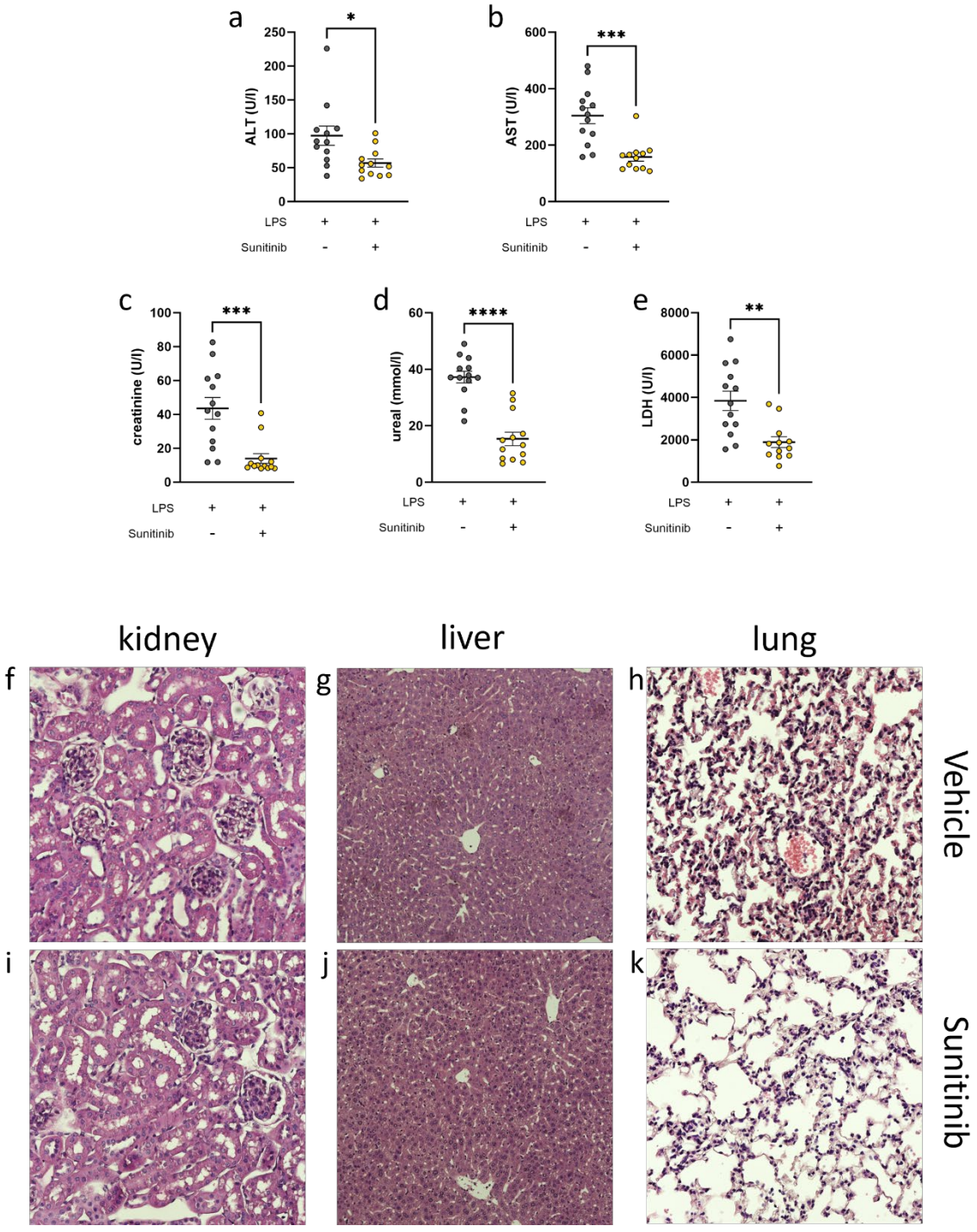


Figure 4.12: Sunitinib reduces markers of organ damage in endotoxaemia at 24 hours. Serum concentration of alanine aminotransferase (ALT) **(a)**, aspartate aminotransferase (AST) **(b)**, creatinine **(c)**, urea **(d)**, and lactate dehydrogenase (LDH) **(e)** in 24 hour endotoxaemia mice. Data points represent individual animals (n=13). Error bars show S.E.M. *p<0.05, **p<0.01, ***p<0.001, ****p<0.0001. Statistical significance determined by T-test. H&E stained tissue sections of kidney **(f,i)**, liver **(g,h)** and lung **(h,k)** from vehicle treated **(f-h)** and lps treated **(j-k)** endotoxaemia mice.

4.4 Discussion

In this chapter I set out to determine effects of sunitinib on inflammatory processes *in vivo*. I report that sunitinib treatment reduces NF-κB signalling, inflammatory cytokine production, inflammatory gene expression, organ damage, and attenuates macrophage polarisation in an endotoxaemia model of acute inflammation in mice.

4.4.1 Characterising anti-inflammatory effects of sunitinib *in vivo*

This endotoxaemia model has allowed interrogation of different parts of the inflammatory cascade through the use of three different timepoints post LPS challenge with different readouts at each stage, so that the kinetics of the inflammatory response and its attenuation by sunitinib can be analysed in depth. An important finding from this chapter is the inhibition of NF-κB p65 translocation *in vivo* early in the inflammatory response (Figure 4.4). Although the exact mechanism of sunitinib's anti-inflammatory effects remains elusive both *in vitro* and *in vivo,* it can be determined that a major element of sunitinib's *in vivo* activity in endotoxaemia is due to this inhibition of NF-κB signalling as early as 60 minutes following LPS administration.

At 1 hour post-LPS challenge, inflammation is characterised by a peak in production of the early response cytokine TNFα, while other cytokines continue to rise and peak later. Here, sunitinib was found to inhibit TNFα production (Figure 4.2), potentially having knock-on consequences for subsequent inflammatory signalling such as inflammatory gene expression (Figure 4.3, 4.7) and organ damage (Figure 4.12). For example, it has been shown that TNFα can stimulate iNOS expression in macrophages [274], and induce endothelial cell ICAM-1 and VCAM-1 [275], thereby promoting vasodilation, immune cell recruitment and tissue damage in systemic inflammation. At the protein level, sunitinib did not inhibit other cytokines to the same degree as TNFα at any of the time points assessed. This raises the question as to why TNFα is disproportionately affected by sunitinib compared to other NF-κB transcriptional targets such as IL-6 and CCL2. One explanation could be that while macrophages and T cells are the main source of TNFα, other cells such as B cells, neutrophils, dendritic cells, endothelial cells, smooth muscle cells, fibroblasts, adipocytes and more contribute to TNFα production [230]. Sunitinib could act on multiple cell types in this broad range of

hematopoietic and non-haematopoietic cells to inhibit TNFα production, either through a common pathway or *via* targeting different kinases in different cell types.

Given the possibility that *in vivo* effects of sunitinib may be largely TNFα mediated, it is pertinent to address here the failure of TNFα inhibitors in clinical trials for sepsis where despite consistent efficacy in animals models of endotoxaemia TNFα inhibition has little to no benefit in sepsis patients [253,256]. Whether sunitinib will show a similar lack of translatability remains to be determined. On the other hand, TNFα inhibition is highly successful in a large proportion of patients with rheumatoid arthritis (RA) [276]. It would therefore be interesting to observe the efficacy of sunitinib in disease models of RA.

An unexpected result of this chapter was the inefficacy of IKK-16 in the 1 hour endotoxaemia model (Figure 4.2). IKK-16 was chosen as a control for these experiments due to previous use in inflammatory models in the literature, as well as efficacy in cell based assays in this project [272,273]. However, in the 1 hour model performed here IKK-16 did not inhibit pro-inflammatory cytokine production and unexpectedly increased CCL2 production. One possibility is that the dose of IKK-16 used was not appropriate and could be titrated to an efficacious dose. An alternative positive control for these experiments could have been Ibrutinib. Previous work in the Greaves lab and by others has shown that Ibrutinib inhibits NF-κB activity and inhibits inflammation and organ dysfunction in a CLP model of sepsis [92,97]. Although targeted to BTK, competition binding assays reveal that Ibrutinib has off-target activity against other tyrosine kinases such as Kit and Flt3 [277] and may therefore share important kinase targets with sunitinib.

Another curious finding of this chapter is that sunitinib reduces both M1 and M2 polarisation in the 24 hour endotoxaemia model. In the previous chapter I reported that sunitinib increases M1 polarisation and decreases M2 polarisation *in vitro*. A likely explanation for the *in vitro versus in vivo* discrepancy is the shortcomings of the *in vitro* M1/M2 polarisation framework, which is not sufficient to recapitulate the full spectrum of macrophage phenotypes *in vivo*. Additionally, only one cell surface marker was used to define each polarisation state (MHCII for M1; CD206 for M2), and the use of more markers may have allowed for more detailed analyses. Nevertheless, signalling

pathways are typically associated with one or the other of M1/M2, and therefore the simultaneous inhibition of both of these phenotypes with sunitinib is unexpected. In a recent screen for inhibitors of M2 macrophage polarisation, He *et al.* report that IKK inhibitors TPCA-1 and bardoxolone methyl inhibit both M1 and M2 polarisation markers [278], suggesting that sunitinib could be acting in a similar way *via* NF-κB.

LPS induces an acute inflammatory response, with high levels of cytokine production and inflammatory signalling pathway activation. It will be interesting therefore to study the effects of sunitinib in chronic inflammation, where this signalling acts at a lower level over an extended period.

4.4.2 Limitations of study

This chapter hinges on the use of endotoxaemia as a model of the acute inflammatory response. Although parallels have been used between sepsis and endotoxaemia, it is important to reemphasize that endotoxaemia is a model of systemic inflammation and not a model of sepsis. The inability to perform true sepsis models such as CLP is a limitation of the current study, and it would be interesting to monitor the effects of sunitinib on pathologically relevant features of this model such as cardiac function. Another limitation of this study is the sole use of male mice throughout. This was done to minimise variation due to sex differences and therefore reduce number of animals required. However, the importance of including female animals in pre-clinical and clinical studies is becoming increasingly evident [279–281]. Notably, epidemiological studies have reported higher incidence of sepsis in males [282,283] , with male patients also having a 70% increased rate of mortality in sepsis [284].

Similarly, circadian control of immune and inflammatory processes is now widely appreciated, with cytokine production and TLR expression all displaying rhythmicity [285,286]. Indeed it has previously been found that cytokine response in endotoxaemia is dependent on macrophage circadian clock regulation [287]. Bearing this in mind, all batches within individual experiments (e.g. all 1 hour endotoxaemia animals) were performed at the same time of day. However, across different time points, time of day could not be kept consistent. Furthermore, 1 hour and 6 hour endotoxaemia mice were challenged with LPS throughout the course of the day, a mouse's usual resting period. It is not

known whether the effects seen with sunitinib may have been different if these experiments were performed in a mouse's normal waking period.

The model design used in this chapter saw sunitinib administered as an oral dose prior to the onset of inflammation. This decision was made in part because sunitinib is an orally available drug and is prescribed as an oral tablet for its current indications in cancer. The second reason a pre-dose was opted for, rather than an intervention strategy, was to maximise the chance of sunitinib having an effect in this short term model, particularly at the 1 hour time point. As a follow up experiment, it would be interesting to administer sunitinib *via* intraperitoneal or intravenous injection after an inflammatory challenge in order to create a more clinically relevant scenario. Given sunitinib's strong activity against TNFα signalling in the early stages of the inflammatory response in particular, it will be informative to examine anti-inflammatory activity when sunitinib is given only after this TNFα signalling wave has been initiated.

The *in vitro* experiments of the previous chapter largely focused on effects of sunitinib in macrophages. As NF-κB signalling is ubiquitous and the cell specificity of sunitinib molecular targets remains unknown, the contribution of macrophages to the phenotypes described in this chapter is unclear. To address this limitation, endotoxaemia experiments could be repeated in macrophage-depleted mice, for example by chlodronate liposomes [288]. This model would also allow the option of reconstituting macrophages treated with sunitinib *ex vivo* to determine macrophage-specific drug effects [288].

Moreover, sunitinib may have other biological targets relevant to inflammatory disease in addition to NF-κB. In a study by Zhao *et al.* (2019), sunitinib (25mg kg^{-1}) was administered to mice by intraperitoneal injection following LPS challenge. In the study, much like the experiments of the current chapter, the authors found that sunitinib reduced TNFα levels as well as also reporting reduced IL-6 production and mouse survival. Through *in vitro* experiments, the authors attributed this *in vivo* activity to inhibition of PDGFR signalling, and ERK1/2 and p38 phosphorylation [199]. Although not directly measured here due to evidence of NF-κB inhibition by sunitinib, it is possible

that these pathways and others are also important in the endotoxaemia experiments of this chapter and this could be further explored, particularly due to sunitinib's broad biological activity.

Finally, although the reason for using a 30mg kg^{-1} dose was validated by previously published data [270], it is possible that this dose could be further optimised for use in the short term endotoxaemia model. Using a published dose conversion framework by Nair and Jacob that accounts for body weight and surface area [289], I calculated that a 30mg kg^{-1} dose in mice corresponds to a 2.4mg kg^{-1} dose in humans, or 144mg for a typical 60kg patient. Given that sunitinib is typically prescribed as daily 50mg tablets for treatment of cancer, this dose is outside of the typical therapeutic range and therefore could amplify existing or present new adverse drug effects if repurposed at this dose. However, administration as a single bolus for short term use rather than continued daily use could mean that adverse effects are reduced. Nevertheless, these factors should be considered when repurposing sunitinib for acute systemic inflammation.

4.4.3 Summary

In this chapter I have shown that oral administration of the multi tyrosine kinase inhibitor and drug-repurposing candidate sunitinib reduces inflammatory signalling in an endotoxaemia mouse model of acute inflammation. At the very earliest stages of inflammation in this model, sunitinib attenuates TNFα production, NF-κB nuclear translocation, and inflammatory gene expression . At later stages of inflammation, sunitinib alters macrophage polarisation and is protective against organ damage.

Chapter 5: Effects of sunitinib in chronic inflammation *in vivo*

5.1 Introduction:[iv]

5.1.1 Targeting inflammation in cardiovascular disease

Chronic inflammation drives several important human diseases, including atherosclerosis, the disease process underpinning chronic cardiovascular disease (CVD). Current treatments for CVD aims to reduce circulating lipid levels through inhibition of HMG|-CoA reductase in cholesterol biosynthesis (statins) or reduce LDL receptor degradation (PSCK9 inhibitors), or to reduce hypertension (ACE inhibitors, beta blockers)[290–292]. Although lipid dysregulation is a key aspect of atherogenesis, the contribution of inflammation to atherosclerosis development and progression in animal models and in humans is widely recognised. For instance, the inflammatory marker C-reactive protein (CRP) has been found to correlate with cardiovascular risk in patients regardless of blood lipid levels [112], and increased risk of CVD has long been noted in patients with existing inflammatory conditions like rheumatoid arthritis (RA) [111,293,294]. Furthermore, although used primarily for their ability to reduce cholesterol production, some of the efficacy of statins has been attributed to their anti-inflammatory actions [295]. Consequently, many attempts have been made to therapeutically target the inflammatory compartment of CVD, with varied levels of success.

Most studies that have attempted to target inflammation in CVD have taken the form of clinical trials involving anti-inflammatory drugs repurposed from inflammatory conditions such as RA (Table 5.1). Moreover, new drug approvals for cardiovascular indications lag significantly behind those of other fields, accounting for just 2% of new drug approvals by the U.S Food and Drug Administration (FDA) in 2018 *versus* 16% in 1997 [296]. For these reasons, and the aforementioned benefits of drug repurposing outlined in Chapter 3, there is a strong case to pursue drug repurposing strategies in the treatment of CVD and a precedent for such studies has been set.

[iv] The introduction to this chapter has been adapted from Chaffey, Roberti and Greaves, 2022. See Appendix 3

Table 5.1: Drug Repurposing Cardiovascular Clinical Trials of anti-inflammatory medicines

Pharmacological agent (Trial name)	Biological target	Start date	Patient population	Intervention	Key findings
Anakinra (MRC-ILA Heart Study) [297]	IL-1β	2007	NSTEMI within 48 hours (n=182)	Placebo vs anakinra 100mg s.c daily for 14 days	49% reduction in CRP levels over first 7 days Significant increase in MACE at 1 year follow up
Anakinra (VCU-ART I, II, III) [298]	IL-1 β	2008	STEMI within 24 hours (n=10,30,99)	Placebo vs anakinra 100mg s.c. daily or twice daily for 14 days	No difference in LV end systolic volume index or LV function Significant reduction in CRP for 14 days of treatment
Canakinumab (CANTOS) [299]	IL-1β	2011	previous MI CRP ≥ 2mg/L (n=10,061)	Placebo vs canakinumab 50/150/300mg s.c every 3 months	15% reduction in MACE in 150mg group only No difference in blood lipids Adverse effects include neutropenia, increased death due to infection or sepsis
Tocilizumab (ASSAIL-MI) [300]	IL-6	2017	STEMI within 6 hours (n=199)	Placebo vs tocilizumab 280mg single dose i.v	5.6% increase in myocardial salvage index No significant difference in infarct size at 6 months Significant reduction in CRP
Etanercept (RENEWAL) [301]	TNFα	1999	Chronic heart failure (n=2048)	Placebo vs etanercept 25mg weekly/ twice weekly, s.c	Trials terminated early due to lack of benefit No significant difference in clinical status, hospitalisation for heart failure or CV death, at 24 weeks
Infliximab (ATTACH) [302]	TNFα	2000	Chronic heart failure (n=150)	Placebo vs infliximab 5/10 mg kg^{-1} at 0, 2, 6 weeks	No significant difference in clinical score at 14 or 28 weeks follow up Increased incidence of MACE in 10 mg kg^{-1} infliximab group at 28 weeks TNF levels initially reduced by then significantly increased above baseline up to 28 weeks in both infliximab groups
Colchicine (LoDoCo) [303]	cytoskeletal rearrangement, non-specific NLRP3 inflammasome	2008	Coronary artery disease (n=352)	Untreated vs colchicine 0.5mg daily, p.o	Significant reduction in incidence of acute coronary syndrome, cardiac arrest, stroke
Colchicine (COLCHICINE-PCI) [304]	cytoskeletal rearrangement, NLRP3 inflammasome	2013	Patients referred for PCI (n=713)	Placebo vs 1.2mg colchicine pre coronary angiography, then 0.6mg pre-PCI, p.o	No significant difference in PCI-related myocardial injury or MACE within 30 days Elevation of plasma IL-6 and CRP from baseline - 24hrs significantly reduced in colchicine group Increased adverse gastrointestinal symptoms in colchicine group
Colchicine (LoDoCo2) [305]	cytoskeletal rearrangement, NLRP3 inflammasome	2014	Coronary artery disease (n=5522)	Placebo vs colchicine 0.5 mg daily, p.o	31% reduction in MACE
Colchicine (COLCOT) [306]	cytoskeletal rearrangement, NLRP3 inflammasome	2015	MI within 30 days (n=4445)	Placebo vs colchicine 0.5mg daily, p.o	Significant reduction in MACE in colchicine group No significant difference in incidence of infection, but increased risk of pneumonia with colchicine

Colchicine (COPS) [307]	cytoskeletal rearrangement, NLRP3 inflammasome	2015	Acute coronary syndrome (n=795)	Placebo vs colchicine 0.5mg twice daily for 1 month, then daily for 11 months , p.o	No significant difference in MACE Increased total death incidence in colchicine group, mostly related to sepsis
Colchicine (COVERT-MI) [308]	cytoskeletal rearrangement, NLRP3 inflammasome	2018	STEMI within 12 hours (n=192)	Placebo vs colchicine 2mg p.o, then colchicine 0.5mg twice daily, p.o for 5 days	No significant reduction in infarct size at 5 days No significant reduction in MACE at 3 months follow up No difference in inflammatory marker (WBC count, CRP) at 48 hours
Methotrexate (METIS) [309]	T cell activation, adenosine signalling	2007	Ischemic chronic heart failure (n=50)	Placebo vs methotrexate 7.5mg weekly, p.o for 12 weeks	No difference in 6 minute walk time before vs after treatment No effect on CRP levels No effect on incidence of MACE
Methotrexate (CIRT) [310]	T cell activation, adenosine signalling	2013	Previous MI or coronary artery disease, plus T2D (n=4768)	Placebo vs methotrexate 5-20mg weekly, p.o	Trial terminated early due to lack of benefit No difference in incidence of MACE No difference in inflammatory markers (WBC count, CRP, IL-1β, IL-6) at 8 months Increased incidence of leukopenia, non-basal-cell skin cancer
Methotrexate (TETHYS) [311]	T cell activation, adenosine signalling	2013	STEMI within 12 hours (n=84)	Placebo vs methotrexate 0.05 mg kg^{-1} for 6 hours	No effect on creatine kinase release over first 72 hours No difference in CRP levels Significantly worse LVEF in methotrexate group at 3 months No effect on incidence of MACE
Cyclosporine (CIRCUS) [312]	T cell activation, macrophage ROS/cytokine production	2011	STEMI within 12 hours (n=970)	Placebo vs cyclosporine A 2.5 mg kg^{-1}, i.v	No effect on any cause death No effect on LV remodelling or MACE incidence at 6 months
Cyclosporine (CYCLE) [313]	T cell activation, macrophage ROS/cytokine production	2012	STEMI within 6 hours (n=203)	Placebo vs cyclosporine A 2.5 mg kg^{-1}, i.v	No effect on ST-segment resolution at 1 hour No effect on LV remodelling or incidence of MACE at 6 months
Allopurinol (ALL-HEART)[314]	xanthine oxidase	2013	Ischemic Heart Disease (n=5215 target)	Placebo vs allopurinol 600mg daily, p.o	No effect on incidence of CV events
Aldesleukin (LILACS) [315]	IL-2 receptor Treg cells	2017	Ischaemic heart disease (n=25) and NSTEMI (n=16)	Placebo vs aldesleukin 0.3 - 3x10^6 (IU) daily for 5 days, s.c	Increase in Tregs but not CD4+ effector T cells

Key: NSTEMI, non-ST segment elevation myocardial infarction; STEMI, ST segment elevation myocardial infarction; s.c, subcutaneous; CRP, C-reactive protein; MACE, major adverse cardiovascular event; LV, left-ventricular; MI, myocardial infarction; CV, cardiovascular; i.v, intravenous; p.o, per os; WBC, white blood cell; T2D, Type 2 Diabetes; LVEF, left ventricular ejection fraction; ROS, reactive oxygen species

5.1.2 Drug repurposing in atherosclerosis

IL-1β inhibiting therapies

IL-1β has been implicated in atherogenesis in pre-clinical studies and observation of reduced plaque burden in *Apoe*$^{-/-}$ lacking IL-1β has helped ascribe pro-atherogenic status to IL-1β signalling [132]. Several mechanisms involving various cell types such as activation of macrophages, pro-inflammatory programming of endothelial cells (ECs), increased immune cell trafficking *via* induction ICAM-1, VCAM-1, and CCL2, and proliferation of vascular smooth muscle cells (VSMCs) *via* induction of platelet derived growth factor (PDGF) have been proposed to underpin the pro-atherogenic functions of IL-1β[132,316,317].

A pivotal development in the field of atherosclerosis came with the landmark Canakinumab Anti-Inflammatory Thrombosis Outcomes Study (CANTOS) trial, in which the IL-1β inhibitor canakinumab was administered to patients following myocardial infarction (MI) in attempt to reduce subsequent cardiovascular events [299]. The decades preceding CANTOS had provided vast amounts of pre-clinical and clinical evidence that inflammation contributed to atherosclerosis, however until CANTOS, the 'inflammatory hypothesis of atherosclerosis' had not been directly addressed in the clinic. Canakinumab, had been used since its FDA approval in 2009 for the treatment of the rare inherited disorder cryopyrin-associated periodic syndromes (CAPS), in which IL-1β is dysregulated, as well as for the treatment of other inflammatory conditions such as gout and periodic fever syndromes [299].

The CANTOS trial found that patients receiving canakinumab had reduced incidence of major adverse CV events (defined as MI, stroke, and CV related death) compared with placebo, although this difference was a mild 15% reduction and only statistically significant at one of the trialled doses. Importantly for the 'inflammatory hypothesis', this reduction was found to be independent of lowering circulating lipid levels, suggesting that lipids are not the sole driver of atherosclerosis progression in the patient cohort studied. Furthermore, the greatest benefit was seen in patients who achieved a substantial reduction in CRP, once again supporting the notion that systemic inflammation has a causal role in atherogenesis and CVD [299]. Despite modest risk reduction, this study has

undoubtably paved the way for future clinical studies into the inhibition of inflammatory signalling as a therapeutic approach for chronic CVD. On the other hand, canakinumab was not without the adverse effects expected of a potent anti-inflammatory drug, with treatment causing increased infections due to neutropenia, as well as a significantly increased incidence of death due to infection or sepsis, although this did not affect overall death rates [299].Furthermore, the widespread use of canakinumab, a human monoclonal antibody therapeutic for CVD is economically unfeasible [318]. Notably, another IL-1 receptor antagonist, anakinra, has failed to improve outcomes in cardiovascular trials [297,298].

TNFα inhibitors

TNFα signalling and its role in the progression of cardiovascular disease has been studied extensively however animal studies have found conflicting effects of TNFα inhibition [62]. Nevertheless, due to its key role in chronic inflammation, and heavily influenced by the success of TNFα inhibition in autoimmune conditions such as RA [229], TNFα inhibitors were among the first biologics to be clinically investigated for CVD. Between 1999 and 2001, the RECOVER and RENAISSANCE trials investigated the effects of subcutaneous etanercept in a total of 2048 patients with chronic heart failure (CHF). The combined analyses of these trials (termed RENEWAL) concluded that etanercept showed no benefit with no difference in incidence of death or hospitalisation for CHF at 24 weeks, causing both trials to be terminated early due to lack of efficacy [301].

In a separate trial of CHF in 150 patients (ATTACH), TNFα inhibitor infliximab was given intravenously at 5 or 10mg kg^{-1} doses over a 6 week period [302]. Similarly to RENEWAL, it was found that infliximab treatment had no significant effect on clinical status at follow up 14 or 28 weeks after intervention, although serious adverse events including death or hospitalisation for HF were increased in the 10mg kg^{-1} infliximab group at 28 weeks follow up. Interestingly in this trial, analysis of blood markers of inflammation showed that although treatment initially reduced TNFα, levels were raised above baseline by 28 weeks follow up in both infliximab groups although other inflammatory markers CRP and IL-6 remained significantly reduced up to 14 weeks [302]. This effect could suggest induction of a compensatory TNFα mechanism, which may be partially responsible

for the adverse effects seen in the 10mg kg^{-1} group. Curiously, meta-analyses of RA patients show that although anti-TNFα therapy does not affect incidence of MI in itself, patients who respond to TNFα therapy have significantly reduced MI risk compared to those who do not respond [319].

Overall, the disappointing results of the above trials suggest that single cytokine inhibition, although useful in helping us to decipher the contribution of individual cytokines to CVD pathogenesis, is not likely to be a successful therapeutic strategy in the complex multicellular processes of post-MI recovery and chronic CVD.

Colchicine

A perhaps more pragmatic alternative drug repurposing candidate that fulfils criteria of being inexpensive and widely available is colchicine, a plant-derived medicine that's use dates back to Ancient Egypt in 1500BC. Colchicine is a standard treatment for gout and familial Mediterranean fever and its immunomodulatory effects are achieved by inhibiting tubulin polymerisation, thereby impeding cellular processes that involve cytoskeletal rearrangement [320]. Although this effect is not cell-type specific, neutrophils are disproportionately affected by colchicine due to their lack of P-glycoprotein membrane efflux pump leading to colchicine accumulation and impaired neutrophil chemotactic functionality [320]. Additionally, the NLRP3 inflammasome is believed to be inhibited by colchicine [321]. Despite having reduced specificity, such pleiotropic effects of colchicine may provide advantage over single cytokine inhibiting therapies with reduced chance for compensatory mechanisms to be triggered.

Colchicine has been assessed in several clinical trials for cardiovascular disease and has largely been found to reduce risk of major CV events [303,305,306], although other studies of colchicine have failed to observe benefit [307,308]. Notably, colchicine treatment correlated with adverse immunosuppressive effects such as an increased risk of pneumonia (in COLCOT) and increased rate of all-cause death (in COPS), largely owing to increased incidence of sepsis[306,307]. These adverse effects are unsurprising and are indicative of the inherent challenges of inhibiting inflammation, yet may be overlooked if overall disease burden is sufficiently reduced with treatment. It should also be noted that colchicine has toxicity-associated adverse effects, particularly gastrointestinal symptoms, with

which comes a particularly narrow therapeutic window[320]. This may also present an additional challenge to its repurposing.

Methotrexate

Despite promising results in pre-clinical studies, some anti-inflammatory medicines have been less successful in CVD trials. The Cardiovascular Inflammation Reduction Trial (CIRT) was run in parallel to CANTOS and aimed to assess the efficacy of methotrexate in CVD [310]. The trial was conceived based upon clinical observations that RA patients who were taking low dose methotrexate had reduced incidence of major CV events [322,323]. The mechanism by which methotrexate exerts its anti-inflammatory effects are not fully understood, however possible mechanisms are *via* the inhibition of cytokine production through blocking T cell activation, and enhancing signalling *via* adenosine receptors [324]. Similarly to colchicine, multiple biological effects of methotrexate may be advantageous to treatment of CVD.

In CIRT, no difference in the major CV events was seen between methotrexate and placebo groups, and additionally methotrexate was found to have no effect on inflammatory markers such as CRP, IL-1β, IL-6 or total white blood cell count at 8 months follow up [310]. Additional trials with smaller patient cohorts have also failed to see benefit of methotrexate in chronic CVD [309,311].

Cyclosporine

Cyclosporine is an immunosuppressive agent used to prevent immune rejection after organ transplantation and was thought to be a good candidate for drug repurposing in CVD due to its multifaceted anti-inflammatory modes of action. Cyclosporine is a calcineurin inhibitor that inhibits activity of T cells and myeloid cells via inhibition of the essential transcription factor NFAT [325]. However, in two separate trials of patients experiencing STEMI, cyclosporine failed to show beneficial effect on ST-segment resolution, LV remodelling or incidence of CV events within the trial periods of 6 months and 1 year respectively [312,313].

The above findings demonstrate the frustrations faced by targeting inflammation in CVD with repurposed or novel drugs. While overwhelming evidence indicates that inflammation is a driver of

chronic CVD as well as detrimental to repair processes following acute CV events, broad inhibition of these pathways using existing anti-inflammatories has so far not been successful. Future studies may aim to alter the timing of intervention, for example in MI recovery where initial inflammation is beneficial, or to investigate efficacy in just a subset of patients, such as in CANTOS where treatment was limited to patients whose inflammatory state was already elevated above baseline.

5.1.3 Emerging anti-inflammatory drug repurposing candidates and molecular targets for cardiovascular disease

Many repurposing-candidates with anti-inflammatory activity have been investigated in various *in vitro* assays and animal models of CVD with some promising results. This new generation of repurposed anti-inflammatory drugs have largely been pursued for their activity against specific molecular targets and pathways known to be involved in CVD, such as the NLRP3 inflammasome [94,97], rather than based on clinical observations as has historically been the case with drug repurposing. Many drugs that have not been originally developed as anti-inflammatory medicines are now being identified to have novel anti-inflammatory activity in CVD relevant animal models (Table 5.2). This new approach provides an opportunity to look for drugs which actively enhance the processes of inflammation resolution and tissue repair in the context of chronic CVD, rather than simply suppress inflammation in a broad manner.

Table 5.2: Anti-inflammatory drug repurposing candidates for use in cardiovascular disease

Pharmacological agent	Biological Target	Original indication	CVD relevant animal Model	Key findings
Digoxin	ATPase, stimulates parasympathetic nervous system	Heart failure and arrhythmias	Diet-induced obesity in mice	Digoxin inhibits IL-17A production, alleviates metabolic disorder, promotes glucose homeostasis, adipose-tissue browning, thermogenesis and energy expenditure [326]
Disulfiram	Acetaldehyde dehydrogenase	Supports the treatment of chronic alcoholism	Diet-induced obesity in rats	Reduced body weight gain and decreased body weight of obese animals [327]
Flurbiprofen	Cyclooxygenase 1/2	Osteoarthritis, rheumatoid arthritis	Diet-induced obesity in mice	Reduced body weight gain after onset of obesity, visceral fat accumulation and leptin resistance [328]
Gefitinib	Epidermal Growth Factor Receptor (EGFR)	Non-small cell lung carcinoma	Diet-induced obesity in mice	Gefitinib lowers blood glucose in all mice and glucose-stimulated insulin secretion in *Ripk2*$^{-/-}$ mice [329]
Ibrutinib	Bruton's Tyrosine Kinase (BTK), NLRP3 inflammasome	mantle cell lymphoma, chronic lymphocytic leukaemia	Diet-induced obesity in mice	Ibrutinib improves glycemic control, reduces myeloid cell recruitment to liver, adipose tissue and kidney. Decreases NF-kB and NLRP3 inflammasome activation [162]
Imatinib	Tyrosine kinases e.g. c-Abl, PDGFR, c-Kit, c-Fms, Lck	Philadelphia chromosome^{+} leukaemias, gastrointestinal stromal tumors	Diet-induced obesity in mice	Imatinib lowers blood glucose in all mice and increases glucose-stimulated insulin secretion in *Ripk2*$^{-/-}$ mice [329]
Lamivudine	Reverse transcriptase, NLRP3 inflammasome	HIV, Hepatitis B	Diet-induced obesity in mice	improves glucose tolerance and insulin sensitivity, inhibits inflammasome activity Reverses insulin resistance in tissues of type 2 diabetic patients [330]
Niclosamide	Inhibitor of oxidative phosphorylation and stimulator of ATPase activity in mitochondria	Helminth infection	*Ldlr*$^{-/-}$ high fat diet mouse model of atherosclerosis	Decreased aortic and carotid artery calcification, improved fatty liver features, decreased cholesterol levels. Inhibits Wnt/ß-catenin, mTORC1, STAT3, NF-kB and Notch signaling pathways [331]
Nitazoxanide	pyruvate:ferredoxin oxidoreductase (PFOR)	Protozoa, helminth, viral and bacterial infections	Peripheral Blood Mononuclear Cells (PBMCs) from patients with type 2 diabetes	Inhibits T cell proliferation, secretion of (IL)-1β, IL-2, IL-6, IL-10, and IL-12, decreases M1 and increases M2 macrophage population [332]

5.2 Rationale and experimental aims of chapter

In chapter 4, I found sunitinib to attenuate acute inflammatory responses *in vivo* through inhibition of NF-κB. The main consequence of this was reduced pro-inflammatory cytokine production, particularly of TNFα, which lead to a reduction in inflammatory signalling and damage in the acute disease model tested.

As discussed in the introduction to this chapter, drug repurposing in an attractive strategy for the treatment of CVD and precedent exists for studying repurposed drugs such as colchicine, canakinumab etc. in inflammation and disease progression in CVD. Inflammation induced by hypercholesterolaemia is a driver of atherosclerosis in CVD and this disease process is in part mediated by NF-κB signalling (reviewed in [143])

Therefore, given the anti-inflammatory activity of sunitinib *in vivo* and the success of using repurposed anti-inflammatory drugs in CVD, in this chapter I aim to study the effect of sunitinib in an animal model of hypercholesterolaemia induced atherosclerosis. I hypothesise that due to the involvement of NF-κB in driving inflammatory signalling in atherosclerosis, sunitinib treatment will overall reduce disease burden in hypercholesterolaemic mice.

The specific aims of this chapter are:

1. Assess the effect of sunitinib on the development of hypercholesterolaemia in a *Ldlr*$^{-/-}$ high fat diet-fed mouse model
2. Assess the effect of sunitinib on the inflammatory state in hypercholesterolaemia induced atherosclerosis in *Ldlr*$^{-/-}$ mice by studying cytokine production, inflammatory gene expression and inflammatory cell recruitment to sites of inflammation
3. Determine the effect of sunitinib on atherosclerotic plaque burden and plaque cellular composition in hypercholesterolaemic *Ldlr*$^{-/-}$ mice.

5.3 Results:

5.3.1 Safety and effect of sunitinib on the induction of hypercholesterolaemia in a *Ldlr*$^{-/-}$ mouse model

Ldlr-/- mice were used for this hypercholesterolaemia study. Ldlr-/- -mice have been well characterised and are commonly used in atherosclerosis studies [333]. Loss of functional LDL receptor in livers of these mice results in increased circulating LDL, causing hypercholesterolaemia and formation of atherosclerotic lesions upon feeding a high-fat diet [333]. Male mice were used in this study in order to reduce variation due to sex differences, as female mice have been shown to develop larger atherosclerotic lesions [334]. At 8-9 weeks old, mice were placed onto a high fat Paigen diet containing 15% Cocoa butter, 1.25% cholesterol (see methods and materials for exact composition). After 4 weeks, once hypercholesterolaemia had been induced, mice were treated with either vehicle or sunitinib (30mg kg^{-1}) five days a week by oral gavage for another 4 weeks (Figure 5.1a). This dose was chosen based on effectivity to exert anti-inflammatory activity in the short term experiments of Chapter 4, and was presumed to be safe to use long-term based on long-term dosing schedules used in cancer models in the literature [245,270,335]. The 8-week model length and oral dosing schedule was also influenced by a similar *Ldlr*$^{-/-}$ mouse model performed in the Greaves lab investigating the effects of BTK inhibitor Ibrutinib (G Purvis, data not published).

To monitor food intake and potential indicators of drug toxicity, mice were weighed weekly. Both groups were found to have a steady increase in body weight, with no significant differences between groups (Figure 5.1b). To ensure that sunitinib does not display hepatotoxicity over the 4 week dosing schedule in this model, plasma levels of liver damage markers alanine aminotransferase (ALT) and aspartate aminotransferase (AST) were measured at the final end point. No significant differences were found between vehicle and sunitinib treated groups in either ALT or AST levels (Figure 5.1c-d), indicating that sunitinib did not cause significant hepatotoxicity in this model.

To determine whether hypercholesterolaemia was successfully induced and to determine whether this was affected by sunitinib, plasma lipid levels of total cholesterol, triglycerides, LDL cholesterol, and free fatty acids (FFA) were also characterised in this model. Baseline lipid levels in *ldlr*$^{-/-}$ mice

on the same C57Bl/6 background fed a standard chow diet have been reported at 10mmol^{-1} for total cholesterol, 5moll^{-1} for LDL cholesterol, and 1.5mmol^{-1} for triglycerides [336]. Plasma levels in the current study are reported in Table 5.3 and indicate presence of hypercholesterolaemia. No significant differences were found between sunitinib and vehicle mice in any of the lipid analytes measured, indicating that sunitinib does not alter lipid or cholesterol handling (Figure 4e-h). This important result suggests that any other phenotypic changes observed with sunitinib treatment are not due to altered circulating lipids.

Table 5.3: Plasma lipid concentration in *Ldlr*$^{-/-}$ high-fat diet fed mice

Plasma concentration (mmol^{-1} ± S.E.M)	**vehicle**	**sunitinib**
total cholesterol	46.9 ± 5.1	44.7 ± 5.6
LDL cholesterol	25.8 ± 3.2	21.1 ± 1.6
triglycerides	5.7 ± 0.3	6.3 ± 0.5
free fatty acids	0.6 ± 0.04	0.7 ± 0.07
	n=14	*n=15*

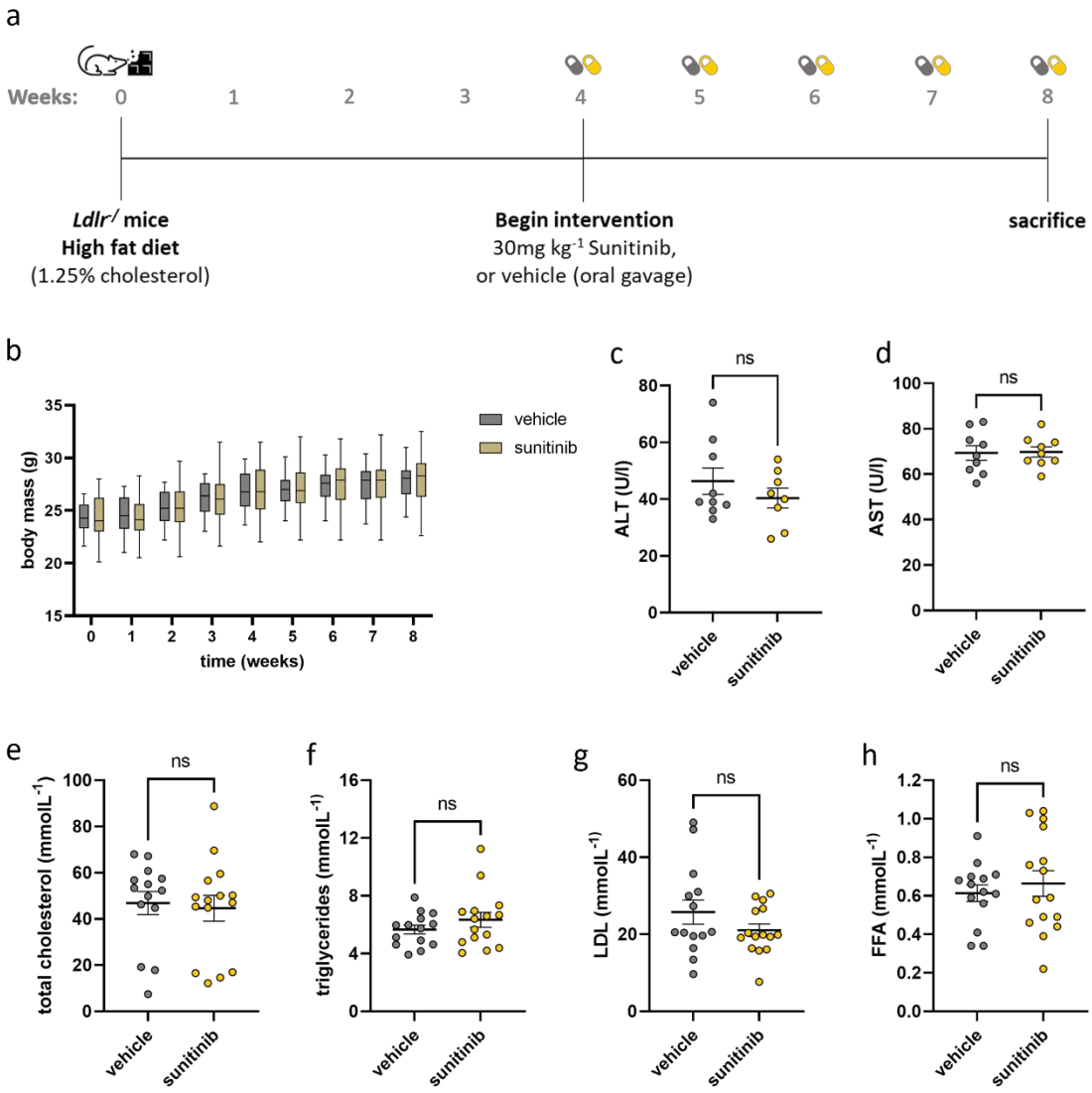


Figure 5.1: Sunitinib does not affect circulating lipid levels in a mouse model of hypercholesterolaemia. (a) Hypercholesterolaemia model design. Male *ldlr*$^{-/-}$ mice aged 7-9 weeks (n=29) were fed a high-fat diet containing 1.25% cholesterol for 8 weeks. After 4 weeks, mice were assigned to groups to receive either sunitinib (30mg kg^{-1}) or vehicle (denoted by yellow and grey symbols, respectively) by oral gavage, daily five times per week. **(b)** Body weight was recorded weekly over the duration of the experiment. Box and whisker plots show median and interquartile range. c-d) plasma levels of alanine aminotransferase (ALT) **(c)** and aspartate aminotransferase (AST) **(d)**. **(e-h)** plasma levels of total cholesterol **(e)**, triglycerides **(f)**, LDL **(g)** and free fatty acids **(h)** in hypercholesteraemic mice. Data points in panels c-h represent individual animals (n=9 in **c-d**; n=14-15 in **e-h**). Data pooled from 3 independent experiments (in **b**, **e-h**) or 2 independent experiments (**c-d**) Error bars show S.E.M. Statistical significance measured by student's T test.

5.3.2 Effect of sunitinib on hypercholesterolaemia induced inflammatory mediator production

Hypercholesterolaemia is known to induce inflammation in both humans and mice [337,338]. To assess the effect of sunitinib on the inflammatory compartment of hypercholesterolaemia and atherosclerosis, serum concentration of the pro-atherogenic cytokines TNFα, IL-1β, and chemokine CCL2 were measured by ELISA. Additionally, production of cytokines such as TGFβ and IL-10 are believed to have anti-atherogenic properties [127] and so these cytokines were also measured. Serum TNFα was found to be significantly reduced in sunitinib-treated *versus* vehicle-treated hypercholesterolaemia mice by 55% ($p<0.001$; Figure 5.2a), whereas CCL2, IL-1β and TGFβ were not significantly altered (Figure 5.2b-d). IL-10 was not detectable by ELISA in hypercholesterolaemia serum samples.

Next, inflammatory gene expression was assessed in the liver of hypercholesteraemic mice (Figure 5.3. In addition to reducing TNFα at the protein level, sunitinib treatment was found to significantly reduce gene expression of *tnf, il1b,* and *ccl2* in the liver ($p<0.05$; Figure 5.3). Other pro-inflammatory genes cxcl1, Nos2, ifng, and il6 were not significantly altered by sunitinib (Figure 5.3). Interestingly, expression of *tgfb* was reduced in sunitinib treated mice, despite no change in the serum ($p<0.05$; Figure 5.3). Expression of anti-atherogenic *il10* and the macrophage scavenger receptor CD36 were not changed with sunitinib treatment (Figure 5.3).

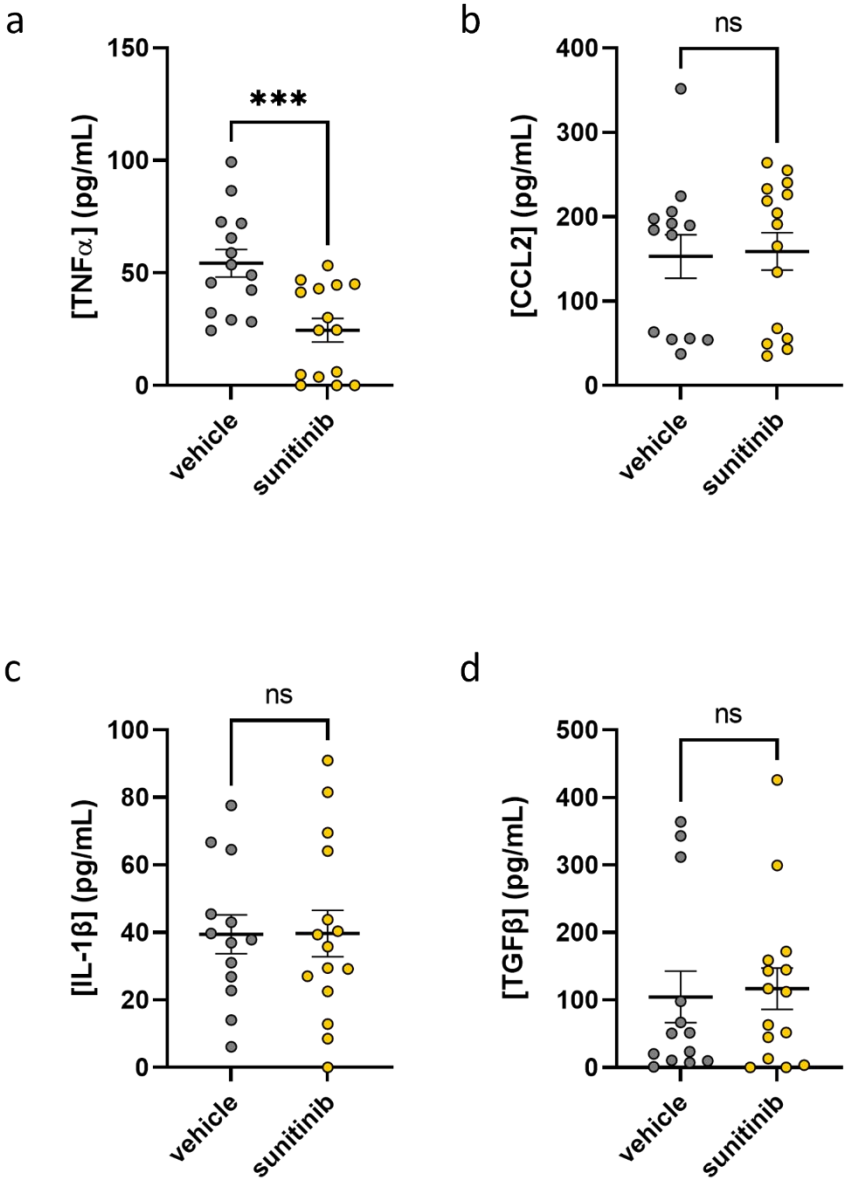


Figure 5.2: Sunitinib reduces TNFα production in hypercholesterolaemic mice. Serum cytokine levels of TNFα **(a)**, CCL2 **(b)**, IL-1β **(c)**, and TGFβ **(d)** in hypercholesterolaemic mice measured by ELISA. Data points represent individual animals (n=14-15). Data pooled from 3 independent experiments. Error bars show S.E.M. Statistical significance measured by student's T test, ***p<0.001.

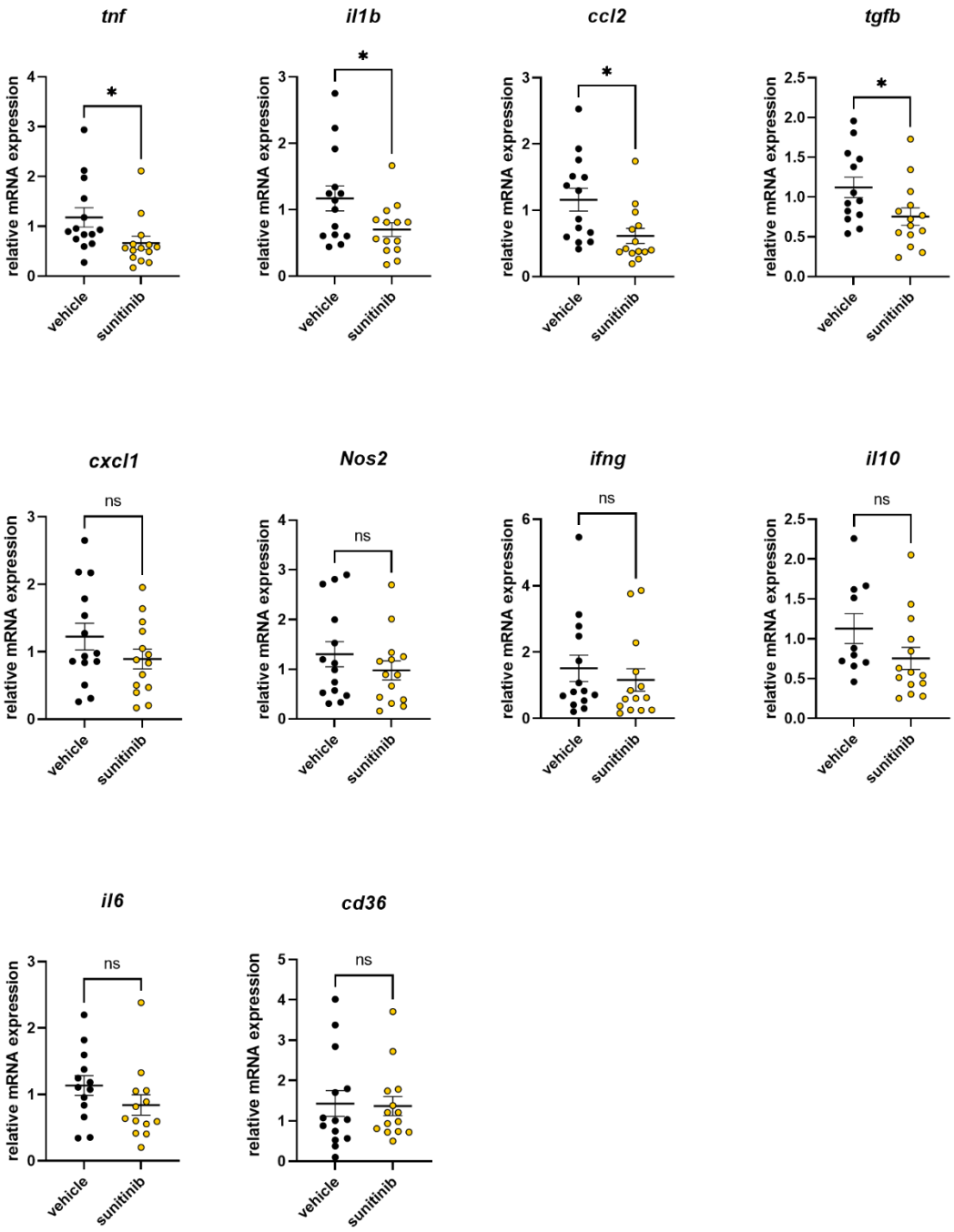


Figure 5.3: Sunitinib reduces inflammatory gene expression in hypercholesterolaemic mice. mRNA expression in the liver of hypercholesterolaemic mice was measured by RT-qPCR using the ΔΔCT method. Data points represent individual animals (n=14-15). Data pooled from 3 independent experiments. Error bars show S.E.M. Statistical significance measured by student's T test, *p<0.05.

5.3.3 Effect of sunitinib on immune cell populations in hypercholesterolaemia

Hypercholesterolaemia can alter immune cell profiles and in particular, has been shown to promote monocytosis measured by increased numbers of Ly6C^{hi} monocytes in blood [339]. To further examine the immune phenotype of sunitinib-treated hypercholesterolaemic mice, I assessed immune cell populations in the peritoneal exudate, blood, and aorta by flow cytometry (Figures 5.4-6). In the peritoneum, the proportion of total macrophages (CD11b+, F4/80+), M1 macrophages (CD11b+, F4/80+, MHCII+), and B cells (CD11b-, F4/80-, B220+), a prominent immune cell population in the peritoneum, was measured according to the gating strategy shown in Figure 5.4a. No significant difference was seen between vehicle- and sunitinib-treated mice in any of these populations (Figure 5.4b-d). In the blood, populations of total monocytes (CD11b+, CD115+, Ly6G-), activated Ly6C^{high} monocytes (CD11b+, CD115+, Ly6G-, Ly6C^{hi}), patrolling Ly6C^{low} monocytes (CD11b+, CD115+, Ly6G-, Ly6C^{lo}), neutrophils (CD11b+, CD115-, L6G+), and eosinophils (CD11b+, Siglec F+) were assessed according to the gating strategy shown (Figure 5.5). Similarly to the peritoneum, no difference was seen between groups in these populations and together these results suggests that sunitinib does not alter the myeloid immune cell profiles in peripheral tissues or in the circulation in hypercholesterolaemia.

Next, I wanted to assess whether sunitinib altered immune cell recruitment to sites of inflammation in hypercholesterolaemia. To do this, whole aortas were enzymatically digested and homogenised and single cell suspensions were then assessed by flow cytometry, as performed by Rumianek *et al.,* 2022 [340]. Total macrophages (CD45+, CD11b+, F4/80+, CD64+), M1 macrophages (CD45+, CD11b+, F4/80+, CD64+, MHCII+) and M2 macrophages (CD45+, CD11b+, F4/80+, CD64+,CD206+), monocytes (CD45+, CD11b+, F4/80-, CD64-, Ly6G-, Ly6C+), and neutrophils (CD45+, CD11b+, F4/80-, CD64-, Ly6G+) were measured according to the gating strategy in Figure 5.6a. Sunitinib treatment was found to not affect the proportion of these immune cell populations (Figure 5.6b-e), suggesting that it does not alter immune cell recruitment to atherosclerotic aortic plaques in these hypercholesterolaemic mice.

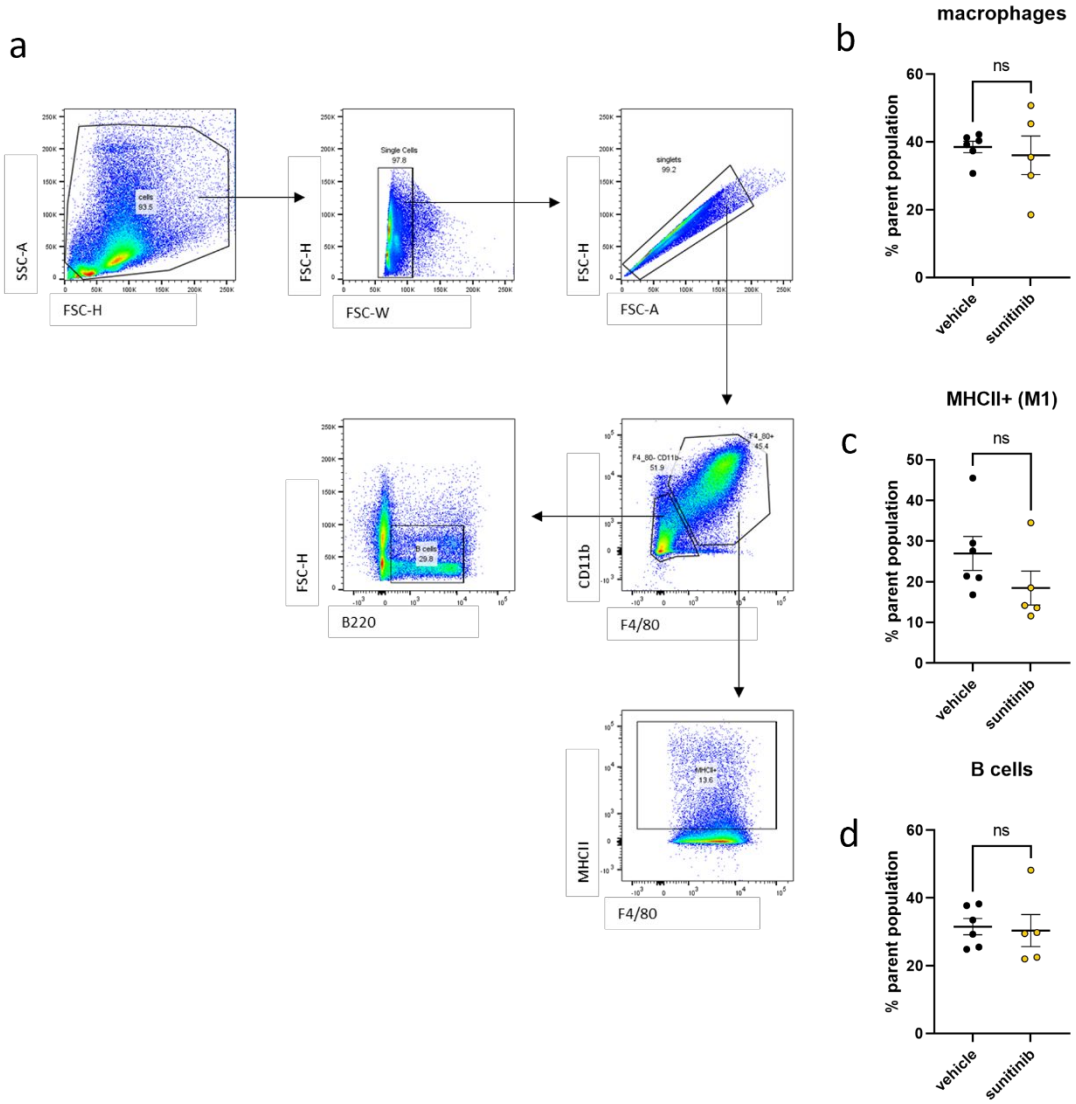


Figure 5.4: Sunitinib does not alter peritoneal immune cell populations in hypercholesterolaemic mice. (a) flow cytometry gating strategy for peritoneal lavage cells in hypercholesterolaemic mice for macrophages (CD11b+, F4/80+), M1 macrophages (CD11b+, F480+, MHCII+), and B cells (CD11b-, F4/80-, B220+). **(b-d)** immune cell populations of **(b)** macrophages, **(c)** M1 macrophages, **(d)** B cells as percentage of parent population in peritoneum of hypercholesterolaemic mice . Data points in panels **b-d** represent individual animals (n=6). Error bars show S.E.M. Statistical significance measured by Mann-Whitney test.

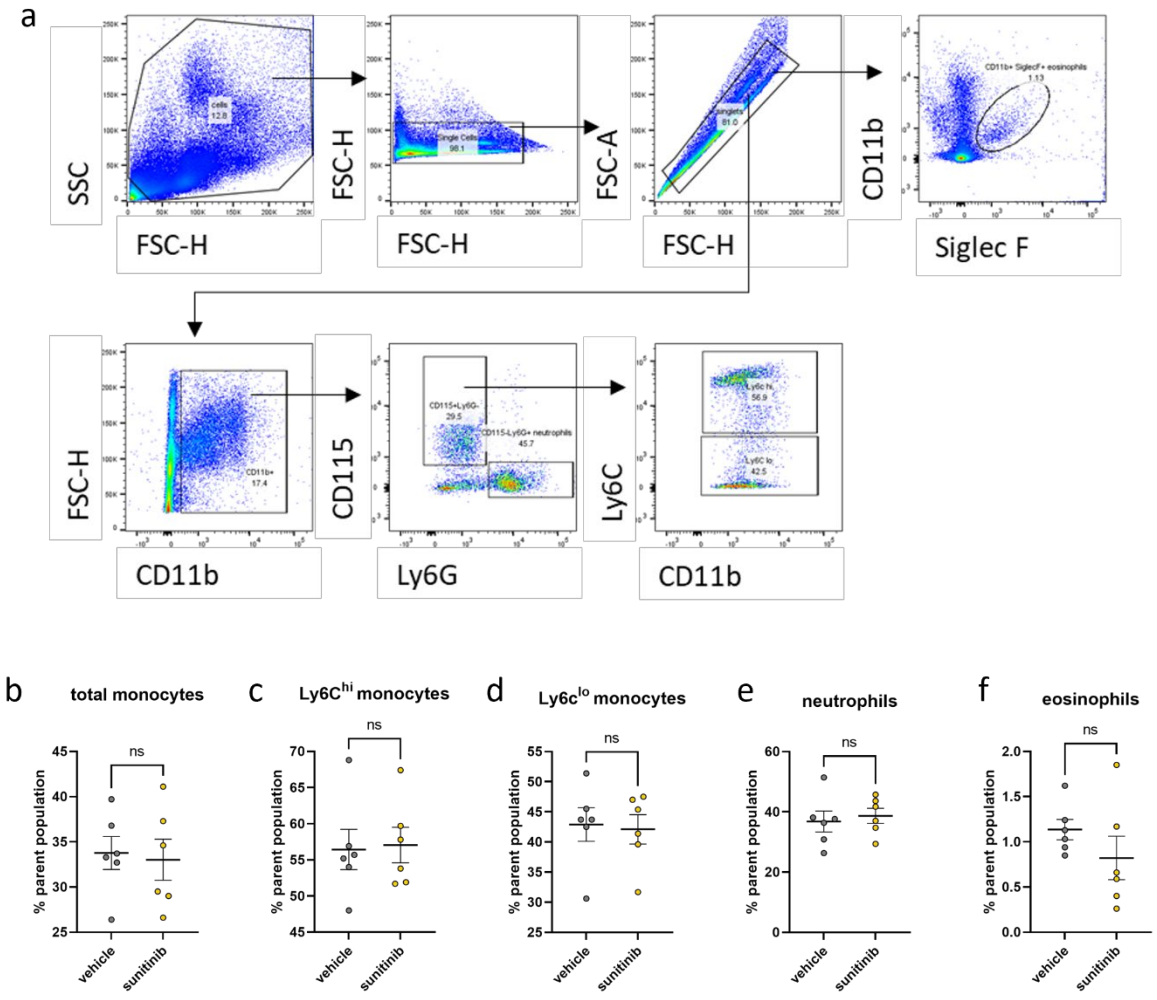


Figure 5.5: Sunitinib does not alter blood immune cell populations in hypercholesterolaemic mice. (a) flow cytometry gating strategy for blood cells in hypercholesteraemic mice for total monocytes (CD11b+, CD115+, Ly6G-), Ly6C^{high} and Ly6C^{low} monocytes (CD11b+, CD115+, Ly6G-, Ly6C^{hi}; CD11b+, CD115+, Ly6G-, Ly6C^{lo} respectively), neutrophils (CD11b+, CD115-, L6G+), and eosinophils (CD11b+, Siglec F+). **(b-f)** immune cell populations of **(b)** total, **(c)** Ly6C^{hi}, **(d)** Ly6C^{lo} monocytes, **(e)** neutrophils and **(f)** eosinophils in blood. Data points in panels **b-e** represent individual animals (n=6). Error bars show S.E.M. Statistical significance measured by Mann-Whitney test.

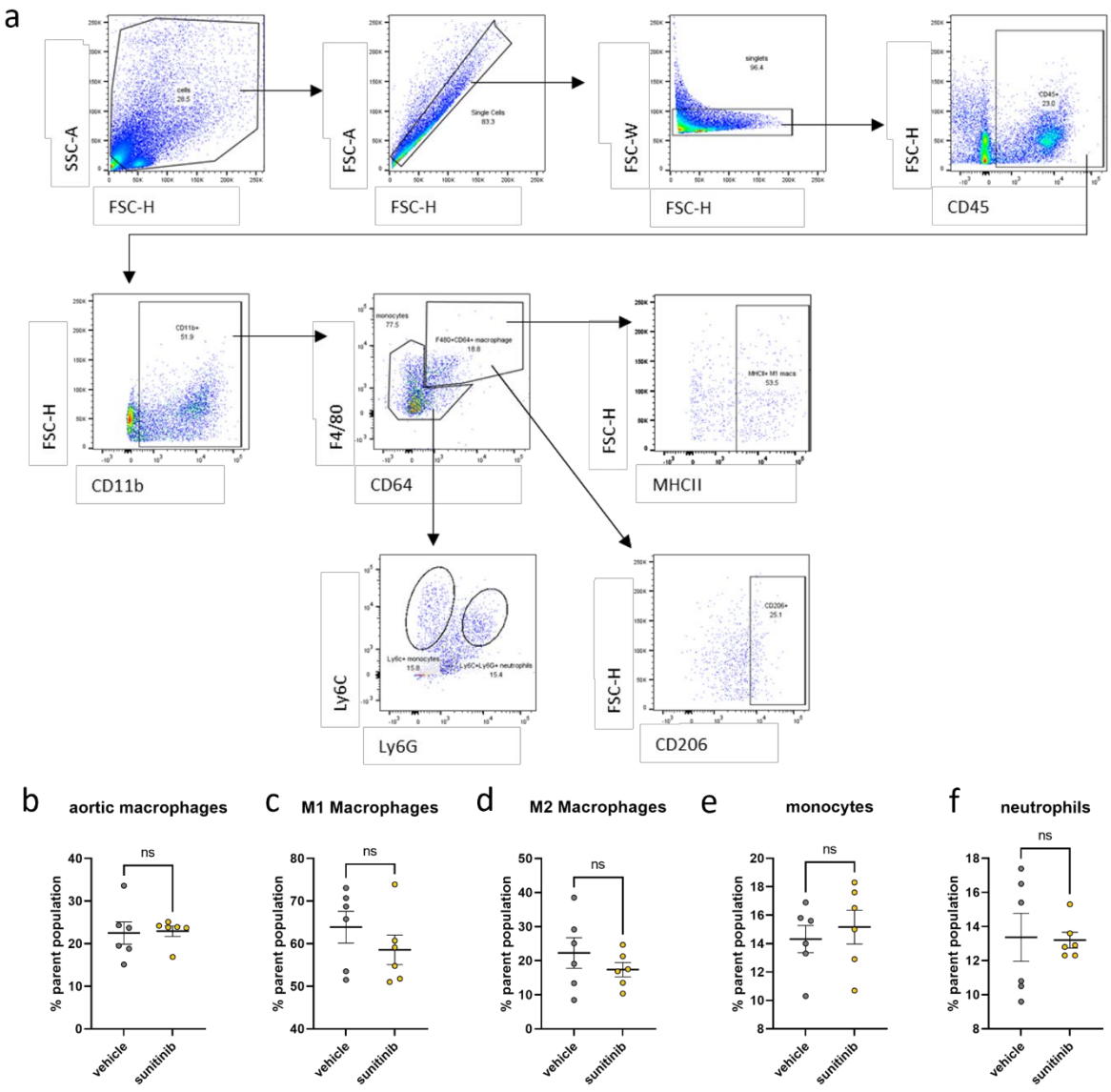


Figure 5.6: Sunitinib does not alter immune cell composition in the aorta of hypercholesterolaemic mice. Whole aortas from hypercholesterolaemic mice were enzymatically digested then analysed by flow cytometry. **(a)** flow cytometry gating strategy to identify total aortic macrophages (CD45+, CD11b+, F4/80+, CD64+), M1 and M2 macrophages (CD45+, CD11b+, F4/80+, CD64+, MHCII+; CD45+, CD11b+, F4/80+, CD64+,CD206+ respectively), monocytes (CD45+, CD11b+, F4/80-, CD64-, Ly6G-, Ly6C+), and neutrophils (CD45+, CD11b+, F4/80-, CD64-, Ly6G+). **(b-f)** immune cell populations for **(b)** total, **(c)** M1 and **(d)** M2 aortic macrophages, **(e)** monocytes, and **(f)** neutrophils in whole aorta samples. Data points in panels **b-f** represent individual animals (n=6). Error bars show S.E.M. Statistical significance measured by Mann-Whitney test.

5.3.4 Effect of sunitinib on atherosclerotic plaque development

A consequence of hypercholesterolaemia in *Ldlr*$^{-/-}$ mice is the formation of atherosclerotic lesions, particularly in the aortic root and arch [336]. As inflammation is a driver of atherogenesis I wanted to determine whether sunitinib-induced inhibition of systemic inflammation evidenced by reduced circulating TNFα would reduce plaque burden in hypercholesterolaemic mice.

Two methods were used to quantify plaque burden in the aortic arch and aortic root, respectively. Aortic arches that were not used for flow cytometry in 5.3.2 were prepared for *en face* staining with Oil-red O to visualise lipid content (Figure 5.7a). Quantification of plaque area proportionate to total arch area reveals no difference between sunitinib and vehicle groups (Figure 5.7b). Due to differences in aorta microdissection between samples and challenges with standardising total arch area, variation among individual animals is high.

To assess plaque burden in the aortic root, cross-sections containing a view of all three aortic valves were stained with Masson-Goldner's trichrome stain, which allows visualisation of collagen (green), muscle (red), erythrocytes (orange), and nuclei (black) (Figure 5.7c). To obtain an accurate measure of plaque area across samples, average plaque area as a proportion of total aorta area was calculated in at least three sections at 40nm intervals. This image analysis was performed by a graduate student, Liliana Som, as part of a lab rotation project. Analysis revealed no difference in plaque area between vehicle and sunitinib groups (Figure 5.7d).

Necrotic core formation can serve as a surrogate marker of plaque stability and is thought to be indicative of impaired efferocytosis [26,125]. Therefore necrotic core area was also measured in aortic root cross-sections. Again, no significant difference was revealed between sunitinib and vehicle treated mice (Figure 5.7e).

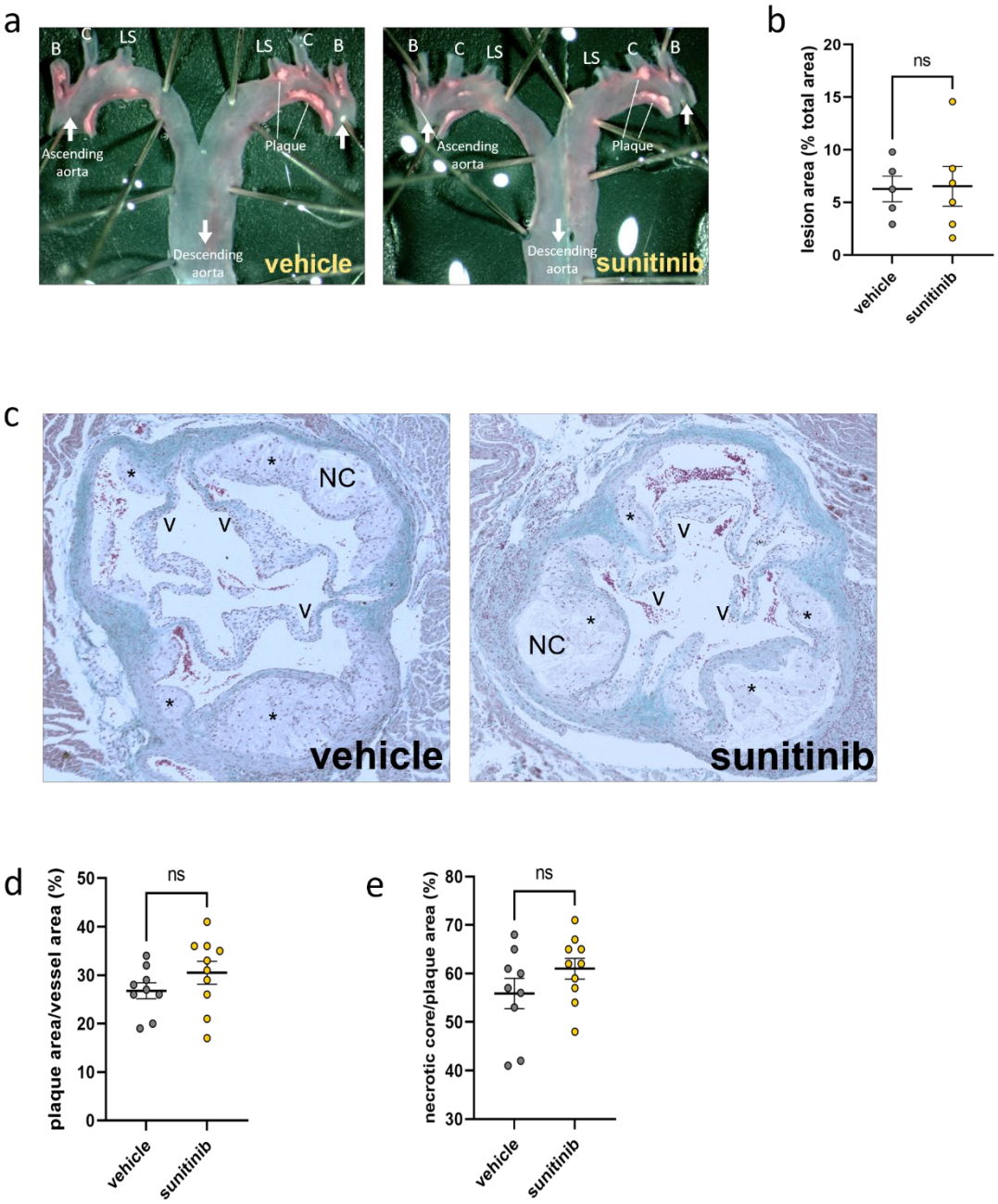


Figure 5.7: Sunitinib does not affect atherosclerotic plaque burden in hypercholesterolaemic mice. (a) representative images of oil red o-stained aortic arches from hypercholesterolaemic mice treated with vehicle (left) or sunitinib (right). Ascending aorta, descending aorta and plaque are labelled. B=brachiocephalic artery, C= carotid artery, LS= Left subclavian artery. **(b)** quantification of atherosclerotic lesion area relative to total aortic arch. **(c)** representative images of aortic sinus sections stained with Masson Goldner trichrome. v=valve, NC= necrotic core, *= plaque. **(d-e)** quantification of **(d)** plaque area and **(e)** necrotic core area in aortic sinus. Data points represent individual animals (n=5-6 in **b**, n=9-10 in **d-e**). Error bars show S.E.M. Statistical significance measured by Mann-Whitney test **(b)** or T-test **(d-e).**

Having identified no effect of sunitinib on necrotic core size, I next measured an indicator of plaque stability, fibrous cap thickness. A key feature of stable plaques is the presence of a fibrous cap formed by proliferation and migration of VSMC to the plaque surface, reducing likelihood of plaque rupture [341]. Here, immunohistochemistry of aortic root sections was performed to examine plaque fibrous cap content, using smooth muscle α actin (αSMA) to identify VSMCs.

Stained sections reveal VSMC content in the aortic wall and surrounding cardiac microvasculature. However, little VSMC positive staining was observed within plaques indicating the absence of a fibrous cap (Figure 5.8). For this reason, quantification of VSMC staining was not performed on these samples.

Finally, I sought to further explore plaque immunophenotype by examining plaque macrophage content. Monocytes are recruited to atherosclerotic lesions in large numbers where they differentiate into macrophages and lipid-laden foam cells. High plaque macrophage content has been correlated with necrotic core size and increased release of pro-inflammatory factors that promote plaque instability [116]. The lectin Galectin 3, which is highly expressed on lesional macrophages [342], was used as a macrophage marker in aortic sinus sections from hypercholesterolaemic mice and sections showed a high level of staining, indicating high macrophage content (Figure 5.8a). However, when quantified, there was no difference in Galectin 3 staining between vehicle and sunitinib groups (Figure 5.8a). This finding concurs with flow cytometry analysis of the aortic arch in which the aortic macrophage population was not affected by sunitinib (Figure 5.6b). Together, these findings suggest that sunitinib does not alter plaque myeloid immunophenotype in atherosclerotic mice.

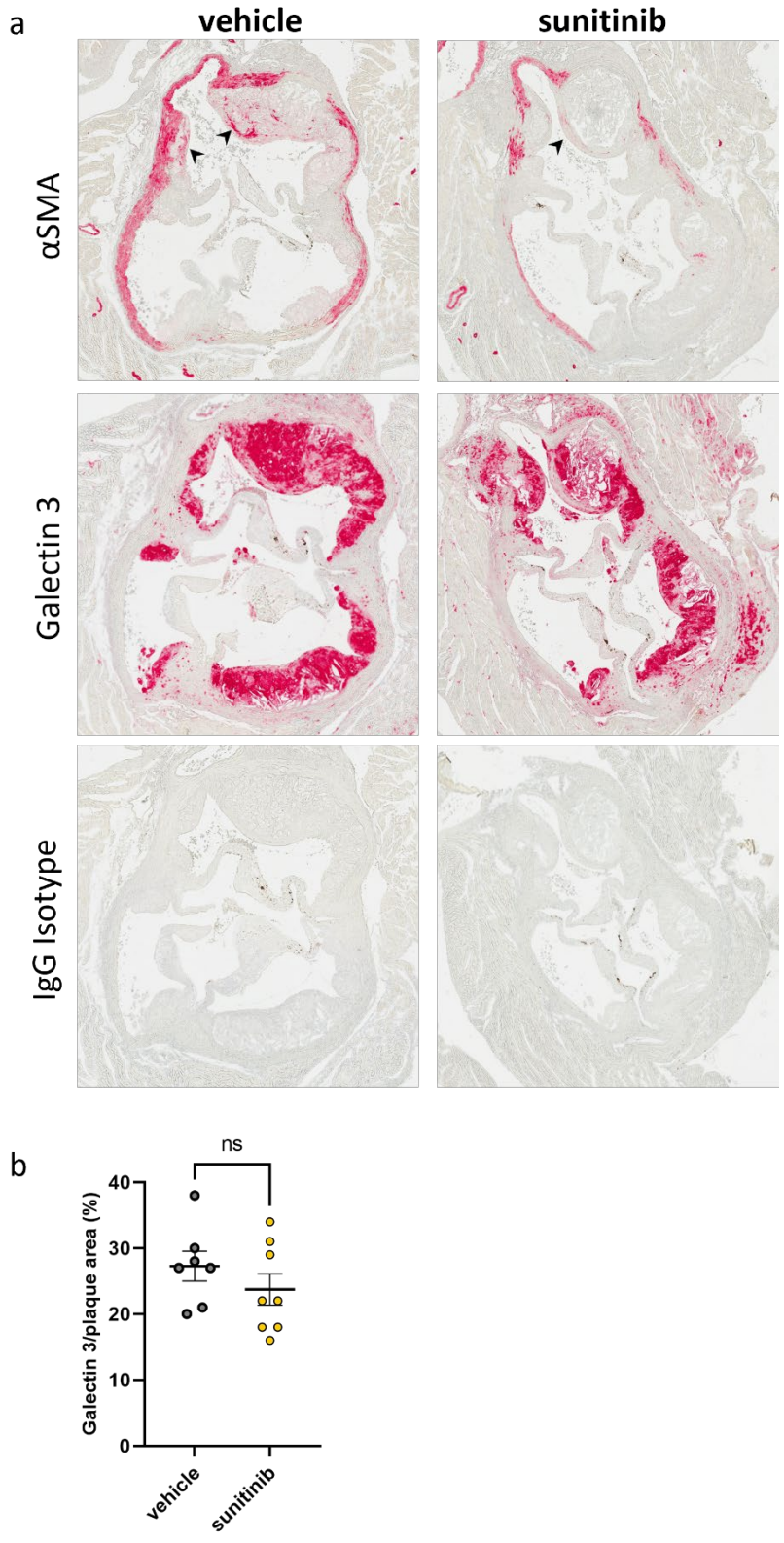


Figure 5.8: Sunitinib does not affect plaque composition in hypercholesterolaemic mice. (a) representative immunohistochemistry images of aortic sinus sections stained for smooth muscle α actin (αSMA), galectin 3, or isotype control. Arrowheads indicate VSMC fibrous cap. **(b)** quantification of galectin 3 staining in aortic sinus sections relative to vessel size. Data points represent individual animals (n=7-8). Error bars show S.E.M. Statistical significance measured by T-test.

5.4 Discussion

5.4.1 Sunitinib reduces inflammation but not atherosclerosis development in a model of hypercholesterolaemia

In this chapter I have expanded upon the findings from the previous chapter examining sunitinib's immunomodulation in a short term *in vivo* model of acute inflammation by studying its effects in a mouse model of chronic inflammation. In a widely used model of hypercholesterolaemia, I find that a 4 week oral sunitinib intervention strikingly reduces serum TNFα, a key cytokine involved in atherogenesis (Figure 5.2), as well as tissue expression of some other CVD-relevant inflammatory genes (Figure 5.3).

Importantly, sunitinib was found not to alter plasma lipid levels in this model (Figure 5.1). Although reducing circulating cholesterol is beneficial for the development of CVD and so overall would not be an undesirable consequence of sunitinib treatment, in the current study this effect would preclude any cardioprotective effects of sunitinib being attributed to its anti-inflammatory activity alone. In a similar study investigating BTK inhibitor Ibrutinib, another TKI with anti-inflammatory activity *via* NF-κB inhibition, in an *Ldlr*$^{-/-}$ model of hypercholesterolaemia, Purvis *et al.* report that Ibrutinib alters *in vivo* macrophage phenotype and reduces circulating lipid levels (data not published). I therefore speculated that this could also be observed with sunitinib. However, the results shown here are more akin to that seen with loss of IL-1β signalling, both in *ApoE*$^{-/-}$ mice [132], and in humans in the CANTOS trial [299], where lipid levels were not affected despite reduced inflammatory signalling.

In this chapter, I report that despite the above mentioned immunomodulatory effects, sunitinib does not alter immune cell recruitment to atherosclerotic plaques in this model and has no effect on plaque size or immunophenotype (Figures 5.6-8). An unexpected observation was the trend towards increased plaque size and necrotic core with sunitinib treatment. Cardiotoxicity and increased risk of major CV events is a widely reported clinical side effect of sunitinib in cancer patients [343–345]. However, little is known about its cardiac effects in the general population. In rats, 4 week dosing of sunitinib has been reported to increase blood pressure but not alter cardiac function [346]. Furthermore, it is possible that attenuation of dose or treatment schedule may limit undesirable cardiac qualities.

Nevertheless, these clinical observations in cancer patients may partially explain the trend towards increased plaque burden seen in this hypercholesterolaemia study. Any future studies in hypercholesterolaemic mice should carefully examine cardiac function and cardiomyocyte viability upon sunitinib treatment.

5.4.2 Potential anti-inflammatory mechanisms of sunitinib in hypercholesterolaemia

Although NF-κB activation was not measured directly in this model, data from previous chapters have shown that sunitinib exerts its anti-inflammatory effects through inhibition of NF-κB signalling, a pathway which is known to drive the inflammatory and pro-atherogenic phenotype of macrophages in hypercholesterolaemia [138,139]. Additionally, NF-κB signalling in a variety of non-macrophage cell types can promote atherogenesis. For example, loss of vascular endothelial cell NF-κB signalling achieved through the endothelial cell specific knock out of IKKγ or IκBα has been shown to result in significantly reduced atherosclerotic plaque formation in *ApoE*$^{-/-}$ mice [347]. NF-κB signalling has also been found to increase with age, a key risk factor for CVD, in aortic endothelial cells in rats [348]. Interestingly, this same study found a corresponding increase with age in signalling of PDGF, another target of sunitinib [348]. PDGF has a key role in VSMC regulation in atherosclerosis and acts to promote VSMC migration and proliferation within plaques [349]. Furthermore, PDGF signalling in VSMCs has been found to promote immune cell accumulation in atherosclerotic plaques *via* induction of VSMC chemokine production [350].

Together these results suggest that sunitinib could have both macrophage- and NF-κB-independent anti-atherogenic activity, and drug repurposing studies of CVD have found that drugs with pleiotropic effects e.g. colchicine, may show benefit over highly targeted therapeutics such as biologics. These possible cardioprotective mechanisms warrant further investigation, particularly analysis of sunitinib's effect on VSMC phenotype in atherosclerosis, given the role that these cells play in atherogenesis [341]. Unfortunately, here I was not able to study the effect of sunitinib on VSMC phenotype as fibrous caps were not visible in samples from this model of hypercholesterolaemia (Figure 5.8).

5.4.3 Targeting TNFα in chronic cardiovascular inflammation

Here, as with the endotoxaemia experiments of the previous chapter, the strongest effect of sunitinib in this hypercholesterolaemia model was inhibition of TNFα. TNFα has a causal role in atherogenesis, as evidenced by a reduction in plaque size in TNFα knock-out *ApoE*$^{-/-}$ mice [128,351]. Furthermore, studies involving bone marrow chimeras have confirmed bone marrow derived cells to be an important source of TNFα in atherogenesis [352]. Given these reports, it would be expected that a sunitinib driven reduction in TNFα production would lead to reduced lesion development, however this is not the case in this *Ldlr*$^{-/-}$ model. Additionally, as TNFα signalling has a role in efferocytosis impairment in atherosclerosis *via* CD47 upregulation [126], a sunitinib-driven reduction in TNFα signalling would be expected to enhance efferocytosis and decrease necrotic core area, a commonly used surrogate marker for efferocytosis [106,107]. However, in this study sunitinib was not found to affect necrotic core size, suggesting that efferocytosis is not affected by sunitnib.

Clinical studies involving small numbers of patients with rheumatoid arthritis, a group with increased risk of CVD, have shown that anti-TNFα therapy in these patients reduces endothelial dysfunction, an early event in atherogenesis [353,354], as well as arterial stiffness [355] and insulin sensitivity [356,357]. Furthermore, CVD risk is lower in patients who respond to anti-TNFα therapy *versus* those who do not, suggesting that CVD risk in RA is directly linked to TNFα [319]. Outside of RA, elevated TNFα levels have been linked with obesity and insulin resistance, both significant risk factors for CVD [358,359]. However, as discussed in 5.1.2, anti-TNFα therapies do not show clinical benefit in large scale trials of CVD, and in the present study, reduction of systemic TNFα did not effect atherogenesis. Discrepancies between these findings and previous reports finding benefit of TNFα inhibition could arise due to pre-existing inflammation present in RA patients, and species differences in animal models of atherosclerosis [115].

Given benefit of TNFα inhibition in RA alone, plus the CVD- protective effects of anti-TNFα treatment seen in these patients, an interesting follow up study would be to investigate sunitinib in a mouse model of both RA and atherosclerosis, using a specifically designed mouse model (K/BxAg7) [360]. Although sunitinib may be of limited use in CVD more broadly due to the failure seen here in

preventing atherogenesis, in this specific yet clinically-relevant setting, treatment sunitinib may prove beneficial.

5.4.2 Limitations of study

There are several technical limitations of this study. They include limited number of mice used due to small colony size, and exclusion of female mice from the study. While including both males and females in this study would have overcome the overall small study size, sex differences in extent of atherosclerosis development in *Ldlr*$^{-/-}$ mice are well documented with females developing significantly more severe lesions than males [361]. For this reason, only male mice were studied in order to minimise variation. Female mice could be used instead of males in a future study.

Additionally, as this model was performed in three batches with different analyses being carried out for different batches, some experiments (such as *en face* lesion staining of the aortic arch and flow cytometry experiments) were underpowered with numbers too low for thorough analysis. It is therefore challenging to draw meaningful conclusions from these experiments, particularly as biological variation is so high. Similarly, some heart samples were lost during processing and so aortic root plaque burden could not be quantified in all samples.

It is possible that the dosing regimen used here, oral sunitinib 30mg kg^{-1} daily for 4 weeks, or the high fat diet model were not the optimal conditions for testing my hypothesis. The dose was chosen based on successful inhibition of inflammation in short term experiments described in Chapter 4, and the dosing schedule was influenced by a previous study in the Greaves lab (G. Purvis, unpublished data). A higher dose of sunitinib may enhance its NF-κB inhibiting ability, however this would have to be carefully balanced against increased toxicity risks with high dose sunitinib and an extended treatment period, and as discussed in the previous chapter, this dose already corresponds to a high human dose [289]. Furthermore, 8 weeks of Paigen diet generates small plaques in *Ldlr*$^{-/-}$ mice and mouse models of atherosclerosis can span up to 12 months [336], at which stage plaques are present throughout the descending aorta, not just in the arch, and root and display advanced lesion morphology with large necrotic cores and fibrous cap presence. It may therefore be easier to determine effect of sunitinib on plaque composition when more advanced plaque is present.

5.4.3 Summary

In this chapter I have found that the multi tyrosine kinase inhibitor and NF-κB inhibitor sunitinib inhibits inflammatory gene expression in a mouse model of hypercholesterolaemia and reduces TNFα production by 55%. Despite this, sunitinib does not alter atherosclerotic plaque development or stability in hypercholesterolaemic mice and thus its prospects as a drug repurposing candidate in CVD are limited.

Chapter 6: Conclusions

6.1 Summary of key findings

Over the course of my DPhil studies, I sought to identify and explore anti-inflammatory activity of drug repurposing candidates. Following an initial screen, I identified sunitinib as a promising potential anti-inflammatory drug repurposing candidate and investigated its activity in several *in vitro* and *in vivo* models of inflammation.

The first aim of my thesis was to identify novel anti-inflammatory drug repurposing candidates and validate their activity in macrophages *in vitro*. With regards to this aim, I made the following key findings:

- Tyrosine kinase inhibitors bosutinib and sunitinib dose-dependently supress NF-κB activity in the RAW-Blue macrophage reporter cell line without compromising cell viability
- Bosutinib and sunitinib inhibit production of pro-inflammatory mediator NF-κB transcriptional targets in RAW-Blue cells, primary murine BMDMs, and L929 fibroblasts in response to LPS stimulation
- Sunitinib attenuates BMDM polarisation
- Sunitinib exerts its NF-κB inhibitory effects via a mechanism independent from TLR4 internalisation and IκB degradation

The second major aim of my thesis was to investigate the effects of sunitinib *in vivo* using an endotoxaemia mouse model of acute inflammation. The key findings relating to this aim were:

- Oral treatment with sunitinib caused a significant 51% decrease in serum TNFα following 1 hour LPS challenge and inhibited expression of inflammatory genes in liver tissue at 1 and 6 hours post-LPS challenge

- Sunitinib inhibits NF-κB nuclear translocation in liver tissue of mice following 1 hour of LPS challenge
- Sunitinib reduces plasma markers of organ damage and improves lung histological features following 24 hours of LPS challenge

The final aim of this thesis was to investigate effects of sunitinib in an animal model of chronic cardiovascular inflammation. With regard to this aim, I made the following key findings:

- Oral sunitinib treatment does not affect circulating lipid levels of high-fat diet fed *Ldlr*$^{-/-}$ mice
- Sunitinib alters the immunophenotype of HFD-fed *Ldlr*$^{-/-}$ mice by substantially reducing plasma TNFα by 55% and reducing expression of CVD-relevant inflammatory genes in liver tissue
- Sunitinib treatment in HFD-fed *Ldlr*$^{-/-}$ mice does not alter immune cell populations and does not affect immune cell recruitment to atherosclerotic plaques
- Sunitinib treatment in HFD-fed *Ldlr*$^{-/-}$ mice does not affect atherosclerotic plaque size, histological markers of plaque stability, or plaque immunophenotype

6.2 The future of sunitinib as a drug repurposing candidate for inflammatory disease

The results presented in this thesis show that sunitinib can act as a potent inhibitor of NF-κB activity and downstream pro-inflammatory mediator production in macrophages *in vitro* and in mouse models of inflammation. Despite these findings, there are several key points that require addressing for sunitinib to be considered a feasible anti-inflammatory drug repurposing candidate.

Firstly, although several attempts were made during this thesis, the molecular mechanism by which sunitinib inhibits NF-κB remains unknown. As a tyrosine kinase inhibitor, it is presumed that sunitinib binds to and inhibits a tyrosine kinase target upstream of NF-κB activation. However, as sunitinib's kinase target profile is particularly broad [240] and the NF-κB signalling is an intricate pathway involving many molecular components, it is probable that simultaneous inhibition of several

kinases is responsible for sunitinib's anti-inflammatory effects. Likely candidates remain RTKs such as CSFR-1, PDGFR and VEGFR, or non-receptor tyrosine kinases such as Src.

To a certain extent, determining exact mechanistic details of sunitinib's anti-inflammatory activity may not be essential, with the knowledge that the ultimate effect is inhibition of NF-κB induced gene transcription. Indeed, drugs including colchicine, methotrexate, and sulfasalazine have safely and successfully been used in the treatment of inflammatory diseases for decades, despite their mechanisms of action remaining incompletely understood [320,324]. However, shedding light on the important kinase targets of sunitinib in inflammation could allow for other inhibitors of those targets that may have fewer side effects to be explored in models of inflammation.

The next consideration, as discussed in chapters 4 and 5, is that the largest *in vivo* effect of sunitinib in both the endotoxaemia and hypercholesterolaemia mouse models was on TNFα production, while some other cytokines such as IL-6 and IL-1β were unaffected in the models used here. The reason for sunitinib's TNFα specific effects require further exploration, however it could be due to targeting both myeloid and non-immune cell types. Due to this TNFα specific effect, an appropriate comparison for sunitinib in future studies would be other TNFα targeted therapies, such as biologic DMARDs which have revolutionised RA treatment [362], and recently developed small molecule TNFα inhibitors [362,363].

In sepsis and in CVD, TNFα inhibitors have seen limited success [256,302,364], therefore these patient populations may not be the most appropriate for treatment with sunitinib. Indeed, here in chapter 5 I found that sunitinib suppression of TNFα signalling in hypercholesterolaemic mice was not sufficient to reduce atherogenesis. On the other hand, RA is a largely TNFα-driven inflammatory disease and as such anti-TNFα therapies have been highly successful in RA patients [276]. Sunitinib could also prove to be beneficial in this context, and would provide a cheaper alternative to anti-TNF biologics, although its efficacy compared to DMARDs such as methotrexate would have to be evaluated.

The next major hurdle to repurposing sunitinib is its toxicity profile. As a second line treatment for advanced renal cell carcinoma (RCC), the side effects of sunitinib in the patient populations for which it is currently used are acceptable given its efficacy at slowing disease progression. Commonly reported adverse effects associated with sunitinib use include fatigue, diarrhoea, nausea, hypertension, thrombocytopenia, and neutropenia, and in early studies of sunitinib for RCC, between 8-10% of patients discontinued sunitinib therapy due to adverse effects [365]. A potential serious adverse effect of sunitinib is cardiac toxicity. In a phase III trial of sunitinib in RCC, 10% of patients experienced reduced ejection fraction, although most instances of this change were mild [345]. Furthermore, a retrospective study found that of 224 patients with RCC or other solid tumours taking sunitinib, 6 developed clinically significant congestive heart failure, with a mean onset of 22 days after initiation of sunitinib treatment [366]. Additional work is required to determine the cause of sunitinib associated cardiac toxicity, although VEGF/VEGFR inhibitors have been linked to such adverse effects [365]. Nevertheless, the risk of serious adverse effects with sunitinib may prevent its use in most patient populations, particularly those with slow progressing inflammatory disease such as RA, or those with prior cardiovascular impairment, such as those with chronic heart failure.

A possibility of drug repurposing is that new indications may require a lower dose in order to have the desired biological effect, particularly if a different patient population or different biological pathway is being targeted from the original indication. In the case of sunitinib, it could be that the dose required to inhibit NF-κB mediated inflammatory gene transcription is lower than the dose required to prevent tumour growth, providing a potential chance to minimise some of the adverse effects discussed above. I calculated that the effective *in vivo* dose used here in mice (30mg kg^{-1}) corresponds to an approximate 144mg dose in humans [289]. This is in fact much higher than that normally used in RCC (daily 50mg tablets), however future animal experiments could explore anti-inflammatory effects with a reduced sunitinib dose.

An alternative option that aims to reduce off target effects and to increase selectivity of repurposed drugs is to utilise novel targeted drug delivery technologies. This strategy, which gained interest in recent years, has seen anti-inflammatory drugs packaged within various nanocarriers including

liposomes, exosomes and hydrogels to increase drug potency, solubility, or specificity (reviewed in [367]). Many such strategies exploit the naturally high phagocytic capacity of macrophages to selectively target these cells in inflammatory disease. For example, Wu *et al.* utilised PS-containing liposomes as a delivery system to successfully target a peroxisome proliferator- activated receptor γ agonist to macrophages in an *ApoE*$^{-/-}$ mouse model of atherosclerosis [368]. These PS-containing liposomes act as apoptotic cell mimetics, and therefore have the dual benefit of selectively targeting the chosen drug to macrophages as well as inducing pro-repair pathways that are triggered by efferocytosis. Such a method could be employed with sunitinib or other repurposed drugs to not only reduce off target effects, but to potentially confer additional anti-inflammatory and pro-repair activity.

If side effects of sunitinib cannot be mitigated, rather than remaining a repurposing candidate itself, sunitinib's future in inflammation biology could lie in its use as a tool to identify structurally similar drug repurposing candidates with preferable side effect profiles and increased potency. Published literature of TKIs in models of inflammation [87,185,199,239], as well as the finding here that both sunitinib and bosutinib have anti-inflammatory activity in macrophages, warrant the further investigation of TKIs in inflammatory signalling and could indicate an emerging class of novel anti-inflammatory drugs. Similarly, drug re-engineering that uses sunitinib as a chemical scaffold for the development of novel compounds may be able to identify compounds with the same anti-inflammatory activity but fewer adverse effects. Although this approach lacks some of the cost and time benefits of drug repurposing and is more akin to *de novo* drug discovery, it could lead to the development of highly potent anti-inflammatory compounds.

Regardless of sunitinib's future for treatment of inflammatory disease, I have shown here that this framework — drug repurposing by phenotypic screening — can be used to identify anti-inflammatory drug activity in macrophages. This and other drug repurposing approaches will help to address the ongoing unmet clinical need for novel anti-inflammatory medicines.

References

1. Doudna, J. A. & Charpentier, E. The new frontier of genome engineering with CRISPR-Cas9. *Science (1979)* **346**, (2014).
2. Cavaillon, J.-M. The historical milestones in the understanding of leukocyte biology initiated by Elie Metchnikoff. *J Leukoc Biol* **90**, 413–424 (2011).
3. Cavaillon, J. M. Once upon a time, inflammation. *Journal of Venomous Animals and Toxins including Tropical Diseases* **27**, (2021).
4. Gordon, S. Elie Metchnikoff, the Man and the Myth. *J Innate Immun* **8**, 223 (2016).
5. Ginhoux, F. & Jung, S. Monocytes and macrophages: developmental pathways and tissue homeostasis. *Nature Reviews Immunology 2014 14:6* **14**, 392–404 (2014).
6. Jenkins, S. J. & Allen, J. E. The expanding world of tissue-resident macrophages. *Eur J Immunol* **51**, 1882–1896 (2021).
7. Blériot, C., Chakarov, S. & Ginhoux, F. Determinants of Resident Tissue Macrophage Identity and Function. *Immunity* **52**, 957–970 (2020).
8. Taylor, P. R. *et al.* MACROPHAGE RECEPTORS AND IMMUNE RECOGNITION. *https://doi.org/10.1146/annurev.immunol.23.021704.115816* **23**, 901–944 (2004).
9. Iqbal, A. J., Fisher, E. A. & Greaves, D. R. Inflammation—a Critical Appreciation of the Role of Myeloid Cells. *Myeloid Cells in Health and Disease* **4**, 325–342 (2016).
10. Hume, D. A. & MacDonald, K. P. A. Therapeutic applications of macrophage colony-stimulating factor-1 (CSF-1) and antagonists of CSF-1 receptor (CSF-1R) signaling. *Blood* **119**, 1810–1820 (2012).
11. Epelman, S., Lavine, K. J. & Randolph, G. J. Origin and Functions of Tissue Macrophages. *Immunity* **41**, 21 (2014).
12. Gschwandtner, M., Derler, R. & Midwood, K. S. More Than Just Attractive: How CCL2 Influences Myeloid Cell Behavior Beyond Chemotaxis. *Front Immunol* **10**, 2759 (2019).
13. Stanley, E. R. & Chitu, V. CSF-1 Receptor Signaling in Myeloid Cells. *Cold Spring Harb Perspect Biol* **6**, a021857 (2014).
14. Rumianek, A. N. & Greaves, D. R. How Have Leukocyte In Vitro Chemotaxis Assays Shaped Our Ideas about Macrophage Migration? *Biology 2020, Vol. 9, Page 439* **9**, 439 (2020).
15. Martinez, F. O. & Gordon, S. The M1 and M2 paradigm of macrophage activation: time for reassessment. *F1000Prime Rep* **6**, (2014).
16. Murray, P. J. Macrophage Polarization. *https://doi.org/10.1146/annurev-physiol-022516-034339* **79**, 541–566 (2017).
17. Nathan, C. F., Murray, H. W., Wlebe, I. E. & Rubin, B. Y. Identification of interferon-gamma as the lymphokine that activates human macrophage oxidative metabolism and antimicrobial activity. *J Exp Med* **158**, 670–689 (1983).
18. Roszer, T. Understanding the mysterious M2 macrophage through activation markers and effector mechanisms. *Mediators Inflamm* **2015**, (2015).

19. Li, M., Hou, Q., Zhong, L., Zhao, Y. & Fu, X. Macrophage Related Chronic Inflammation in Non-Healing Wounds. *Front Immunol* **12**, 2289 (2021).

20. Viola, A., Munari, F., Sánchez-Rodríguez, R., Scolaro, T. & Castegna, A. The metabolic signature of macrophage responses. *Front Immunol* **10**, 1462 (2019).

21. O'Rourke, S. A., Dunne, A. & Monaghan, M. G. The Role of Macrophages in the Infarcted Myocardium: Orchestrators of ECM Remodeling. *Front Cardiovasc Med* **6**, 101 (2019).

22. Kim, Y., Nurakhayev, S., Nurkesh, A., Zharkinbekov, Z. & Saparov, A. Macrophage Polarization in Cardiac Tissue Repair Following Myocardial Infarction. *Int J Mol Sci* **22**, 1–15 (2021).

23. Xuan, W., Qu, Q., Zheng, B., Xiong, S. & Fan, G.-H. The chemotaxis of M1 and M2 macrophages is regulated by different chemokines. *J Leukoc Biol* **97**, 61–69 (2015).

24. Vogel, D. Y. S. *et al.* Macrophages migrate in an activation-dependent manner to chemokines involved in neuroinflammation. *J Neuroinflammation* **11**, 1–11 (2014).

25. Gordon, S. Phagocytosis: An Immunobiologic Process. *Immunity* **44**, 463–475 (2016).

26. Kojima, Y., Weissman, I. L. & Leeper, N. J. The Role of Efferocytosis in Atherosclerosis. *Circulation* **135**, 476–489 (2017).

27. Elliott, M. R. & Ravichandran, K. S. The Dynamics of Apoptotic Cell Clearance. *Developmental Cell* vol. 38 147–160 Preprint at https://doi.org/10.1016/j.devcel.2016.06.029 (2016).

28. Green, D. R., Oguin, T. H. & Martinez, J. The clearance of dying cells: Table for two. *Cell Death and Differentiation* vol. 23 915–926 Preprint at https://doi.org/10.1038/cdd.2015.172 (2016).

29. Fadok, V. A. *et al.* Macrophages that have ingested apoptotic cells in vitro inhibit proinflammatory cytokine production through autocrine/paracrine mechanisms involving TGF-β, PGE2, and PAF. *Journal of Clinical Investigation* **101**, 890–898 (1998).

30. Henson, P. M. & Bratton, D. L. Antiinflammatory effects of apoptotic cells. *Journal of Clinical Investigation* **123**, 2773–2774 (2013).

31. Yurdagul, A. *et al.* Macrophage Metabolism of Apoptotic Cell-Derived Arginine Promotes Continual Efferocytosis and Resolution of Injury. *Cell Metab* **31**, 518-533.e10 (2020).

32. Cui, D. *et al.* Pivotal advance: macrophages become resistant to cholesterol-induced death after phagocytosis of apoptotic cells. *J Leukoc Biol* **82**, 1040–50 (2007).

33. Morioka, S. *et al.* Efferocytosis induces a novel SLC program to promote glucose uptake and lactate release. *Nature* **563**, 714–718 (2018).

34. Schebb, N. H. *et al.* Formation, Signaling and Occurrence of Specialized Pro-Resolving Lipid Mediators—What is the Evidence so far? *Front Pharmacol* **13**, 475 (2022).

35. Feehan, K. T. & Gilroy, D. W. Is Resolution the End of Inflammation? *Trends Mol Med* **25**, 198–214 (2019).

36. Elliott, M. R., Koster, K. M. & Murphy, P. S. Efferocytosis Signaling in the Regulation of Macrophage Inflammatory Responses. *The Journal of Immunology* **198**, 1387–1394 (2017).

37. Serhan, C. N. The resolution of inflammation: the devil in the flask and in the details. *The FASEB Journal* **25**, 1441 (2011).

38. Chiang, N. & Serha, C. N. Specialized pro-resolving mediator network: an update on production and actions. *Essays Biochem* **64**, 443–462 (2020).

39. Anderson, K. V., Bokla, L. & Nüsslein-Volhard, C. Establishment of dorsal-ventral polarity in the drosophila embryo: The induction of polarity by the Toll gene product. *Cell* **42**, 791–798 (1985).

40. Fitzgerald, K. A. & Kagan, J. C. Toll-like Receptors and the Control of Immunity. *Cell* **180**, 1044–1066 (2020).

41. Lannoy, V., Côté-Biron, A., Asselin, C. & Rivard, N. Phosphatases in toll-like receptors signaling: the unfairly-forgotten. *Cell Communication and Signaling 2021 19:1* **19**, 1–15 (2021).

42. Pålsson-McDermott, E. M. & O'Neill, L. A. J. Signal transduction by the lipopolysaccharide receptor, Toll-like receptor-4. *Immunology* **113**, 153 (2004).

43. Kawasaki, T. & Kawai, T. Toll-like receptor signaling pathways. *Front Immunol* **5**, 461 (2014).

44. Chattopadhyay, S. & Sen, G. C. Tyrosine Phosphorylation in Toll-Like Receptor Signaling. *Cytokine Growth Factor Rev* **25**, 533 (2014).

45. Karin, M. *How NF-kB is activated: the role of the IkB kinase (IKK) complex*. http://www.stockton-press.co.uk/onc.

46. Sen, R. & Baltimore, D. Multiple nuclear factors interact with the immunoglobulin enhancer sequences. *Cell* **46**, 705–716 (1986).

47. Liu, T., Zhang, L., Joo, D. & Sun, S. C. NF-κB signaling in inflammation. *Signal Transduction and Targeted Therapy 2017 2:1* **2**, 1–9 (2017).

48. Christian, F., Smith, E. L. & Carmody, R. J. The Regulation of NF-κB Subunits by Phosphorylation. *Cells* **5**, (2016).

49. Dorrington, M. G. & Fraser, I. D. C. NF-κB Signaling in Macrophages: Dynamics, Crosstalk, and Signal Integration. *Front Immunol* **10**, (2019).

50. Jin, J. *et al.* Noncanonical NF-κB Pathway Controls the Production of Type I Interferons in Antiviral Innate Immunity. *Immunity* **40**, 342–354 (2014).

51. Sun, S. C. The non-canonical NF-κB pathway in immunity and inflammation. *Nature Reviews Immunology 2017 17:9* **17**, 545–558 (2017).

52. Sanjabi, S., Hoffmann, A., Liou, H. C., Baltimore, D. & Smale, S. T. Selective requirement for c-Rel during IL-12 P40 gene induction in macrophages. *Proc Natl Acad Sci U S A* **97**, 12705–12710 (2000).

53. Litvak, V. *et al.* Function of C/EBPdelta in a regulatory circuit that discriminates between transient and persistent TLR4-induced signals. *Nat Immunol* **10**, 437–443 (2009).

54. Courtine, E. *et al.* Combined loss of cRel/p50 subunits of NF-κB leads to impaired innate host response in sepsis. *Innate Immun* **18**, 753–763 (2012).

55. Grigoriadis, G. *et al.* The Rel subunit of NF-kappaB-like transcription factors is a positive and negative regulator of macrophage gene expression: distinct roles for Rel in different macrophage populations. *EMBO J* **15**, 7099–7107 (1996).

56. Nelson, D. E. *et al.* Oscillations in NF-κB signaling control the dynamics of gene expression. *Science (1979)* **306**, 704–708 (2004).

57. Fujioka, S. *et al.* NF-κB and AP-1 Connection: Mechanism of NF-κB-Dependent Regulation of AP-1 Activity. *Mol Cell Biol* **24**, 7806 (2004).

58. Kelley, N., Jeltema, D., Duan, Y. & He, Y. The NLRP3 Inflammasome: An Overview of Mechanisms of Activation and Regulation. *Int J Mol Sci* **20**, (2019).

59. Karasawa, T. & Takahashi, M. Role of NLRP3 Inflammasomes in Atherosclerosis. *J Atheroscler Thromb* **24**, 443 (2017).

60. Carswell, E. A. *et al.* An endotoxin-induced serum factor that causes necrosis of tumors. *Proceedings of the National Academy of Sciences* **72**, 3666–3670 (1975).

61. Holbrook, J., Lara-Reyna, S., Jarosz-Griffiths, H. & McDermott, M. Tumour necrosis factor signalling in health and disease. *F1000Res* **8**, (2019).

62. Rolski, F. & Błyszczuk, P. Complexity of TNF-α Signaling in Heart Disease. *J Clin Med* **9**, 1–25 (2020).

63. Webster, J. D. & Vucic, D. The Balance of TNF Mediated Pathways Regulates Inflammatory Cell Death Signaling in Healthy and Diseased Tissues. *Front Cell Dev Biol* **8**, 365 (2020).

64. Jang, D. I. *et al.* The Role of Tumor Necrosis Factor Alpha (TNF-α) in Autoimmune Disease and Current TNF-α Inhibitors in Therapeutics. *International Journal of Molecular Sciences 2021, Vol. 22, Page 2719* **22**, 2719 (2021).

65. Parameswaran, N. & Patial, S. Tumor Necrosis Factor-α Signaling in Macrophages. *Crit Rev Eukaryot Gene Expr* **20**, 87 (2010).

66. Rose-John, S., Winthrop, K. & Calabrese, L. The role of IL-6 in host defence against infections: immunobiology and clinical implications. *Nature Reviews Rheumatology 2017 13:7* **13**, 399–409 (2017).

67. Luo, Y. & Zheng, S. G. Hall of fame among pro-inflammatory cytokines: Interleukin-6 gene and its transcriptional regulation mechanisms. *Front Immunol* **7**, 604 (2016).

68. Benveniste, E. N. Cytokines. *Encyclopedia of the Neurological Sciences* 921–925 (2014) doi:10.1016/B978-0-12-385157-4.00175-5.

69. Tanaka, T., Narazaki, M. & Kishimoto, T. IL-6 in Inflammation, Immunity, and Disease. *Cold Spring Harb Perspect Biol* **6**, 16295–16296 (2014).

70. Scheller, J., Chalaris, A., Schmidt-Arras, D. & Rose-John, S. The pro- and anti-inflammatory properties of the cytokine interleukin-6. *Biochimica et Biophysica Acta (BBA) - Molecular Cell Research* **1813**, 878–888 (2011).

71. Chen, Q. *et al.* Fever-range thermal stress promotes lymphocyte trafficking across high endothelial venules via an interleukin 6 trans-signaling mechanism. *Nature Immunology 2006 7:12* **7**, 1299–1308 (2006).

72. Xing, Z. *et al.* Enhanced Acute Inflammatory Responses in IL-6-deficient Mice IL-6 Is an Antiinflammatory Cytokine Required for Controlling Local or Systemic Acute Inflammatory Responses. *J. Clin. Invest* **101**, 311–320 (1998).

73. Mauer, J. *et al.* Signaling by IL-6 promotes alternative activation of macrophages to limit endotoxaemia and obesity-associated resistance to insulin. *Nat Immunol* **15**, 423–430 (2014).

74. Kaneko, N., Kurata, M., Yamamoto, T., Morikawa, S. & Masumoto, J. The role of interleukin-1 in general pathology. *Inflammation and Regeneration 2019 39:1* **39**, 1–16 (2019).

75. Chan, A. H. & Schroder, K. Inflammasome signaling and regulation of interleukin-1 family cytokines. *Journal of Experimental Medicine* **217**, (2020).

76. Palmieri, E. M., McGinity, C., Wink, D. A. & McVicar, D. W. Nitric Oxide in Macrophage Immunometabolism: Hiding in Plain Sight. *Metabolites* **10**, 1–34 (2020).

77. Brunet, L. R. Nitric oxide in parasitic infections. *Int Immunopharmacol* **1**, 1457–1467 (2001).

78. Tripathi, P., Tripathi, P., Kashyap, L. & Singh, V. The role of nitric oxide in inflammatory reactions. *FEMS Immunol Med Microbiol* **51**, 443–452 (2007).

79. Rath, M., Müller, I., Kropf, P., Closs, E. I. & Munder, M. Metabolism via arginase or nitric oxide synthase: Two competing arginine pathways in macrophages. *Front Immunol* **5**, 532 (2014).

80. Aleshin, A. & Finn, R. S. SRC: A Century of Science Brought to the Clinic. *Neoplasia* **12**, 599–607 (2010).

81. Zen, K. & Liu, Y. Role of different protein tyrosine kinases in fMLP-induced neutrophil transmigration. *Immunobiology* **213**, 13–23 (2008).

82. Johnsen, I. B. *et al.* Toll-like receptor 3 associates with c-Src tyrosine kinase on endosomes to initiate antiviral signaling. *EMBO J* **25**, 3335–3346 (2006).

83. Hsieh, H. L., Wang, H. H., Wu, C. Y., Tung, W. H. & Yang, C. M. Lipoteichoic acid induces matrix metalloproteinase-9 expression via transactivation of PDGF receptors and NF-kappaB activation in rat brain astrocytes. *Neurotox Res* **17**, 344–359 (2010).

84. Tang, C. H., Hsu, C. J., Yang, W. H. & Fong, Y. C. Lipoteichoic acid enhances IL-6 production in human synovial fibroblasts via TLR2 receptor, PKCdelta and c-Src dependent pathways. *Biochem Pharmacol* **79**, 1648–1657 (2010).

85. Meng, F. & Lowell, C. A. Lipopolysaccharide (LPS)-induced Macrophage Activation and Signal Transduction in the Absence of Src-Family Kinases Hck, Fgr, and Lyn. *J Exp Med* **185**, 1661 (1997).

86. Leu, T. H., Charoenfuprasert, S., Yen, C. K., Fan, C. W. & Maa, M. C. Lipopolysaccharide-induced c-Src expression plays a role in nitric oxide and TNFα secretion in macrophages. *Mol Immunol* **43**, 308–316 (2006).

87. Kang, J. L. *et al.* Inhibition of Src tyrosine kinases suppresses activation of nuclear factor-κB, and serine and tyrosine phosphorylation of IκB-α in lipopolysaccharide-stimulated raw 264.7 macrophages. *J Toxicol Environ Health A* **68**, 1643–1662 (2005).

88. Chen, Y. J. *et al.* Eps8 Protein Facilitates Phagocytosis by Increasing TLR4-MyD88 Protein Interaction in Lipopolysaccharide-stimulated Macrophages. *J Biol Chem* **287**, 18806 (2012).

89. Neys, S. F. H., Hendriks, R. W. & Corneth, O. B. J. Targeting Bruton's Tyrosine Kinase in Inflammatory and Autoimmune Pathologies. *Front Cell Dev Biol* **9**, 1078 (2021).

90. Karlsson, M. *et al.* A single–cell type transcriptomics map of human tissues. *Sci Adv* **7**, (2021).

91. Weber, A. N. R. *et al.* Bruton's tyrosine kinase: An emerging key player in innate immunity. *Front Immunol* **8**, 1454 (2017).

92. Purvis, G. S. D., Aranda-Tavio, H., Channon, K. M. & Greaves, D. R. Bruton's TK regulates myeloid cell recruitment during acute inflammation. *Br J Pharmacol* **179**, 2754–2770 (2022).

93. de Porto, A. P. *et al.* Bruton's Tyrosine Kinase-Mediated Signaling in Myeloid Cells Is Required for Protective Innate Immunity During Pneumococcal Pneumonia. *Front Immunol* **12**, 3623 (2021).

94. Ito, M. *et al.* Bruton's tyrosine kinase is essential for NLRP3 inflammasome activation and contributes to ischaemic brain injury. *Nature Communications 2015 6:1* **6**, 1–11 (2015).

95. Weber, A. N. R. Targeting the NLRP3 Inflammasome via BTK. *Front Cell Dev Biol* **9**, 139 (2021).

96. O'Riordan, C. E. *et al.* Bruton's Tyrosine Kinase Inhibition Attenuates the Cardiac Dysfunction Caused by Cecal Ligation and Puncture in Mice. *Front Immunol* **10**, (2019).

97. Purvis, G. S. D. *et al.* Inhibition of Bruton's TK regulates macrophage NF-κB and NLRP3 inflammasome activation in metabolic inflammation. *Br J Pharmacol* **177**, 4416 (2020).

98. Irvine, K. M. *et al.* A CSF-1 receptor kinase inhibitor targets effector functions and inhibits pro-inflammatory cytokine production from murine macrophage populations. *The FASEB Journal* **20**, 1921–1923 (2006).

99. Zhao, B. *et al.* Constitutive Receptor-independent Low Density Lipoprotein Uptake and Cholesterol Accumulation by Macrophages Differentiated from Human Monocytes with Macrophage-Colony-stimulating Factor (M-CSF). *Journal of Biological Chemistry* **281**, 15757–15762 (2006).

100. Paolino, M. & Penninger, J. M. The Role of TAM Family Receptors in Immune Cell Function: Implications for Cancer Therapy. *Cancers (Basel)* **8**, (2016).

101. Camenisch, T. D., Koller, B. H., Earp2, H. S. & Matsushima, G. K. A Novel Receptor Tyrosine Kinase, Mer, Inhibits TNF-α Production and Lipopolysaccharide-Induced Endotoxic Shock. *The Journal of Immunology* **162**, 3498–3503 (1999).

102. Lu, Q. & Lemke, G. Homeostatic regulation of the immune system by receptor tyrosine kinases of the Tyro 3 family. *Science* **293**, 306–11 (2001).

103. Lumbroso, D. *et al.* Macrophage-derived protein S facilitates apoptotic polymorphonuclear cell clearance by resolution phase macrophages and supports their reprogramming. *Front Immunol* **9**, (2018).

104. Zagórska, A., Través, P. G., Lew, E. D., Dransfield, I. & Lemke, G. Diversification of TAM receptor tyrosine kinase function. *Nat Immunol* **15**, 920–928 (2014).

105. Sharif, M. N. *et al.* Twist mediates suppression of inflammation by type I IFNs and Axl. *Journal of Experimental Medicine* **203**, 1891–1901 (2006).

106. Cai, B. *et al.* MerTK receptor cleavage promotes plaque necrosis and defective resolution in atherosclerosis. *Journal of Clinical Investigation* **127**, 564–568 (2017).

107. Thorp, E., Cui, D., Schrijvers, D. M., Kuriakose, G. & Tabas, I. Mertk receptor mutation reduces efferocytosis efficiency and promotes apoptotic cell accumulation and plaque necrosis in atherosclerotic lesions of Apoe-/- mice. *Arterioscler Thromb Vasc Biol* **28**, 1421–1428 (2008).

108. DeBerge, M. *et al.* Macrophage AXL receptor tyrosine kinase inflames the heart after reperfused myocardial infarction. *Journal of Clinical Investigation* **131**, (2021).

109. Hotchkiss, R. S. *et al.* Sepsis and septic shock. *Nature Reviews Disease Primers 2016 2:1* **2**, 1–21 (2016).

110. Wiersinga, W. J., Leopold, S. J., Cranendonk, D. R. & van der Poll, T. Host innate immune responses to sepsis. *https://doi.org/10.4161/viru.25436* **5**, 36–44 (2013).

111. Conrad, N. *et al.* Autoimmune diseases and cardiovascular risk: a population-based study on 19 autoimmune diseases and 12 cardiovascular diseases in 22 million individuals in the UK. *The Lancet* **400**, 733–743 (2022).

112. Ridker, P. M., Cushman, M., Stampfer, M. J., Tracy, R. P. & Hennekens, C. H. Inflammation, aspirin, and the risk of cardiovascular disease in apparently healthy men. *N Engl J Med* **336**, 973–979 (1997).

113. Berk, B. C., Weintraub, W. S. & Alexander, R. W. Elevation of C-reactive protein in 'active' coronary artery disease. *Am J Cardiol* **65**, 168–172 (1990).

114. Tabas, I. & Lichtman, A. H. Monocyte-Macrophages and T Cells in Atherosclerosis. *Immunity* **47**, 621–634 (2017).

115. Engelen, S. E., Robinson, A. J. B., Zurke, Y. X. & Monaco, C. Therapeutic strategies targeting inflammation and immunity in atherosclerosis: how to proceed? *Nature Reviews Cardiology 2022 19:8* **19**, 522–542 (2022).

116. Moore, K. J., Sheedy, F. J. & Fisher, E. A. Macrophages in atherosclerosis: a dynamic balance. *Nat Rev Immunol* **13**, 709 (2013).

117. Ruparelia, N. & Choudhury, R. Inflammation and atherosclerosis: what is on the horizon? *Heart* **106**, 80–85 (2020).

118. Libby, P. Inflammation during the life cycle of the atherosclerotic plaque. *Cardiovasc Res* **117**, 2525 (2021).

119. Susser, L. I. & Rayner, K. J. Through the layers: how macrophages drive atherosclerosis across the vessel wall. (2022) doi:10.1172/JCI157011.

120. Barrett, T. J. Macrophages in Atherosclerosis Regression. *Arterioscler Thromb Vasc Biol* **40**, 20–33 (2020).

121. Elhage, R. *et al.* Involvement of interleukin-6 in atherosclerosis but not in the prevention of fatty streak formation by 17beta-estradiol in apolipoprotein E-deficient mice. *Atherosclerosis* **156**, 315–320 (2001).

122. Huber, S. A., Sakkinen, P., Conze, D., Hardin, N. & Tracy, R. Interleukin-6 exacerbates early atherosclerosis in mice. *Arterioscler Thromb Vasc Biol* **19**, 2364–2367 (1999).

123. Schieffer, B. *et al.* Impact of interleukin-6 on plaque development and morphology in experimental atherosclerosis. *Circulation* **110**, 3493–3500 (2004).

124. Maguire, E. M., Pearce, S. W. A. & Xiao, Q. Foam cell formation: A new target for fighting atherosclerosis and cardiovascular disease. *Vascul Pharmacol* **112**, 54–71 (2019).

125. Thorp, E. B. Mechanisms of failed apoptotic cell clearance by phagocyte subsets in cardiovascular disease. *Apoptosis* vol. 15 1124–1136 Preprint at https://doi.org/10.1007/s10495-010-0516-6 (2010).

126. Kojima, Y. *et al.* CD47-blocking antibodies restore phagocytosis and prevent atherosclerosis. *Nature* **536**, 86–90 (2016).

127. Fatkhullina, A. R., Peshkova, I. O. & Koltsova, E. K. The Role of Cytokines in the Development of Atherosclerosis. *Biochemistry (Mosc)* **81**, 1358 (2016).

128. Ohta, H. *et al.* Disruption of tumor necrosis factor-alpha gene diminishes the development of atherosclerosis in ApoE-deficient mice. *Atherosclerosis* **180**, 11–17 (2005).

129. Zhu, M. *et al.* Excess TNF-α in the blood activates monocytes with the potential to directly form cholesteryl ester-laden cells. *Acta Biochim Biophys Sin (Shanghai)* **47**, 899–907 (2015).

130. Wuttge, D. M. *et al.* CXCL16/SR-PSOX is an interferon-gamma-regulated chemokine and scavenger receptor expressed in atherosclerotic lesions. *Arterioscler Thromb Vasc Biol* **24**, 750–755 (2004).

131. Davenport, P. & Tipping, P. G. The Role of Interleukin-4 and Interleukin-12 in the Progression of Atherosclerosis in Apolipoprotein E-Deficient Mice. *Am J Pathol* **163**, 1117 (2003).

132. Kirii, H. *et al.* Lack of interleukin-1beta decreases the severity of atherosclerosis in ApoE-deficient mice. *Arterioscler Thromb Vasc Biol* **23**, 656–660 (2003).

133. Mallat, Z. *et al.* Protective role of interleukin-10 in atherosclerosis. *Circ Res* **85**, (1999).

134. Caligiuri, G. *et al.* Interleukin-10 Deficiency Increases Atherosclerosis, Thrombosis, and Low-density Lipoproteins in Apolipoprotein E Knockout Mice. *Molecular Medicine* **9**, 10 (2003).

135. Mallat, Z. *et al.* Inhibition of transforming growth factor-beta signaling accelerates atherosclerosis and induces an unstable plaque phenotype in mice. *Circ Res* **89**, 930–934 (2001).

136. Grainger, D. J., Mosedale, D. E., Metcalfe, J. C. & Bottinger, E. P. Dietary fat and reduced levels of TGFbeta1 act synergistically to promote activation of the vascular endothelium and formation of lipid lesions. *J Cell Sci* **113 (Pt 13)**, 2355–2361 (2000).

137. Brand, K. *et al.* Activated transcription factor nuclear factor-kappa B is present in the atherosclerotic lesion. *J Clin Invest* **97**, 1715–1722 (1996).

138. Liao, F., Andalibi, A., DeBeer, F. C., Fogelman, A. M. & Lusis, A. J. Genetic control of inflammatory gene induction and NF-kappa B-like transcription factor activation in response to an atherogenic diet in mice. *J Clin Invest* **91**, 2572–2579 (1993).

139. Real, J. T. *et al.* Circulating mononuclear cells nuclear factor-kappa B activity, plasma xanthine oxidase, and low grade inflammatory markers in adult patients with familial hypercholesterolaaemia. *Eur J Clin Invest* **40**, 89–94 (2010).

140. Aiello, R. J. *et al.* Monocyte Chemoattractant Protein-1 Accelerates Atherosclerosis in Apolipoprotein E-Deficient Mice. *Arterioscler Thromb Vasc Biol* **19**, 1518–1525 (1999).

141. Cybulsky, M. I. *et al.* A major role for VCAM-1, but not ICAM-1, in early atherosclerosis. *J Clin Invest* **107**, 1255–1262 (2001).

142. Collins, R. G. *et al.* P-Selectin or Intercellular Adhesion Molecule (Icam)-1 Deficiency Substantially Protects against Atherosclerosis in Apolipoprotein E–Deficient Mice. *Journal of Experimental Medicine* **191**, 189–194 (2000).

143. De Winther, M. P. J., Kanters, E., Kraal, G. & Hofker, M. H. Nuclear Factor κB Signaling in Atherogenesis. *Arterioscler Thromb Vasc Biol* **25**, 904–914 (2005).

144. Chaffey, L., Roberti, A. & Greaves, D. R. Drug repurposing in cardiovascular inflammation: Successes, failures, and future opportunities. *Front Pharmacol* **13**, 4500 (2022).

145. Timmermans, S., Souffriau, J. & Libert, C. A general introduction to glucocorticoid biology. *Front Immunol* **10**, 1545 (2019).

146. Weikum, E. R., Knuesel, M. T., Ortlund, E. A. & Yamamoto, K. R. Glucocorticoid receptor control of transcription: precision and plasticity via allostery. *Nature Reviews Molecular Cell Biology 2017 18:3* **18**, 159–174 (2017).

147. Yang, R. & Yu, Y. Glucocorticoids are double-edged sword in the treatment of COVID-19 and cancers. *Int J Biol Sci* **17**, 1530 (2021).

148. Scheinman, R. I., Cogswell, P. C., Lofquist, A. K. & Baldwin, A. S. Role of transcriptional activation of I kappa B alpha in mediation of immunosuppression by glucocorticoids. *Science* **270**, 283–286 (1995).

149. Bekhbat, M., Rowson, S. A. & Neigh, G. N. Checks and Balances: the Glucocorticoid Receptor and NFκB in Good Times and Bad. *Front Neuroendocrinol* **46**, 15 (2017).

150. Widén, C., Gustafsson, J. Å. & Wikström, A. C. Cytosolic glucocorticoid receptor interaction with nuclear factor-kappa B proteins in rat liver cells. *Biochem J* **373**, 211–220 (2003).

151. Hench, P. S., Kendall, E. C., Slocumb, C. H. & Polley, H. F. The effect of a hormone of the adrenal cortex (17-hydroxy-11-dehydrocorticosterone: compound E) and of pituitary adrenocortical hormone in arthritis: preliminary report. *Ann Rheum Dis* **8**, 97 (1949).

152. Habib, I., Mazulis, A., Roginsky, G. & Ehrenpreis, E. D. Nonsteroidal Anti-inflammatory Drugs and Inflammatory Bowel Disease: Pathophysiology and Clinical Associations. *Inflamm Bowel Dis* **20**, 2493–2502 (2014).

153. Wang, B. *et al.* Metabolism pathways of arachidonic acids: mechanisms and potential therapeutic targets. *Signal Transduction and Targeted Therapy 2021 6:1* **6**, 1–30 (2021).

154. Ricciotti, E. & Fitzgerald, G. A. Prostaglandins and Inflammation. *Arterioscler Thromb Vasc Biol* **31**, 986 (2011).

155. Williams, J. A. & Shacter, E. Regulation of Macrophage Cytokine Production by Prostaglandin E 2 DISTINCT ROLES OF CYCLOOXYGENASE-1 AND-2*. (1997) doi:10.1074/jbc.272.41.25693.

156. Akaogi, J. *et al.* Prostaglandin E2 receptors EP2 and EP4 are up-regulated in peritoneal macrophages and joints of pristane-treated mice and modulate TNF-alpha and IL-6 production. *J Leukoc Biol* **76**, 227–236 (2004).

157. Luan, B. *et al.* CREB pathway links PGE2 signaling with macrophage polarization. *Proc Natl Acad Sci U S A* **112**, 15642–15647 (2015).

158. Benjamin, O., Bansal, P. & Goyal, A. et al. Disease Modifying Anti-Rheumatic Drugs (DMARD). *StatPearls* (2022).

159. Botz, B., Bölcskei, K. & Helyes, Z. Challenges to develop novel anti-inflammatory and analgesic drugs. *Wiley Interdiscip Rev Nanomed Nanobiotechnol* **9**, e1427 (2017).

160. Junhee Seok *et al.* Genomic responses in mouse models poorly mimic human inflammatory diseases. *Proc Natl Acad Sci U S A* **110**, 3507–3512 (2013).

161. Kapellos, T. S. *et al.* A novel real time imaging platform to quantify macrophage phagocytosis. *Biochem Pharmacol* **116**, 107–119 (2016).

162. Purvis, G. S. D. *et al.* Inhibition of Bruton's TK regulates macrophage NF-κB and NLRP3 inflammasome activation in metabolic inflammation. *Br J Pharmacol* **177**, 4416–4432 (2020).

163. Englen, M. D., Valdez, Y. E., Lehnert, N. M. & Lehnert, B. E. Granulocyte/macrophage colony-stimulating factor is expressed and secreted in cultures of murine L929 cells. *J Immunol Methods* **184**, 281–283 (1995).

164. Park, I. *et al.* C-type lectin receptor CLEC4A2 promotes tissue adaptation of macrophages and protects against atherosclerosis. *Nat Commun* **13**, (2022).

165. Livak, K. J. & Schmittgen, T. D. Analysis of relative gene expression data using real-time quantitative PCR and the 2(-Delta Delta C(T)) Method. *Methods* **25**, 402–408 (2001).

166. Douglas, G. *et al.* Roles for endothelial cell and macrophage Gch1 and tetrahydrobiopterin in atherosclerosis progression. *Cardiovasc Res* **114**, 1385–1399 (2018).

167. Montinari, M. R., Minelli, S. & De Caterina, R. The first 3500 years of aspirin history from its roots - A concise summary. *Vascul Pharmacol* **113**, 1–8 (2019).

168. Vane, J. R. Inhibition of Prostaglandin Synthesis as a Mechanism of Action for Aspirin-like Drugs. *Nature New Biology 1971 231:25* **231**, 232–235 (1971).

169. Nosengo, N. Can you teach old drugs new tricks? *Nature* **534**, 314–316 (2016).

170. W, T. D. *et al.* Clinical Development Success Rates 2006–2015.

171. J A. DiMasi, L. Feldman, A. Seckler & A. Wilson. Trends in risks associated with new drug development: success rates for investigational drugs. *Clin Pharmacol Ther* **87**, 272–277.

172. Hay, M., Thomas, D. W., Craighead, J. L., Economides, C. & Rosenthal, J. Clinical development success rates for investigational drugs. *Nat Biotechnol* **32**, 40–51 (2014).

173. Wong, C. H., Siah, K. W. & Lo, A. W. Estimation of clinical trial success rates and related parameters. *Biostatistics* **20**, 273–286 (2019).

174. Dexamethasone in Hospitalized Patients with Covid-19. *New England Journal of Medicine* **384**, 693–704 (2021).

175. Cruz-Burgos, M. *et al.* New Approaches in Oncology for Repositioning Drugs: The Case of PDE5 Inhibitor Sildenafil. *Front Oncol* **11**, 208 (2021).

176. Jourdan, J. P., Bureau, R., Rochais, C. & Dallemagne, P. Drug repositioning: a brief overview. *Journal of Pharmacy and Pharmacology* **72**, 1145–1151 (2020).

177. Teo, S. K. *et al.* Thalidomide in the treatment of leprosy. *Microbes Infect* **4**, 1193–1202 (2002).

178. Sheskin, J. Thalidomide in the treatment of lepra reactions. *Clin Pharmacol Ther* **6**, 303–306 (1965).

179. Millrine, D. & Kishimoto, T. A Brighter Side to Thalidomide: Its Potential Use in Immunological Disorders. *Trends Mol Med* **23**, 348–361 (2017).

180. Roberti, A., Chaffey, L. E. & Greaves, D. R. NF-κB Signaling and Inflammation—Drug Repurposing to Treat Inflammatory Disorders? *Biology 2022, Vol. 11, Page 372* **11**, 372 (2022).

181. Rihel, J. *et al.* Zebrafish behavioral profiling links drugs to biological targets and rest/wake regulation. *Science (1979)* **327**, 348–351 (2010).

182. Hall, C. J. *et al.* Repositioning drugs for inflammatory disease-fishing for new anti-inflammatory agents. *DMM Disease Models and Mechanisms* **7**, 1069–1081 (2014).

183. Ferguson, F. M. & Gray, N. S. Kinase inhibitors: the road ahead. *Nature Reviews Drug Discovery 2018 17:5* **17**, 353–377 (2018).

184. Zarrin, A. A., Bao, K., Lupardus, P. & Vucic, D. Kinase inhibition in autoimmunity and inflammation. *Nature Reviews Drug Discovery 2020 20:1* **20**, 39–63 (2020).

185. Guo, K. *et al.* Treatment Effects of the Second-Generation Tyrosine Kinase Inhibitor Dasatinib on Autoimmune Arthritis. *Front Immunol* **9**, (2018).

186. Baig, M. S. *et al.* Repurposing Thioridazine (TDZ) as an anti-inflammatory agent. *Scientific Reports 2018 8:1* **8**, 1–10 (2018).

187. Auphan, N., DiDonato, J. A., Rosette, C., Helmberg, A. & Karin, M. Immunosuppression by glucocorticoids: inhibition of NF-kappa B activity through induction of I kappa B synthesis. *Science* **270**, 286–290 (1995).

188. Barnes, P. J. How corticosteroids control inflammation: Quintiles Prize Lecture 2005. *Br J Pharmacol* **148**, 245 (2006).

189. Chong, W. *et al.* Histone Deacetylase Inhibitor SAHA Attenuates TLR4 Signaling in LPS-Stimulated Mouse Macrophages. *J Surg Res* **178**, 851 (2012).

190. Beduschi, M. G., Guimarães, C. L., Buss, Z. S. & Dalmarco, E. M. Mycophenolate mofetil has potent anti-inflammatory actions in a mouse model of acute lung injury. *Inflammation* **36**, 729–737 (2013).

191. Lee, J. *et al.* Mycophenolate mofetil promotes down-regulation of expanded B cells and production of TNF-α in an experimental murine model of colitis. *Cytokine* **44**, 49–56 (2008).

192. Jonsson, C. A. & Carlsten, H. Mycophenolic acid inhibits inosine 5′-monophosphate dehydrogenase and suppresses production of pro-inflammatory cytokines, nitric oxide, and LDH in macrophages. *Cell Immunol* **216**, 93–101 (2002).

193. Tariq, M. *et al.* Gefitinib inhibits M2-like polarization of tumor-associated macrophages in Lewis lung cancer by targeting the STAT6 signaling pathway. *Acta Pharmacol Sin* **38**, 1501–1511 (2017).

194. Wang, L. *et al.* Doxorubicin-Induced Systemic Inflammation Is Driven by Upregulation of Toll-Like Receptor TLR4 and Endotoxin Leakage. *Cancer Res* **76**, 6631–6642 (2016).

195. MichelL, Jomard & Démarchez. Pharmacology of adapalene. *British Journal of Dermatology* **139**, 3–7 (1998).

196. Oliveira, L. D. M., Teixeira, F. M. E. & Sato, M. N. Impact of Retinoic Acid on Immune Cells and Inflammatory Diseases. *Mediators Inflamm* **2018**, (2018).

197. Li, Z. *et al.* Protective effects of Nebivolol against interleukin-1β (IL-1β)-induced type II collagen destruction mediated by matrix metalloproteinase-13 (MMP-13). *Cell Stress Chaperones* **22**, 767–774 (2017).

198. Xie, Q. *et al.* Nebivolol ameliorates cardiac NLRP3 inflammasome activation in a juvenile-adolescent animal model of diet-induced obesity. *Sci Rep* **6**, 1–12 (2016).

199. Zhao, S. *et al.* Suppressive effects of sunitinib on a TLR activation-induced cytokine storm. *Eur J Pharmacol* **854**, 347–353 (2019).

200. Miller, S. C. *et al.* Identification of known drugs that act as inhibitors of NF-κB signaling and their mechanism of action. *Biochem Pharmacol* **79**, 1272–1280 (2010).

201. Van Dongen, M. *et al.* Anti-inflammatory M2 type macrophages characterize metastasized and tyrosine kinase inhibitor-treated gastrointestinal stromal tumors. *Int J Cancer* **127**, 899–909 (2010).

202. Jiang, M. *et al.* Tamoxifen inhibits macrophage FABP4 expression through the combined effects of the GR and PPARγ pathways. *Biochem J* **454**, 467–477 (2013).

203. Chang, Y. -C & Malone, M. H. Anti-Inflammatory and Liver Sulfhydryl Content-Altering Effects of Certain Nonsteroids in the Rat. *J Pharm Sci* **60**, 416–419 (1971).

204. Mumuni A., M., Kenechukwu, F. C., Chime, S. A., Ogbonna, J. D. & Mora, A. T. Anti-inflammatory and pharmacokinetics evaluation of PEGylated ibuprofen tablet formulation. *Drug Deliv* **21**, 315–319 (2014).

205. Scheuren, N., Bang, H., Münster, T., Brune, K. & Pahl, A. Modulation of transcription factor NF-κB by enantiomers of the nonsteroidal drug ibuprofen. *Br J Pharmacol* **123**, 645–652 (1998).

206. Canan, C. H. *et al.* Characterization of lung inflammation and its impact on macrophage function in aging. *J Leukoc Biol* **96**, 473–480 (2014).

207. Hossain, M. M. *et al.* The anti-parkinsonian drug zonisamide reduces neuroinflammation: Role of microglial Na v 1.6. *Exp Neurol* **308**, 111–119 (2018).

208. Xu, J. *et al.* Methylprednisolone inhibition of TNF-α expression and NF-κB activation after spinal cord injury in rats. *Molecular Brain Research* **59**, 135–142 (1998).

209. Johnson, M. The anti-inflammatory profile of fluticasone propionate. *Allergy* **50**, 11–14 (1995).

210. Escotte, S. *et al.* Fluticasone reduces IL-6 and IL-8 production of cystic fibrosis bronchial epithelial cells via IKK-β kinase pathway. *European Respiratory Journal* **21**, 574–581 (2003).

211. Mogensen, T. H., Berg, R. S., Paludan, S. R. & Østergaard, L. Mechanisms of dexamethasone-mediated inhibition of toll-like receptor signaling induced by Neisseria meningitidis and Streptococcus pneumoniae. *Infect Immun* **76**, 189–197 (2008).

212. Gibson, P. G., Saltos, N. & Fakes, K. Acute anti-inflammatory effects of inhaled budesonide in asthma: A randomized controlled trial. *Am J Respir Crit Care Med* **163**, 32–36 (2001).

213. Wilson, S. J., Wallin, A., Della-Cioppa, G., Sandström, T. & Holgate, S. T. Effects of budesonide and formoterol on NF-κB, adhesion molecules, and cytokines in asthma. *Am J Respir Crit Care Med* **164**, 1047–1052 (2001).

214. Dandona, P. *et al.* A mixed anti-inflammatory and pro-inflammatory response associated with a high dose of corticosteroids. *Curr Mol Med* **14**, 793–801 (2014).

215. Carneiro, P. J. *et al.* Bosutinib Therapy Ameliorates Lung Inflammation and Fibrosis in Experimental Silicosis. *Front Physiol* **8**, (2017).

216. Ma, L. *et al.* Bosutinib attenuates inflammation via inhibiting salt-inducible kinases in experimental model of intracerebral hemorrhage on mice. *Stroke* **48**, 3108–3116 (2017).

217. Cabozantinib inhibits Listeria monocytogenes infection in mice. *Journal of Southern Medical University* **36**, 56 (2016).

218. Wang, L., Lu, Q., Gao, W. & Yu, S. Recent advancement on development of drug-induced macrophage polarization in control of human diseases. *Life Sci* **284**, 119914 (2021).

219. Purvis, G. S. D. *et al.* Bruton's TK regulates myeloid cell recruitment during acute inflammation. *Br J Pharmacol* **179**, 2754–2770 (2022).

220. Nowak-Sliwinska, P. *et al.* Photoactivation of lysosomally sequestered sunitinib after angiostatic treatment causes vascular occlusion and enhances tumor growth inhibition. *Cell Death Dis* **6**, e1641 (2015).

221. Richard, K., Vogel, S. N. & Perkins, D. J. Quantitation of TLR4 Internalization in Response to LPS in Thioglycollate Elicited Peritoneal Mouse Macrophages by Flow Cytometry. *Bio Protoc* **9**, 3369 (2019).

222. Wang, X. *et al.* Post-translational Modifications of IκBα: The State of the Art. *Front Cell Dev Biol* **8**, 1285 (2020).

223. Koneczny, I., Cossins, J. & Vincent, A. The role of muscle-specific tyrosine kinase (MuSK) and mystery of MuSK myasthenia gravis. *J Anat* **224**, 29 (2014).

224. Spadaro, O. *et al.* IGF1 Shapes Macrophage Activation in Response to Immunometabolic Challenge. *Cell Rep* **19**, 225–234 (2017).

225. Cho, K. A., Park, M., Kim, Y. H., Woo, S. Y. & Ryu, K. H. Conditioned media from human palatine tonsil mesenchymal stem cells regulates the interaction between myotubes and fibroblasts by IL-1Ra activity. *J Cell Mol Med* **21**, 130–141 (2017).

226. Mussbacher, M. *et al.* Cell type specific roles of nf-kb linking inflamation and thrombosis. *Front Immunol* **10**, 85 (2019).

227. Ramadass, V., Vaiyapuri, T. & Tergaonkar, V. Small molecule nf-kb pathway inhibitors in clinic. *International Journal of Molecular Sciences* vol. 21 1–43 Preprint at https://doi.org/10.3390/ijms21145164 (2020).

228. Bennett, J. *et al.* NF-κB in the crosshairs: Rethinking an old riddle. *Int J Biochem Cell Biol* **95**, 108 (2018).

229. McKellar, G. E., McCarey, D. W., Sattar, N. & McInnes, I. B. Role for TNF in atherosclerosis? Lessons from autoimmune disease. *Nature Reviews Cardiology 2009 6:6* **6**, 410–417 (2009).

230. Zelová, H. & Hošek, J. TNF-α signalling and inflammation: Interactions between old acquaintances. *Inflammation Research* **62**, 641–651 (2013).

231. Hilgendorff, A. *et al.* Statins differ in their ability to block NF-kappaB activation in human blood monocytes. *Int J Clin Pharmacol Ther* **41**, 397–401 (2003).

232. Choi, J. & Fenando, A. Sulfasalazine. *Intraocular Inflammation* 373–377 (2022) doi:10.1007/978-3-540-75387-2_30.

233. Medvedev, A. E. *et al.* Role of TLR4 tyrosine phosphorylation in signal transduction and endotoxin tolerance. *J Biol Chem* **282**, 16042–16053 (2007).

234. Kang, J. L., Jung, H. J., Lee, K. & Kim, H. R. Src Tyrosine Kinases Mediate Crystalline Silica-Induced NF-jB Activation through Tyrosine Phosphorylation of IjB-a and p65 NF-jB in RAW 264.7 Macrophages. doi:10.1093/toxsci/kfj096.

235. Byeon, S. E. *et al.* The Role of Src Kinase in Macrophage-Mediated Inflammatory Responses. *Mediators Inflamm* **2012**, (2012).

236. Ito, M. *et al.* Bruton's tyrosine kinase is essential for NLRP3 inflammasome activation and contributes to ischaemic brain injury. *Nature Communications 2015 6:1* **6**, 1–11 (2015).

237. Isfort, S. *et al.* Bosutinib: A Potent Second-Generation Tyrosine Kinase Inhibitor. *Recent Results Cancer Res* **212**, 87–108 (2018).

238. Randall, N., Courville, E. L., Baughn, L., Afrin, L. & Ustun, C. Bosutinib, a Lyn/Btk inhibiting tyrosine kinase inhibitor, is ineffective in advanced systemic mastocytosis. *Am J Hematol* **90**, E74–E74 (2015).

239. Ozanne, J., Prescott, A. R. & Clark, K. The clinically approved drugs dasatinib and bosutinib induce anti-inflammatory macrophages by inhibiting the salt-inducible kinases. *Biochemical Journal* **465**, 271–279 (2015).

240. Kitagawa, D. *et al.* Activity-based kinase profiling of approved tyrosine kinase inhibitors. *Genes to Cells* **18**, 110–122 (2013).

241. Stanley, E. R. & Chitu, V. CSF-1 Receptor Signaling in Myeloid Cells. *Cold Spring Harb Perspect Biol* **6**, (2014).

242. Ko, J. S. *et al.* Direct and differential suppression of myeloid-derived suppressor cell subsets by sunitinib is compartmentally constrained. *Cancer Res* **70**, 3526–3536 (2010).

243. HM, C. *et al.* Myeloid-Derived Suppressor Cells as an Immune Parameter in Patients with Concurrent Sunitinib and Stereotactic Body Radiotherapy. *Clin Cancer Res* **21**, 4073–4085 (2015).

244. Xin, H. *et al.* Sunitinib Inhibition of Stat3 Induces Renal Cell Carcinoma Tumor Cell Apoptosis and Reduces Immunosuppressive Cells. *Cancer Res* **69**, 2506–2513 (2009).

245. Hipp, M. M. *et al.* Sorafenib, but not sunitinib, affects function of dendritic cells and induction of primary immune responses. *Blood* **111**, 5610–5620 (2008).

246. Pu, S. Y. *et al.* Feasibility and biological rationale of repurposing sunitinib and erlotinib for dengue treatment. *Antiviral Res* **155**, 67–75 (2018).

247. Laurila, J. P., Laukkanen, M. O., Joensuu, H., Salmi, M. & Jalkanen, S. Leukocyte trafficking is not affected by multikinase inhibitors sunitinib or sorafenib in mice. *Int J Cancer* **139**, 2270–2276 (2016).

248. Detry, B. *et al.* Sunitinib Inhibits Inflammatory Corneal Lymphangiogenesis. *Investigative Opthalmology & Visual Science* **54**, 3082 (2013).

249. Sanchez, A. *et al.* Sunitinib enhances neuronal survival in vitro via NF-κB-mediated signaling and expression of cyclooxygenase-2 and inducible nitric oxide synthase. *J Neuroinflammation* **10**, 857 (2013).

250. Glenn, G. & van der Geer, P. Toll-like receptors stimulate regulated intramembrane proteolysis of the CSF-1 receptor through Erk activation. *FEBS Lett* **582**, 911–915 (2008).

251. Tang, J. *et al.* EGFR signaling augments TLR4 cell surface expression and function in macrophages via regulation of Rab5a activation. *Protein Cell* **11**, 144–149 (2020).

252. Patil, T., Soni, A. & Acharya, S. A brief review on in vivo models for Gouty Arthritis. *Metabol Open* **11**, 100100 (2021).

253. Lewis, A. J., Seymour, C. W. & Rosengart, M. R. Current Murine Models of Sepsis. *Surg Infect (Larchmt)* **17**, 385 (2016).

254. Cash, J. L., White, G. E. & Greaves, D. R. Chapter 17 Zymosan-Induced Peritonitis as a Simple Experimental System for the Study of Inflammation. *Methods Enzymol* **461**, 379–396 (2009).

255. Nandi, M. *et al.* Rethinking animal models of sepsis – working towards improved clinical translation whilst integrating the 3Rs. *Clin Sci* **134**, 1715–1734 (2020).

256. Lv, S. *et al.* Anti-TNF-α therapy for patients with sepsis: a systematic meta-analysis. *Int J Clin Pract* **68**, 520–528 (2014).

257. Cavaillon, J. M. & Adib-Conquy, M. Bench-to-bedside review: Endotoxin tolerance as a model of leukocyte reprogramming in sepsis. *Crit Care* **10**, 233 (2006).

258. Murphey, E. D., Fang, G. & Sherwood, E. R. Endotoxin pretreatment improves bacterial clearance and decreases mortality in mice challenged with Staphylococcus aureus. *Shock* **29**, 512–518 (2008).

259. Siempos, I. I. *et al.* Cecal Ligation and Puncture-induced Sepsis as a Model To Study Autophagy in Mice. *J Vis Exp* **84**, 51066 (2014).

260. Matute-Bello, G., Frevert, C. W. & Martin, T. R. Animal models of acute lung injury. *Am J Physiol Lung Cell Mol Physiol* **295**, L379 (2008).

261. Caraballo, C. & Jaimes, F. Focus: Death: Organ Dysfunction in Sepsis: An Ominous Trajectory From Infection To Death. *Yale J Biol Med* **92**, 629 (2019).

262. Hughes, K. T. & Beasley, M. B. Pulmonary Manifestations of Acute Lung Injury: More Than Just Diffuse Alveolar Damage. *Arch Pathol Lab Med* **141**, 916–922 (2017).

263. Hefler, J. *et al.* Preclinical models of acute liver failure: a comprehensive review. *PeerJ* **9**, (2021).

264. Hukriede, N. A. *et al.* Experimental models of acute kidney injury for translational research. *Nature Reviews Nephrology 2022 18:5* **18**, 277–293 (2022).

265. Huen, S. C. & Cantley, L. G. Macrophages in Renal Injury and Repair. *https://doi.org/10.1146/annurev-physiol-022516-034219* **79**, 449–469 (2017).

266. Kosaka, J., Lankadeva, Y. R., May, C. N. & Bellomo, R. Histopathology of Septic Acute Kidney Injury: A Systematic Review of Experimental Data. *Crit Care Med* **44**, e897–e903 (2016).

267. Lee, S. J. *et al.* Drug repositioning of TANK-binding kinase 1 inhibitor CYT387 as an alternative for the treatment of Gram-negative bacterial sepsis. *Int Immunopharmacol* **73**, 482–490 (2019).

268. Li, X. *et al.* Sorafenib inhibits LPS-induced inflammation by regulating Lyn-MAPK-NF-kB/AP-1 pathway and TLR4 expression. *Cell Death Discov* **8**, (2022).

269. Wang, T., Zheng, R. & Sun, S. Drug Repurposing: Escitalopram attenuates acute lung injury by inhibiting the SIK2/ HDAC4/ NF-κB signaling cascade. *Biochem Biophys Res Commun* **599**, 1–8 (2022).

270. Welti, J. C. *et al.* Contrasting effects of sunitinib within in vivo models of metastasis. *Angiogenesis* **15**, 623–641 (2012).

271. Hu, J. J. *et al.* FDA-approved disulfiram inhibits pyroptosis by blocking gasdermin D pore formation. *Nature Immunology 2020 21:7* **21**, 736–745 (2020).

272. Coldewey, S. M., Rogazzo, M., Collino, M., Patel, N. S. A. & Thiemermann, C. Inhibition of IκB kinase reduces the multiple organ dysfunction caused by sepsis in the mouse. *Dis Model Mech* **6**, 1031 (2013).

273. Waelchli, R. *et al.* Design and preparation of 2-benzamido-pyrimidines as inhibitors of IKK. *Bioorg Med Chem Lett* **16**, 108–112 (2006).

274. Sanders, B., Larson, D. F., Hunter, K., Gorman, M. & Yang, B. Comparison of tumor necrosis factor-effect on the expression of iNOS in macrophage and cardiac myocytes. *Perfusion* **16**, 67–74 (2001).

275. Chandrasekharan, U. M. *et al.* Tumor necrosis factor α (TNF-α) receptor-II is required for TNF-α–induced leukocyte-endothelial interaction in vivo. *Blood* **109**, 1938–1944 (2007).

276. Taylor, P. C. & Feldmann, M. Anti-TNF biologic agents: still the therapy of choice for rheumatoid arthritis. *Nature Reviews Rheumatology 2009 5:10* **5**, 578–582 (2009).

277. Barf, T. *et al.* Acalabrutinib (ACP-196): A covalent Bruton tyrosine kinase inhibitor with a differentiated selectivity and in vivo potency profile. *Journal of Pharmacology and Experimental Therapeutics* **363**, 240–252 (2017).

278. He, L. *et al.* Global characterization of macrophage polarization mechanisms and identification of M2-type polarization inhibitors. *Cell Rep* **37**, 109955 (2021).

279. Rathod, K. *et al.* Sex differences in the inflammatory response and inflammation-induced vascular dysfunction. *The Lancet* **389**, S20 (2017).

280. Klein, S. L. & Flanagan, K. L. Sex differences in immune responses. *Nature Reviews Immunology 2016 16:10* **16**, 626–638 (2016).

281. Varghese, M. *et al.* Sex Differences in Inflammatory Responses to Adipose Tissue Lipolysis in Diet-Induced Obesity. *Endocrinology* **160**, 293 (2019).

282. Annane, D., Aegerter, P., Jars-Guincestre, M. C. & Guidet, B. Current Epidemiology of Septic Shock. *https://doi.org/10.1164/rccm.2201087* **168**, 165–172 (2012).

283. Xie, J. *et al.* The Epidemiology of Sepsis in Chinese ICUs: A National Cross-Sectional Survey. *Crit Care Med* **48**, E209–E218 (2020).

284. Nasir, N. *et al.* Mortality in Sepsis and its relationship with Gender. *Pak J Med Sci* **31**, 1201 (2015).

285. Scheiermann, C., Kunisaki, Y. & Frenette, P. S. Circadian control of the immune system. *Nat Rev Immunol* **13**, 190 (2013).

286. Baxter, M. & Ray, D. W. Circadian rhythms in innate immunity and stress responses. *Immunology* **161**, 261 (2020).

287. Gibbs, J. E. *et al.* The nuclear receptor REV-ERBα mediates circadian regulation of innate immunity through selective regulation of inflammatory cytokines. *Proc Natl Acad Sci U S A* **109**, 582–587 (2012).

288. Nguyen, T., Du, J. & Li, Y. C. A protocol for macrophage depletion and reconstitution in a mouse model of sepsis. *STAR Protoc* **2**, 101004 (2021).

289. Nair, A. & Jacob, S. A simple practice guide for dose conversion between animals and human. *J Basic Clin Pharm* **7**, 27 (2016).

290. Oesterle, A., Laufs, U. & Liao, J. K. Pleiotropic Effects of Statins on the Cardiovascular System. *Circ Res* **120**, 229 (2017).

291. Roth, E. M. & Davidson, M. H. PCSK9 Inhibitors: Mechanism of Action, Efficacy, and Safety. *Rev Cardiovasc Med* **19**, S31–S46 (2018).

292. Fretheim, A. *et al.* Comparative effectiveness of antihypertensive medication for primary prevention of cardiovascular disease: Systematic review and multiple treatments meta-analysis. *BMC Med* **10**, 1–14 (2012).

293. Agca, R., Smulders, Y. & Nurmohamed, M. Cardiovascular disease risk in immune-mediated inflammatory diseases: recommendations for clinical practice. *Heart* **108**, 73–79 (2022).

294. Hansildaar, R. *et al.* Cardiovascular risk in inflammatory arthritis: rheumatoid arthritis and gout. *Lancet Rheumatol* **3**, e58–e70 (2021).

295. Ridker, P. M. The JUPITER trial: Results, controversies, and implications for prevention. *Circ Cardiovasc Qual Outcomes* **2**, 279–285 (2009).

296. Zannad, F. *et al.* What can heart failure trialists learn from oncology trialists? *Eur Heart J* **42**, 2373–2383 (2021).

297. Morton, A. C. *et al.* The effect of interleukin-1 receptor antagonist therapy on markers of inflammation in non-ST elevation acute coronary syndromes: the MRC-ILA Heart Study. *Eur Heart J* **36**, 377–384 (2015).

298. Abbate, A. *et al.* Interleukin-1 blockade inhibits the acute inflammatory response in patients with st-segment–elevation myocardial infarction. *J Am Heart Assoc* **9**, (2020).

299. Ridker, P. M. *et al.* Antiinflammatory Therapy with Canakinumab for Atherosclerotic Disease. *New England Journal of Medicine* **377**, 1119–1131 (2017).

300. Broch, K. *et al.* Randomized Trial of Interleukin-6 Receptor Inhibition in Patients With Acute ST-Segment Elevation Myocardial Infarction. *J Am Coll Cardiol* **77**, 1845–1855 (2021).

301. Mann, D. L. *et al.* Targeted Anticytokine Therapy in Patients With Chronic Heart Failure. *Circulation* **109**, 1594–1602 (2004).

302. Chung, E. S., Packer, M., Lo, K. H., Fasanmade, A. A. & Willerson, J. T. Randomized, Double-Blind, Placebo-Controlled, Pilot Trial of Infliximab, a Chimeric Monoclonal Antibody to Tumor Necrosis Factor-α, in Patients With Moderate-to-Severe Heart Failure. *Circulation* **107**, 3133–3140 (2003).

303. Nidorf, S. M., Eikelboom, J. W., Budgeon, C. A. & Thompson, P. L. Low-Dose Colchicine for Secondary Prevention of Cardiovascular Disease. *J Am Coll Cardiol* **61**, 404–410 (2013).

304. Shah, B. *et al.* Effects of Acute Colchicine Administration Prior to Percutaneous Coronary Intervention: The COLCHICINE-PCI Randomized Trial. *Circ Cardiovasc Interv* **13**, e008717 (2020).

305. Nidorf, S. M. *et al.* Colchicine in Patients with Chronic Coronary Disease. *New England Journal of Medicine* **383**, 1838–1847 (2020).

306. Tardif, J.-C. *et al.* Efficacy and Safety of Low-Dose Colchicine after Myocardial Infarction. *New England Journal of Medicine* **381**, 2497–2505 (2019).

307. Tong, D. C. *et al.* Colchicine in Patients With Acute Coronary Syndrome. *Circulation* **142**, 1890–1900 (2020).

308. Mewton, N. *et al.* Effect of Colchicine on Myocardial Injury in Acute Myocardial Infarction. *Circulation* **144**, 859–869 (2021).

309. Moreira, D. M., Vieira, J. L. & Mascia Gottschall, C. A. The Effects of METhotrexate Therapy on the Physical Capacity of Patients With ISchemic Heart Failure: A Randomized Double-Blind, Placebo-Controlled Trial (METIS Trial). *J Card Fail* **15**, 828–834 (2009).

310. Ridker, P. M. *et al.* Low-Dose Methotrexate for the Prevention of Atherosclerotic Events. *New England Journal of Medicine* **380**, 752–762 (2019).

311. Moreira, D. M., Lueneberg, M. E., da Silva, R. L., Fattah, T. & Gottschall, C. A. M. MethotrexaTE THerapy in ST-Segment Elevation MYocardial InfarctionS. *J Cardiovasc Pharmacol Ther* **22**, 538–545 (2017).

312. Cung, T.-T. *et al.* Cyclosporine before PCI in Patients with Acute Myocardial Infarction. *New England Journal of Medicine* **373**, 1021–1031 (2015).

313. Ottani, F. *et al.* Cyclosporine A in Reperfused Myocardial Infarction: The Multicenter, Controlled, Open-Label CYCLE Trial. *J Am Coll Cardiol* **67**, 365–374 (2016).

314. Mackenzie, I. S. *et al.* Allopurinol versus usual care in UK patients with ischaemic heart disease (ALL-HEART): a multicentre, prospective, randomised, open-label, blinded-endpoint trial. *The Lancet* **400**, 1195–1205 (2022).

315. Zhao, T. X. *et al.* Low dose interleukin-2 in patients with stable ischaemic heart disease and acute coronary syndrome (LILACS). *Eur Heart J* **41**, (2020).

316. van Tassell, B. W., Toldo, S., Mezzaroma, E. & Abbate, A. Targeting Interleukin-1 in Heart Disease. *Circulation* **128**, 1910 (2013).

317. Szekely, Y. & Arbel, Y. A Review of Interleukin-1 in Heart Disease: Where Do We Stand Today? *Cardiol Ther* **7**, 25 (2018).

318. Sehested, T. S. G. *et al.* Cost-effectiveness of Canakinumab for Prevention of Recurrent Cardiovascular Events. *JAMA Cardiol* **4**, 128–135 (2019).

319. Dixon, W. G. *et al.* Reduction in the incidence of myocardial infarction in patients with rheumatoid arthritis who respond to anti–tumor necrosis factor α therapy: Results from the British Society for Rheumatology Biologics Register. *Arthritis Rheum* **56**, 2905–2912 (2007).

320. Deftereos, S. G. *et al.* Colchicine in Cardiovascular Disease: In-Depth Review. *Circulation* **145**, 61–78 (2022).

321. Demidowich, A. P., Davis, A. I., Dedhia, N. & Yanovski, J. A. Colchicine to decrease NLRP3-activated inflammation and improve obesity-related metabolic dysregulation. *Med Hypotheses* **92**, 67–73 (2016).

322. Choi, H. K., Hernán, M. A., Seeger, J. D., Robins, J. M. & Wolfe, F. Methotrexate and mortality in patients with rheumatoid arthritis: a prospective study. *The Lancet* **359**, 1173–1177 (2002).

323. Micha, R. *et al.* Systematic Review and Meta-Analysis of Methotrexate Use and Risk of Cardiovascular Disease. *Am J Cardiol* **108**, 1362–1370 (2011).

324. Chan, E. S. L. & Cronstein, B. N. Molecular action of methotrexate in inflammatory diseases. *Arthritis Res* **4**, 266–273 (2002).

325. Liddicoat, A. M. & Lavelle, E. C. Modulation of innate immunity by cyclosporine A. *Biochem Pharmacol* **163**, 472–480 (2019).

326. Teijeiro, A., Garrido, A., Ferre, A., Perna, C. & Djouder, N. Inhibition of the IL-17A axis in adipocytes suppresses diet-induced obesity and metabolic disorders in mice. *Nature Metabolism 2021 3:4* **3**, 496–512 (2021).

327. Omran, Z., Sheikh, R., Baothman, O. A., Zamzami, M. A. & Alarjah, M. Repurposing Disulfiram as an Anti-Obesity Drug: Treating and Preventing Obesity in High-Fat-Fed Rats. *Diabetes Metab Syndr Obes* **13**, 1473 (2020).

328. Hosoi, T., Baba, S. & Ozawa, K. Therapeutic potential of flurbiprofen against obesity in mice. *Biochem Biophys Res Commun* **449**, 132–134 (2014).

329. Duggan, B. M., Cavallari, J. F., Foley, K. P., Barra, N. G. & Schertzer, J. D. RIPK2 Dictates Insulin Responses to Tyrosine Kinase Inhibitors in Obese Male Mice. *Endocrinology* **161**, 1–16 (2020).

330. Ambati, J. *et al.* Repurposing anti-inflammasome NRTIs for improving insulin sensitivity and reducing type 2 diabetes development. *Nature Communications 2020 11:1* **11**, 1–12 (2020).

331. Tanaka, T. *et al.* Computational Screening Strategy for Drug Repurposing Identified Niclosamide as Inhibitor of Vascular Calcification. *Front Cardiovasc Med* **8**, 826529 (2021).

332. Castillo-Salazar, M. *et al.* Nitazoxanide Exerts Immunomodulatory Effects on Peripheral Blood Mononuclear Cells from Type 2 Diabetes Patients. *Biomolecules* **11**, (2021).

333. Getz, G. S. & Reardon, C. A. Animal Models of Atherosclerosis. *Arterioscler Thromb Vasc Biol* **32**, 1104 (2012).

334. Mansukhani, N. A. *et al.* Sex Differences in the LDL Receptor Knockout Mouse Model of Atherosclerosis. *Artery Res* **20**, 8 (2017).

335. Zhang, L. *et al.* In Vivo Antitumor and Antimetastatic Activity of Sunitinib in Preclinical Neuroblastoma Mouse Model. *Neoplasia* **11**, 426 (2009).

336. Ma, Y. *et al.* Hyperlipidaemia and Atherosclerotic Lesion Development in Ldlr-Deficient Mice on a Long-Term High-Fat Diet. *PLoS One* **7**, (2012).

337. Tahir, A. *et al.* An evaluation of lipid profile and pro-inflammatory cytokines as determinants of cardiovascular disease in those with diabetes: a study on a Mexican American cohort. *Scientific Reports 2021 11:1* **11**, 1–12 (2021).

338. Ferroni, P. *et al.* Enhanced interleukin-1β in hypercholesterolaemia: Effects of simvastatin and low-dose aspirin. *Circulation* **108**, 1673–1675 (2003).

339. Swirski, F. K. *et al.* Ly-6Chi monocytes dominate hypercholesterolaemia-associated monocytosis and give rise to macrophages in atheromata. *J Clin Invest* **117**, 195–205 (2007).

340. Rumianek, A. N., Davies, B., Channon, K. M., Greaves, D. R. & Purvis, G. S. D. A Human CD68 Promoter-Driven Inducible Cre-Recombinase Mouse Line Allows Specific Targeting of Tissue Resident Macrophages. *Front Immunol* **13**, (2022).

341. Harman, J. L. & Jørgensen, H. F. The role of smooth muscle cells in plaque stability: Therapeutic targeting potential. *Br J Pharmacol* **176**, 3741 (2019).

342. Papaspyridonos, M. *et al.* Galectin-3 Is an Amplifier of Inflammation in Atherosclerotic Plaque Progression Through Macrophage Activation And Monocyte Chemoattraction. *Arterioscler Thromb Vasc Biol* **28**, 433–440 (2008).

343. Chu, T. F. *et al.* Cardiotoxicity Associated with the Tyrosine Kinase Inhibitor Sunitinib. *Lancet* **370**, 2011 (2007).

344. Schmidinger, M. *et al.* Cardiac toxicity of sunitinib and sorafenib in patients with metastatic renal cell carcinoma. *Journal of Clinical Oncology* **26**, 5204–5212 (2008).

345. Di Lorenzo, G. *et al.* Cardiovascular toxicity following sunitinib therapy in metastatic renal cell carcinoma: a multicenter analysis. *Ann Oncol* **20**, 1535–1542 (2009).

346. Blasi, E. *et al.* Sunitinib, a Receptor Tyrosine Kinase Inhibitor, Increases Blood Pressure in Rats without Associated Changes in Cardiac Structure and Function. *Cardiovasc Ther* **30**, 287–294 (2012).

347. Gareus, R. *et al.* Endothelial cell-specific NF-kappaB inhibition protects mice from atherosclerosis. *Cell Metab* **8**, 372–383 (2008).

348. Zhou, L., Dong, J., Yu, M., Yin, H. & She, M. Age-dependent increase of NF-κB translocation and PDGF-B expression in aortic endothelial cells of hypercholesterolaemic rats. *Exp Gerontol* **38**, 1161–1168 (2003).

349. Raines, E. W. PDGF and cardiovascular disease. *Cytokine Growth Factor Rev* **15**, 237–254 (2004).

350. He, C. *et al.* PDGFRβ signalling regulates local inflammation and synergizes with hypercholesterolaaemia to promote atherosclerosis. *Nature Communications 2015 6:1* **6**, 1–14 (2015).

351. Xiao, N. *et al.* Tumor necrosis factor-alpha deficiency retards early fatty-streak lesion by influencing the expression of inflammatory factors in apoE-null mice. *Mol Genet Metab* **96**, 239–244 (2009).

352. Brånén, L. *et al.* Inhibition of tumor necrosis factor-alpha reduces atherosclerosis in apolipoprotein E knockout mice. *Arterioscler Thromb Vasc Biol* **24**, 2137–2142 (2004).

353. Irace, C. *et al.* Effect of anti TNFalpha therapy on arterial diameter and wall shear stress and HDL cholesterol. *Atherosclerosis* **177**, 113–118 (2004).

354. Hürlimann, D. *et al.* Anti–Tumor Necrosis Factor-α Treatment Improves Endothelial Function in Patients With Rheumatoid Arthritis. *Circulation* **106**, 2184–2187 (2002).

355. Mäki-Petäjä, K. M. *et al.* Rheumatoid Arthritis Is Associated With Increased Aortic Pulse-Wave Velocity, Which Is Reduced by Anti–Tumor Necrosis Factor-α Therapy. *Circulation* **114**, 1185–1192 (2006).

356. Yazdani-Biuki, B. *et al.* Improvement of insulin sensitivity in insulin resistant subjects during prolonged treatment with the anti-TNF-α α α α antibody infliximab. *Eur J Clin Invest* **34**, 641–642 (2004).

357. Kiortsis, D. N., Mavridis, A. K., Vasakos, S., Nikas, S. N. & Drosos, A. A. Effects of infliximab treatment on insulin resistance in patients with rheumatoid arthritis and ankylosing spondylitis. *Ann Rheum Dis* **64**, 765–766 (2005).

358. Hotamisligil, G. S., Arner, P., Caro, J. F., Atkinson, R. L. & Spiegelman, B. M. Increased adipose tissue expression of tumor necrosis factor-alpha in human obesity and insulin resistance. *Am Soc Clin Investig*.

359. Dandona, P., Weinstock, R., … K. T.-T. J. of & 1998, undefined. Tumor necrosis factor-α in sera of obese patients: fall with weight loss. *academic.oup.com*.

360. Rose, S. *et al.* A novel mouse model that develops spontaneous arthritis and is predisposed towards atherosclerosis. *Ann Rheum Dis* **72**, 89 (2013).

361. Mansukhani, N. A. *et al.* Sex Differences in the LDL Receptor Knockout Mouse Model of Atherosclerosis. *Artery Res* **20**, 8 (2017).

362. Dömling, A. & Li, X. TNF-α: The shape of small molecules to come? *Drug Discov Today* **27**, 3–7 (2022).

363. Dietrich, J. D. *et al.* Development of Orally Efficacious Allosteric Inhibitors of TNFα via Fragment-Based Drug Design. *J Med Chem* **64**, 417–429 (2021).

364. Bozkurt, B. *et al.* Results of Targeted Anti–Tumor Necrosis Factor Therapy With Etanercept (ENBREL) in Patients With Advanced Heart Failure. *Circulation* **103**, 1044–1047 (2001).

365. Schwandt, A., Wood, L. S., Rini, B. & Dreicer, R. Management of side effects associated with sunitinib therapy for patients with renal cell carcinoma. *Onco Targets Ther* **2**, 51 (2009).

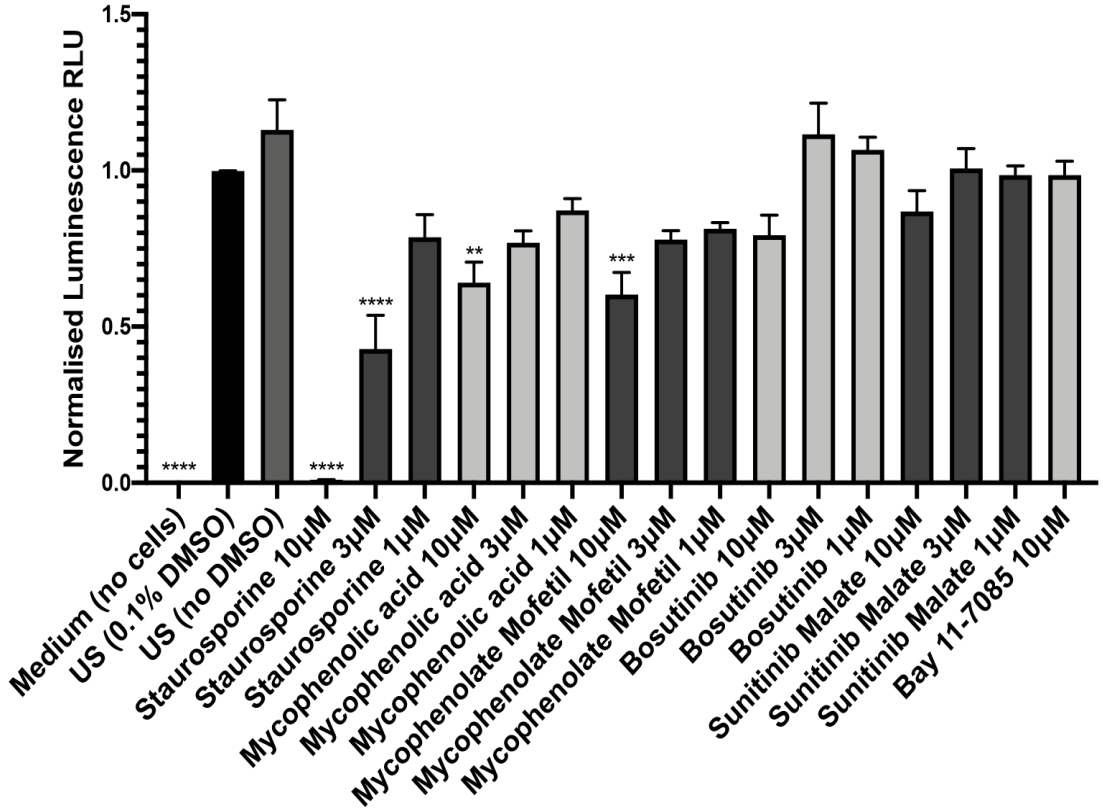
366. Khakoo, A. Y. *et al.* Heart failure associated with sunitinib malate: a multitargeted receptor tyrosine kinase inhibitor. *Cancer* **112**, 2500–2508 (2008).

367. Wang, H. *et al.* Update on Nanoparticle-Based Drug Delivery System for Anti-inflammatory Treatment. *Front Bioeng Biotechnol* **9**, (2021).

368. Wu, Y. *et al.* An apoptotic body-biomimic liposome in situ upregulates anti-inflammatory macrophages for stabilization of atherosclerotic plaques. *Journal of Controlled Release* **316**, 236–249 (2019).

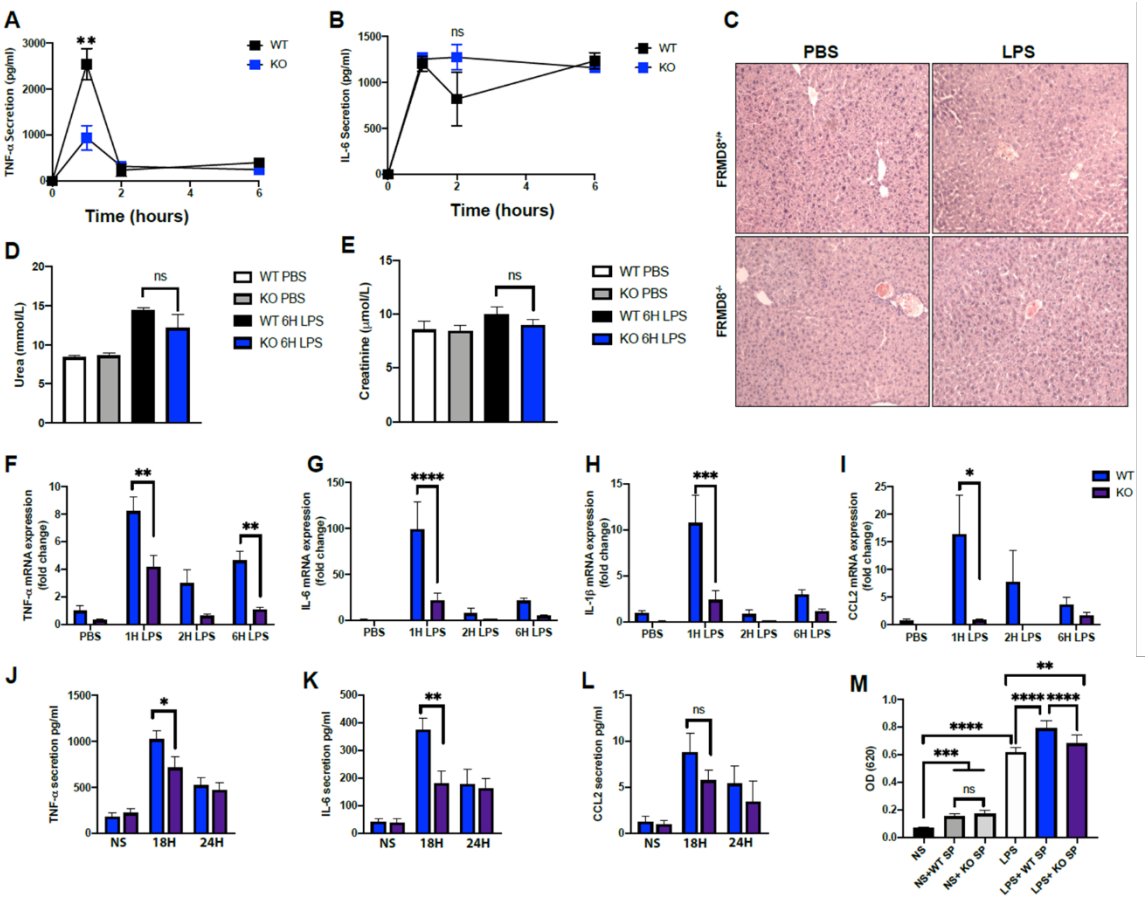
Appendices

Appendix 1: Amelia Bowman FHS Project Cytotoxicity data



Effect of candidates on cell viability. RAW-blue cells were stimulated with LPS (100ng/mL) and treated with the compounds at 10µM, 3µM and 1µM for 6 hours before being lysed and luminescence measured using CellTiter-Glo. Cell viability; data is normalised to US (0.1% DMSO), *n=4*. Data are presented as mean ±SEM of 4 independent experiments preformed in quadruplicate. Statistical significance was evaluated using a one-way ANOVA with Dunnett's multiple comparisons test against 0.1% DMSO (**P*<0.05, ***P*<0.01, ****P*<0.001, *****P*<0.0001). RLU=relative light unit.

Appendix 2: Lynda Zeboudj Endotoxaemia data



FRMD8 deficiency protects against acute inflammation. FRMD8+/+ and FRMD8-/- male mice were i.p injected with 10 mg kg^{-1} of LPS for the indicated time or PBS (control) and cytokine levels was examined in the sera by ELISA (n=4-8). **A** TNF-a levels in the serum from FRMD8+/+ and FRMD8-/- animals after LPS injection (n=4-8), **B** IL-6 levels in the serum from FRMD8+/+ and FRMD8-/- after LPS injection at the indicated time points (n=4-8), **C** H&E staining of representative section of liver obtained from FRMD8+/+ and FRMD8-/- mice injected with PBS or LPS for 6 hours. **D** Urea **E** Creatinine levels in the sera from FRMD8+/+ and FRMD8-/- injected with PBS or LPS for 6 hours. **F** TNF-a, **G** IL-6, **H** IL-1B, **I** CCL2 mRNA expression in the liver after i.p injection of PBS or LPS for the indicated time points (n=4-8). **J** TNF-a, **K** IL-6, **L** CCL2 secretion on splenocytes LPS stimulated in vitro at the indicated time points. **M** Raw blue cells (macrophage cell line) stably transfected with a secreted alkaline phosphatase (SEAP) under the transcription of NF-KB and AP-1 were co-incubated with splenocytes from FRMD8+/+ (WT) or FRMD8-/- (KO), and stimulated with LPS, after 6 hours SEAP was measured by spectrophotometry at OD 620. Data are expressed as mean ± SEM, * represents $P < 0.05$, ** represents $P < 0.01$, *** represents P<0,001 and **** represents P<0,0001.

Appendix 3: Publication contributions

Chaffey L, Roberti A, Greaves DR. Drug repurposing in cardiovascular inflammation: Successes, failures, and future opportunities. Front Pharmacol. 2022 Oct 21;13:4500.

Roberti A, **Chaffey LE**, Greaves DR. NF-κB Signaling and Inflammation: Drug Repurposing to Treat Inflammatory Disorders? Biology, 2022 Feb 26;11(3):372. Available from: https://www.mdpi.com/2079-7737/11/3/372/htm